TRANSACTIONS OF THE AMERICAN SOCIETY FOR METALS

L 04073
639 Alcoa Hist
793 C F
1816 O W A
Zimmer

SEPTEMBER, 1942

Volume XXX

Number 3

The TRANSACTIONS of the AMERICAN SOCIETY FOR METALS

Published quarterly and Copyrighted, 1942, by the AMERICAN SOCIETY FOR METALS
7301 Euclid Avenue, Cleveland, Ohio

SUBSCRIPTIONS: (members) $2.50 per year
(non-members) $5.00 per year, $2.00 per copy
Foreign (non-members) $6.50 per year, $2.50 per copy

Entered as second class matter, November 9, 1931, at the Post Office at Cleveland, Ohio, under the Act of March 3, 1879

RAY T. BAYLESS, *Editor*

Vol. XXX September 1942 No. 3

The object of the Society shall be to promote the arts and sciences connected with either the manufacture or treatment of metals, or both.

Officers and Trustees

BRADLEY STOUGHTON, President
Lehigh University, Bethlehem, Pa.

H. J. FRENCH, Vice-President
International Nickel Co., New York

F. B. FOLEY, Treasurer
The Midvale Co., Nicetown, Philadelphia

W. H. EISENMAN, Secretary
7301 Euclid Ave., Cleveland

TRUSTEES

O. E. HARDER, Past President
Battelle Memorial Institute, Columbus, Ohio

E. L. BARTHOLOMEW
United Shoe Machinery Corp.
Beverly, Mass.

C. Y. CLAYTON
Missouri School of Mines & Metallurgy
Rolla, Mo.

N. F. TISDALE
Molybdenum Corporation of America
Pittsburgh

K. R. VAN HORN
Aluminum Company of America
Cleveland

Publication Committee

MAXWELL GENSAMER, Chairman '42
Carnegie Institute of Technology
Pittsburgh

RAY T. BAYLESS, Secretary
7301 Euclid Ave., Cleveland

Members:

J. B. Austin, New York '44
L. S. Bergen, New York '42
Walter Crafts, Buffalo '44
T. G. Digges, Washington '43
E. H. Dix, Jr., Pittsburgh '43
W. E. Jominy, Detroit '44
E. G. Mahin, Notre Dame '43
J. F. Oesterle, Milwaukee '42
Gilbert Soler, Canton-Mass. '44
Clair Upthegrove, Detroit '44
J. P. Walsted, Worcester '42
A. W. Winston, Detroit '42
L. L. Wyman, Schenectady '43
J. F. Wyzalek, New Jersey '43

Table of Contents

Page

Heat Etching as a General Method for Revealing the Austenite Grain Size of Steels—By O. O. Miller and M. J. Day 541

Discussion 563

The Transformation of Retained Austenite in High Speed Steel at Subatmospheric Temperatures—By Paul Gordon and Morris Cohen 569

Discussion 588

The Temperature and Manner of Growth of Shatter Cracks in Steel Rails—By H. B. Wishart, E. P. Epler and R. E. Cramer 592

Discussion 601

The Nickel-Molybdenum System—By Finley H. Ellinger 607

Discussion 638

Problems in the Drawability of Deep Drawing Sheets—By M. Asimow and J. N. Crombie 639

Discussion 689

The Carbon-Oxygen Equilibrium in Liquid Iron—By Shadburn Marshall and John Chipman 695

Discussion 741

Application of Oscillograph to Determination of Cooling Rates of Quenched Steels—By Charles R. Austin, R. M. Allen and W. G. Van Note 747

Discussion 773

Urea Process for Nitriding Steels—By Ray P. Dunn, W. B. F. Mackay and Ralph L. Dowdell 776

Discussion 791

A Study of Cutting Oils With and Without Added Sulphur—By O. W. Boston and J. C. Zimmer 793

Discussion 808

THERMALLOY

X-RAY INSPECTED HEAT and CORROSION RESISTANT CASTINGS

- ★ RETORTS
- ★ MUFFLES
- ★ TRAYS
- ★ BOXES
- ★ LEAD POTS
- ★ SALT POTS
- ★ CYANIDE POTS

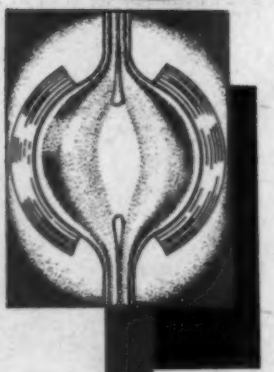

Progress Impels X-Ray Inspection

THERMALLOY *the "EYE" of QUALITY*

THE ELECTRO ALLOYS COMPANY

CASTINGS FOR HEAT CORROSION

ELYRIA, OHIO

QUALITY CASTINGS SINCE 1919

HEAT ETCHING AS A GENERAL METHOD FOR REVEALING THE AUSTENITE GRAIN SIZE OF STEELS

By O. O. Miller and M. J. Day

Abstract

Experimental evidence shows that the method of heat etching, as a means of revealing austenite grain size, is generally applicable provided that the heating is done in an inert atmosphere with an oxygen pressure so low that no appreciable amount of oxide of any of the metals commonly added to deoxidize steel, such as aluminum, zirconium and silicon, is produced at the surface of the specimen. If the oxygen pressure is not low enough the oxide thus produced effectively retards the austenite grain coarsening at the surface long after the remainder of the specimen has coarsened. The procedure for achieving this high degree of purification of hydrogen and for maintaining it in the heat treating furnace is described; the permissible oxygen pressure is less the higher the aluminum content of the steel.

This procedure was employed to reveal the true austenite grain size of steels over a wide range of composition with respect to carbon, silicon, aluminum, chromium, nickel, molybdenum, vanadium and tungsten; the results are in good accord with those obtained by the well known and generally accepted metallographic methods. Accordingly, heat etching is, we believe, applicable to any steel whatever, independent of carbon content, and even to pure iron. This investigation corroborates directly the view, now generally held, that alumina, rather than aluminum or oxygen, is the effective agent in inhibiting the growth of austenite grains in steel.

Introduction

THE method of revealing austenite grain size by heat etching was introduced by Day and Austin (1)[1] who gave a survey of the literature covering the observations which led them to develop it, and applied it to a number of steels. In this method a polished specimen

[1]The figures appearing in parentheses refer to the bibliography appended to this paper.

A paper presented before the Twenty-third Annual Convention of the Society held in Philadelphia, October 20 to 24, 1941. The authors are members of the staff of the Research Laboratory, United States Steel Corporation, Kearny, N. J. Manuscript received July 25, 1941.

is held in an inert atmosphere at the temperature and for the time of the heat treatment to be employed, and is then quenched in mercury; it differs from others in that the surface exposed during heating, and not a section cut and prepared later, is used for rating the grain size, and consequently all tarnishing or scaling of this surface must be prevented.

Instances came to our attention in which the method, as described by Day and Austin, indicated an austenite grain size much smaller than that revealed by the usual methods and consistent with the response of the steel to heat treatment. This discrepancy led us to make the investigation, described in this paper, which demonstrates that it arose from the fact that ordinary methods of purifying hydrogen do not bring the oxygen pressure down to a level low enough to prevent oxidation of elements such as aluminum at the surface to be examined. In other words, if the grain size observed at the surface is to be that characteristic of the steel as heat treated, the surface metal must remain essentially unaltered during the heating process. When care is taken to insure a low enough oxygen pressure, the heat etching method yields correct results on any steel, as the evidence to be presented demonstrates.

Experimental

The first experiments were made on three samples of S.A.E. 1060 steel, all from a single heat, which happened to be available; they were chosen because they were alike except in aluminum content, as shown in Table I. In order to insure similar initial structure in all three cases, these Steels (1, 2, 3, with 0.005, 0.02, 0.1 per cent aluminum, respectively), in the form of bars 1 inch in diameter and 10 inches long, were heated for 30 minutes at 1625, 1825, 2100 degrees Fahr. (885, 995, 1150 degrees Cent.), respectively, followed by air cooling. The heat etching technique, as described by Day and Austin, was applied to these steels and the result compared with that obtained by the ferrite network method (2, 3). The former indicated no coarsening of Steel 3 after 30 minutes at any temperature up to 2200 degrees Fahr. (1205 degrees Cent.) while the latter showed that extensive coarsening had occurred. A specimen of Steel 3, which had been heat etched at 2200 degrees Fahr. (1205 degrees Cent.) for 30 minutes, and quenched, was tempered in vacuum and polished lightly on a cloth so as to remove the heat etch but not the surface

Table I
Chemical Composition of Steels

Steel Number	Type of Steel	Deoxidizer	Chemical Analyses, Per Cent*				
			Carbon	Manganese	Silicon	Aluminum	Added Alloying Elements
1	S.A.E. 1060	Silicon	0.60	0.89	0.13	0.005	None
2	S.A.E. 1060	Si + 0.5 lb. Al per ton	0.59	0.89	0.15	0.02	None
3	S.A.E. 1060	Si + 2.0 lb. Al per ton	0.59	0.89	0.15	0.1	None
4**	C-0.5% Mo	Silicon + Zirconium	0.20	0.73	0.23	0.004	0.51 Mo
5	0.05% C	Aluminum	0.05	0.34	0.008	0.1	None
6	S.A.E. 1020	Silicon	0.20	0.61	0.23	0.001	None
7	S.A.E. 1020	Silicon + Aluminum	0.20	0.53	0.24	0.03	None
8	1.20% C	Silicon	1.19	0.31	0.25	0.004	None
9	C-0.5% Mo	Silicon + Aluminum	0.12	0.41	0.15	0.03	0.44 Mo
10***	C-0.5% Mo	Aluminum	0.11	0.46	0.02	0.08	0.43 Mo
11***	C-2% Mo	Aluminum	0.13	0.33	0.01	0.05	1.95 Mo
12	Cr-Mo-Si-Al	Silicon + Aluminum	0.07	0.28	1.28	0.6	4.96 Cr, 0.54 Mo, 1.28 Si, 0.6 Al
13	S.A.E. 4815	Silicon	0.16	0.52	0.27	0.006	3.36 Ni, 0.19 Mo
14	S.A.E. 6140	Silicon + Aluminum	0.43	0.74	0.23	0.03	0.92 Cr, 0.16 V
15	13% Cr	Silicon + Aluminum	0.09	0.38	0.36	0.02	12.7 Cr
16	1.25% W	Silicon	0.56	0.19	0.06	0.008	1.28 W

*Phosphorus and sulphur are well within commercial limits. Results for aluminum are to be regarded as relative rather than absolute.
**Steel 4 contains 0.04% zirconium.
***Small experimental heat in laboratory furnace.

grains; upon etching this surface with Vilella reagent (4) (made by dissolving 1 gram of picric acid and 5 milliliters of concentrated hydrochloric acid in 95 milliliters of ethyl alcohol), the austenite grains there were observed to have the same small size as indicated by heat etching, though a cross section of the same specimen showed

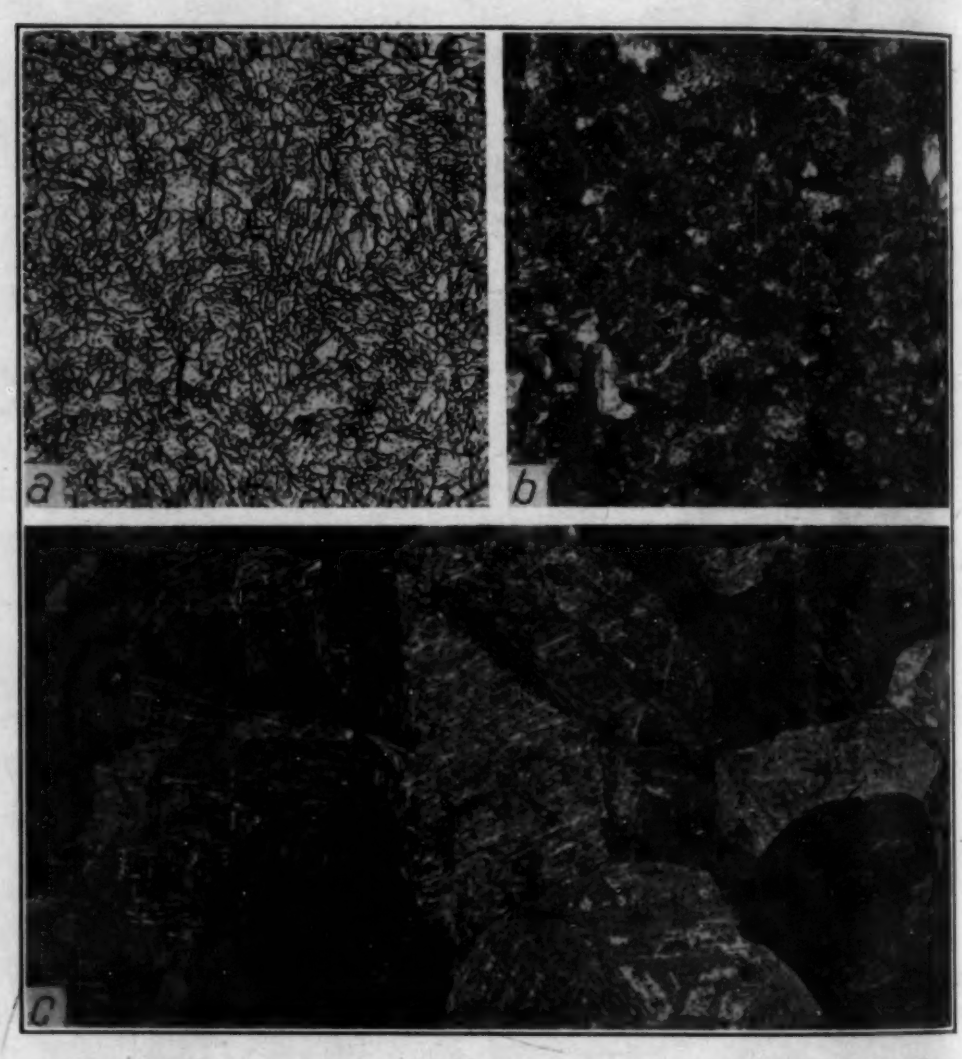

Fig. 1—Austenite Grain Size of Steel 3, S.A.E. 1060 Containing 0.1 Per Cent Aluminum, Heat Etched 30 Minutes at 2200 Degrees Fahr. in Hydrogen Containing Sufficient Oxygen to Retard the Surface Grain Growth. × 100. (a) Heat Etch. (b) Tempered Martensite Etch of Surface Grains. (c) Tempered Martensite Etch of Interior Grains.

large austenite grains in the interior. Photomicrographs of the heat etch, of the tempered martensite etch of the same surface and of the interior of the specimen, are presented in Fig. 1. This same specimen was sectioned at an angle of 5 to 10 degrees to the heat etched surface to determine the depth of the zone of retarded

coarsening, and this sectioned surface was etched with Vilella reagent. The photomicrograph (Fig. 2) shows that the zone of retarded coarsening extended approximately 1 inch from the line corresponding to the original heat etched surface; from the angle of sectioning and the magnification (100 diameters), it is apparent that this zone was about 0.001-inch thick.

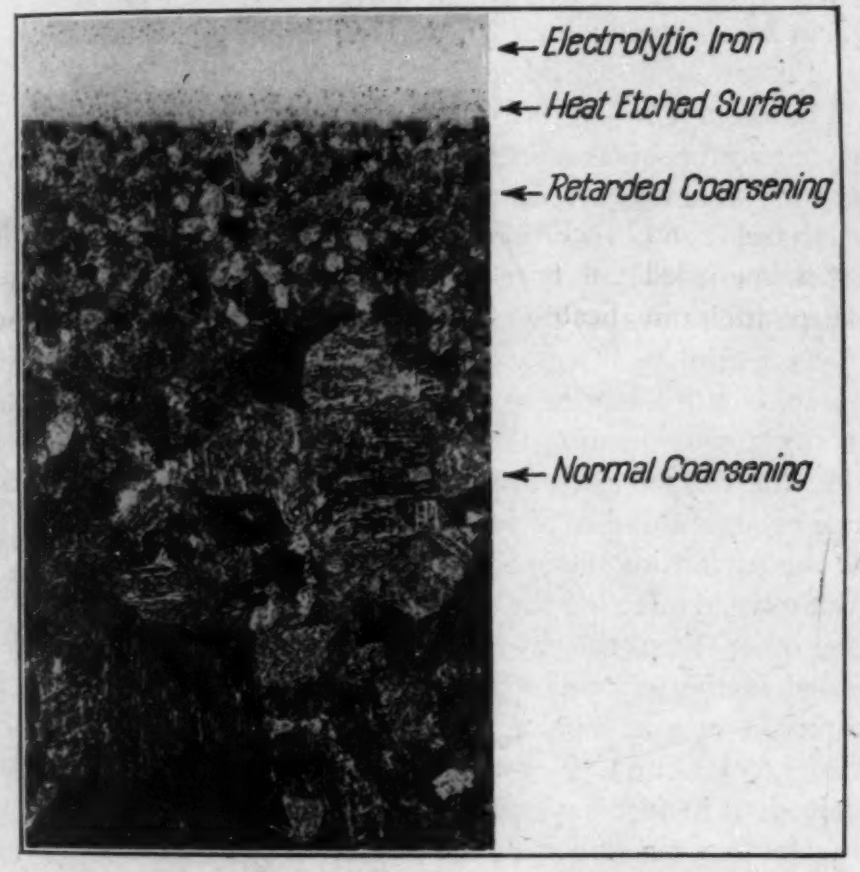

Fig. 2—The Influence of Oxygen in Hydrogen Upon the Austenite Grain Size on and Near the Surface During Heat Etching, 30 Minutes at 2200 Degrees Fahr., Steel 3, S.A.E. 1060 Containing 0.1 Per Cent Aluminum. The Surface Shown is a Cross Section at an Angle of 5 to 10 Degrees to the Original Heat Etched Surface, Tempered Martensite Etch. × 100.

These observations suggested the presence, in the hydrogen in contact with the specimen, of oxygen or oxidizing impurities at a partial pressure large enough to oxidize the aluminum in solid solution at and close to the surface of the steel, producing alumina particles which effectively retarded austenite grain growth at the surface, while the interior of the specimen coarsened in the usual manner. This line of reasoning indicated that the partial pressure of oxygen

in the atmosphere surrounding the specimen in the furnace should be lowered. As a first step in this direction, the hydrogen purification train was rebuilt using new platinized asbestos and desiccants but with a single passage of the hydrogen over the platinized asbestos. Observations on the tarnishing of 18 per cent chromium-8 per cent nickel steel wire heated in a porcelain tube in this hydrogen indicated a much lower equivalent partial pressure of oxygen when the train had been rebuilt; for then at 1300 degrees Fahr. (705 degrees Cent.) this atmosphere did not oxidize this alloy whereas before it did. The occurrence of tarnishing serves as a sensitive and satisfactory indicator of the presence of oxygen at concentrations too small for accurate determination by ordinary methods of gas analysis; and such observations can be used regularly if the specimen is suspended in the furnace by a wire of 18-8. Thermodynamic calculation indicates that hydrogen, purified even by repeated passage over hot platinized asbestos followed each time by phosphorus pentoxide, is still likely to oxidize any aluminum present in solution in the steel; consequently, the most that one can hope to achieve is to bring the oxygen pressure down to a level at which it does not produce enough alumina to influence appreciably the austenite grain size at the surface of the specimen.

But oxygen affecting the surface of the specimen may come from sources other than the hydrogen. For instance, from scale, as illustrated in the photomicrographs compared in Fig. 3; even from the porcelain tube at high temperatures such as 2200 degrees Fahr. (1205 degrees Cent.). For at such temperatures, the silica in the porcelain does in fact have an oxygen pressure high as compared to that of alumina (in line with the relatively poor deoxidizing power of silicon) as shown by Fig. 4 which provides a comparison of the result of heat etching Steel 3 in a porcelain tube and in a sintered pure alumina tube, all other conditions being identical. There is obviously less coarsening in the former (4a) than in the latter (4b). This indicates the advisability of using alumina in place of porcelain for work at high temperatures on steels containing appreciable amounts of aluminum as such.

In any case, the suitability or otherwise of the atmosphere in actual contact with the specimen while it is being heated can be told, after a little experience, by inspection of the polished surface itself. If surface is still bright, the metal has remained unaffected and the atmosphere is suitable for that particular steel; if there is any indica-

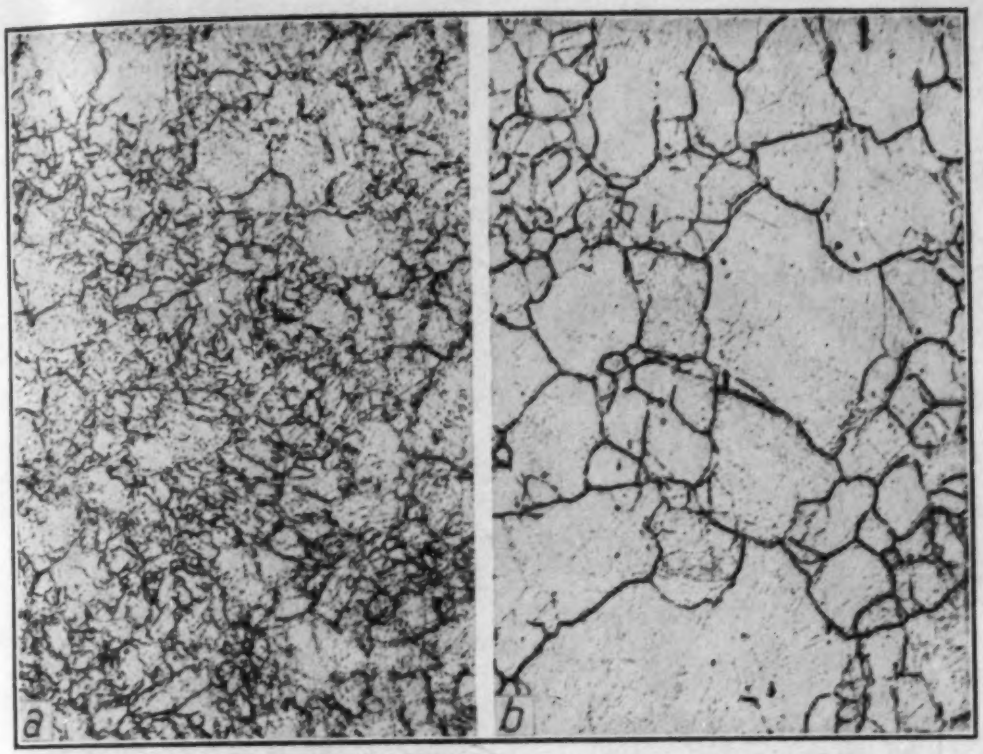

Fig. 3—The Influence of Oxygen from Iron Oxide Upon the Austenite Grain Size Indicated by Heat Etching, 30 Minutes at 2000 Degrees Fahr., Steel 3, S.A.E. 1060 Containing 0.1 Per Cent Aluminum. × 100. (a) Specimen with Mill Scale on Unpolished Side. (b) Scale-Free Specimen.

tion of a bloom or film on the surface, the atmosphere is not low enough in oxidizing power for the steel and temperature concerned.

With these points established, the improved technique was applied successfully to Steels 5 to 16 which cover a wide range of composition and of differences in deoxidation practice, as shown in Table I. The austenite grain size of a cross section of these same specimens was also revealed by tempering and etching with Vilella reagent, which worked well on all of them with the single exception of the plain steel containing less than 0.1 per cent carbon. In this case it was found that etching with a 5 per cent aqueous solution of ferric chloride delineates the austenite grains of untempered or slightly tempered low carbon martensite, with or without a network of ferrite at the boundaries of the prior austenite grains; this procedure was used on Steel 5.

A graphic comparison of the weighted average[2] austenite grain size delineated by the heat etch and tempered martensite etch on the

[2]The derivation and use of this weighted average is discussed later; in any case, the kind of average used does not affect this comparison.

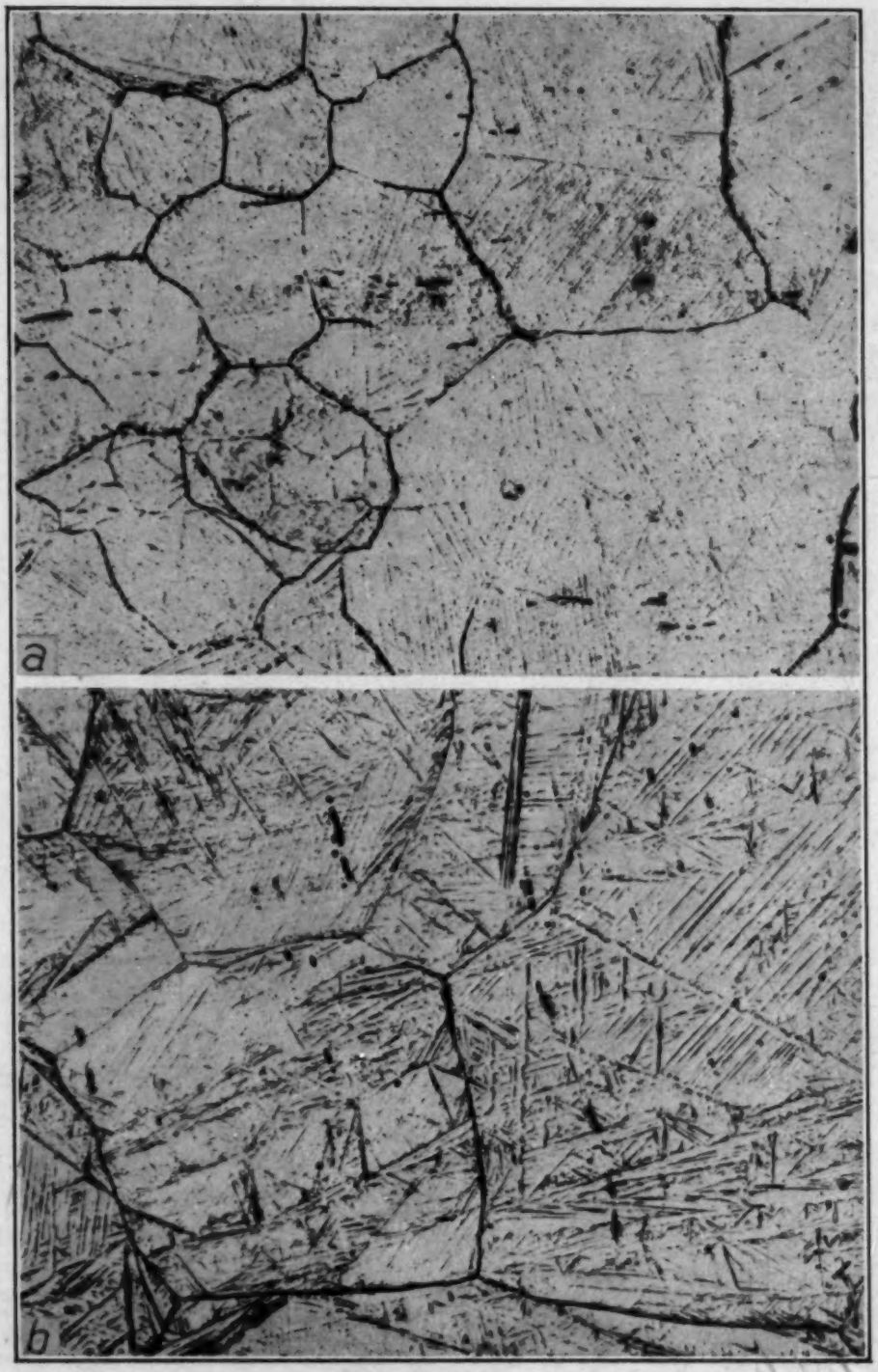

Fig. 4—The Influence of Oxygen from the Refractory Tube Upon the Austenite Grain Size Indicated by Heat Etching, 30 Minutes at 2200 Degrees Fahr., Steel 3, S.A.E. 1060 Containing 0.1 Per Cent Aluminum. × 100. (a) Porcelain Tube. (b) Sintered Pure Alumina Tube.

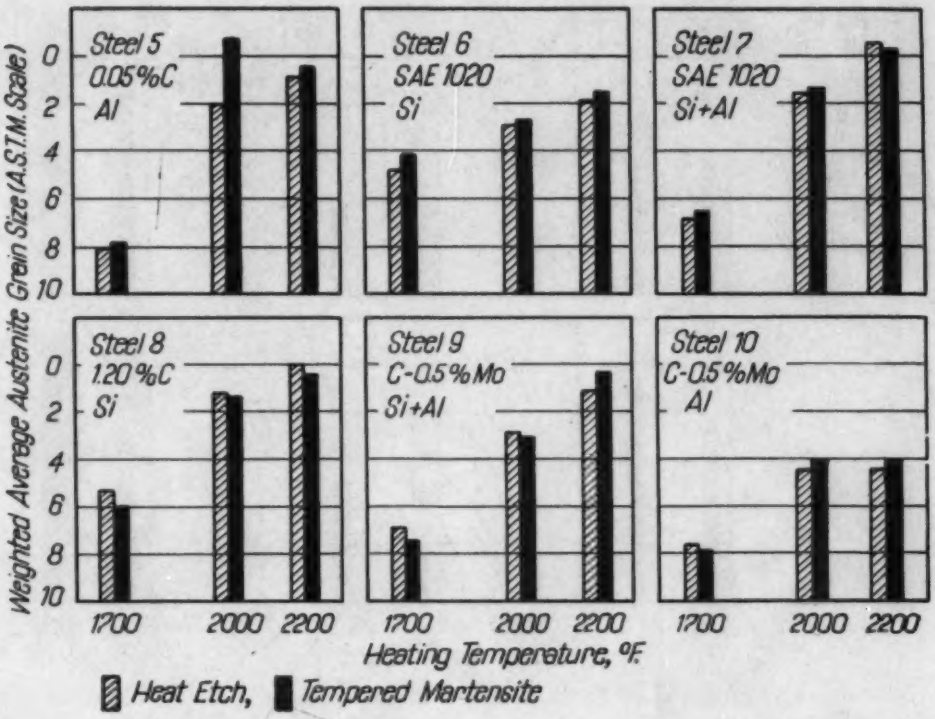

Fig. 5—Comparison of Heat Etch and Tempered Martensite Methods for Determining the Austenite Grain Size of Steels 5, 6, 7, 8, 9 and 10. The Type of Steel and Added Deoxidizers are Indicated on Each Graph. All Specimens Were at Temperature for 30 Minutes.

steels which had been heated for 30 minutes at a temperature of 1700, 2000, or 2200 degrees Fahr. (925, 1095, 1205 degrees Cent.) is presented in Figs. 5 and 6 for Steels 5 to 16. The agreement between the two methods is excellent and more than sufficient for all practical purposes. Photomicrographs illustrating this close agreement between the two methods are presented in Figs. 7, 8 and 9 for three of these steels.

The composition of Steels 12 and 15 is such that they are not entirely austenitic at any of the heat treating temperatures which were employed, and therefore do not show the usual increase in austenite grain size with temperature. The percentage of ferrite was appreciable at 1700 degrees Fahr. (925 degrees Cent.), almost zero at 2000 degrees Fahr. (1095 degrees Cent.), and high at 2200 degrees Fahr. (1205 degrees Cent.) where there was so much of it that the austenite grains appeared more or less as islands in a sea of ferrite. Obviously, no appreciable coarsening of austenite grains is likely to occur under the conditions which existed at 2200 degrees Fahr. (1205 degrees Cent.).

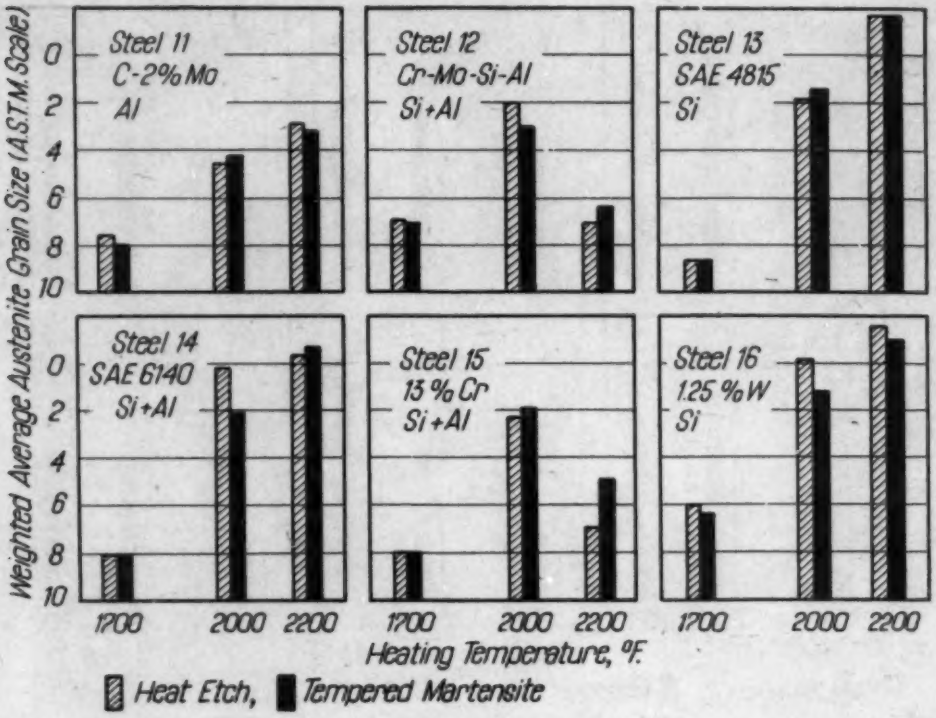

Fig. 6—Comparison of Heat Etch and Tempered Martensite Methods for Determining the Austenite Grain Size of Steels 11, 12, 13, 14, 15 and 16. The Type of Steel and Added Deoxidizers are Indicated on Each Graph. All Specimens Were at Temperature for 30 Minutes.

As an illustration of what may happen if the atmosphere is not sufficiently oxygen-free, let us revert to Steels 1, 2, 3 (S.A.E. 1060 with increasing amounts of residual aluminum) and compare the results of the tempered martensite etch or ferrite network method with those of the heat etch done both under proper conditions and otherwise. These results are plotted as weighted average austenite grain size against heating temperature, the time being always 30 minutes, in Fig. 10. Curve A shows that when the atmosphere is low enough in oxidizing power, all three methods give identical results over the whole temperature range. Curve B shows that a porcelain tube, though all right for Steel 2 (0.02 per cent aluminum) is unsatisfactory for Steel 3 (0.1 per cent aluminum). Curve C shows the delay of coarsening caused by the presence of some scale on the specimens of Steels 2 and 3; Curve D the still greater delay produced by scale in presence of insufficiently purified hydrogen, this delay being greater the higher the residual aluminum. In all cases, the grain size of a cross section of the specimen falls on Curve A. If the concentration of oxygen is great enough, it may even affect the superficial grain

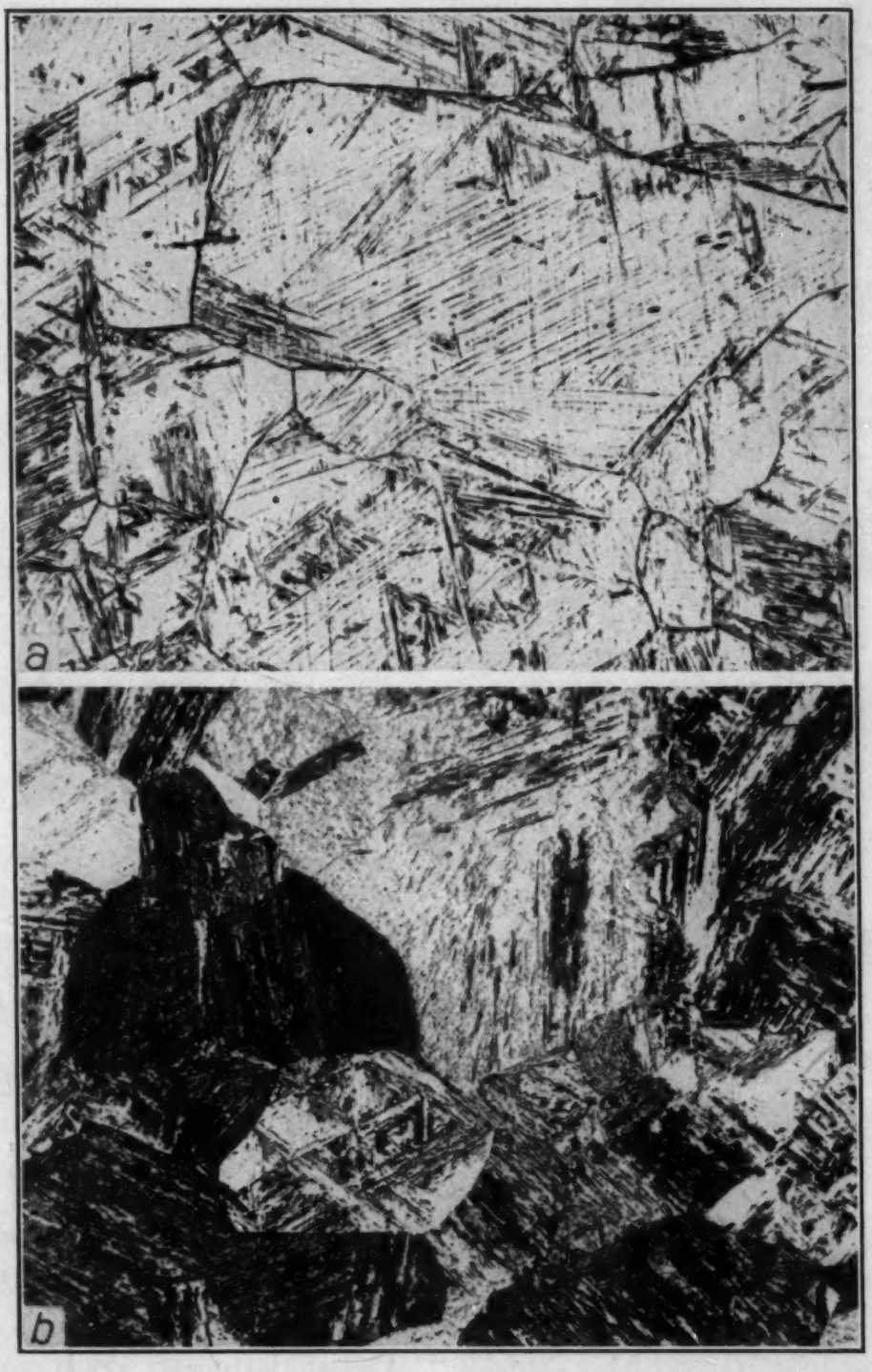

Fig. 7—Austenite Grain Size of Steel 7, S.A.E. 1020 Containing 0.03 Per Cent Aluminum, 30 Minutes at 2200 Degrees Fahr. × 100. (a) Heat Etch. (b) Tempered Martensite Etch.

size of a steel containing silicon but very little aluminum, as illustrated by Curve D for Steel 1, and by the difference between Fig.

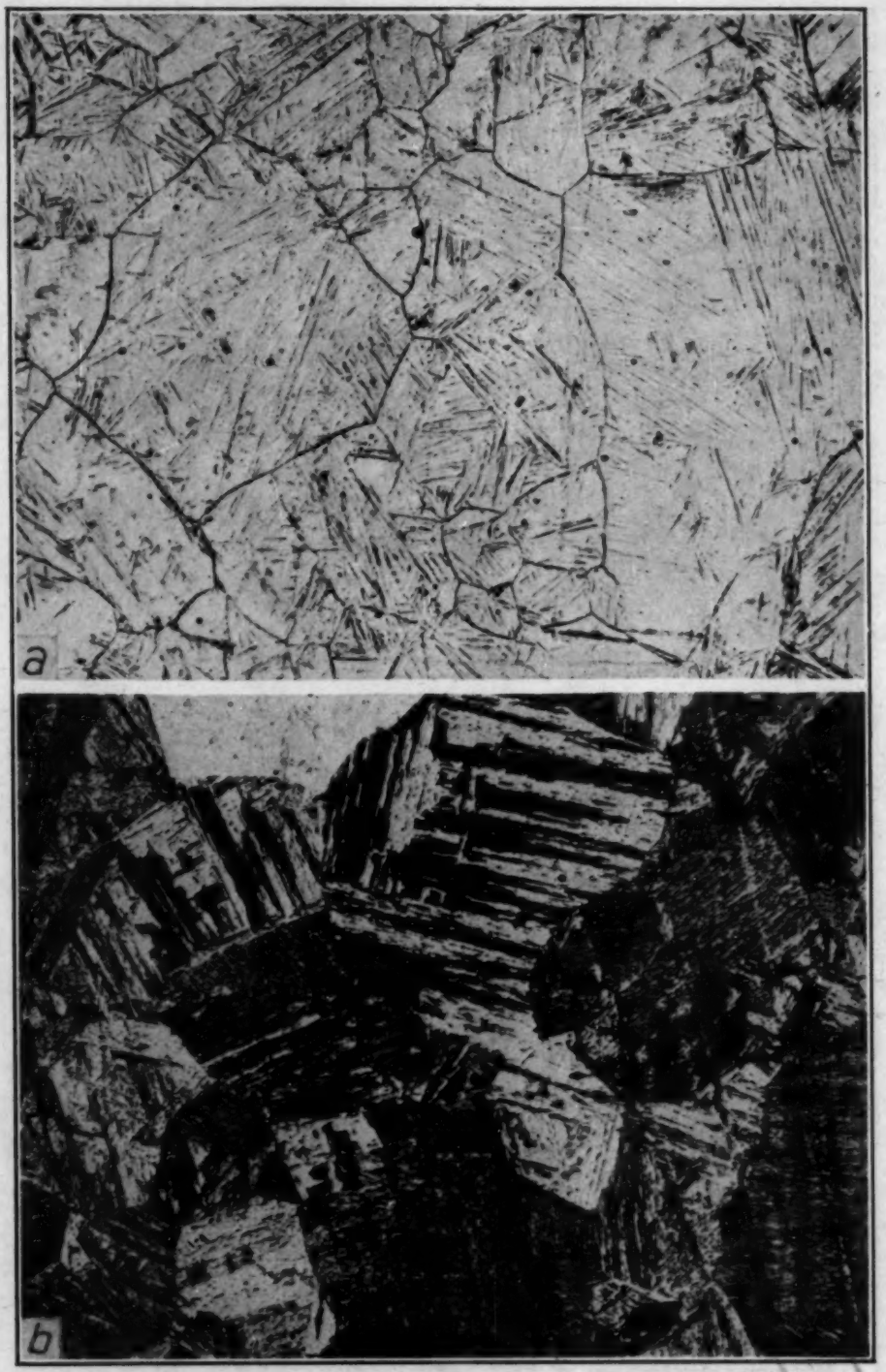

Fig. 8—Austenite Grain Size of Steel 9, Carbon-0.5 Per Cent Molybdenum Steel Containing 0.03 Per Cent Aluminum, 30 Minutes at 2200 Degrees Fahr. × 100. (a) Heat Etch. (b) Tempered Martensite Etch.

11a and 11b or 11c. An analogous comparison for Steel 3 is illustrated in Fig. 12.

Fig. 9—Austenite Grain Size of Steel 14, S.A.E. 6140 Containing 0.03 Per Cent Aluminum, 30 Minutes at 2200 Degrees Fahr. × 100. (a) Heat Etch. (b) Tempered Martensite Etch.

The behavior of Steel 4, which contains 0.04 per cent zirconium, shows that residual zirconium reacts with oxygen in much the same

way as aluminum; after being heated in an improper atmosphere the difference in grain size between surface and interior was unmistakable though less marked than in Steel 2 when it was treated similarly.

All of these observations corroborate the belief that dispersed

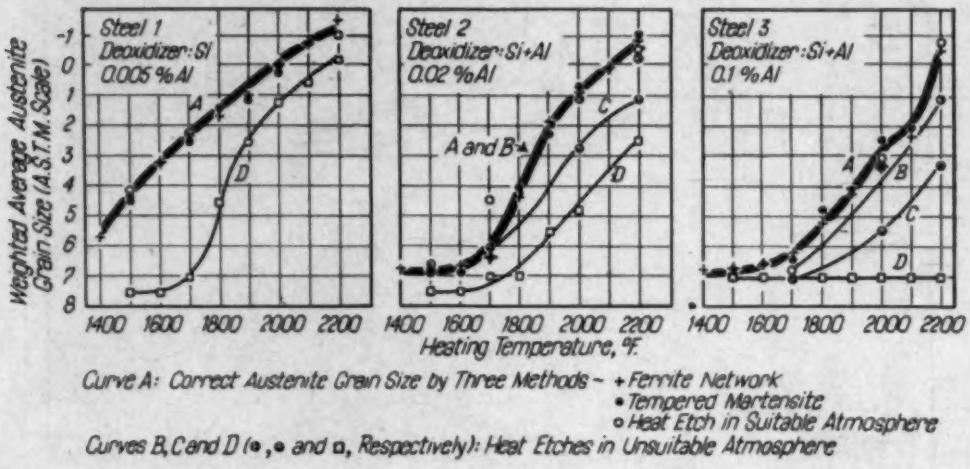

Fig. 10—Austenite Grain Size of Steels 1, 2 and 3, S.A.E. 1060. Curve A Represents the Correct Austenite Grain Size by Ferrite Network Method, Tempered Martensite Method, and Heat Etching in Hydrogen of Sufficient Purity for Good Results. Curves B, C, and D Represent the Austenite Grain Size by Heat Etching in Hydrogen Containing Too Much Oxygen for Good Results. The Oxygen Pressure Increases from B to D. All Specimens Were at Temperature for 30 Minutes.

alumina particles, rather than aluminum or oxygen in solid solution, are the effective agent in retarding grain growth. For so long as oxidation of the aluminum is prevented, there is no difference in grain size at any temperature between surface and interior; but as soon as oxidation begins at the surface, grain growth is retarded there. That oxygen is not itself the effective agent is evident from the observation that, when exposed to the same atmosphere capable of oxidizing aluminum but not iron, surface coarsening is retarded more as the aluminum content is greater.

Re-examination of the steels used by Day and Austin showed that all contained less than 0.01 per cent aluminum. That they observed no discrepancy between the results of heat etching and of the other methods is due to this low content of aluminum and to the fact that the oxygen pressure of the heating atmosphere was low enough.

All of this emphasizes the necessity of insuring that the procedure used to develop the grain pattern does not of itself alter the metal at the surface which is to be examined. Usually any such altera-

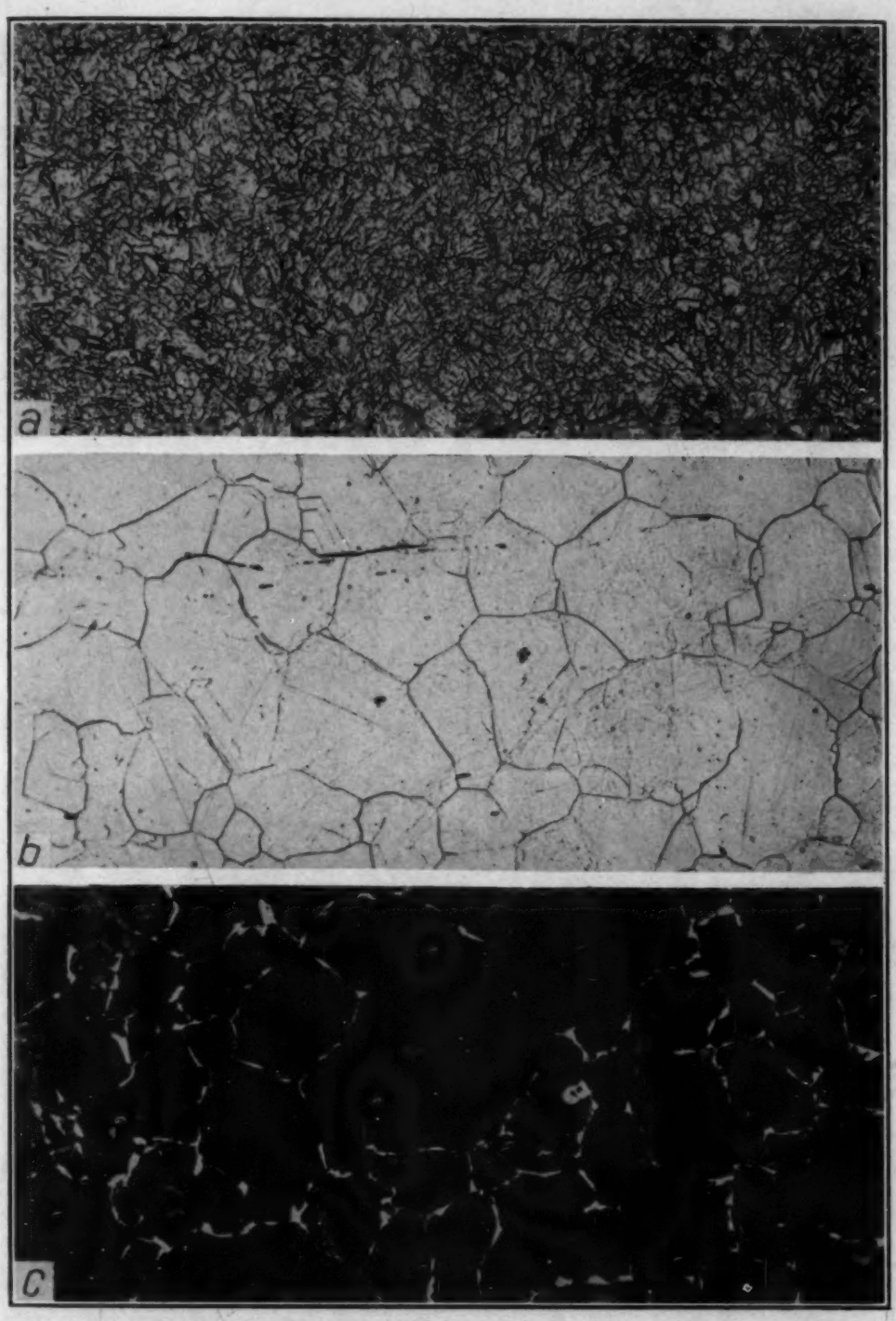

Fig. 11—Austenite Grain Size of Steel 1, S.A.E. 1060 Containing 0.13 Per Cent Silicon and 0.005 Per Cent Aluminum, 30 Minutes at 1700 Degrees Fahr. × 100. (a) Heat Etch in Hydrogen Containing Enough Oxygen to Retard the Grain Growth. (b) Heat Etch in Hydrogen of Sufficient Purity for Good Results. (c) Ferrite Network.

tion will not extend far below the surface exposed during heat treatment. The carburizing, oxidation and heat etching methods are, how-

Fig. 12—Austenite Grain Size of Steel 3, S.A.E. 1060 Containing 0.1 Per Cent Aluminum, 30 Minutes at 2200 Degrees Fahr. × 100. (a) Heat Etch in Hydrogen Containing Enough Oxygen to Retard the Grain Growth. (b) Heat Etch in Hydrogen of Sufficient Purity for Good Results. (c) Ferrite Network.

ever, concerned with the austenite grain size at or near the surface which was exposed during heat treatment. In carburized specimens it

is not unusual to find austenite grains in the case much finer than in the core; whether this is caused by the carbon or the oxygen which diffuse in from the surface, or by both, the grain size observed is influenced by this chemical action as well as by the thermal treatment. In the oxidation method (5) oxygen is required and some chemical alteration of the surface is unavoidable; consequently, this method cannot be expected always to delineate the true austenite grain size of the specimen as a whole, especially at higher heat treating temperatures. Heat etching differs from the carburizing and oxidation methods in that no chemical alteration of the surface is needed to delineate the grain boundaries; in fact, one of the first requirements established for the thermal treatment of heat etched specimens was that oxidation, deoxidation, carburization and decarburization must be avoided. Of these reactions, oxidation is the only one which shows any appreciable tendency to occur during heat etching and it is reduced to a negligible quantity when the oxygen pressure of the hydrogen is sufficiently low.

Weighted Average Grain Size

All measurements of austenite grain size were made on the scale of the American Society for Testing Materials (6) by estimating the percentage of the area covered by the grains of each size; typical examples of measurements when several distinct sizes were present are:

(a) 10 per cent No. 3; 40 per cent No. 4; 30 per cent No. 5; 20 per per cent No. 6
(b) 10 per cent No. 1; 20 per cent No. 2; 5 per cent No. 3 and 35 per cent No. 6; 30 per cent No. 7

Steels which coarsen gradually with increase of temperature, and the wholly fine or coarse zones of those which coarsen abruptly, are similar to (a) in which the sizes of the grains are not widely different. On the other hand, for a steel which coarsens abruptly with increase of temperature, the grain size picture in the zone of abrupt coarsening is similar to (b) in which two ranges of widely different sizes of grains are present.

Such results cannot be presented graphically in this form, and when recorded in tables they present a serious problem to the reader who tries to compare them or to follow trends. For this reason the data on austenite grain size in this paper are presented graphically as a weighted average for each specimen. This procedure is unques-

tionable for cases such as (a) where the range of austenite grain size is not great and the weighted average is really a mean grain size, and particularly where, as in this paper, comparison is nearly always between two very similar distributions. We are, however, well aware that this is a questionable procedure in cases such as (b) where the weighted average may prove to be a size that is not actually present in the steel; yet we believe that in this paper it is not only permissible, but desirable for several reasons. First, the graphical presentation makes it far easier for the reader to grasp the results. Second, a relatively small number of the measurements are of the type (b). For comparison with Figs. 5 and 10, the range and weighted average value for all measurements of the type (b) determined by the ferrite network, tempered martensite, and the correct heat etching methods are presented in Table II. It may be observed that both the range and the weighted average indicate quite close agreement between the three methods. A few measurements of austenite grain size, after heat etching in an unsuitable atmosphere, which were used in Curves B, C, and D in Fig. 10, are of the type (b), but they are not included in Table II; here again the weighted average indicates the same trend as the range.

We wish to emphasize again that the weighted average method of reporting measurements similar to (b) is not desirable for any purpose other than to show trends in austenite grain coarsening or to compare results of several methods in good agreement. A weighted average of measurements such as (b) should under no circumstances be used for relating austenite grain size to hardenability and the mechanical properties of steel. The reason for this is obvious: if a steel contains 50 per cent No. 1 and 50 per cent No. 7 austenite grains, the weighted average is No. 4, yet its hardenability and mechanical properties cannot be expected to be those characteristic of a steel made up of No. 4 grains.

To calculate the weighted average, multiply the fractional part of the total area by the grain size number (A.S.T.M.), repeat this for each grain size, add the products algebraically; the sum is the weighted average grain size. For the grain sizes designated as 00, 000, 0000 by the American Society for Testing Materials, —1, —2, —3, respectively, are used. This is a logical modification because the scale is really logarithmic (to base 2) and negative numbers must be used not only in calculating the weighted average grain size but also in considering the basic relation between these grain size numbers and

Table II

Comparison of Specimens Containing Two Ranges of Widely Different Sizes of Austenite Grains as Revealed By Three Methods

Steel Number	Heating* Temperature Degrees Fahr.	Range of Austenite Grain Size			Weighted Average Austenite Grain Size		
		Ferrite Network	Tempered Martensite	Heat Etching**	Ferrite Network	Tempered Martensite	Heat Etching**
2	1600	2 to 4 and 6 to 8	5 to 8	....	6.7	6.9	...
2	1700	1 to 4 and 6 to 8	2 to 3 and 5 to 8	1 to 3 and 5 to 8	6.4	6.4	4.5
2	1800	1 to 3 and 5 to 7	1 to 3 and 5 to 7	....	4.4	4.1	...
3	1700	1 to 4 and 6 to 8	2 to 4 and 6 to 8	4 and 6 to 8	6.2	6.4	6.8
3	1800	0 to 3 and 6 to 8	0 to 3 and 6 to 8	....	5.2	4.7	...
3	1900	0 to 3 and 6 to 8	0 to 3 and 6 to 8	....	4.2	4.1	...
3	2000	1 to 4 and 6 to 7	0 to 3 and 6 to 8	0 to 5	3.3	2.4	3.0
7	1700	....	1 to 4 and 7 to 8	2 to 3 and 7 to 8	...	6.5	6.6

*All specimens were at temperature for 30 minutes.
**The heat etching was done in hydrogen of sufficient purity for good results.

the mean number of grains per square inch (7). An example of the calculation of weighted average grain size may be cited where negative numbers are involved: a specimen contains 20 per cent No. (−2); 30 per cent No. (−1); 40 per cent No. 0; 10 per cent No. 1 grains. Multiplying, we have $0.2 \times (-2) = -0.4$; $0.3 \times (-1) = -0.3$; $0.4 \times 0 = 0$; $0.1 \times 1 = 0.1$; the algebraic sum of the products is −0.6 which is the weighted average grain size. Unpub-

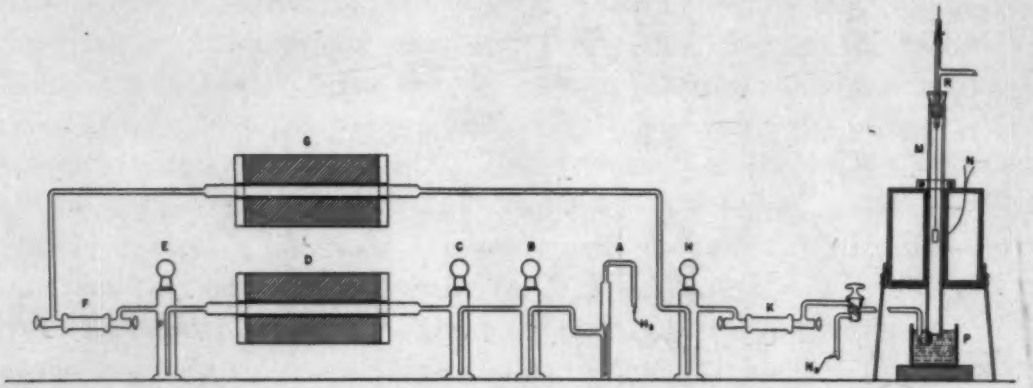

Fig. 13—Hydrogen Purification Train and Heat Treating Furnace for Heat Etching.

lished data show that in measuring grain size, different observers, and the same observer on different days, usually agree on the weighted average value within plus or minus 0.5 grain size number (A.S.T.M.).

Recommended Procedure

The apparatus is the same as that described by Day and Austin except for two modifications: the hydrogen should preferably be passed through a second purifying treatment, and the porcelain tube which was used previously for the heating chamber should be replaced by a tube of sintered pure alumina free from less stable oxides. The double purification of the hydrogen is suggested because experimental indications are that after a single purification the oxygen pressure in the hydrogen is too near the borderline for safety, especially for steels containing sizable amounts of residual aluminum. Nevertheless, a single purifying train suffices for many steels provided that the tank hydrogen contains not more than 0.1 per cent oxygen.

Fig. 13 is a diagrammatic sketch of the apparatus. Hydrogen of commercial cylinder quality passes through sulphuric acid (A), soda lime (B) and Drierite (C) for preliminary drying and removal of

carbon dioxide; then over a catalyst of platinized asbestos (D) at 1000 degrees Fahr. (540 degrees Cent.) to convert much of the oxygen present to water vapor which is absorbed subsequently by activated alumina (E) and phosphorus pentoxide (F). To effect the double purification the hydrogen is passed over a second catalyst (G) and again dried with alumina (H) and phosphorus pentoxide (K). The sintered alumina tube (M) is placed in a platinum wound furnace whose temperature is controlled by means of a thermocouple (N) and appropriate equipment. The lower end of this tube is sealed by immersion in the water-cooled mercury quenching bath (P), which arrangement also permits the introduction of purified hydrogen through pyrex tubing from the purification train; its upper end is fitted with a rubber stopper (R) or a suitable cap, a convenient means of support for the specimen, and an escape for the gas.

When an atmosphere of hydrogen exceedingly low in oxygen pressure is desired, it is necessary to select for the heating chamber a refractory oxide that will not be reduced by the gas. This requirement is met satisfactorily by a sintered pure alumina tube; less stable oxides, such as silica, are reduced by hydrogen at elevated temperatures, particularly in the presence of iron vapor. Silica, porcelain, and even glass are not reduced readily at lower temperatures, so that they may be used if the specimen is heated by induction. In fact, a fused silica tube and induction heating were used successfully during a period when a sintered pure alumina tube was not available; adaptation of the apparatus in Fig. 13 to induction heating presents no serious problems.

The procedure followed in heating and quenching austenite grain size specimens is the same as described in the earlier paper. In practice the period required between specimens is reduced to a minimum by maintaining at all times a hydrogen atmosphere in the furnace. This requires that the specimen be introduced through a gas lock, or by accelerating the flow of hydrogen through the furnace so that the upper end of the tube can be opened and closed without danger of explosion. Before the specimen is lowered into the heating zone, sufficient time is allowed to free the furnace of the traces of oxygen which entered when the specimen was introduced. The specimen is suspended by a wire unhardenable by rapid cooling, such as iron or 18 per cent chromium-8 per cent nickel steel; this facilitates its removal from the mercury bath after quenching without need of opening the furnace. In order to avoid the danger of an explosion at

high temperature when the tube is filled with air, flush and fill with nitrogen before admitting hydrogen and use nitrogen in an equivalent way when going from hydrogen to air. Hydrogen may directly follow or precede air if the tube is at room temperature.

For good results from heat etching, it is necessary to prepare the specimen so that it is entirely free from iron oxide in any form.

Summary

1. Heat etching accurately delineates the austenite grains actually present at the surface of the heat treated specimen. These grains are of the same size as those in the interior of a specimen provided that during the heat treatment the austenite grain coarsening behavior of the metal at the surface has not been altered by chemical reaction with the furnace atmosphere.

2. If the partial pressure of oxygen in the atmosphere during heat treatment is not low enough, aluminum, or other deoxidizing metal, is oxidized at the surface in such quantity that its oxide is effective in retarding austenite grain growth at the surface long after the remainder of the specimen has coarsened. In one instance where a steel containing 0.1 per cent aluminum had been heat treated for 30 minutes at 2200 degrees Fahr. (1205 degrees Cent.), the depth of the zone of retarded coarsening was approximately 0.001 inch.

3. Heat etching properly carried out indicates successfully and accurately the austenite grain size of any steel. This implies that the hydrogen be purified sufficiently and maintained in this condition in the heat treating furnace. This is achieved by the use of a hydrogen purification train in good condition, removal of all visible scale and oxides from the surface of the specimen, and the use of a sintered pure alumina tube for enclosing the hydrogen and specimen in the furnace. A silica tube may be used if induction heating is employed.

Acknowledgments

We wish to express appreciation for assistance from associates at the Research Laboratory of the United States Steel Corporation. The assistance of Messrs. E. T. Gioia and R. T. Davis, Jr., has been most helpful. The helpful interest of Messrs. J. B. Austin, E. S. Davenport, John Johnston, R. P. Smith and J. R. Vilella is acknowledged gratefully.

Bibliography

1. M. J. Day and J. B. Austin, "Heat Etching as a Means of Revealing Austenite Grain Size," TRANSACTIONS, American Society for Metals, Vol. 28, 1940, p. 354.
2. J. R. Vilella, "The Grain Size of Steel," *Mechanical Enginering,* Vol. 62, 1940, p. 293.
3. N. F. Ward and J. E. Dorn, "Grain Size of Steel: A Critical Review," *Metals and Alloys,* Vol. 10, 1939, p. 74, 115, 212, 246.
4. E. C. Bain and J. R. Vilella, "Austenite Grain Size in Steel," METALS HANDBOOK, American Society for Metals, 1939, p. 754.
5. Harry Tobin and Reid L. Kenyon, "Austenite Grain Size of Eutectoid Steel," TRANSACTIONS, American Society for Metals, Vol. 26, 1938, p. 133.
6. "Austenite Grain Size in Steels," *Standards,* Part I, Metals, American Society for Testing Materials, 1939, p. 1175.
7. J. J. B. Rutherford, R. H. Aborn and E. C. Bain, "The Relation Between the Grain Areas on a Plane Section and the Grain Size of a Metal," *Metals and Alloys,* Vol. 8, 1937, p. 345.

DISCUSSION

Written Discussion: By Harry Tobin and Reid L. Kenyon, research laboratory, American Rolling Mill Co., Middletown, O.

The studies reported by these authors are further evidence of the continued interest in developing improved methods for determining the austenite grain size of steels. While the method they described doubtless has some application in laboratory studies, it does not appear to be suitable for studies of large sections of forgings as processed in actual operations. This is often of considerable importance and is possible by the oxidation method, which was the subject of a study made by us several years ago, and reported before the American Society for Metals in a paper at the 1937 Annual Meeting.

One of the interesting things brought out by the authors is the evidence as shown in their Fig. 2 of the formation in some steels of a very thin layer of fine grains on the surface when subjected to oxidizing conditions. With the technique that they have employed, this would naturally affect the results of any attempt to estimate the grain size from a study of the extreme surface grains, inasmuch as it is their practice to polish very lightly so as to remove the heat etch but not the surface grains.

The authors mention this as a factor affecting the results obtained by the method described in our 1937 paper, but we would like to call their attention to the difference in our polishing technique as compared with theirs. In their Fig. 2 the depth of the fine-grained layer is approximately 0.001 inch whereas in our practice we always remove many times this much metal from the surface, in many cases as much as $\frac{1}{32}$ inch. This depends, of course, on the time and temperature at which the material has been heated.

Evidence was given in the previous paper already referred to that the oxide penetration method gave an accurate indication of the size of the grains, not only near the surface, but in the interior of the metal.

Further evidence that the surface oxidation method gives accurate indications of austenite grain size are furnished by the accompanying micrographs. Pieces of half-inch round bar of two different steels were heated 30 minutes at 1600, 1800 and 2000 degrees Fahr. (870, 980 and 1095 degrees Cent.). Duplicate pieces were treated in each case, one of which was slow-cooled and the other quenched in a brine solution. It will be seen from the following analysis that Steel A was fine-grained, while Steel B was not.

	Steel A Per Cent	Steel B Per Cent
Carbon	0.60	0.46
Manganese	0.63	0.70
Aluminum	0.071	0.005

Figs. A and B show the two samples of the fine-grained steel after heating 30 minutes at 1600 degrees Fahr. (870 degrees Cent.). Although the pearlitic structure of the slow-cooled sample is slightly banded, it is easily seen that the grain size is comparable to that shown in the martensitic structure outlined by the oxide films around the grain boundaries in the companion sample. The pearlitic structure is that shown on a section taken through the middle of the specimen, far removed from any surface oxidation condition, while the microstructure of the other specimen was taken just under the surface as described in our previous paper.

Figs. C and D show a similar comparison of the two specimens heated 30 minutes at 1800 degrees Fahr. (980 degrees Cent.). Here again the pearlitic structure was that shown on a sample polished through the middle of the half-inch bar and the martensitic structure outlined by oxide films around the grain boundaries was developed just under the surface by polishing away the excessive oxidation after the sample was quenched. Some of the pits are still visible in certain portions of this micrograph.

Figs. E and F in a like manner show the comparison of the companion sample heated 30 minutes at 2000 degrees Fahr. (1095 degrees Cent.), and here again the grain size developed on the two pieces is closely comparable.

A similar series of micrographs is shown for the somewhat lower carbon steel which was not fine-grained. Figs. G and H illustrate the appearance of the two samples heated 30 minutes at 1600 degrees Fahr. (870 degrees Cent.), Figs. I and J the two samples heated 30 minutes at 1800 degrees Fahr. (980 degrees Cent.), and Figs. K and L the two samples heated 30 minutes at 2000 degrees Fahr. (1095 degrees Cent.). In all cases the grain size indicated by the two procedures is practically identical.

The oxidation method has been used in our laboratory for several years now, and in no case has it failed to show the austenite grain size developed in the interior of the specimen by other suitable means. It is important, however, to grind down the surface far enough to remove any severely decarburized material, but not far enough to remove all of the oxide penetration around the grains. This can best be done by polishing on a slight taper similar to the way in which the authors of this paper have done, and as described in our paper of 1937, choosing for grain size estimation a portion which has been ground down to the proper degree as judged by the oxide films around the grain boundaries of quenched steels or the ferrite boundaries of pearlitic steels.

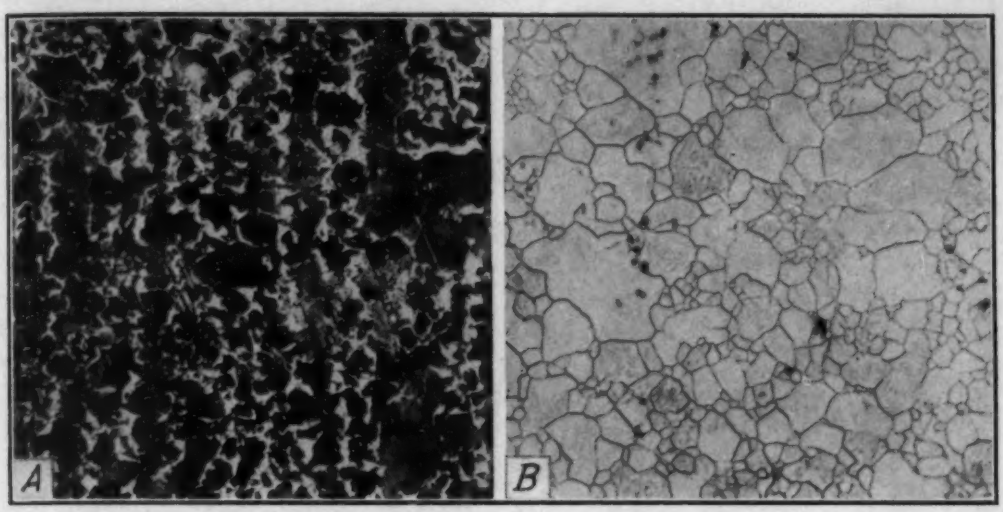

Figs. A and B—Austenitic Grain Size of Two Samples From Steel A After Heating 30 Minutes at 1600 Degrees Fahr. × 100.

(A) M-24568—Pearlitic Structure of Slow Cooled Sample Polished Through the Middle of the Half-Inch Bar and Showing the Austenitic Grain Size Outlined by the Ferrite. Etched With Nital.

(B) M-24567—Martensitic Structure of Quenched Companion Sample Polished Somewhat Under the Surface and Showing the Austenitic Grain Size Outlined by the Oxide Films. Etched With 15 Per Cent HCl in Ethyl Alcohol.

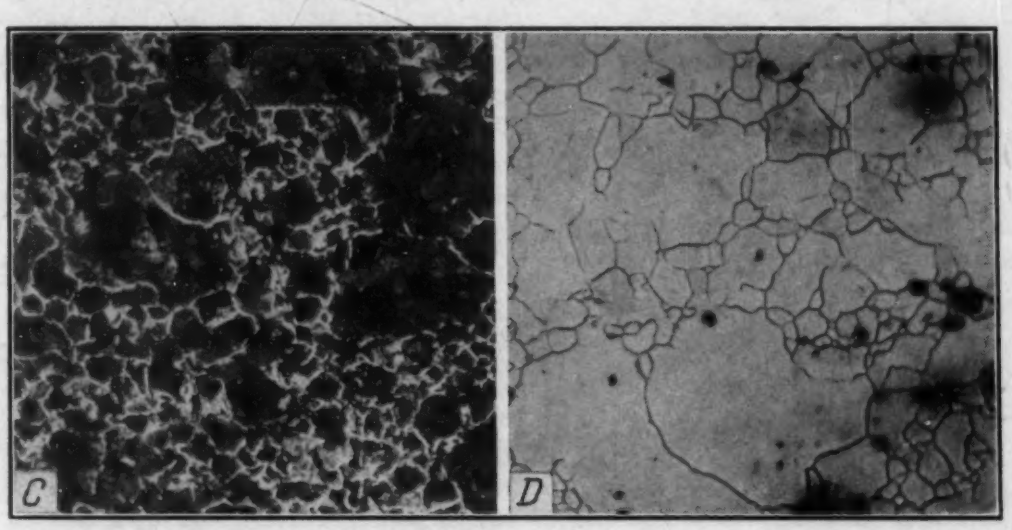

Figs. C and D—Austenitic Grain Size of Two Samples From Steel A After Heating 30 Minutes at 1800 Degrees Fahr. × 100.

(C) M-24572—Pearlitic Structure of Slow Cooled Sample Polished Through the Middle of the Half-Inch Bar and Showing the Austenitic Grain Size Outlined by the Ferrite. Etched With Nital.

(D) M-24571—Martensitic Structure of Quenched Companion Sample Polished Somewhat Under the Surface Showing the Austenitic Grain Size Outlined by the Oxide Films. Etched With 15 Per Cent HCl in Ethyl Alcohol.

In conclusion, we would like to point out that the method which we have described does not require any special equipment, such as a hydrogen purifying train and special furnace, and furthermore, it is applicable to pieces of any size, such as forgings that have been produced in regular mill operations. As a

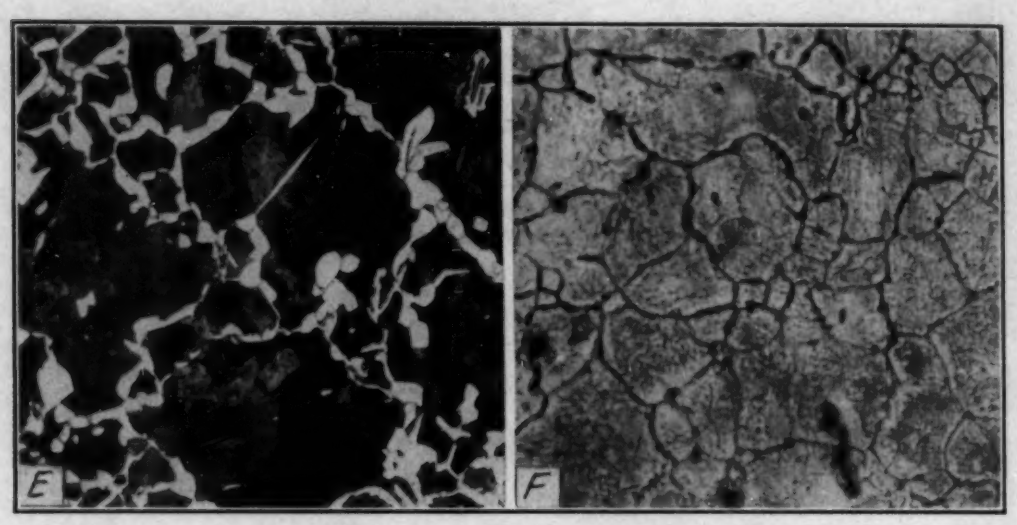

Figs. E and F—Austenitic Grain Size of Two Samples From Steel A After Heating 30 Minutes at 2000 Degrees Fahr. × 100.

(E) M-24575—Pearlitic Structure of Slow Cooled Sample Polished Through the Middle of the Half-Inch Bar and Showing the Austenitic Grain Size Outlined by the Ferrite. Etched With Nital.

(F) M-24576—Martensitic Structure of Quenched Companion Sample Polished Somewhat Under the Surface Showing the Austenitic Grain Size Outlined by the Oxide Films. Etched With 15 Per Cent HCl in Ethyl Alcohol.

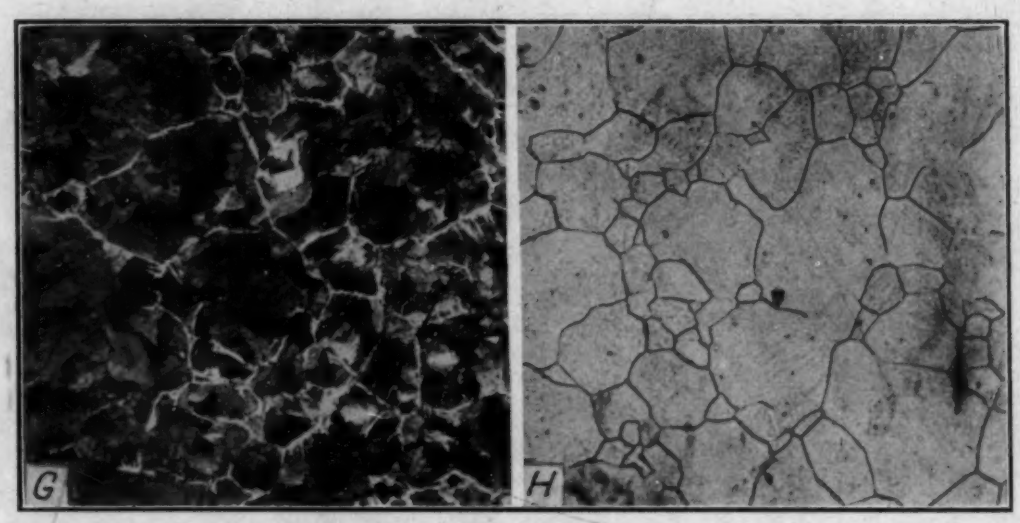

Figs. G and H—Austenitic Grain Size of Two Samples From Steel B After Heating 30 Minutes at 1600 Degrees Fahr. × 100.

(G) M-24570—Pearlitic Structure of Slow Cooled Sample Polished Through the Middle of the Half-Inch Bar and Showing the Austenitic Grain Size Outlined by the Ferrite. Etched With Nital.

(H) M-24569—Martensitic Structure of Quenched Companion Sample Polished Somewhat Under the Surface Showing the Austenitic Grain Size Outlined by the Oxide Films. Etched With 15 Per Cent HCl in Ethyl Alcohol.

matter of fact, any piece which has been heated under oxidizing conditions sufficient to produce a surface scale, can be polished with proper technique in such a way that the oxide penetration around the austenite grain boundaries can be developed, and thus the effect of the previous treatment determined.

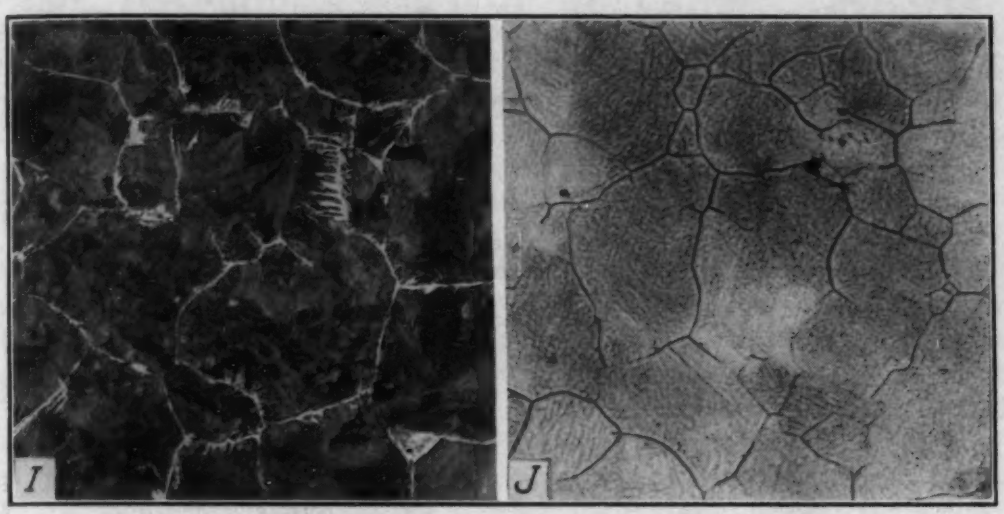

Figs. I and J—Austenitic Grain Size of Two Samples From Steel B After Heating 30 Minutes at 1800 Degrees Fahr. × 100.

(I) M-24573—Pearlitic Structure of Slow Cooled Sample Polished Through the Middle of the Half-Inch Bar and Showing the Austenitic Grain Size Outlined by the Ferrite. Etched With Nital.

(J) M-24574—Martensitic Structure of Quenched Companion Sample Polished Somewhat Under the Surface Showing the Austenitic Grain Size Outlined by the Oxide Films. Etched With 15 Per Cent HCl in Ethyl Alcohol.

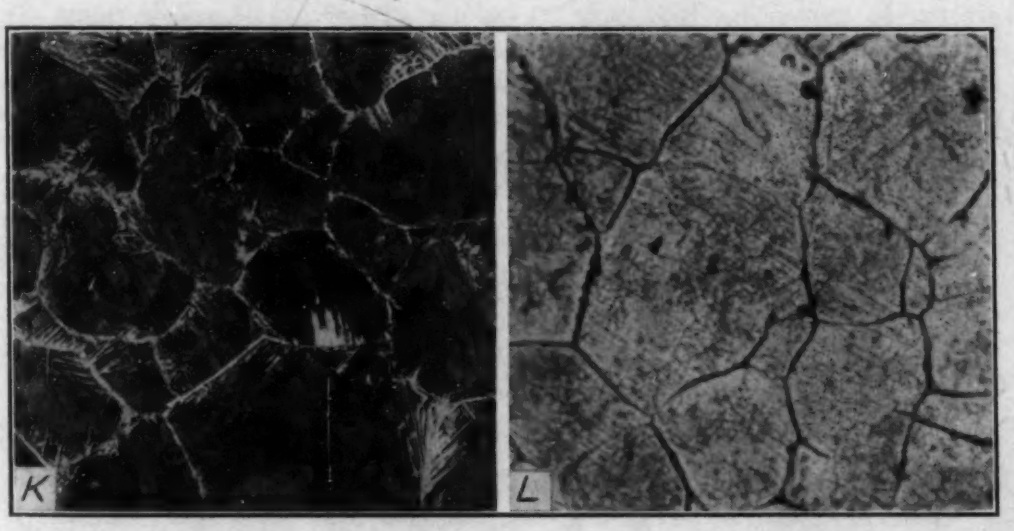

Figs. K and L—Austenitic Grain Size of Two Samples From Steel B After Heating 30 Minutes at 2000 Degrees Fahr. × 100.

(K) M-24578—Pearlitic Structure of Slow Cooled Sample Polished Through the Middle of the Half-Inch Bar and Showing the Austenitic Grain Size Outlined by the Ferrite. Etched With Nital.

(L) M-24577—Martensitic Structure of Quenched Companion Sample Polished Somewhat Under the Surface Showing the Austenitic Grain Size Outlined by the Oxide Films. Etched With 15 Per Cent HCl in Ethyl Alcohol.

Authors' Reply

It is gratifying to have the interesting discussion by Messrs. Tobin and Kenyon, who present evidence that the oxidation method can be used for deter-

mining austenite grain size provided proper care and technique are employed. However, several instances have come to our attention in which the oxidation method indicated an austenite grain size smaller than was consistent with other observations. Possibly their procedure was not followed closely enough; but we are somewhat skeptical of any method which involves any change in composition of the steel, and in the oxidation method the composition is changed by an increase in the percentage of oxygen near the surface.

Our remarks on the oxidation method were intended to suggest caution in its interpretation, for our results show that when steel containing an appreciable amount of aluminum is heated in an atmosphere even very slightly oxidizing to aluminum, the austenite grains in the neighborhood of the surface may be much smaller than those in the interior of the specimen. The necessity of bearing this fact in mind is evident also from the discussion of Tobin and Kenyon, who state, "It is important, however, to grind down the surface far enough to remove any severely decarburized material, but not far enough to remove all of the oxide penetration around the grains." In trying to remove the decarburized zone, one may remove the zone in which the aluminum has been oxidized; if this is achieved, the oxidation method should give satisfactory results, but unfortunately, some investigators have not been careful enough to achieve it.

We wish to correct the statement by Tobin and Kenyon that it is our practice to remove the heat etch but not the surface grains. This is not our regular practice for heat etching, but was used only in exploratory experiments to determine the reason why heat etching sometimes indicates austenite grains smaller at the surface than in the interior of a specimen.

THE TRANSFORMATION OF RETAINED AUSTENITE IN HIGH SPEED STEEL AT SUBATMOSPHERIC TEMPERATURES

By Paul Gordon and Morris Cohen

Abstract

The behavior of the retained austenite in hardened 18-4-1 high speed steel before, during, and after treatment in liquid nitrogen (—310 degrees Fahr., —190 degrees Cent.) has been studied by means of specific volume, hardness, dilatometric, X-ray diffraction, and magnetic measurements. The retained austenite undergoes partial transformation during the cooling to —310 degrees Fahr. The extent of this low temperature transformation is not affected by variations in the rate of cooling or time of holding at —310 degrees Fahr. but is greatly suppressed by room temperature aging of the hardened steel prior to the subatmospheric cooling. Tempering at sufficiently high temperatures after the liquid nitrogen treatment conditions the remaining austenite for transformation during the subsequent cooling to room temperature. This tempering causes the same fundamental changes as tempering after ordinary hardening.

The extra hardness achieved by the subzero treatment is relatively persistent even after tempering at 1050 degrees Fahr. On the basis of transverse bend tests, it appears that subzero hardening and tempering of 18-4-1 high speed steel may produce combinations of hardness, strength, and ductility not attainable by ordinary hardening and tempering.

THE recent work of Cohen and Koh (1)[1] has shown that the retained austenite in 18-4-1 high speed steel is responsible for the secondary hardening which accompanies the tempering operation. It was found that the retained austenite decomposes by first precipitat-

[1]The figures appearing in parentheses refer to the bibliography appended to this paper.

This paper is based on a thesis submitted by Paul Gordon to the Department of Metallurgy of the Massachusetts Institute of Technology, October, 1940, in partial fulfillment of the requirements for the degree of Master of Science in Metallurgy.

A paper presented before the Twenty-third Annual Convention of the Society held in Philadelphia, October 20 to 24, 1941. The authors, Paul Gordon and Morris Cohen, are associated with the Department of Metallurgy, Massachusetts Institute of Technology, Cambridge, Massachusetts. Manuscript received June 23, 1941.

ing alloy carbides at the tempering temperature and then transforming into martensite during the cooling from the tempering temperature. Some isothermal decomposition of the retained austenite may occur, but this is of a minor order compared with the transformation that takes place during the cooling to room temperature. It was also demonstrated that the characteristics of this transformation during cooling depend on the tempering treatment: The higher the tempering temperature and the longer the tempering time, the higher is the temperature at which the retained austenite begins to transform during cooling, and the greater is the extent of this transformation when room temperature is reached. The basis of these relationships lies in the carbide precipitation which occurs during the tempering treatment. At high tempering temperatures and during long tempering treatments, this carbide precipitation lowers the carbon and alloy content of the retained austenite, and thereby raises the transformation range sufficiently to allow the transformation to take place during the cooling to room temperature. Short tempering times and low tempering temperatures cause little or no change in the retained austenite composition, and, hence, the austenite does not transform after such treatments.

These phenomena immediately suggest that the transformation range of the retained austenite in the as-hardened 18-4-1 steel lies below room temperature and that this austenite may undergo transformation without preliminary carbide precipitation if the hardened steel is cooled to subatmospheric temperatures. In fact, the occurrence of these low temperature transformations in high speed steel has already been demonstrated by Dowdell and Harder (2), Scott (3), and Gulyaev (4), (5). Moreover, numerous investigators have studied such transformations in plain carbon and other alloy steels (2), (5-14). It appears that only Gulyaev (5) has investigated the kinetics of the subatmospheric austenite transformation in high speed steel. By making magnetic measurements during the cooling to —297 degrees Fahr. (—183 degrees Cent.), Gulyaev showed that after hardening at the usual temperatures the austenite transformation range extends well below room temperature, but complete transformation is not attained by such subzero cooling. He also found that room temperature aging of hardened high speed steel stabilizes the retained austenite so that the subatmospheric transformation is partially suppressed.

The present research was planned to shed further light on the

behavior of retained austenite in 18-4-1 high speed steel before, during, and after subatmospheric cooling. In particular, the following factors were investigated:

1. Effect of rate of cooling the hardened steel to —310 degrees Fahr. (—190 degrees Cent.)
2. Effect of holding the hardened steel at —310 degrees Fahr.
3. Effect of aging the hardened steel at room temperature before cooling to —310 degrees Fahr.
4. Effect of tempering the hardened steel before cooling to —310 degrees Fahr.
5. Effect of tempering the hardened steel after cooling to —310 degrees Fahr.

Experimental Details

The compositions of the steels used in this investigation are given in Table I.

Table I
Compositions of High Speed Steels

Stock	C	Mn	S	P	Si	W	Cr	V
½" square	0.73	0.23	Tr.	0.016	0.36	17.94	3.94	1.13
¼" round	0.735	0.22	Tr.	0.018	0.32	17.84	3.98	1.17
5/16" square	0.72	0.32	...	0.022	0.40	17.87	4.08	1.12

Hardness, specific volume, and X-ray diffraction measurements were made on ⅝-inch lengths of the ½-inch square stock, while 4-inch lengths of the ¼-inch round stock were used for dilatometric and magnetic measurements. The preparation of these specimens and details of heat treatment have been described elsewhere (1). Five-inch lengths of the 5/16-inch square stock were ground on all sides to approxmiately ¼-inch square after certain heat treatments, and used for transverse bend tests. All of the specimens were hardened from 2350 ± 10 degrees Fahr. (1285 ± 5 degrees Cent.).

A Vickers machine was used for the hardness testing since the subzero cooled specimens exhibited some tendency to crack under the Rockwell indentor. However, inasmuch as most of the previous hardness work on high speed steel has been expressed in terms of Rockwell C units, the hardness values throughout this paper have been converted accordingly. In order to obtain an accurate conversion, several high speed steel specimens in different states of heat

treatment were tested for hardness on both the Vickers and Rockwell machines. The results are shown in Table II together with the conversion values given by Scott and Gray (15). It is believed the hardness readings are accurate to ± 10 Vickers numbers or ± 0.3 Rockwell C units.

Table II
Relationship Between Vickers and Rockwell C Hardness for 18-4-1 High Speed Steel

Measured Vickers Hardness (30-kg. Load)	Measured Rockwell C Hardness (150-kg. Load)	Rockwell C Hardness as Converted from Vickers (Scott and Gray)
883	66.7	66.9
875	66.3	66.7
870	66.2	66.6
866	66.1	66.5
850	65.5	66.0
830	64.7	65.2
800	64.0	64.1

The details of the specific volume, X-ray diffraction, and dilatometric determinations have already been reported (1). All specific volumes have been referred to a room temperature of 72 degrees Fahr. (22 degrees Cent.), and are accurate to ± 0.02 per cent. The changes in length were measured to within ± 0.001 per cent. An accuracy of ± 0.1 per cent was attained in the magnetic measurements which were carried out in a field of 770 gauss. The apparatus employed will be described in the literature soon. In the case of the transverse bend tests,[2] a 4½-inch span was used with a two-point loading system to provide pure bending over the middle third of the specimen. The transverse load was applied in small increments and the resulting tensile stresses in the outer surface were calculated from simple beam theory. Corresponding tensile strains were measured up to the breaking point with a modified SR-4 electrical resistance strain gage (16) cemented on the tension side of the specimen. The stress-strain curves determined in this way usually departed only slightly from linearity between the proportional limit and the breaking point.

Liquid nitrogen (—310 degrees Fahr., —190 degrees Cent.) was used for the subatmospheric cooling. For the most part, the specimens to be cooled were immersed directly into the liquid nitrogen. In certain cases the rate of cooling was retarded by insulating the specimens from the nitrogen. At first, considerable difficulty was encountered due to the cracking of the specific volume specimens dur-

[2]These transverse tests were carried out as part of a Bachelor's Thesis at the Massachusetts Institute of Technology by J. L. Klein.

ing the subzero treatment. However, it was found that this cracking could be reduced to a minimum by rounding off the sharp corners and edges of the specimens before the hardening operation. In the subatmospheric dilatometric experiments, a rate of cooling slow enough to permit measurements on the way down (approximately 20 degrees Fahr. per minute) was obtained by pouring controlled amounts of liquid nitrogen into the annular space between the quartz tube of the dilatometer and a concentrically suspended Dewar flask.

Discussion of Results

Preliminary Results—Preliminary hardness, specific volume, and X-ray diffraction measurements indicated definitely that the cooling in liquid nitrogen of hardened 18-4-1 steel causes part of the retained austenite to transform. For example, if the subzero cooling is carried out immediately after the hardening quench, the resulting transformation is manifested by an increase in hardness of one full point on the Rockwell C scale, a marked increase in volume, and a disappearance of the austenite diffraction lines from the X-ray photogram. (The last finding should not be construed as evidence that the retained austenite completely transforms during the subzero treatment since the X-ray method is relatively insensitive to small traces of a dispersed phase.)

Effect of Rate of Cooling to —310 Degrees Fahr. (—190 Degrees Cent.) and Time of Holding at —310 Degrees Fahr.—It was originally suspected that the thermal shock produced by immersing the hardened steel directly into the liquid nitrogen might be an important factor in the transformation of the retained austenite during the subatmospheric cooling. In order to minimize this possible effect, hardened specimens were cooled to —310 degrees Fahr. at considerably slower rates, after which the hardness and specific volume values were determined as criteria of the extent of retained austenite transformation. All of these specimens were maintained at —310 degrees Fahr. for 1 hour before heating back to room temperature. The data in Table III show that the rate of cooling to —310 degrees Fahr., at least within the limits studied, has no measurable effect on the extent of the subatmospheric transformation, and that the cause of this transformation cannot be ascribed to thermal shock. Consequently, in all the following experiments, except for the dilatometric runs, the cooling to —310 degrees Fahr.

was accomplished by direct immersion in the liquid nitrogen. The cooling rate of 20 degrees Fahr. per minute employed for the dilatometric runs lies within the range covered by Table III.

Table III
Effect of Cooling Rate to —310 Degrees Fahr.
(Time Between Hardening Quench and Subzero Cooling = 10 Minutes)

Insulation Between Specimen and Liquid Nitrogen	Cooling Rate Degrees Fahr. Per Minute	Rockwell C Hardness	Specific Volume Cubic Centimeters Per Gram
As Hardened	...	66.0	0.11550
None	150	67.0	0.11588
Air	40	67.0	0.11587
Asbestos	25	67.1	0.11588
Oil	15	67.0	0.11589

The time of holding at —310 degrees Fahr. was likewise found to have no influence on the subzero transformation as demonstrated in Table IV. In view of these results, an arbitrary holding time of 1 hour in the liquid nitrogen was adopted.

Table IV
Effect of Time of Holding at —310 Degrees Fahr.
(Time Between Hardening Quench and Subzero Cooling = 3 Hours)

Time at —310 Degrees Fahr. Hours	Rockwell C Hardness	Specific Volume Cubic Centimeters Per Gram
As Hardened	66.0	0.11550
0.08	66.5	0.11576
1.0	66.4	0.11579
6.0	66.5	0.11577
16.0	66.4	0.11577

These critical experiments not only served the purpose for which they were intended, but also revealed that the time of room temperature aging between the hardening quench and the subzero cooling is a very important factor in these transformation studies. By comparing the data in Tables III and IV, it becomes obvious that the extent of subatmospheric transformation was appreciably less in the latter series of specimens than in the former, and that the only likely variable at play was the difference in the room temperature aging time prior to the subzero cooling, i.e., 3 hours versus 10 minutes. Accordingly, the effect of such room temperature aging was then investigated more thoroughly.

Effect of Room Temperature Aging Between the Hardening Quench and the Cooling to —310 Degrees Fahr. (—190 Degrees Cent.)—A set of specimens was hardened, aged at room temperature

for times ranging from 0 to 650 hours, immersed in liquid nitrogen for 1 hour, and then returned to room temperature. The changes in hardness and specific volume due to the subzero cooling are plotted in Fig. 1 as a function of the time of room temperature aging prior

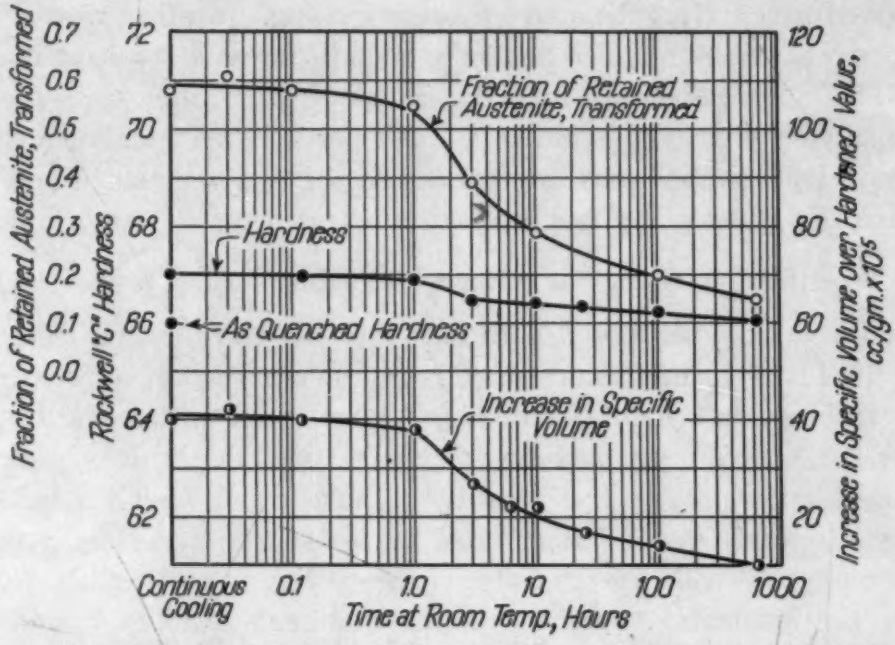

Fig. 1—Changes in Hardness, Specific Volume, and Fraction of Retained Austenite Transformed Due to Cooling Hardened 18-4-1 High Speed Steel to —310 Degrees Fahr. After Aging for Different Periods of Time at Room Temperature.

to the cooling. The liquid nitrogen treatment on the freshly hardened steel causes the hardness to increase from Rockwell C 66.0 to 67.0 and the volume to increase by approximately 0.00040 cubic centimeter per gram or 0.35 per cent as measured at room temperature. If the hardened steel is aged at room temperature, however, particularly for more than 1 hour, the subsequent low temperature transformation is considerably reduced. For example, after room temperature aging for 10 hours and then cooling to —310 degree Fahr., the hardness increases to 66.4 and the volume increases by only 0.17 per cent.

The retained austenite in the as-hardened steel does not transform completely during the liquid nitrogen treatment even if the subzero cooling follows the hardening quench immediately. This is nicely demonstrated by the fact that specimens treated in this way will undergo further austenite transformation if they are subsequently tempered, as described on page 584. The increase in volume accompanying the latter increment of transformation is 0.18 per cent

when the transformation product is martensite. Since the transformation of all the retained austenite by tempering (after ordinary hardening) is attended by a volume increase of 0.43 per cent (1), it appears that $\frac{0.18}{0.43}$ or 42 per cent of the retained austenite remains untransformed after the above subzero cooling. In other words, only 58 per cent of the retained austenite transforms as a result of cooling to —310 degrees Fahr. immediately after hardening, and the accompanying change in volume is 0.35 per cent as previously mentioned. By assuming that the fraction of the retained austenite which transforms during any low temperature treatment is proportional to the corresponding change in volume, and using $\frac{58}{.35}$ as a proportionality constant it becomes possible to calculate the third curve shown in Fig. 1. The indicated values should only be regarded as approximate.

It is quite evident from Fig. 1 that room temperature aging after the hardening quench has a potent stabilizing influence on the retained austenite, as has already been reported by Gulyaev (5). Whereas nearly $\frac{6}{10}$ of the retained austenite transforms as a result of cooling to —310 degrees Fahr. if the cooling is accomplished right after the hardening, only $\frac{3}{10}$ of the retained austenite transforms during subzero cooling if the steel is previously aged at room temperature for 10 hours, and only $\frac{2}{10}$ transforms if the room temperature aging time is 100 hours.

In view of these striking results, it was decided to follow the course of the austenite transformation with a dilatometer so that measurements could be made, not only before and after the treatments, but also during the cycle of operations. The resulting curves are shown in Fig. 2. When the high speed steel is cooled continuously from the hardening temperature (2350 degrees Fahr., 1285 degrees Cent.) through room temperature to —310 degrees Fahr. (Fig. 2a), the primary austenite transformation sets in at about 420 degrees Fahr. (215 degrees Cent.) (the so-called M-point) with a vigorous expansion superimposed upon the natural thermal contraction. The transformation proceeds during cooling to approximately —150 degrees Fahr. (—100 degrees Cent.), after which the steel contracts normally down to the liquid nitrogen temperature. The dilation curve in the vicinity of 70 degrees Fahr. (Fig. 2a) is quite smooth, thus signifying that the austenite transformation progresses in a regular fashion while the steel is cooling through

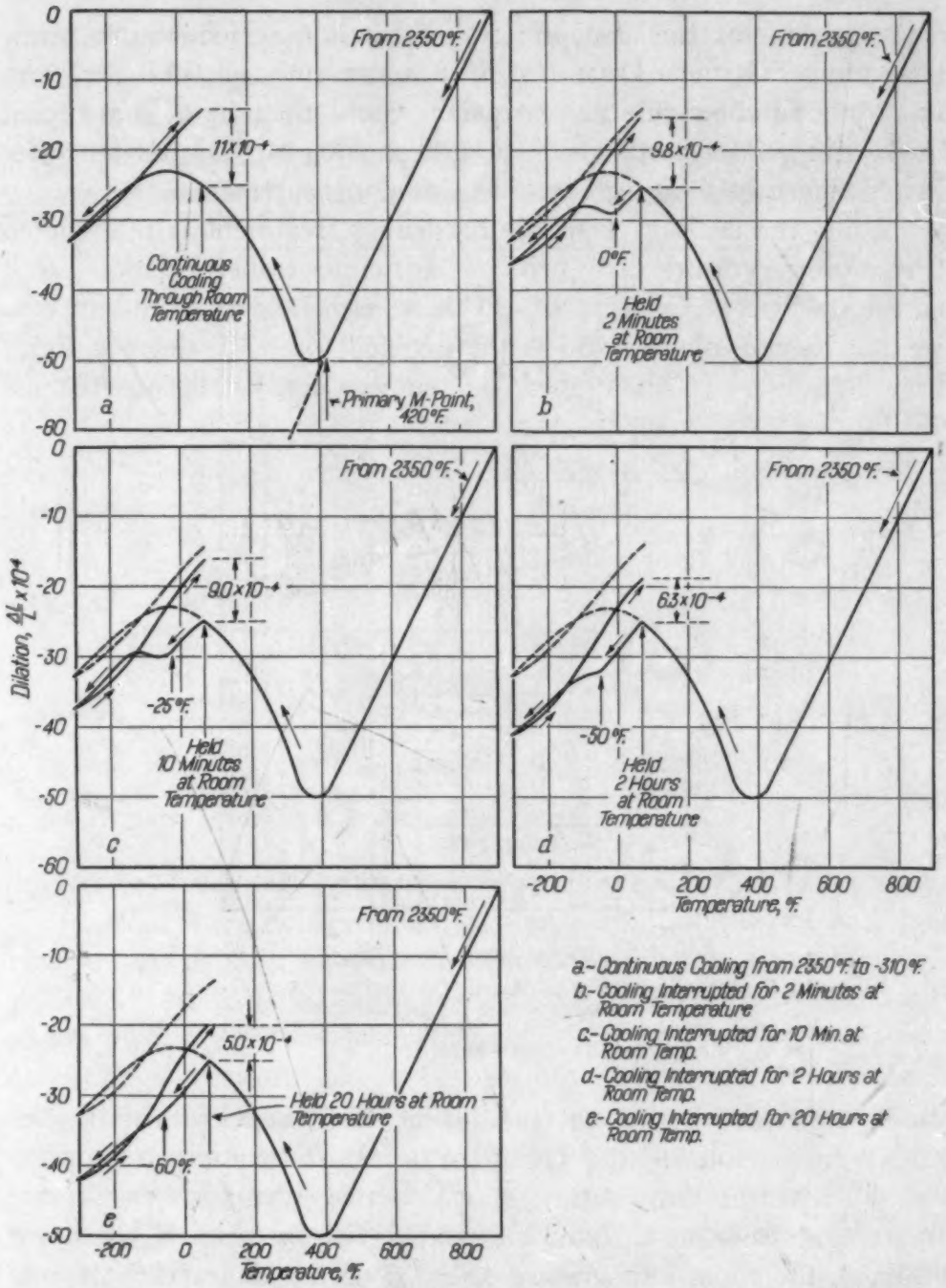

Fig. 2—Dilation Curves Showing the Effect on the Austenite Transformation of Interrupting the Hardening Quench at Room Temperature for Varying Periods of Time.
Fig. 2a—Continuous Cooling from 2350 to —310 Degrees Fahr.
Fig. 2b—Cooling Interrupted for 2 Minutes at Room Temperature.
Fig. 2c—Cooling Interrupted for 10 Minutes at Room Temperature.
Fig. 2d—Cooling Interrupted for 2 Hours at Room Temperature.
Fig. 2e—Cooling Interrupted for 20 Hours at Room Temperature.

room temperature. After the steel is cooled to —310 degrees Fahr. and heated back to room temperature, the net increase in length due

to the portion of the austenite transformation which occurs below room temperature is 11 x 10^{-4} inches per inch or 0.11 per cent. The corresponding cubical expansion would then be 0.33 per cent which is in good agreement with the expansion of 0.35 per cent previously determined by the specific volume measurements.

When the cooling from the hardening treatment is interrupted at room temperature, the primary austenite transformation stops and the steel ceases to expand.* If the steel is held at room temperature for only 2 minutes and is then cooled to —310 degrees Fahr. (Fig. 2b), there is an appreciable temperature lag before the remaining austenite begins to transform. This temperature lag becomes more pronounced the longer the holding time at room temperature, whereas the temperature at which the subatmospheric transformation stops is not affected materially. In other words, as shown in Fig. 3, the room temperature aging does not displace the transformation range of the retained austenite to lower temperatures, but suppresses only the upper part of the range. The corresponding decrease in the extent of the subatmospheric transformation is indicated in Fig. 2 by the decrease in the net expansion as measured on the dilatometer curves at room temperature.

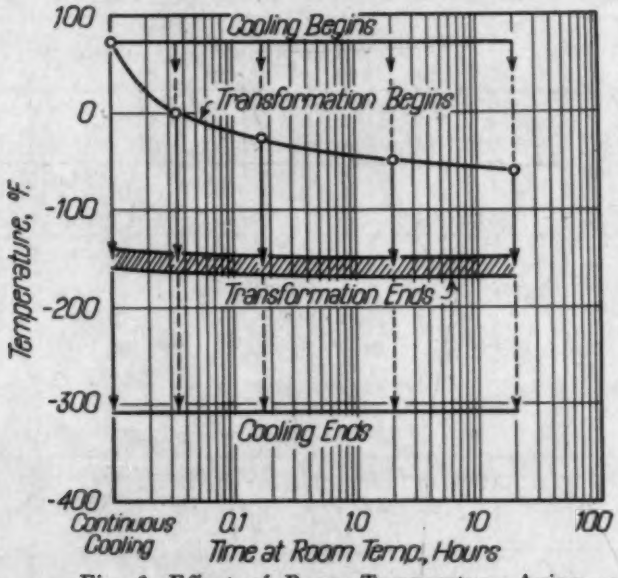

Fig. 3—Effect of Room Temperature Aging on the Transformation Range of the Retained Austenite in Hardened 18-4-1 Steel During Subsequent Cooling to —310 Degrees Fahr.

*Experiments indicate that this is true only if room temperature is approached at a fairly rapid rate. If room temperature is approached asymptotically, some transformation does occur at room temperature, as shown by Grossmann and Bain (17).

The room temperature aging of the hardened high speed steel was then investigated by many dilatometric, magnetic and specific volume measurements in order to ascertain the cause of the above stabilizing effect on the retained austenite. It was possible to obtain the change-in-length measurements immediately after the harden-

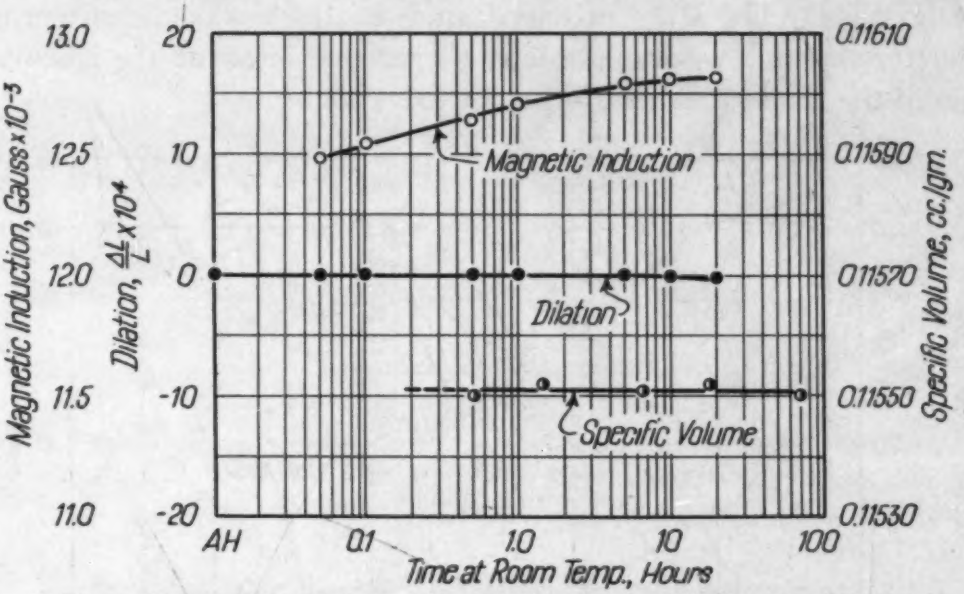

Fig. 4—Effect of Room Temperature Aging on the Dilation, Specific Volume, and Magnetic Induction of Hardened 18-4-1 Steel.

ing quench, magnetic measurements within 3 minutes after the quench, and the specific volume measurements within one-half hour after the quench. The results of these experiments are summarized in Fig. 4. An appreciable increase in the intensity of magnetization occurs during the room temperature aging. This increase in magnetization amounts to about 11 per cent of the change effected by complete transformation of the retained austenite, and, at first glance, suggests that a considerable part of the retained austenite undergoes isothermal transformation during room temperature aging. However, there is no corresponding change in the length or volume of the steel despite the fact that the extent of austenite transformation necessary to account for the magnetic changes could be readily detected by the dilatometric and specific volume measurements. It is not likely, therefore, that the retained austenite transforms at room temperature, and certainly not in sufficient quantities to account for the decreasing amounts of transformation during subsequent cooling to —310 degrees Fahr. It is more probable that the principal effect of room temperature aging lies in a partial relief of the internal

stresses set up by the hardening transformation. Such a stress relief would be attended by an increase in magnetization, no change in volume and, very possibly, compensating internal movements which would cause no consistent overall change in length in the specimens used. Furthermore, it is conceivable that even a relatively slight relief at room temperature of the austenite-martensite transformation stresses might have a profound effect on the resumption of the transformation during further cooling.

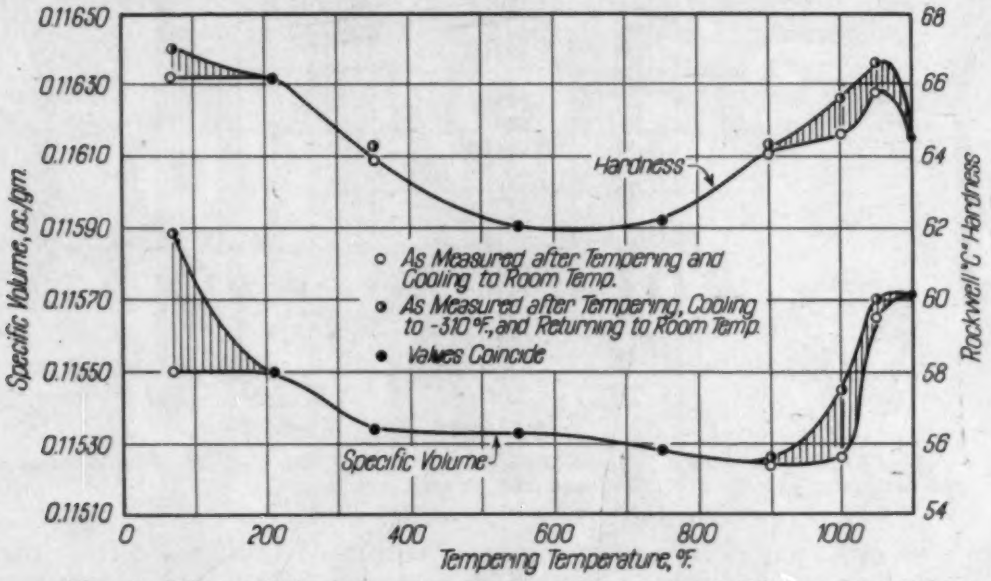

Fig. 5—Effect of Tempering the Hardened 18-4-1 Steel Prior to the Subzero Cooling. Tempering Time, 1 Hour.

Effect of Tempering the Hardened Steel Before Cooling to —310 Degrees Fahr. (—190 Degrees Cent.)—On the basis of the above stress relief hypothesis, it may be expected that heating the hardened steel to elevated temperatures would retard the subatmospheric transformation even more effectively than does the room temperature aging. To test this possibility, two groups of hardened specimens were tempered for 1 hour at temperatures between 70 degrees Fahr. and 1050 degrees Fahr. One group of specimens was simply cooled to room temperature from the tempering treatment while the second group was continuously cooled to —310 degrees Fahr. for 1 hour and then returned to room temperature. The hardness and specific volume measurements on these two series of specimens are plotted in Fig. 5 as a function of the tempering temperature. The effect of the subzero cooling (after tempering) is represented by the shaded regions between the two sets of curves.

The hardness and specific volume values of the as-tempered specimens are in excellent agreement with previously published work (1). The decrease in hardness and volume on tempering above 200 degrees Fahr. (95 degrees Cent.) is due to the decomposition of the tetrago-

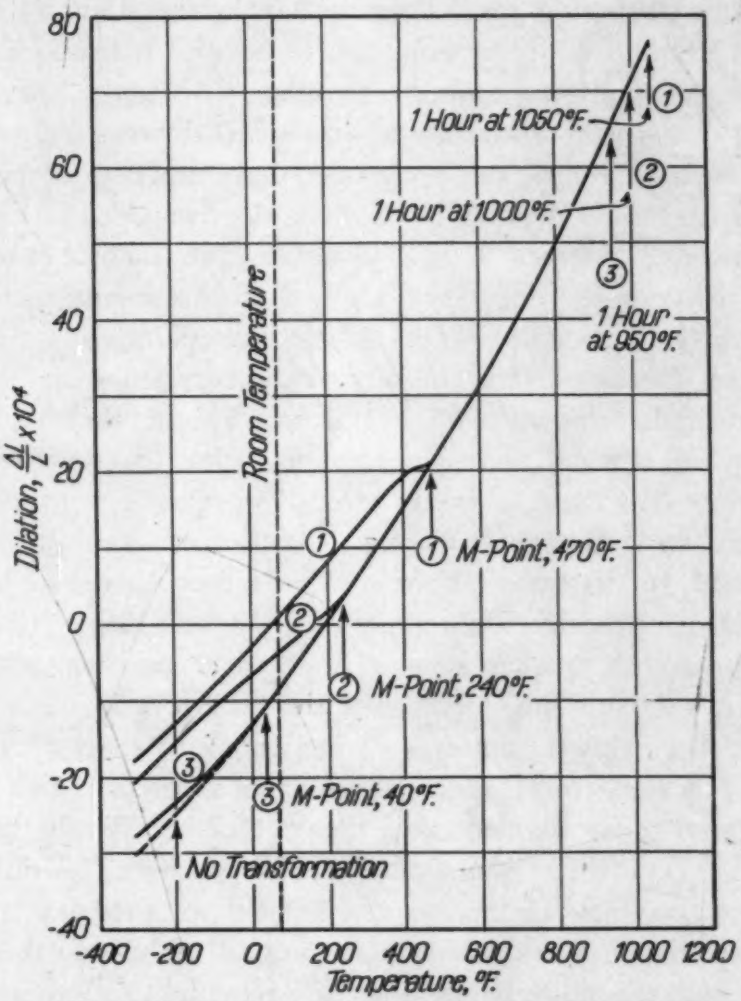

Fig. 6—Dilation Curves Showing Effect of Tempering Between Hardening and Cooling to —310 Degrees Fahr.

nal martensite in the hardened steel. Above 600 degrees Fahr. (315 degrees Cent.) the increase in hardness coincident with further contraction is caused by the precipitation of carbides from the retained austenite, while the additional hardening and marked expansion resulting from tempering above 950 degrees Fahr. (510 degrees Cent.) are due to the transformation of the retained austenite. It will be shown in connection with the dilatometric curves in Fig. 6 that the latter transformation occurs during the cooling from the tempering temperature.

Turning now to the shaded regions in Fig. 5 which depict the effect of subzero cooling after each tempering treatment, it is evident that the extent of the low temperature transformation decreases markedly as the tempering temperature is raised above room temperature. After tempering for 1 hour at 200 degrees Fahr., the retained austenite is stabilized to the point where none of it transforms during the subsequent subzero cooling. In other words, the previously determined transformation range above —310 degrees Fahr. ceases to exist. Similar stabilization is obtained by tempering at higher temperatures up to 875 degrees Fahr. (460 degrees Cent.). On tempering above 875 degrees Fahr., however, the carbide precipitation changes the composition of the retained austenite sufficiently to permit its transformation during the subsequent cooling to —310 degrees Fahr. This decrease in the stability of the retained austenite by tempering at high temperatures is clarified by the three dilatometric curves in Fig. 6 which show the changes in length during continuous cooling to —310 degrees Fahr. after tempering for 1 hour at 950 degrees Fahr. (510 degrees Cent.), 1000 degrees Fahr. (540 degrees Cent.), and 1050 degrees Fahr (565 degrees Cent.), respectively. With increasing tempering temperature in this range, the retained austenite becomes further impoverished in carbon and alloying elements, and the consequent rising of the transformation range above —310 degrees Fahr. results in austenite transformation when the steel is cooled through this range. When the transformation range is raised above room temperature, the retained austenite transforms during the cooling to room temperature as well as during subatmospheric cooling. In fact, as more and more austenite transforms above room temperature due to tempering at higher and higher temperatures, correspondingly less austenite remains to transform during the subatmospheric cooling, as shown by both Figs. 5 and 6.

When the tempering temperature is such as to cause the retained austenite to transform during cooling to —310 degrees Fahr., interruption of the cooling at room temperature tends to suppress the remaining austenite transformation during the subsequent subzero cooling. This phenomenon is quite analogous to the room temperature aging effect described on page 576. Consequently, in the tempering plus liquid nitrogen treatments which form the basis for Figs. 5 and 6, care was taken to cool the specimens continuously from the tempering temperature to —310 degrees Fahr.

Effect of Tempering After Cooling the Hardened Steel to —310

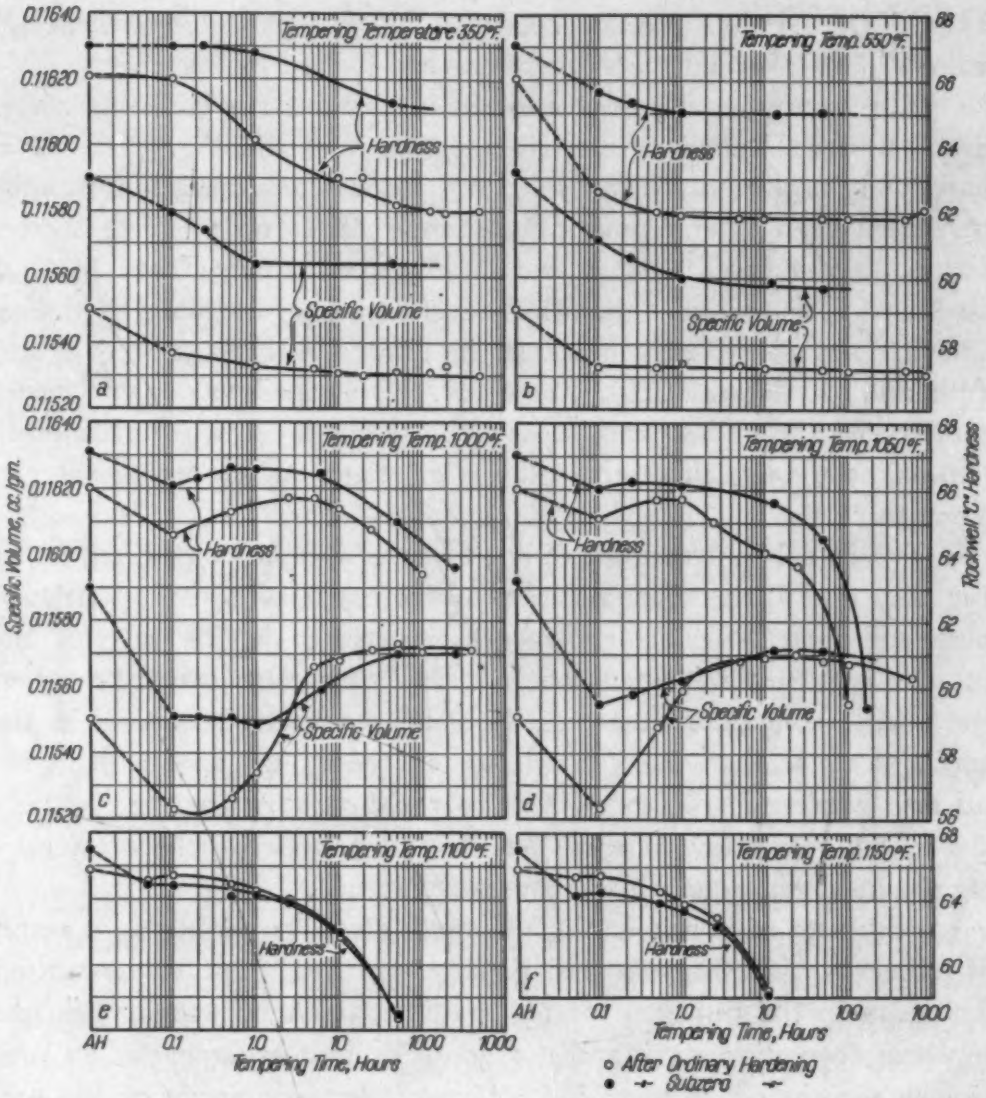

Fig. 7—Comparison of the Effect of Tempering the 18-4-1 Steel After Ordinary Hardening and After Subzero Hardening.

Fig. 7a—Tempering Temperature 350 Degrees Fahr. Fig. 7b—Tempering Temperature 550 Degrees Fahr. Fig. 7c—Tempering Temperature 1000 Degrees Fahr. Fig. 7d—Tempering Temperature 1050 Degrees Fahr. Fig. 7e—Tempering Temperature 1100 Degrees Fahr. Fig. 7f—Tempering Temperature 1150 Degrees Fahr.

Degrees Fahr. (—190 Degrees Cent.)—It remained to investigate the effect of tempering the hardened 18-4-1 steel after, rather than before, the subzero cooling. Two sets of specimens were hardened in the usual way by oil quenching from 2350 degrees Fahr. (1285 degrees Cent.) to room temperature. One set was immediately cooled to —310 degrees Fahr. for 1 hour and returned to room temperature. Then both sets were tempered for varying lengths of time at temperatures between 350 degrees Fahr. (175 degrees Cent.) and

1150 degrees Fahr. (620 degrees Cent.). The hardness and specific volume data taken on these specimens are plotted in Fig. 7.

The tempering process exhibits the same fundamental stages after subzero hardening as after ordinary hardening. The extra hardening produced by the subatmospheric transformation is quite persistent even after tempering at temperatures up to 1050 degrees Fahr. (565 degrees Cent.), the hardness remaining from ½ to 2 Rockwell C units higher than that developed after ordinary hardening and tempering. After tempering at 1100 and 1150 degrees Fahr. (595 and 620 degrees Cent.), however, the hardness values of the subzero cooled specimens drop below those of the specimens hardened in the ordinary way, although in the later stages of tempering the gap tends to close.

The initial contraction exhibited by the specific volume curves of Fig. 7 is due to the decomposition of the martensite in the hardened high speed steels. This contraction is greater in the case of the subzero hardened specimens because the latter contain more martensite and less residual austenite than the specimens hardened in the usual way. At the same time, however, the extra martensite in the subzero hardened specimens is more resistant to softening, possibly due to a higher alloy content, than the martensite which forms during the hardening quench to room temperature.

Both sets of specimens display secondary hardening as a result of tempering (see Figs. 7c and 7d in particular), thus demonstrating that even in the nitrogen treated specimens some austenite remains for transformation during the subsequent tempering cycle, as previously mentioned on page 575. The smaller magnitude of the secondary hardening and attendant volume changes in the case of the subzero cooled specimens compared to the normally hardened specimens is simply a consequence of the subatmospheric transformation of part of the retained austenite which would otherwise be available for secondary hardening during tempering.

The high hardness caused by the subatmospheric transformation may have practical possibilities, especially in view of the relatively slow rate of softening after tempering at 1050 degrees Fahr. (565 degrees Cent.). The question immediately arises, however, as to whether the advantages of this extra hardness are offset by a corresponding lack of ductility. Accordingly, a series of transverse bend tests were made in order to obtain some index of the relative

strength and ductility after various treatments. The pertinent results are shown in Table V. The modulus of rupture is the calculated maximum tensile stress in the specimen at the breaking point, while the ductility or plastic strain is taken as the maximum

Table V
Transverse Bend Tests on 18-4-1 High Speed Steel

Treatment	Rockwell C Hardness	Proportional Limit (Lbs./Sq.In.)	Modulus of Rupture (Lbs./Sq.In.)	Plastic Strain (Inches/Inch)
(A) Ordinary hardening followed by tempering for 2½ hrs. at 1050° F.	65	280,000	386,000	0.0007
(B) Subzero hardening followed by tempering for 2½ hrs. at 1050° F.	66	320,000	412,000	0.0015
(C) Ordinary hardening followed by tempering for 2½ hrs. at 1150° F.	63	220,000	444,000	0.0017
(D) Subzero hardening followed by tempering for 2½ hrs. at 1150° F.	62.5	240,000	435,000	0.0102

departure of the stress-strain curve from the extended straight portion. Comparing treatments (A) and (B), where a tempering temperature of 1050 degrees Fahr. (565 degrees Cent.) is used, it is evident that the subzero cooling not only provides an increase in hardness and strength, but also an improvement in ductility. When the tempering temperature is raised to 1150 degrees Fahr. (620 degrees Cent.) (cf. treatments C and D), the subzero hardening has relatively little effect on the hardness and strength, but results in a remarkable increase in ductility. In other words, it appears that subzero hardening followed by the proper tempering treatment may yield a combination of properties in high speed steel not attainable after ordinary hardening. These findings are in line with the work of Luerssen and Greene (9) who have shown that the hardness, strength, and ductility of 18 per cent chromium + 5 per cent nickel steels are enhanced by cooling to —112 degrees Fahr. (—80 degrees Cent.) and then tempering. Also Gulyaev (4) has reported that the subzero treatment of high speed steel permits higher cutting speeds when working with short chips.

From a practical point of view it is important to note that cooling to temperatures as low as —310 degrees Fahr. (—190 degrees Cent.) is not necessary to achieve subatmospheric transformation in

hardened high speed steel. The dilatometric curves in Fig. 2 show that the transformation stops below —150 degrees Fahr. (—100 degrees Cent.). In fact, only a small amount of transformation occurs below —100 degrees Fahr. (—75 degrees Cent.). Consequently, any readily attainable temperature in the range —100 to —150 degrees Fahr. may be used instead of —310 degrees Fahr. The attendant danger of cracking would also be reduced. In any case, the subatmospheric cooling need not be rapid, but must be started very soon after the hardening quench from 2350 degrees Fahr. in order to avoid the stabilizing effect of room temperature aging on the retained austenite.

Conclusions

(a) During the continuous cooling of 18-4-1 high speed steel from a hardening temperature of 2350 to —310 degrees Fahr. (1285 to —190 degrees Cent.), the austenite transformation sets in at 420 degrees Fahr. (215 degrees Cent.), progresses smoothly through room temperature, and stops at approximately —150 degrees Fahr. (—100 degrees Cent.).

(b) Interrupting the cooling from 2350 degrees Fahr. at room temperature, as is done in the ordinary oil-hardening operation, stops the transformation.

(c) Aging the hardened high speed steel at room temperature before cooling to —310 degrees Fahr. reduces the magnitude of the subatmospheric transformation and lowers the temperature at which the transformation sets in. This stabilizing effect on the retained austenite becomes more pronounced the longer the time of room temperature aging.

(d) The rate of subzero cooling and the time of holding at —310 degrees Fahr. have no measurable effect on the extent of the subatmospheric transformation.

(e) If the hardened 18-4-1 steel is tempered at temperatures between 200 and 875 degrees Fahr. (95 and 470 degrees Cent.) the retained austenite is stabilized sufficiently so that no transformation occurs during subsequent cooling to —310 degrees Fahr. Tempering at temperatures above 875 degrees Fahr., however, produces enough carbide precipitation from the retained austenite to lower its stability to the point where transformation again takes place during cooling from the tempering temperature to —310 degrees Fahr.

(f) Tempering the hardened 18-4-1 steel after subzero cooling completes the retained austenite transformation. Such tempering shows the same fundamental stages as tempering after ordinary hardening.

(g) The increment of hardness developed in hardened 18-4-1 steel by subzero cooling is persistent during tempering up to temperatures as high as 1050 degrees Fahr. (565 degrees Cent.).

(h) The indications are that subzero hardening and tempering of 18-4-1 high speed steel will produce combinations of hardness, strength, and ductility unattainable by ordinary hardening and tempering.

Acknowledgments

The authors desire to express their gratitude to J. P. Gill and R. S. Rose of the Vanadium-Alloys Steel Company who furnished the steel for the specific volume, hardness, X-ray diffraction, dilatometric, and magnetic measurements;

To P. Payson of the Crucible Steel Company who supplied the steel for the bend tests;

To J. Lester Klein who carried out the bend tests;

To Otto Zmeskal who conducted the magnetic measurements.

Bibliography

1. Morris Cohen and P. K. Koh, "The Tempering of High Speed Steel," Transactions, American Society for Metals, Vol. 27, 1939, p. 1015-1051.
2. R. L. Dowdell and O. E. Harder, "The Decomposition of the Austenitic Structure in Steel. Part II, The Decomposition of Austenite in Liquid Oxygen," Transactions, American Society for Steel Treating, Vol. 11, 1927, p. 391.
3. H. Scott, "Relation of the High Temperature Treatment of High Speed Steel to Secondary Hardening and Red Hardness," *Scientific Papers*, Bureau of Standards, Vol. 16, 1920, p. 521-536.
4. A. Gulyaev, "Improved Heat Treatment of High Speed Steel to Improve Cutting Quality," *Metallurg*, Vol. 12, 1937, p. 65-77.
5. A. Gulyaev, "Transformation of Retained Austenite at Subzero Temperatures with High Speed Steel," *Metallurg*, Vol. 14, 1939, p. 64-77.
6. J. A. Matthews, "Retained Austenite—A Contribution to the Metallurgy of Magnetism," Transactions, American Society for Steel Treating, Vol. 8, 1925, p. 565-583.
7. K. Honda and K. Iwase, "On the Transformatoin of Retained Austenite into Martensite by Stress," Transactions, American Society for Steel Treating, Vol. 11, 1927, p. 399.
8. E. C. Bain and W. S. N. Waring, "Austenite Decomposition and Length Changes in Steel," Transactions, American Society for Steel Treating, Vol. 15, 1929, p. 69-95.

9. G. V. Luerssen and O. V. Greene, "The Cold Treatment of Certain Alloy Steels," TRANSACTIONS, Amercian Society for Steel Treating, Vol. 19, 1932, p. 601-552.
10. H. P. Nielson and R. L. Dowdell, "Effect of Thermal Stresses on Austenite," TRANSACTIONS, American Society for Steel Treating, Vol. 22, 1934, p. 810-832.
11. G. Tammann and E. Scheil, "Transformation of Austenite and Martensite in Quenched Steels," *Zeitschrift anorg. allgemeine Chemie,* Vol. 157, 1926.
12. K. Schroeter, "Transformation of Austenite to Martensite in Liquid Air," *Zeitschrift anorg. allgemeine Chemie,* Vol. 169, 1928, p. 157-160.
13. N. Minkevitch, O. Ivanov, and Ya. Dovgelevski, "Influence of Subzero Temperatures upon Cr, W, V Steels in the As Quenched State," *Stal,* Vol. 8, 1938, p. 63.
14. W. P. Sykes and Z. Jeffries, "On the Constitution and Properties of Hardened Steel," TRANSACTIONS, American Society for Steel Treating, Vol. 11, 1927, p. 871-897.
15. H. Scott and T. H. Gray, "Hardness Conversion Relations for Hardened Steels," TRANSACTIONS, American Society for Metals, Vol. 28, 1940, p. 399-423.
16. Baldwin-Southwark Bulletin 155.
17. M. A. Grossmann and E. C. Bain, "High Speed Steel," John Wiley and Sons, Inc., N. Y., 1931, p. 135.

DISCUSSION

Written Discussion: By W. R. Frazer, metallurgist, Union Twist Drill Co., Athol, Mass.

We have studied with considerable interest this excellent paper which gives us more data on the phenomena of austenite transformation in high speed steel. The authors show that as high speed steel cools from its hardening heat, the austenite starts to transform into primary martensite at a temperature of 420 degrees Fahr. (215 degrees Cent.) and progresses on continuous cooling until a temperature of —150 degrees Fahr. (—101 degrees Cent.) is reached. They also find that when the cooling is interrupted at room temperature, the transformation is stopped and considerable subatmospheric cooling is required to again start the change in structure. The longer the steel is held at room temperature, the more resistant the retained austenite is to further transformation. The subatmospheric continuous cooling therefore develops more primary martensite in the as-hardened condition than conventional hardening, which accounts for the increased hardness and specific volume measurements given in Tables III and IV. The authors have calculated that the continuous subatmospheric cooling develops 58 per cent more primary martensite than conventional hardening and consequently there is only 42 per cent of the conventional amount of retained austenite left to transform on tempering.

In Fig. 7, the authors have plotted the changes in hardness and specific volume when samples hardened by subatmospheric cooling and conventionally are tempered at various temperatures for different lengths of time. It is interesting to note that the hardness of the subzero cooled pieces continue to show increased hardness on tempering up to 1050 degrees Fahr. (565 degrees Cent.), with a definite development of secondary hardening, indicating transformation of the retained austenite.

This paper strengthens the argument that tools should be cooled at least to a temperature that can be handled with bare hands, or better yet to room temperature, before tempering, so that as much primary martensite is formed as possible. Apparently the increased toughness obtained by the subzero cooling is directly related to this phenomenon. We should like to inquire if the authors have compared the single tempering with repeat tempering and also interrupted tempering to determine the effect on toughness.

The facts revealed and theory proposed as a result of this investigation have given us food for thought although we anticipate many problems in attempting to put the treatment to practical use due to the increased hazard of developing hardening cracks.

Written Discussion: By W. E. Bancroft, chief metallurgist, Pratt & Whitney Division, Niles-Bement-Pond Co., Hartford, Conn.

In attempting to show what happens when 18-4-1 high speed steel is cooled to a subzero temperature of —310 degrees Fahr. (—190 degrees Cent.) under various conditions the authors have done a very excellent and valuable piece of work. There are only one or two points which seem to be capable of further clarification. For example, in reporting the effect of tempering prior to subzero hardening, why might it not be desirable to construct a set of curves similar to those shown in Fig. 7, so as to demonstrate the effect of tempering time and show what happens under conditions of complete transformation? Or perhaps it might be sufficient to construct another curve similar to Fig. 5, but based on a tempering time of 2.5 hours, whereby, according to Dr. Cohen's previous work on the tempering of 18-4-1 high speed steel, the transformation would be complete. As it now stands Fig. 5 indicates a definite difference in hardness of about one point Rockwell between specimens cooled and not cooled to subzero temperatures after tempering at 1050 degrees Fahr. (565 degrees Cent.) for 1 hour. My question is what happens to the hardness if transformation were completed in the tempering operation—would this difference be eliminated or would it persist as in the case of specimens subzero cooled before tempering? The published data seem to be inconclusive on this point. In any case the dotted extension lines above 1050 degrees Fahr. (565 degrees Cent.) in Fig. 5 do not look right since 1050 degrees Fahr. (565 degrees Cent.) is supposed to produce maximum hardness, and any increase in tempering temperature beyond this point should result in a decrease rather than the increase in hardness indicated by these curves.

It is of particular interest to note that subzero cooling before tempering produces a type of martensite which not only maintains a higher hardness, but also possesses greater ductility after being tempered to the usual range. It is to be hoped that this procedure does not exhibit any unforeseen disadvantages and that it may lend itself to commercial practice since the one thing a heat treater and user of high speed steel is constantly looking for is a method of increasing toughness without impairing the hardness and wearing qualities of cutting tools.

In noting that the authors found it necessary to use the Vickers method for hardness testing because pieces cooled to subzero temperatures showed a tendency to crack, the question arises as to whether this cracking was

observed on all specimens, including those which had been tempered either before or after subzero cooling, or only on those which were tested in the untempered condition.

Finally, would the authors care to explain just how continuous cooling, both from the quenching and tempering temperatures, was accomplished? Was it considered desirable to hold the specimens until they actually reached room temperature before transferring to liquid nitrogen, or was this done from some higher temperature and if so how high?

Oral Discussion

A. R. TROIANO:* The authors have presented what I believe is the first published record of a very interesting and important phenomenon. That is, the stabilization of austenite by aging at room temperature. It should be pointed out here that this phenomenon is not peculiar to high speed steels.

For the last year or more, we have been engaged in a comprehensive study of chromium steels at the University of Notre Dame and have found the same effect. In some of the steels already investigated the effect is even more marked than that reported by the authors for high speed steel. As a typical example, a steel containing approximately 15 per cent chromium and 0.70 per cent carbon, continuously cooled, will show the Ar" point just below room temperature. However, if this same steel is aged 1 hour at room temperature, Ar" (the temperature for the beginning of formation of martensite on cooling) is lowered to well below —77 degrees Cent. (—107 degrees Fahr.). The effect of aging 1 hour or 6 months at room temperature does not appreciably alter these results for this steel.

In all cases, the steels were given a complete carbide solution anneal. This removes as possible variables the ferrite, carbides, etc., that may be present in the high speed steel.

A study of the lowering of Ar" as a function of aging time and temperature is in progress at the present time.

Authors' Reply

We are pleased to learn that Dr. Troiano has also observed the effect of room temperature aging on the stabilization of austenite. It is significant that this phenomenon is not peculiar to high speed steel alone, but likewise appears in high chromium steels in which all the carbides are dissolved.

Dr. Frazer has brought out a very important practical consideration in stating that this paper strengthens the argument that hardened high speed tools should be cooled close to room temperature before the tempering operation. The present work suggests that failure to cool the steel to room temperature between hardening and tempering may result in somewhat inferior properties. However, in the case of complicated shapes where the danger of cracking is present, cooling all the way to room temperature after hardening may have to be avoided. The effect of minimum temperature between hardening and tempering on the mechanical properties of high speed steel is now being investigated at Massachusetts Institute of Technology.

---

*Assistant professor of metallurgy, University of Notre Dame, Notre Dame, Indiana.

Dr. Frazer has mentioned that continuous subatmospheric cooling develops 58 per cent more primary martensite than conventional hardening. This statement requires some rewording: the data show that subzero cooling causes the transformation to martensite of 58 per cent of the austenite which would have been retained at room temperature if the subzero cooling were omitted.

The questions raised by Mr. Bancroft are very pertinent. Time was not studied as a variable in the tempering experiments prior to the nitrogen cooling because the 1-hour treatments seemed to tell a rather complete story. On tempering between 200 and 875 degrees Fahr. (95 and 470 degrees Cent.), the retained austenite is stabilized so that none transforms during subsequent cooling to —310 degrees Fahr. (—190 degrees Cent.). Time variations in this tempering range would show little effect on the subatmospheric transformation. Above 900 degrees Fahr. (480 degrees Cent.), however, the carbide precipitation from the retained austenite causes the latter to transform during the cooling, and variations in tempering time might be expected to result in appreciable effects, as Mr. Bancroft suggests. However, these effects are predictable from Figs. 5 and 6, and it was not felt that more detailed experimentation along these lines would shed further light on the fundamentals of the problem.

We are indebted to Mr. Bancroft for pointing out the discrepancy in the extrapolated hardness curves of Fig. 5. Since the time of Mr. Bancroft's discussion, experimental points for 1100 degrees Fahr. (595 degrees Cent.) have been determined, and the curves above 1050 degrees Fahr. (565 degrees Cent.) have been redrawn. Maximum hardness occurs on tempering at 1050 degrees Fahr. (565 degrees Cent.). After tempering for 1 hour at 1100 degrees Fahr. (595 degrees Cent.), the retained austenite is completely transformed by the time room temperature is reached, and there is no further change in either hardness or specific volume as a result of liquid nitrogen cooling.

The manner of cooling through room temperature after hardening in order to achieve maximum subatmospheric transformation is not critical, so long as the steel is not permitted to stay at room temperature. A convenient and effective procedure is to quench the steel in oil or in air from the high heat temperature, and then transfer to the liquid nitrogen when the steel reaches a temperature of 100-200 degrees Fahr.

The Vickers hardness tester was adopted in the present work because the steels cooled directly in liquid nitrogen showed a tendency toward cracking around Rockwell impressions. Specimens that were tempered either before or after the subzero treatment did not crack around Rockwell impressions. Nevertheless, all of the hardness testing was conducted on the Vickers machine, and the readings were transposed to Rockwell values by means of a conversion chart established for the purpose.

We quite agree with both Dr. Frazer and Mr. Bancroft that the commercial possibilities of subzero hardening should be approached cautiously because of the cracking hazard. On the other hand, this cracking hazard should not be allowed to discourage practical attempts to take advantage of the subzero treatment.

THE TEMPERATURE AND MANNER OF GROWTH OF SHATTER CRACKS IN STEEL RAILS

By H. B. Wishart, E. P. Epler and R. E. Cramer

Abstract

Experiments are described which show the temperatures at which shatter cracks begin to develop in rails of 131-pound section, rolled from ingots treated with hydrogen, a gas which produces shatter-sensitive steel. A series of pictures shows the increase in size and number of shatter cracks as the specimens were cooled from the rolling temperature to lower temperatures or held at room temperature for longer periods of time.

Other experiments are described which show the effect of holding rail specimens of different shatter crack sensitivity at various temperatures for different periods of time. It is emphasized that crack sensitivity of the steel, time and temperatures of cooling, and mass factors have a pronounced influence on the development of shatter cracks in rails or flakes in steel forgings.

Shatter cracks will not form at low temperatures if rail steel is properly controlled, cooled or held at temperatures between 1200 and 400 degrees Fahr. (649 and 204 degrees Cent.) for a sufficient time to relieve the shatter sensitivity before cooling to room temperature.

Introduction

MANY opinions have been advanced as to the temperatures at which flakes or shatter cracks form in steel rails and also on the rate of their growth. As little experimental information is available on these subjects, four experiments were made to obtain additional data. The first two experiments, designated as Tests 1 and 2, were similar and consisted of cooling the rail specimens from their original rolling heat to various temperatures, immediately reheating to 700 degrees Fahr. (370 degrees Cent.), and slow cooling.

The purpose in treating the rail specimens as described was to allow for any development of shatter cracks that might occur on

A paper presented before the Twenty-third Annual Convention of the Society held in Philadelphia, October 20 to 24, 1941. Of the authors, H. B. Wishart is contact representative, Carnegie-Illinois Steel Corp., Chicago, E. P. Epler is metallurgist, Carnegie-Illinois Steel Corp., Gary, Ind., and R. E. Cramer is special research assistant professor of engineering materials, University of Illinois, Urbana, Ill. Manuscript received June 17, 1941.

cooling to the various temperatures. The reheating and slow cooling process was to check and prevent further shatter crack growth which might have taken place and to eliminate any remaining shatter sensitivity. By following this process, it was felt that the approximate temperature of shatter crack formation was indicated.

Tests 3 and 4 were repetitions of Tests 1 and 2 and in addition provided for holding of rail specimens at various temperatures for given lengths of time followed by both air cooling of specimens and reheating of specimens. These last two tests were made to determine whether a time lag existed in shatter crack formation, whereby steel held at a higher temperature, for example, 300 degrees Fahr. (150 degrees Cent.) for 4 hours would shatter crack, whereas steel allowed to cool to 200 degrees Fahr. (95 degrees Cent.) and immediately reheated would not develop shatter cracks. Specimens cooled in air after having been subjected to holding at various temperatures were investigated for the purpose of ascertaining whether holding at low temperatures would be effective in preventing shatter cracks.

General Experimental Procedure

As an insurance that the rail steel used in the tests would flake if cooled in still air, one ingot from each of four heats of steel was treated with hydrogen gas (which has been shown to produce flakes) (1), (2), (3)[1] as they were teemed in the open hearth by a method previously described (4). The chemical analyses of the four heats are shown in Table I. After the ingots were impregnated with hydrogen they followed the routine channels through the strippers, soaking pits, and rail mill to the hot saws. At the hot saws short specimens were cut from the C and D rails of the hydrogen-treated ingots and numbered. In the third and fourth experiments about 60 specimens were required from each ingot. To obtain this number of specimens, it was necessary to cut 6-foot lengths with the hot saws, then have four welders torch cut these lengths to 1-foot specimens while the rails were still at a red heat.

Tests 1 and 2

Rails from Heat Numbers 85128 and 83263 were used in these tests. The ingots from both heats were treated with 20 cubic feet

[1]The figures appearing in parentheses refer to the bibliography appended to this paper.

of hydrogen. It will be shown later that the results obtained are influenced by the amount of hydrogen used, as this governs to a large extent the sensitivity of the rails to shatter cracking. Only 10 specimens were used from each heat. After cutting at the hot saws the specimens were cooled in still air to temperatures of 500, 400,

Table I
Chemical Analyses of Heats of Rail Steel Used in Tests

Heat No.	Chemical Composition—Per Cent				
	Carbon	Manganese	Phosphorus	Sulphur	Silicon
85128	0.75	0.92	0.018	0.031	0.21
83263	0.78	0.90	0.013	0.029	0.23
54007	0.75	0.98	0.017	0.029	0.23
51106	0.79	0.85	0.016	0.038	0.22

300, 200, 100 and 70 degrees Fahr. (260, 205, 150, 95, 40 and 20 degrees Cent.). Upon reaching these temperatures the specimens were immediately placed in a furnace at 700 degrees Fahr. (370 degrees Cent.) for at least 7 hours, then slow cooled over a period of 10 hours. This 700 degrees Fahr. (370 degrees Cent.) temperature and method of cooling have been found in previous tests (2), (4), (5) to completely prevent any further formation of shatter cracks in rails. Also specimens from each heat were held at 70 degrees Fahr. (20 degrees Cent.) for 2, 4, and 6 hours before being placed in the 700 degrees Fahr. (370 degrees Cent.) furnace. In each test a control specimen which was a crop end from the rails was cooled on the mill floor for 72 hours to represent the sensitivity of the steel to the development of shatter cracks.

To determine the presence of shatter cracks, a longitudinal slice 6 inches long and ⅞ inch below the top of the rail head was cut from each specimen. These slices were ground smooth, etched in hot 1-1 hydrochloric acid and examined for shatter cracks with low-power magnifying glasses. The number of longitudinal and transverse cracks found in each specimen is recorded in Table II, while photographs of representative specimens are shown in Figs. 1 and 2, at approximately ¾ natural size. The photographs are especially interesting because they show the increase in size of the shatter cracks as the specimens cooled to lower temperatures or remained at room temperature for incurred periods of time before being placed in the 700 degrees Fahr. (370 degrees Cent.) furnace. This series of pictures furnishes very good evidence that the cracks gradually

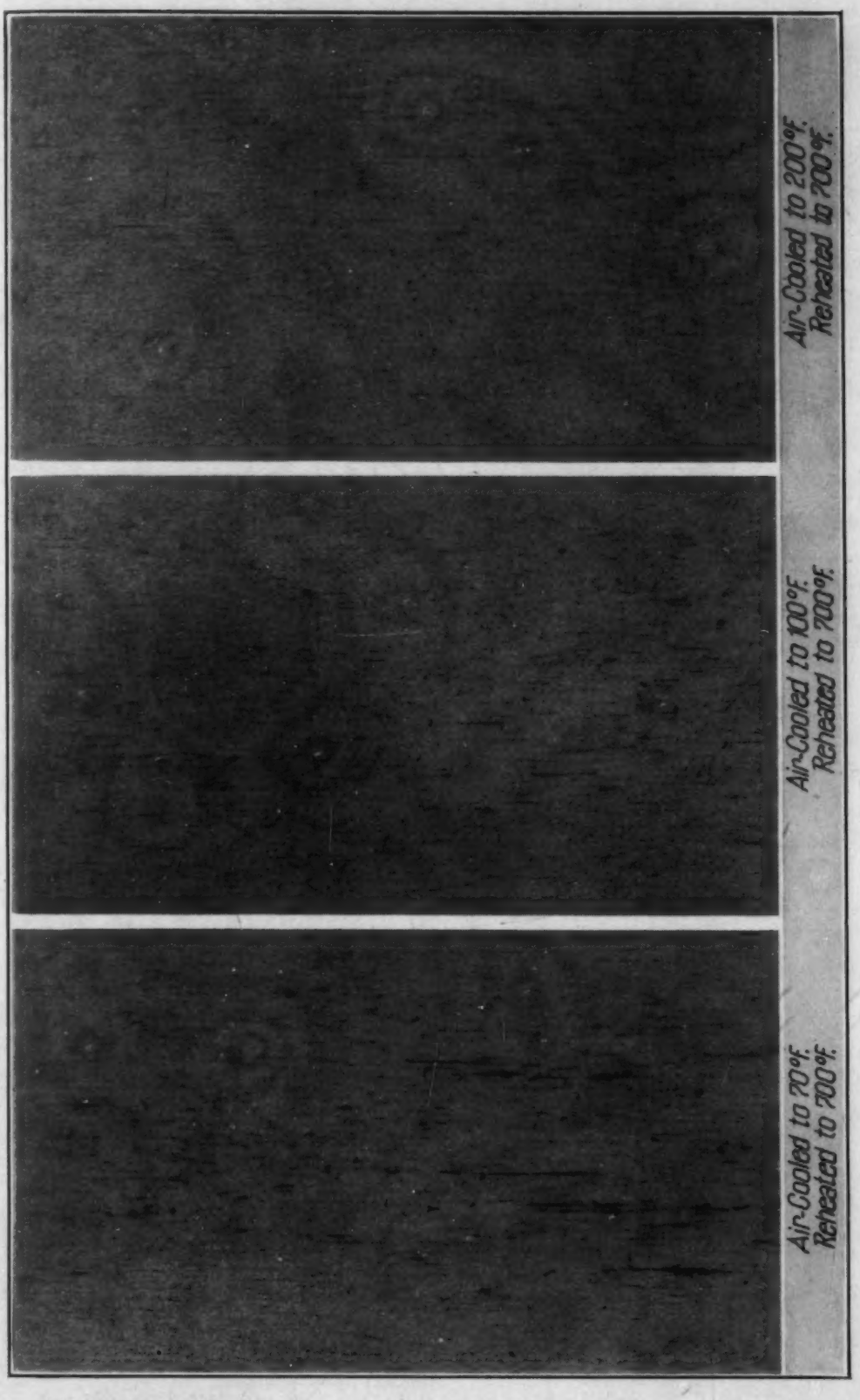

Fig. 1—Etched Rail Specimens. No Shatter Cracks in Top Rail Slice. Shatter Cracks in Bottom Two Slices. Etched in Hot 1-1 Hydrochloric Acid.

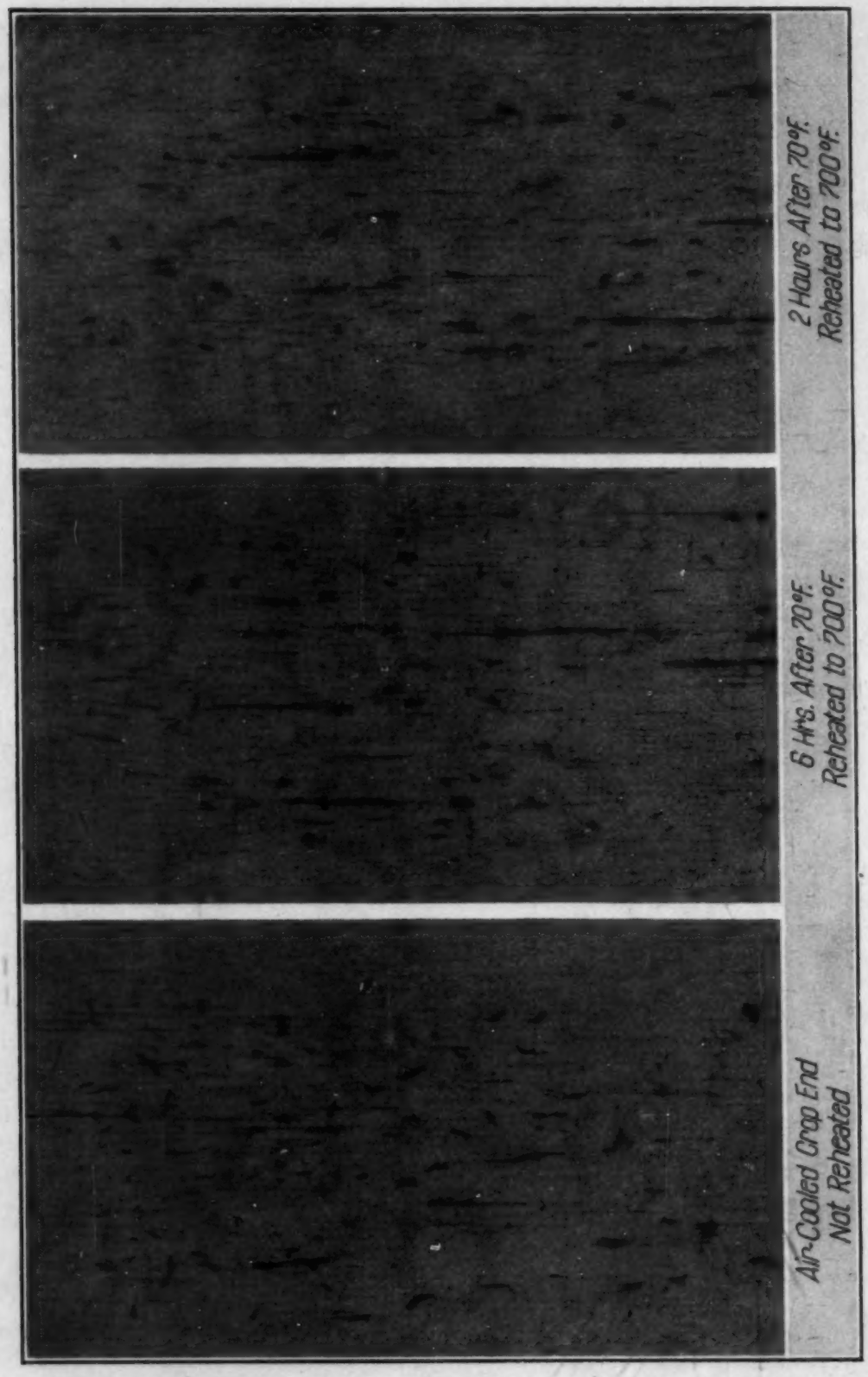

Fig. 2—Etched Rail Specimens. Shatter Cracks in All Rail Slices. Etched in Hot 1-1 Hydrochloric Acid.

Table II
Tests 1 and 2
Cooling Temperatures, Holding Times and Etch Test Results of Rail Specimens

Rail Specimen No.	Temperature Degrees Fahr. Rail Specimen Cooled in Still Air	Time Held Before Placing in Furnace at 700 Degrees Fahr. Hours	Shatter Cracks on 6-In. Specimen			
			Heat 85128		Heat 83263	
			Long.*	Trans.**	Long.*	Trans.**
500	500	0	0	0	0	0
400	400	0	0	0	0	0
300	300	0	0	0	0	0
200	200	0	0	0	0	0
100	100	0	7	1	5	0
70-0	70	0	30	8	25	6
70-2	70	2	50	9	43	7
70-4	70	4	56	8	48	5
70-6	70	6	67	14	55	12
Crop End	Cooled in Air	72 hours	78	27	69	18

*Longitudinal.
**Transverse.

increase both in number and size with time. In the past there has been considerable discussion whether such cracks formed suddenly or grew gradually. This experiment also shows that for the particular steel used in these tests the shatter cracks began to develop in the rails while they were cooling between 200 and 100 degrees Fahr. (93 and 38 degrees Cent.).

Tests 3 and 4

These experiments were designed to determine more completely the effect of holding specimens for varying lengths of time at temperatures between 400 and 100 degrees Fahr. (205 and 40 degrees Cent.) to ascertain if increased holding time at relatively low temperatures would allow the formation of shatter cracks. Further information was gained by using steels of different sensitivity to cracking, by varying the amount of hydrogen used in treating the ingots.

About 60 rail specimens, 1 foot in length, from heats 51106 and 54007 were cut as previously described. These were trucked while still at temperatures above 700 degrees Fahr. (370 degrees Cent.) to the mill heat treating department. In working with steel which may develop shatter cracks all experiments must be made while the specimens are cooling initially after rolling. Two electric furnaces and three steam heated water tanks were previously heated to the holding temperatures shown in Tables III and IV. The rail

Table III
Test 3
Number of Shatter Cracks in 6-inch Slice From Rail Heads
Heat 54007, Ingot 7—40 Cubic Feet Hydrogen

Time in Hours Rail Specimen Held at Temp.	Method of Cooling	Holding Temperature 100 Degrees Fahr.		150 Degrees Fahr.		200 Degrees Fahr.		250 Degrees Fahr.		300 Degrees Fahr.	
		L*	T**	L*	T**	L*	T**	L*	T**	L*	T**
0	Furnace†	113	9	18	3	8	0	0	0	0	0
2	Furnace†	80	7	96	7	58	3	28	0	4	0
4	Furnace†	92	5	74	6	45	1	24	0	9	0
6	Furnace†	97	4	68	5	74	3	25	0	13	0
8	Furnace†	120	13	72	6	70	0	22	0	22	0
10	Furnace†	103	9	83	6	65	3	25	0	20	0
0	Air††	210	10	210	10	210	10	210	10	210	10
2	Air††	52	3	70	6	62	0	25	0	24	0
4	Air††	95	3	75	6	60	2	10	0	36	0
6	Air††	73	7	90	8	80	7	9	0	26	0
8	Air††	104	9	90	5	50	3	21	0	10	0
10	Air††	72	7	60	8	60	6	20	1	15	0

*Longitudinal Cracks. **Transverse Cracks.
†Specimens reheated to 700 degrees Fahr. (370 degrees Cent.) after holding at given temperature.
††Specimens air cooled after holding at given temperature.

specimens were spread out evenly over the shop floor to cool to the holding temperatures. When a group of 11 specimens reached each holding temperature, 10 of them were put in a furnace or water tank at that temperature and one was placed in a reheating furnace operating at 700 degrees Fahr. (370 degrees Cent.). At 2-hour intervals, up to 10 hours, two specimens were removed from each

furnace or tank and one specimen cooled in air while the other was placed in the 700 degrees Fahr. (370 degrees Cent.) reheating furnace. This furnace was operated at temperatures for 7 hours after the last specimen was placed in it then slow cooled over a period of 10 hours.

Table IV
Test 4
Number of Shatter Cracks in 6-Inch Slice from Rail Heads
Heat 51106, Ingot 4—25 Cubic Feet Hydrogen

Time in Hours, Rail Specimen Held at Temp.	Method of Cooling	Holding Temperature 100° F. L*	100° F. T**	150° F. L*	150° F. T**	200° F. L*	200° F. T**	300° F. L*	300° F. T**	400° F. L*	400° F. T**
0	Furnace†	8	1	1	0	0	0	0	0	0	0
2	Furnace†	45	4	2	0	3	0	0	0	0	0
4	Furnace†	43	2	40	0	8	0	0	0	0	0
6	Furnace†	50	2	15	0	14	0	0	0	0	0
8	Furnace†	27	1	12	0	20	0	0	0	0	0
10	Furnace†	25	0	23	0	27	0	0	0	0	0
0	Air††	82	14	82	14	82	14	82	14	82	14
2	Air††	30	0	28	2	40	4	40	6	29	1
4	Air††	15	0	28	3	30	3	24	0	4	0
6	Air††	55	7	19	0	20	2	0	0	0	0
8	Air††	25	2	15	1	25	1	0	0	0	0
10	Air††	20	0	10	0	15	0	0	0	0	0

*Longitudinal Cracks. **Transverse Cracks.
†Specimens reheated to 700 degrees Fahr. (370 degrees Cent.) after holding at given temperature.
††Specimens air cooled after holding at given temperature.

Tables III and IV give the holding temperatures and time of holding for each specimen together with the number of longitudinal and transverse shatter cracks found in a 6-inch slice from each specimen. It will be noted that the control specimen for each test is the specimen held zero hours and cooled in air. The ingot of Heat No. 54007 was treated with 40 cubic feet of hydrogen which produced 210 longitudinal and 10 transverse shatter cracks in the control specimen, while only 25 cubic feet of hydrogen was used in the ingot of Heat No. 51106, producing 82 longitudinal and 14 transverse shatter cracks in the control specimen. This difference in the crack sensitivity of the two heats of steel explains why all the furnace cooled specimens of Heat No. 54007 held 2 hours or longer at 300 degrees Fahr. (150 degrees Cent.) developed shatter cracks while no shatter cracks developed in the specimens from Heat No. 51106, held at this same temperature up to 10 hours and furnace cooled.

It will be further observed from Table III that the specimen treated with 40 cubic feet of hydrogen developed a few shatter cracks when cooled to 200 degrees Fahr. (95 degrees Cent.) and

immediately reheated, and another specimen held at 300 degrees Fahr. (150 degrees Cent.) for only 2 hours developed a few cracks. The tests also show in Table IV that holding rails treated with 25 cubic feet of hydrogen at either 400 degrees Fahr. (205 degrees Cent.) or 300 degrees Fahr. (150 degrees Cent.) for 6 hours followed by cooling in air was sufficient treatment to prevent the formation of shatter cracks.

General Conclusions

The following general conclusions can be drawn from these experiments:

1. Shatter cracks develop gradually both in size and number in shatter sensitive carbon steel rails as they are allowed to cool between the range of 400 and 70 degrees Fahr. (205 and 21 degrees Cent.). The temperature at which shatter cracks were initially observed depended upon the manner in which the rails were cooled through this temperature range.
2. Shatter crack development continues after the rails reach room temperature and are held at this temperature for increasing periods of time.
3. Conclusions 1 and 2 apply only to shatter sensitive air cooled rails which are not controlled or held between temperatures of 1200 degrees Fahr. (650 degrees Cent.) to 400 degrees Fahr. (205 degrees Cent.) for lengths of time sufficient to properly eliminate shatter sensitivity.
4. The temperature at which shatter cracks begin to form and the amount of retarded cooling required to prevent their formation depend on the sensitivity of the steel to the development of shatter cracks.
5. It should be emphasized that besides the sensitivity of the steel to the development of shatter cracks or flakes, the mass factor of the finished product will have a major influence on the development of these defects. For this reason it is necessary to consider each flaking problem individually.

Acknowledgments

The work reported in this paper has been done in the Metallurgical Division, Rail Mill and Heat Treating Department of the Gary Works, Carnegie-Illinois Steel Corporation, which are under

the supervision of Messrs. A. N. Swanson, C. C. Deck, and H. A. V. Lundstrom, respectively. The co-operation and assistance rendered by these gentlemen and other members of their organization during the tests are acknowledged. R. E. Cramer participated in the tests because he is on the staff of the Investigation of Transverse Fissures in Railroad Rails, directed by Professor H. F. Moore at the University of Illinois in co-operation with Committee 4 of the A.R.E.A., of which Mr. W. H. Penfield is Chairman, and the Rail Manufacturers Technical Committee, Mr. L. S. Marsh, Chairman.

Bibliography

1. R. E. Cramer, "The Production of Flakes in Steel by Heating in Hydrogen," TRANSACTIONS, American Society for Metals, Vol. 25, Sept. 1937, p. 923-934.
2. H. B. Wishart and A. N. Swanson, "Methods of Preventing Shatter Cracks or Flakes in Carbon Steels," TRANSACTIONS, American Society for Metals, Vol. 27, Sept. 1939, p. 784-796.
3. C. A. Zapffe and C. E. Sims, "Hydrogen Embrittlement, Internal Stress and Defects in Steel," Technical Publication No. 1307, American Institute of Mining and Metallurgical Engineers, August 1941.
4. R. E. Cramer and E. C. Bast, "The Production of Flakes by Treating Molten Steel with Hydrogen and the Time of Cooling Necessary to Prevent their Formation," TRANSACTIONS, American Society for Metals, Vol. 27, June 1939, p. 433-457.
5. R. E. Cramer and E. C. Bast, "The Prevention of Flakes by Holding Railroad Rails at Various Constant Temperatures," TRANSACTIONS, American Society for Metals, Vol. 27, Dec. 1939, p. 923-934.

DISCUSSION

Written Discussion: By W. H. Penfield, chairman, Association of American Railroads, American Railway Engineering Association, Chicago.

The subject is one that has been of vital interest to the users of railroad rails for many years. Fissures originating in the head of rails and spreading under traffic were of much concern to the railroads and prior to the construction of the Sperry Transverse Fissure Detector equipment there was no method of detecting their presence in the rail heads until they reached the surface or until the rail failed in service.

Investigation finally associated the nuclei of the fissures with shatter cracks and an intensive study was undertaken to determine how shatter cracks in steel rails could be prevented. Various methods have been successfully used. The most practicable to date is to slow up the cooling from the rolling temperature to normal air temperature and prevent the cooling below a temperature of 300 degrees Fahr. (150 degrees Cent.) in less than 7 hours.

The paper prepared by Messrs. Wishart, Epler and Cramer is a splendid contribution to the study of shatter cracks and will be of much value in helping to find improved methods of preventing their formation in railroad rails.

Written Discussion: By L. S. Marsh, chairman, American Iron and Steel Institute, Technical Committee on Rails, Inland Steel Co., Chicago.

Some ten years ago agreement was entered into between the University of Illinois, the American Railway Association (now the Association of American Railroads), and the Rail Manufacturers' Technical Committee, for a cooperative investigation of the cause of failures of railroad rails in service together with their prevention, with particular reference to transverse fissures. The direction of the technical work was to be under Prof. H. F. Moore.

During the course of the investigation evidence was produced that a large percentage of the rails failing from internal transverse fissures, and sent to the University of Illinois Materials Laboratory for examination, also showed the presence of shatter cracks. Rolling load machines were designed to duplicate, as nearly as possible, the pressure and action of car wheels passing over the rails. Actual operating speeds could not be attained, but varying pressures could be applied. Details will not be gone into in this short discussion as they are all available in the reports of the investigation and have been published in the American Railway Engineering Association bulletins.

Suffice it to say however, that it was found possible to produce transverse fissures in many of those specimens of rails which, upon examination by etching, had indicated the presence of shatter cracks. On the contrary, specimens which were free from shatter cracks, did not produce transverse fissures when subjected to the same treatment. A sufficiently large number of specimens were examined during the investigation to warrant the conclusion that the "shatter crack" was the beginning of the internal transverse fissure. While we are not prepared to state that this is the only source of the transverse fissure, it undoubtedly accounts for a very high percentage of this type of defect.

As it was apparent that the shatter crack was responsible for a great deal of the trouble it became necessary to find a practical means for preventing the formation of these defects which were, apparently, the nuclei for the formation of internal transverse fissures.

In 1931 the Canadian metallurgist, I. C. Mackie, began the control cooling of rails and his method, with some changes in equipment and temperatures of charging into and removal from the boxes in which the rails were placed, is being used at the present time.

As a result of the work done by the University of Illinois in connection with the rails investigation previously referred to, much has been learned as to critical temperatures involved in the process. A large amount of data has been tabulated after checking temperatures in the control cooling boxes at the various mills, by the test party from the University of Illinois. All of this work has been done with the idea of obtaining information which could be used in preparing a workable specification for control cooling.

In order that a comparative test could be made between sound rails and those known to contain shatter cracks, it became necessary to resort to the introduction of hydrogen into the molten steel in accordance with the methods referred to in the bibliography appended to the paper under consideration.

As a means of obtaining comparative test specimens this method has been extremely satisfactory. However, from a practical manufacturing standpoint,

it would be unfortunate should the conclusion be drawn that absorption of hydrogen was, or is, the basic cause for the formation of shatter cracks in steel rails.

So far as I know, this has not been proven to be the case. Moreover, it is quite possible that nonmetallic inclusions and gas pockets may have a definite bearing on the problem. There are two points brought out in the paper which are, in my opinion, important, namely: the "sensitivity of the steel to the development of shatter cracks," and the "mass factor of the finished product...." So far as my information goes we have no practical method of predetermining the shatter sensitivity of the steel. The problem of the "mass factor" will become less uncertain as the tonnage of the two standardized rail sections increases.

Control cooling equipment requires a large amount of space in the steel mill and, as rails must be rapidly moved from the hot beds to the control cooling boxes, the distance which they have to be carried by the cranes is restricted because of the possible dropping of temperature to too low a point.

As space for control cooling boxes is at a premium in the rail mill it is therefore important that the capacity of these boxes should be used to the greatest possible extent. This means that rails must be in the boxes the shortest possible time which will result in a satisfactory job of control cooling. Because of this fact the information which has been worked up by the authors of the paper is extremely valuable, largely because it can be used as a basis for specifications covering a practical method of control cooling with, of course, the inclusion of the necessary time and temperature safety factors.

It would be of interest to know, in order to more definitely establish a top limit, whether the steel of Table III, test 3, treated with 40 cubic feet of hydrogen would have been free of shatter cracks at 400 degrees Fahr. (205 degrees Cent.).

To get the experimental work a little closer to the practical problem of commercial rails, it is suggested that the experimenters make a series of rail steel ingots with decreasing hydrogen to the vanishing point and repeat the experiments of the paper.

The authors of the paper deserve commendation for the method of handling specimens and the orderly procedure in carrying out their tests and reporting results.

Written Discussion: By E. C. Bast, metallurgist, Atchison, Topeka and Santa Fe Railway Co., Topeka, Kansas.

The work of Messrs. Wishart, Epler, and Cramer is of considerable interest in giving further evidence of the formation and prevention of shatter cracks in steel rails. There apparently is no doubt that hydrogen is the primary cause for shatter sensitive steel. They have shown that the amount of hydrogen injected in the molten steel influences the sensitivity of the rails to shatter cracking, and that this sensitivity governs the temperature at which shatter cracks begin to form and the amount of retarded cooling required to prevent their formation. It is interesting to note that shatter cracks develop gradually and are not suddenly formed by a trapped gas pocket or burst.

It would be interesting to know if hydrogen can collect in defined areas

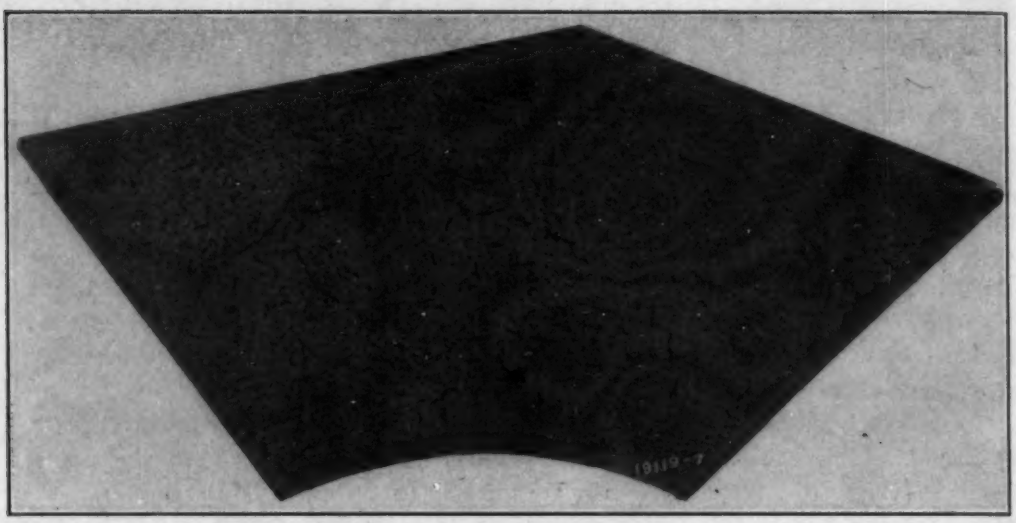

Fig. A—Deep Etched Longitudinal Center Section of the Hub of a Diesel Locomotive Wheel Showing Numerous Large Shatter Cracks Dispersed Throughout the Entire Hub.

in steel rails and yet not show evidences of shatter cracks, but still weaken the rail in these areas so that they may serve as nuclei for fissures.

The seriousness of crack sensitive steel is so important that any information on the formation and prevention of shatter cracks in steel is a welcomed contribution. To cite an example of how shatter cracked rails behave in service; some of the rails sent in by our Detector Car crew were subjected to drop test throughout the full length and showed so brittle and such poor structural condition due to shatter cracks that it is surprising they did not break in service or in handling after removal. One of the 112-pound rails drop tested showed 38 transverse fissures and 11 nuclei in 49 fractures produced in the 39-foot length. It is certainly a relief to know that new rails subjected to the proper controlled cooling will definitely prevent future serious rail conditions of this nature.

It seems most of the contributions on shatter cracks have been related to steel rails. The accompanying photograph of a deep etched longitudinal center section of the hub of a Diesel Locomotive wheel shows numerous large shatter cracks dispersed throughout the entire hub, merely illustrating the formation of shatter cracks in members other than rails with essentially the same chemical composition.

Oral Discussion

B. M. LARSON:[1] First, I noticed that the longitudinal cracks predominate over the transverse ones; there are many more longitudinal ones. I wonder whether that indicates that nonmetallic particles, rolled out in the direction of rolling the rail, serve as nuclei for fissures, perhaps by acting as starting places for build up of pressure due to H_2 or CH_4.

I am also curious as to whether there is any evidence that transverse

[1]Physical chemist, United States Steel Research Laboratory, Kearny, N. J.

fissures in rails start only from transverse cracks or also from longitudinal cracks.

H. STYRI:[2] I should like to know whether you have any proof that these so-called shatter cracks are cracks and not etching lines, and if so, I would like to know the method used to determine whether or not it is a crack.

CHARLES TURNER, JR.:[3] What effect does the degree of work have on flaking?

Authors' Reply

The authors at this time wish to express their appreciation for the comments made in connection with this paper.

We believe that Mr. Penfield's discussion requires no comment.

In connection with Mr. Marsh's comments, the exact method of shatter crack formation has not been definitely determined. However, from the work that has been done on the subject it is indicated that hydrogen has some influence on shatter formation in steel. Shatter cracks apparently are caused by a stress build up in the steel. In all probability the damaging stresses causing shatter results from some combination of cooling stresses and stresses produced by gases as the steel temperature decreases.

With regard to Table III, it was thought in making the test that holding rails at 300 degrees Fahr. (150 degrees Cent.) after air cooling from rolling heat would suffice to relieve shatter sensitivity in the steel. In this case the heat was extremely shatter sensitive and 300 degrees Fahr. (150 degrees Cent.) holding was not sufficient to prevent shatter. The fourth test was, therefore, made involving a holding temperature of 400 degrees Fahr. (205 degrees Cent.). The steel used in this test apparently was not as sensitive to shatter formation as the steel used in the third test. Since the writing of this paper another series of tests have been made in which a comparable amount of hydrogen to that used in the third tests was piped into the steel as it was being teemed into ingot form. No shatter cracks were developed at 400 degrees Fahr. (205 degrees Cent.) holding temperatures on specimens reheated and controlled cooled. Six hours of holding at 400 degrees Fahr. (205 degrees Cent.) were required to prevent shatter in specimens air cooled from this holding temperature. This steel was not quite as sensitive to shatter as the steel from the third test. It is to be mentioned that the amount of hydrogen used is not always an index as to the shatter sensitivity of the steel. Other factors such as chemistry of the steel, apparently have an effect on the final degree of shatter sensitivity.

We agree with Mr. Bast in his discussion that there is a possibility that hydrogen could collect in localized areas in steel and yet while not causing shatter cracks, could produce a region of high localized stress. Where the rails are properly controlled, cooled or held at some temperature between 1250 and 400 degrees Fahr. (675 and 205 degrees Cent.) for a sufficient length of time to relieve the shatter sensitivity, there is a possibility that such areas will not form or if they do will be minimized or relieved by this treatment.

---

[2]Director of research, SKF Industries, Philadelphia.

[3]Assistant metallurgist, Camden Forge Co., Camden, N. J.

Referring to Mr. Larson's questions, it is possible that nonmetallic particles and the direction of rolling has an influence on the direction of shatter crack formation. The particles in some instances apparently act to some degree as hydrogen nucleation zones which in turn produce shatter. The direction of shatter cracks can also be influenced by cooling stresses, such as rim-core stresses which should be instrumental in the development of longitudinal cracks.

The question of whether transverse fissures start from longitudinal or transverse shatter cracks is a difficult one to answer. The writers have examined a number of transverse fissured rails where it would be entirely a guess as to the direction of the shatter crack which was the nucleus of the fissure. Rails have been examined which contained fissures and only longitudinal shatter cracks as indicated by etch tests. Whether the shatter crack causing the fissure in such cases was longitudinal in direction is problematical. In all probability shatter cracks in either direction can be potential nuclei for transverse fissures.

With regard to Dr. Styri's question, the method most generally used to detect shatter cracks is by etching the specimen in a hydrochloric acid solution. There has been some controversy as to whether the cracks which are apparent after etching are etching lines or the enlargement of cracks not apparent to the eye before etching. The writers have on several occasions noticed shatter cracks in specimens which were not etched when examined with the aid of a microscope. Shatter cracks were also observed to open up in tension specimens made from shatter sensitive steel as the specimens were being pulled.

In connection with Mr. Turner's question as to the effect of work on flaking or shatter cracks, it has been indicated that the greater the porosity of the steel the less the tendency to flake. As the steel becomes denser due to rolling, the conditions for shatter formation in a shatter sensitive steel are enhanced to some degree. The mass factor is also an important function in the shatter crack problem. Where shatter sensitive carbon grade steel is rolled into 1½-inch rounds or smaller there is little difficulty experienced with shatter cracks. This is probably due to the gases being able to diffuse from the steel without the formation of localized stressed areas.

THE NICKEL-MOLYBDENUM SYSTEM

By Finley H. Ellinger

Abstract

This paper presents the nickel-molybdenum constitutional diagram as constructed chiefly from metallographic and X-ray data. The diagram shows that the addition of molybdenum to nickel causes the solidus-liquidus temperatures to be gradually lowered from the melting point of pure nickel to the eutectic temperature at 1320 degrees Cent. (2410 degrees Fahr.). The eutectic point occurs at 46.5 per cent molybdenum. At 1370 degrees Cent. (2500 degrees Fahr.) a peritectic reaction occurs between the liquid and the molybdenum-rich solid solution by which is formed the phase corresponding to the ratio NiMo of 62 per cent molybdenum content. At the peritectic temperature the molybdenum-rich solid solution dissolves 0.9 per cent nickel. The solubility of molybdenum in the nickel-rich solid solution decreases from 37 per cent at the eutectic temperature to 30 per cent at 890 degrees Cent. From 890 to 600 degrees Cent. (1635 to 1110 degrees Fahr.) the solubility falls to 20.5 per cent molybdenum.

At 890 degrees Cent. (1635 degrees Fahr.) a peritectoid reaction occurs between the nickel-rich solid solution and the intermetallic constituent NiMo and forms the phase corresponding to the ratio Ni_3Mo. At 840 degrees Cent. (1545 degrees Fahr.) another peritectoid reaction occurs between the nickel-rich solid solution and the phase Ni_3Mo and yields the phase corresponding to the ratio Ni_4Mo.

Age-hardening properties of nickel-rich alloys from 21 to 35 per cent molybdenum content were determined. These age-hardenable compositions fall into two groups, (1) those that harden by the precipitation of Ni_4Mo in the supersaturated nickel-rich solid solution, and (2) those that harden by the decomposition of the supersaturated solid solution into two new phases, Ni_4Mo and Ni_3Mo.

THIS investigation is a continuation of the study of alloy systems involving tungsten and molybdenum with iron, cobalt and nickel,

*Much of the material in this paper is taken from a thesis submitted by Finley H. Ellinger in partial fulfillment of the requirements for the degree of Metallurgical Engineer, Case School of Applied Science, June, 1941.

A paper presented before the Twenty-third Annual Convention of the Society held in Philadelphia, October 20 to 24, 1941. The author, Finley H. Ellinger, is associated with the General Electric Co., Cleveland. Manuscript received June 23, 1941.

which have been a subject of research at the Cleveland Wire Works of General Electric Company for the past number of years.

The most recent study of the nickel-molybdenum system was reported in two parts by Grube and Schlecht (1)[1], and by Grube and Winkler (2) who constructed their diagram chiefly by methods of electrical resistivity and magnetic susceptibility but also investigated the corrosion resistance, hardness, X-ray patterns and microstructure of the alloys. The above authors reported two new constituents, the beta phase and the compound Ni_3Mo, but otherwise the results of their work agree quite well with that of previous investigations. They placed the eutectic horizontal at 1300 degrees Cent. (2370 degrees Fahr.) reaching from 37 to 62 per cent molybdenum and the eutectic point at 50 per cent molybdenum. The peritectic reaction was found to occur at 1345 degrees Cent. (2455 degrees Fahr.) and to yield as a product the compound NiMo of 62 per cent molybdenum. The peritectic horizontal reached from the liquid at 55 per cent molybdenum to 100 per cent molybdenum.

The chief difference, outside of slight variations in transformation temperatures and compositions of phases, between Grube and Winkler's diagram and that of the present investigation is the interpretation of the beta phase. The evidence to support the present interpretation was obtained chiefly by metallographic, X-ray and age-hardening data.

Methods and Materials

The alloys used in this investigation were prepared from hydrogen reduced metal powders in the same manner as has been previously described (3). This consisted essentially of securing an intimate mixture of the powders, briquetting and subsequently sintering or melting in a hydrogen atmosphere. The nickel-rich compositions could be rolled into slabs at 1000 to 1200 degrees Cent. (1830 to 2190 degrees Fahr.) but considerable difficulty was encountered with cracking during the first few passes through the rolls. It is believed that hydrogen in the metal was the chief source of this trouble.

Lines of solid solubility and transformation horizontals in the solid were determined by microscopic examination of samples quenched in water after long periods of homogenization at suc-

[1]The figures appearing in parentheses pertain to the references appended to this paper.

cessively decreasing temperatures. The procedure was to place a group of specimens of like composition in the furnace at a temperature above that being determined and to bring to equilibrium by annealing for 25 to 50 hours. Then a specimen was quenched, the remaining samples being furnace-cooled through an interval of temperature and homogenized again before quenching another specimen. In this way the temperature being determined could be bracketed within the interval of temperature in which a phase change was observed. By making successive runs and decreasing the interval of temperature each time, the change in state was determined to ±10 degrees Cent.

An etchant, made up of 2 parts of 20 per cent hydrochloric acid plus 1 part of hydrogen peroxide and used electrolytically at 0.05 ampere per square centimeter, was found to be a good all around etchant for the Ni-Mo alloys. It attacks all the phases except the molybdenum-rich constituent (epsilon) and for this phase either a $\frac{1}{10}$ normal sodium hydroxide or an alkaline sodium picrate solution, both used electrolytically, was found to be satisfactory. A solution of 1 part of phosphoric acid plus 4 parts of hydrogen peroxide was useful in revealing the intermetallic phase NiMo in a nickel-rich matrix. A solution of 19 parts sulphuric acid plus 1 part of nitric acid, used hot, rapidly etches the intermetallic phase NiMo. This solution is also useful in etching 2-phase structures of alpha plus gamma, it having a preferential attack upon gamma.

Constitutional Diagram

Liquidus-Solidus Temperatures—The phrase diagram as drawn from the results of this investigation is shown in Fig. 1. The solidus curve above the alpha field was determined by visual observation of the point at which alloys of 10, 20, 26 and 30 per cent molybdenum began to fuse, the temperature being read with an optical pyrometer. For these determinations pressed bars sintered at 1300 degrees Cent. (2370 degrees Fahr.) for 65 hours were used because they were much more uniform than melted alloys in which coring is very severe. The specimens were in the form of slender, four-sided pyramids with one side rough polished. This polished side of the cone faced the mouth of the furnace and reflected the dark exterior so that any minute change in the surface was easily detected.

For each determination two cones of different compositions were

mounted in the tube of the hydrogen furnace on an alundum block. Since the temperature had to be read on the furnace wall, an alundum shield was placed directly behind the specimens in order to lessen the cooling effect of the flow of hydrogen through the tube. The specimens were placed in the furnace at 50 to 100 degrees Cent. below their approximate melting point and held at that temperature

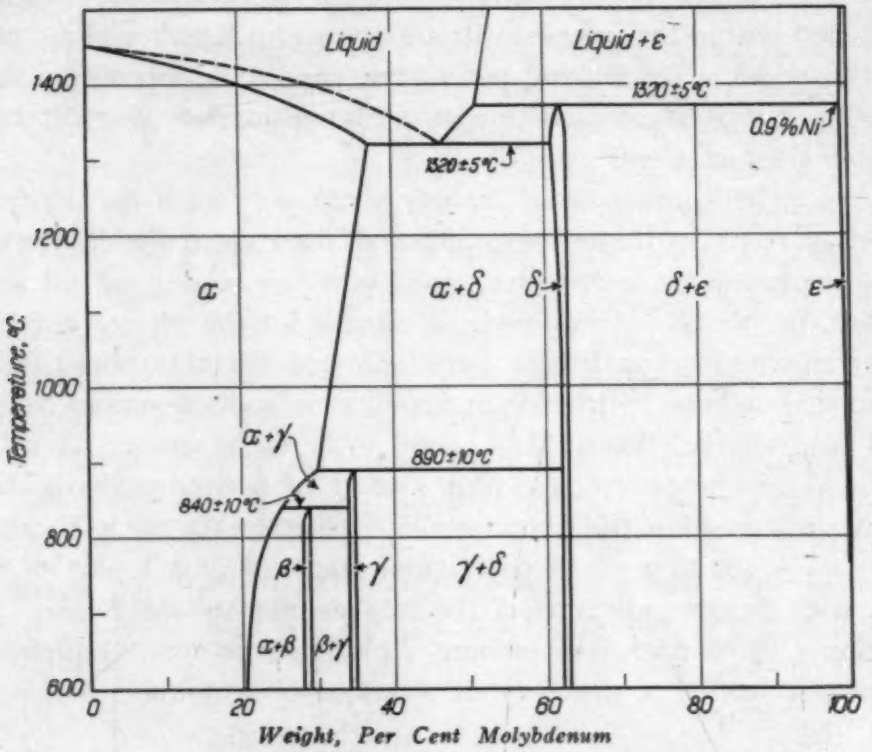

Fig. 1—Constitutional Diagram of Nickel-Molybdenum System.

for 1 hour. Then the temperature was raised at the rate of not more than 1-2 degrees Cent. per minute and read continuously to plus or minus 3 degrees Cent. The first evidence of liquid was a mottled appearance of the surface of the specimen which would shortly become covered with liquid metal. The liquidus temperature could be approximated by noting the temperature at which the cone had completely collapsed and formed into a ball of liquid.

The eutectic temperature was determined by the examination of the microstructures of a series of specimens containing 40 per cent molybdenum, quenched in water from a series of increasing temperatures. Three sections of an ingot that had been solidified slowly to obtain a well formed eutectic structure were placed on an alundum slab in the furnace. The temperature was stabilized at

1300 degrees Cent. (2370 degrees Fahr.) and then raised at the rate of 1-2 degrees per minute. Several determinations were made first in order to approximate the eutectic temperature, the temperature being read with an optical pyrometer. For the final determination the temperature was checked with a platinum-platinum-rhodium thermocouple and a Leeds and Northrup portable potentiometer with automatic cold junction compensation. Fig. 2 shows the structure of a specimen quenched from 1312 degrees Cent. (2395 degrees Fahr.). There is no change from the as-solidified structure which consists of areas of eutectic in a matrix of alpha solid solution. In the specimen quenched at 1320 degrees Cent. (2410 degrees Fahr.) (Fig. 3) the areas of eutectic have been entirely liquid and have now solidified as a fine eutectic structure. In the specimen quenched from 1325 degrees Cent. (2415 degrees Fahr.) (Fig. 4) it is seen that some primary alpha solid solution has melted and on quenching has crystallized as dendrites in the areas of fine eutectic. Accordingly, the eutectic temperature was placed at 1320 $\pm$ 5 degrees Cent. (2410 degrees Fahr.).

To locate the eutectic point, alloys of 45 and 50 per cent molybdenum that had been solidified slowly were examined for the amount of eutectic present. These structures indicated the eutectic composition to be slightly above 45 per cent molybdenum. Alloys of 46 and 47 per cent molybdenum, therefore, were prepared as above. The 46 per cent molybdenum alloy (Fig. 5) contained a slight amount of primary alpha solid solution and the 47 per cent molybdenum alloy (Fig. 6) contained a slight amount of primary delta compound. In view of these structures the eutectic composition was fixed at 46.5 per cent molybdenum.

The peritectic temperature was determined by the examination of the microstructures of a series of previously sintered 60 and 70 per cent molybdenum specimens after quenching from a series of increasing temperatures. The absence of any epsilon in the 60 per cent molybdenum specimens (Fig. 7) and of any liquid in the 70 per cent molybdenum specimens quenched from below 1370 $\pm$5 degrees Cent. (2500 degrees Fahr.) established this temperature as being that of the peritectic horizontal.

The nickel-rich end of the peritectic horizontal was determined by heating previously sintered specimens of 50, 51, 52, and 53 per cent molybdenum to the peritectic temperature and cooling rapidly. The 50 per cent molybdenum specimen showed no epsilon pres-

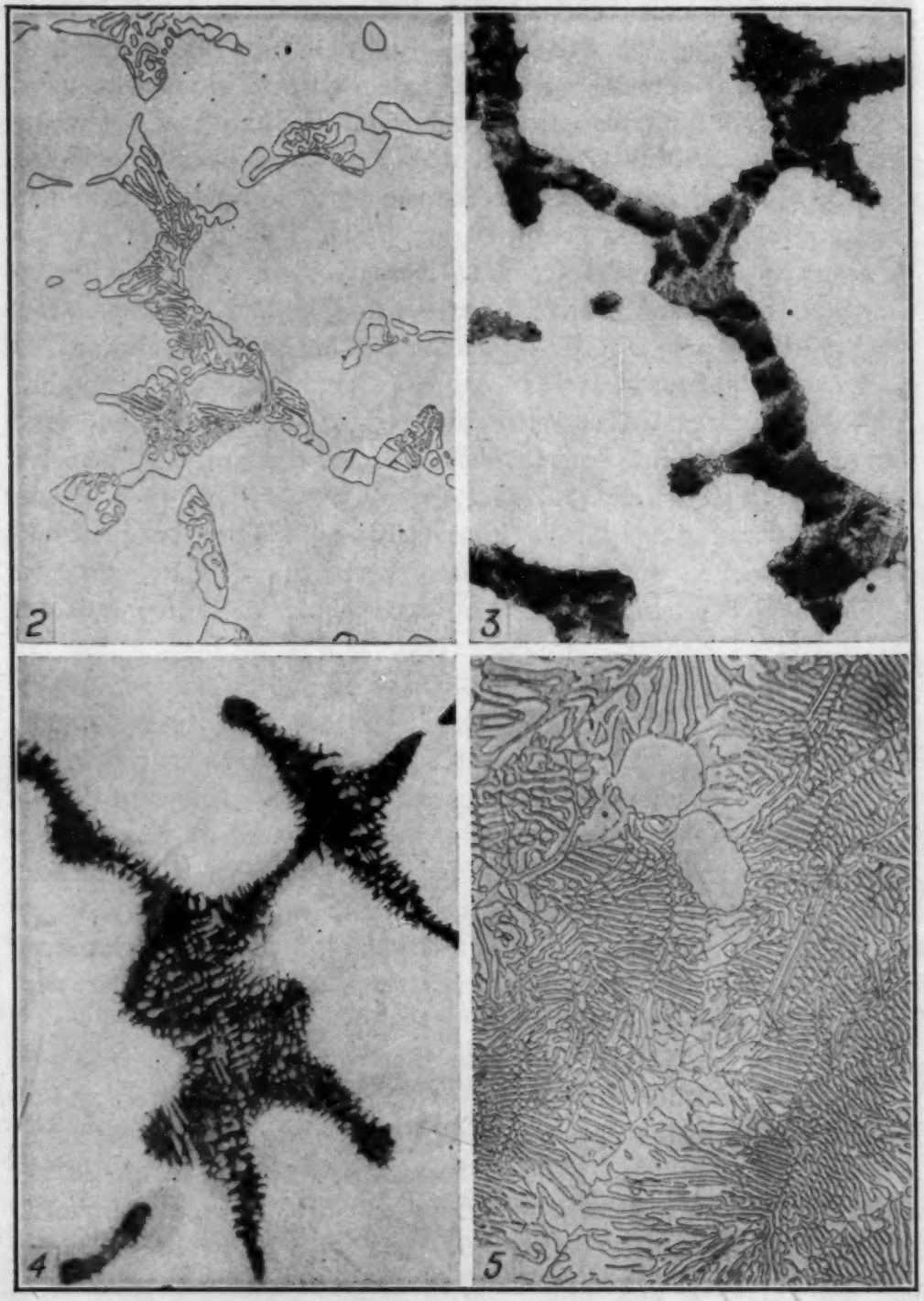

Fig. 2—40 Per Cent Molybdenum. As Solidified from Melt, Reheated and Quenched from 1312 Degrees Cent. Phosphoric Etch. Eutectic Plus Primary Alpha. × 200.

Fig. 3—40 Per Cent Molybdenum. As Solidified from Melt, Reheated and Quenched from 1320 Degrees Cent. Phosphoric Etch. Areas of Eutectic Had Been Liquid at 1320 Degrees Cent. × 200.

Fig. 4—40 Per Cent Molybdenum. As Solidified from Melt, Reheated and Quenched from 1325 Degrees Cent. Phosphoric Etch. Some Primary Alpha Had Been Liquid at 1325 Degrees Cent. × 200.

Fig. 5—46 Per Cent Molybdenum. As Solidified Slowly from Melt. Phosphoric Etch. Eutectic Plus Slight Amount of Primary Alpha. × 200.

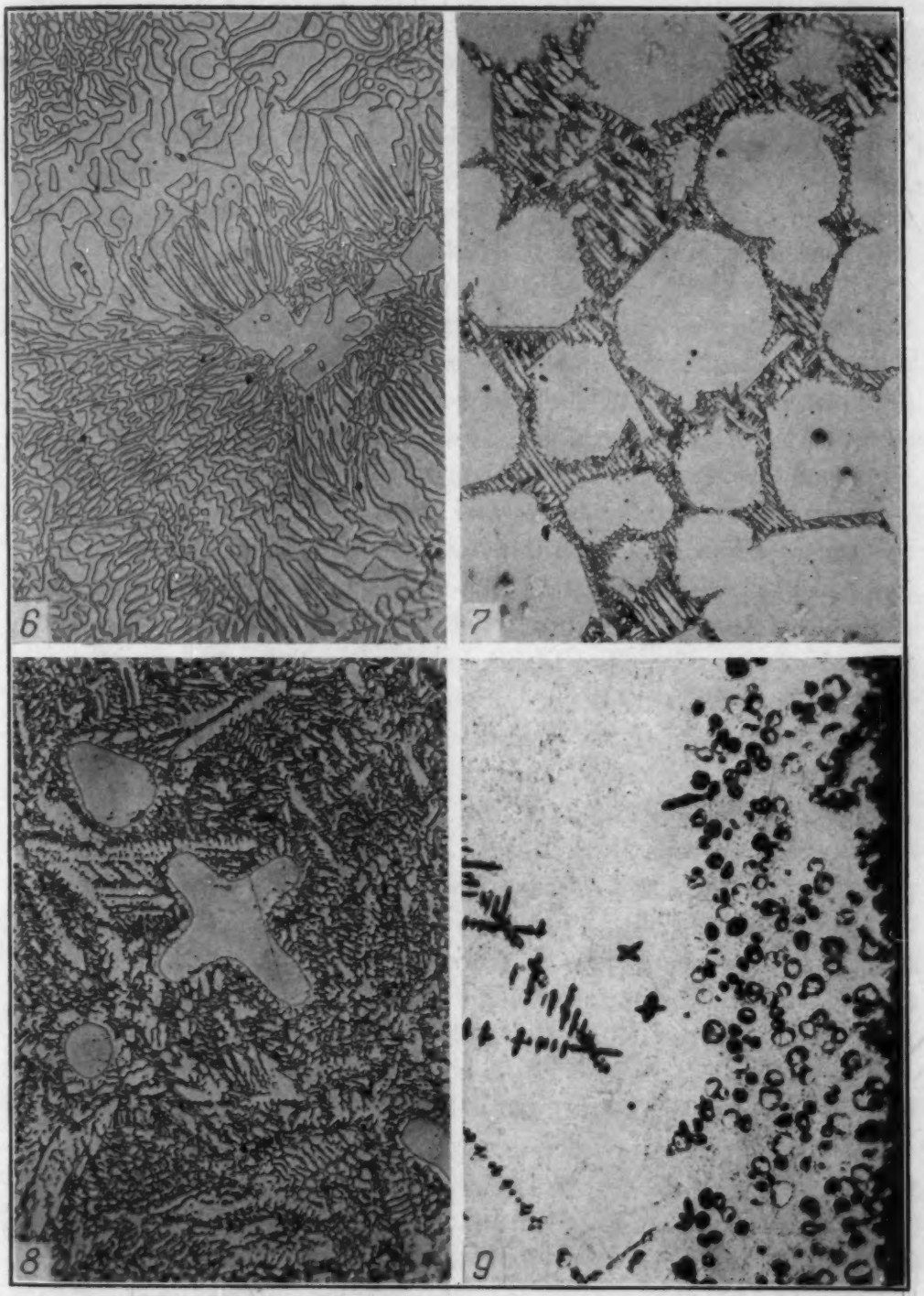

Fig. 6—47 Per Cent Molybdenum. As Solidified from Melt. Phosphoric Etch. Eutectic Plus Slight Amount of Primary Delta. × 200.

Fig. 7—60 Per Cent Molybdenum. Sintered at 1300 Degrees Cent. for 65 Hours. Reheated to 1365 Degrees Cent. and Quenched. Hydrochloric Etch. Delta Plus Liquid. × 200.

Fig. 8—52 Per Cent Molybdenum. Sintered at 1300 Degrees Cent. for 45 Hours. Reheated to 1375 Degrees Cent. and Quenched. Phosphoric Etch. Primary Epsilon Plus Liquid. × 200.

Fig. 9—55 Per Cent Molybdenum. As Cooled Rapidly from Melt at 1550 Degrees Cent. Caustic Etch. Undissolved Globules of Molybdenum at Bottom and Primary Epsilon Dendrites. × 100.

ent; that is, at the peritectic temperature this composition is in the all liquid field. The 51 per cent molybdenum specimen showed just a trace of epsilon and the 52 per cent molybdenum specimen showed considerable primary epsilon (Fig. 8) indicating that these two latter compositions had passed into the liquid plus epsilon field. From this evidence the nickel-rich end of the peritectic horizontal was placed at 51 per cent molybdenum.

The course of the liquidus curve above the epsilon plus liquid field was determined by melting rapidly 55 per cent molybdenum pressed bars at a series of temperatures, cooling rapidly from temperature, and examining the structure for the presence of undissolved molybdenum. Particles of undissolved molybdenum could be readily identified from particles of epsilon by their globular shape and also by their presence at the bottom of the ingot as shown in Fig. 9. At temperatures above 1575 to 1600 degrees Cent. (2865 to 2910 degrees Fahr.) particles of undissolved molybdenum could no longer be detected. Epsilon, which crystallized from the melt on cooling through the epsilon plus liquid field, was always present as small, uniformly distributed dendrites, as also shown in Fig. 9.

Solubility of Molybdenum in Alpha Solid Solution—The maximum solubility of molybdenum in alpha solid solution was placed at 37 per cent molybdenum at the eutectic temperature. This was determined by sintering 35, 36, 37 and 38 per cent molybdenum pressed specimens at 1300 degrees Cent. (2370 degrees Fahr.) for 65 hours, after which period maximum solution of the molybdenum had been obtained. A mere trace of delta phase was observed in the 37 per cent molybdenum alloy which justified making this composition the limit of solubility at the eutectic temperature.

The limit of solid solubility of delta in alpha solid solution with decreasing temperature, as shown in Fig. 1, was determined within 1 per cent molybdenum at all 50 degrees Cent. intervals of temperature between 900 and 1200 degrees Cent. (1650 and 2190 degrees Fahr.). It was found to be very nearly a straight line running between 37 per cent molybdenum at 1320 degrees Cent. (2410 degrees Fahr.) and 30 per cent molybdenum at 890 degrees Cent. (1635 degrees Fahr.). This decrease in solubility is illustrated by Figs. 10 and 11 of 34 per cent molybdenum specimens quenched from 1100 and 900 degrees Cent. (2010 and 1650 degrees Fahr.) respectively. The first precipitate of delta is observed in the grain boundaries of the 1100 degrees Cent. (2010 degrees Fahr.) speci-

men. At lower temperatures precipitation occurs chiefly within the alpha grains.

Below 890 ± 10 degrees Cent. there is, at first, a rapid decrease in the solubility of molybdenum in nickel. With lowering temperatures, however, the rate of decrease gradually diminishes until at 600 degrees Cent. (1110 degrees Fahr.) and 20.5 per cent molybdenum the solubility line becomes practically vertical.

Gamma Phase and Peritectoid Reaction—The intermetallic phase (gamma) of 34 to 35 per cent molybdenum and corresponding to the ratio Ni_3Mo is produced by the peritectoid reaction alpha plus delta $\rightleftarrows$ gamma at 890 ± 10 degrees Cent. (1635 degrees Fahr.).

Evidence of the peritectoid reaction is shown in Figs. 11 to 14 inclusive. By taking a group of specimens of 34 per cent molybdenum which had been homogenized at a temperature just above that of the gamma peritectoid horizontal to produce alpha plus delta (Fig. 11) and reheating them at 850 to 875 degrees Cent. (1560 to 1605 degrees Fahr.) for increasing periods of time, the progress of the alpha plus delta → gamma reaction could be observed. On heating in the alpha plus gamma field, first of all, plates of gamma precipitate, forming banded alpha plus gamma grains (Fig. 12). Then the layers of alpha react with the delta, consequently forming indentations in the particles of delta as shown in Fig. 13. After 200 hours at 875 degrees Cent. (1605 degrees Fahr.) the delta particles appear of very irregular contour due to the reaction as shown in Fig. 14.

Structures consisting almost entirely of the gamma compound were produced in two ways. Fig. 15 shows the structure produced by rapidly cooling a homogenized specimen of gamma composition from 1300 degrees Cent. (2370 degrees Fahr.) to just below the peritectoid temperature and holding there for 300 hours. It consists of large grains, originally alpha, bearing acicular markings.

A finer-grained gamma structure (Fig. 16) was obtained by reheating a cold worked alpha solid solution at 875 degrees Cent. (1605 degrees Fahr.) after which the alpha is seen to have recrystallized to a fine-grained gamma in which the markings are not as evident as in Fig. 15. In this latter specimen a few particles of delta, deeply etched, are also present.

Upon reheating the gamma structure, shown in Fig. 15, just above the peritectoid temperature for several hours, the gamma decomposes to alpha plus a fine dispersion of delta particles as shown in Fig. 17. This same structure reheated to 1100 degrees Cent.

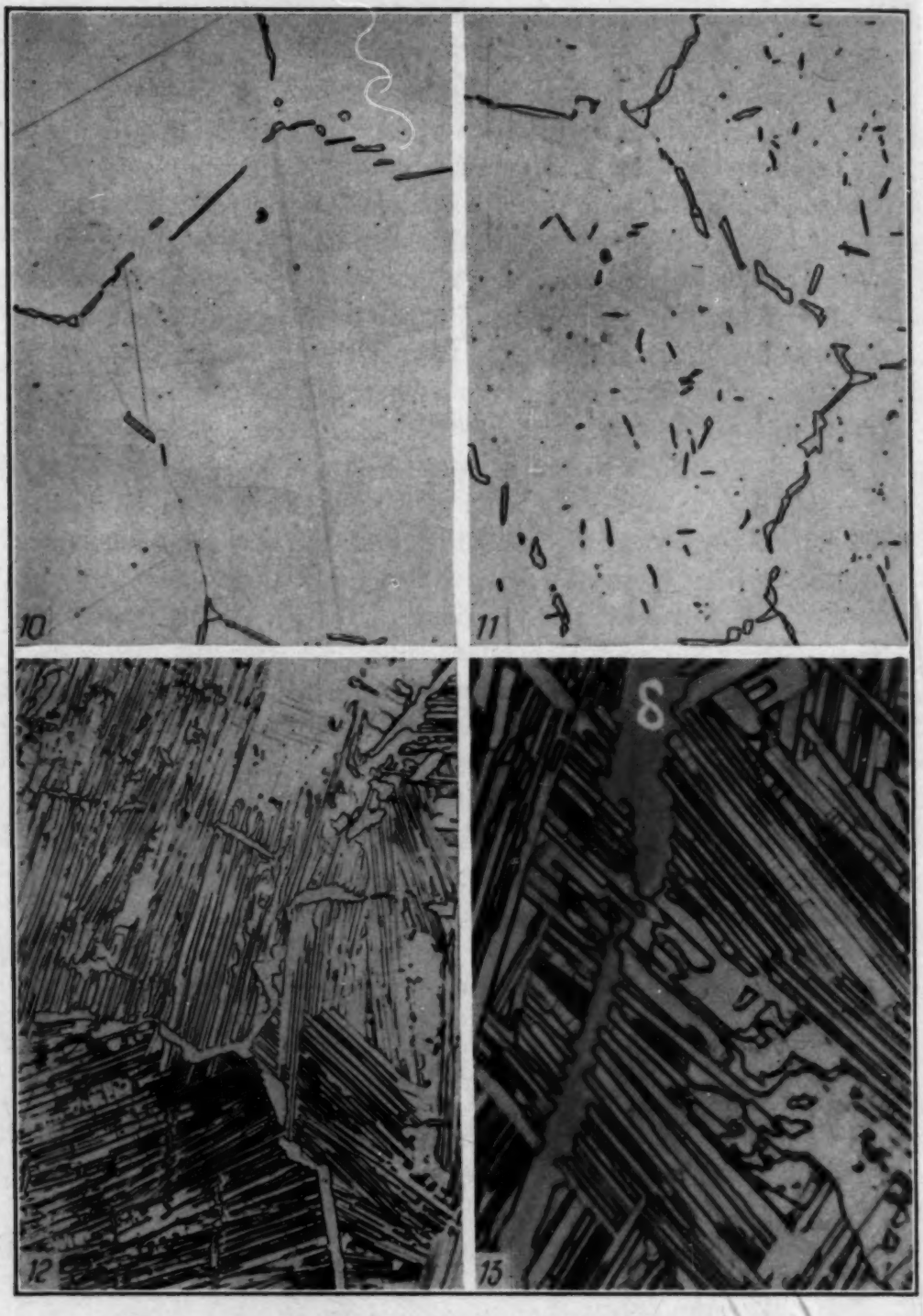

Fig. 10—34 Per Cent Molybdenum. Rolled, Heated Successively 1300 Degrees Cent.—20 Hours, 1200 Degrees Cent.—25 Hours, 1100 Degrees Cent.—65 Hours and Quenched. Phosphoric Etch. Alpha Plus Precipitate of Delta. × 200.

Fig. 11—Same Composition and Treatment of Fig. 10 After Additional 50 Hours at 1000 Degrees Cent. and 100 Hours at 900 Degrees Cent. Phosphoric Etch. Alpha Plus Precipitate of Delta. × 200.

Fig. 12—Same Composition and Treatment of Fig. 11 After Additional 25 Hours at 875 Degrees Cent. Hydrochloric Etch. Banded Grains of Alpha Plus Gamma with Residual Delta. × 500.

Fig. 13—Same Specimen Shown in Fig. 12. × 1500.

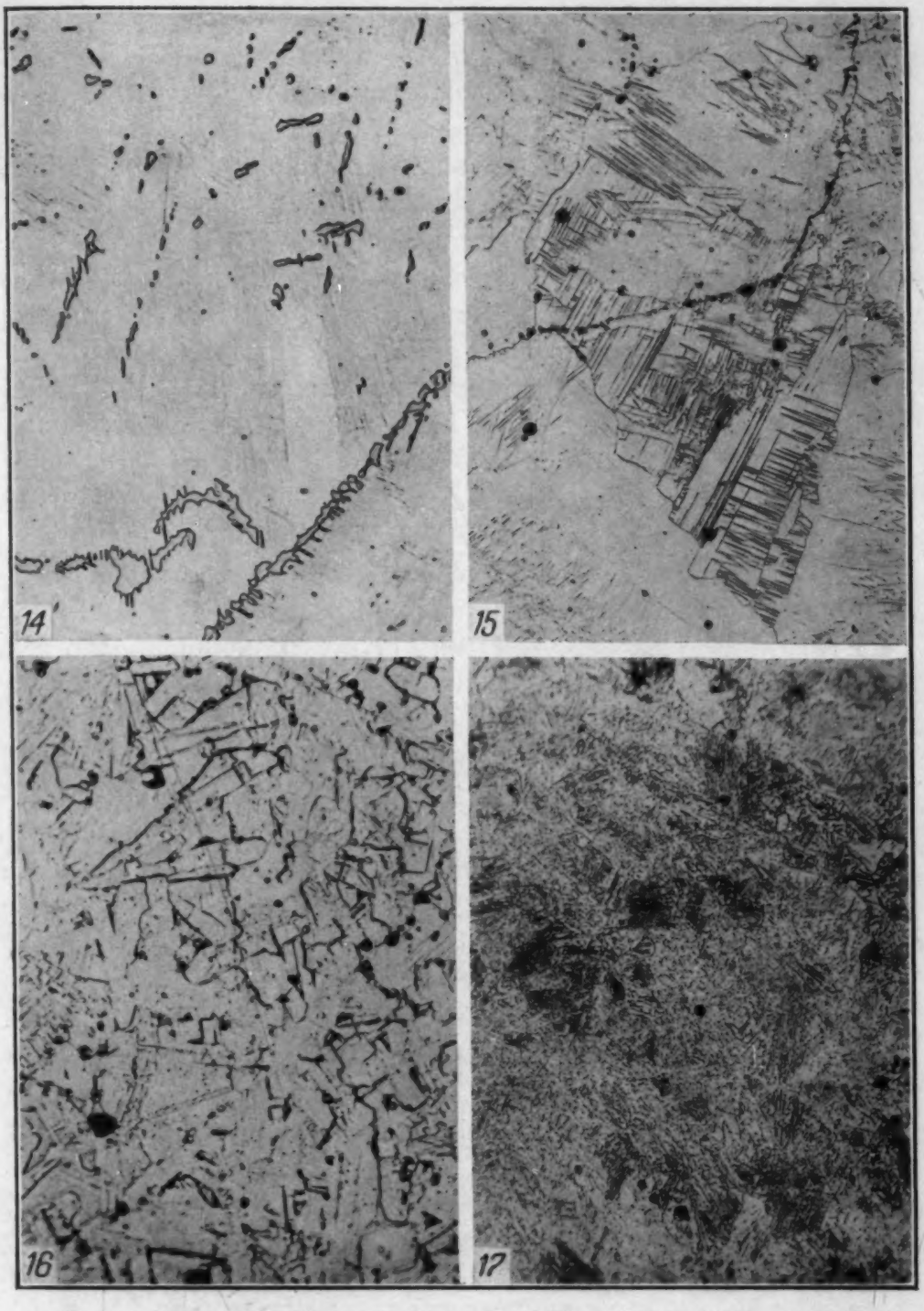

Fig. 14—Same Composition and Treatment of Fig. 12 After Additional 175 Hours at 875 Degrees Cent. Phosphoric Etch. Residual Delta Particles in Matrix of Alpha Plus Gamma. × 500.

Fig. 15—35 Per Cent Molybdenum. Rolled, Heated at 1300 Degrees Cent.—25 Hours, Cooled to 900 Degrees Cent. in 4 Hours, Held Successively for 50 Hours at 900, 850, 800, 750, 700 and 600 Degrees Cent. Hydrochloric Etch. Gamma As Formed from Large Grained Alpha. × 200.

Fig. 16—35 Per Cent Molybdenum. Ingot Homogenized at 1300 Degrees Cent. and Cold Rolled. Heated at 875 Degrees Cent. for 300 Hours. Sulphuric Etch. Fine Grained Gamma Plus Slight Excess of Delta. × 500.

Fig. 17—Structure of Fig. 15 After Heating 45 Hours at 925 Degrees Cent. Hydrochloric Etch. Alpha Plus Fine Dispersion of Delta. × 200.

(2010 degrees Fahr.) shows that the alpha has recrystallized and now the delta particles are of appreciable size (Fig. 18).

In the alpha plus gamma field gamma normally crystallizes as plates, forming banded grains composed of alternate layers of alpha and gamma. Such banded grains are seen in Figs. 19 and 20 of a 30 per cent molybdenum alloy and in Fig. 21 of a 33 per cent molybdenum alloy as formed by cooling from 1300 degrees Cent. (2370 degrees Fahr.) into the alpha plus gamma field and holding there for 50 hours. However, the formation of gamma can be modified by thoroughly homogenizing and then cold working alpha solid solutions prior to heating in the alpha plus gamma field. After such a treatment the alpha grains have recrystallized and the gamma has precipitated uniformly in a 30 per cent molybdenum alloy (Fig. 22). But with greater concentration of molybdenum, the gamma still has some tendency to form banded grains with alpha (Fig. 23).

Beta Phase and Peritectoid Reaction—Another peritectoid reaction, involving alpha and gamma and occurring at 840 $\pm$10 degrees Cent. (1545 degrees Fahr.), results in the formation of the beta phase of 28 to 29 per cent molybdenum and corresponding to the ratio Ni_4Mo.

In the alpha plus beta field beta precipitates in a finely divided form, as shown in Figs. 24 and 25, of 23 and 25 per cent molybdenum alloys respectively. The localized areas of precipitate are characteristic of the cored structures which form from the alpha solid solution. Beta precipitate has very little tendency to coalesce into large particles, even at the highest temperature at which it exists. For instance, the structures of Figs. 24 and 25 had been heated at 800 degrees Cent. (1470 degrees Fahr.) for 1200 hours. However, by cold working the alpha solution prior to reheating just below the peritectoid temperature, a massive form of beta could be produced which appears to form by recrystallization rather than by coalescence. Such structures are shown in Figs. 26 and 27 of 26 and 28 per cent molybdenum specimens respectively, reduced cold 60 per cent in thickness before treating at 800 degrees Cent. (1470 degrees Fahr.) for 300 hours. Here it is seen that fine grains of beta have formed within the darkened areas. In Fig. 28 are shown grains of beta formed by recrystallization on subsequent heating about a Rockwell brale indentation.

In alloys of approximately the beta composition the presence of this phase may be identified by the striations and markings which

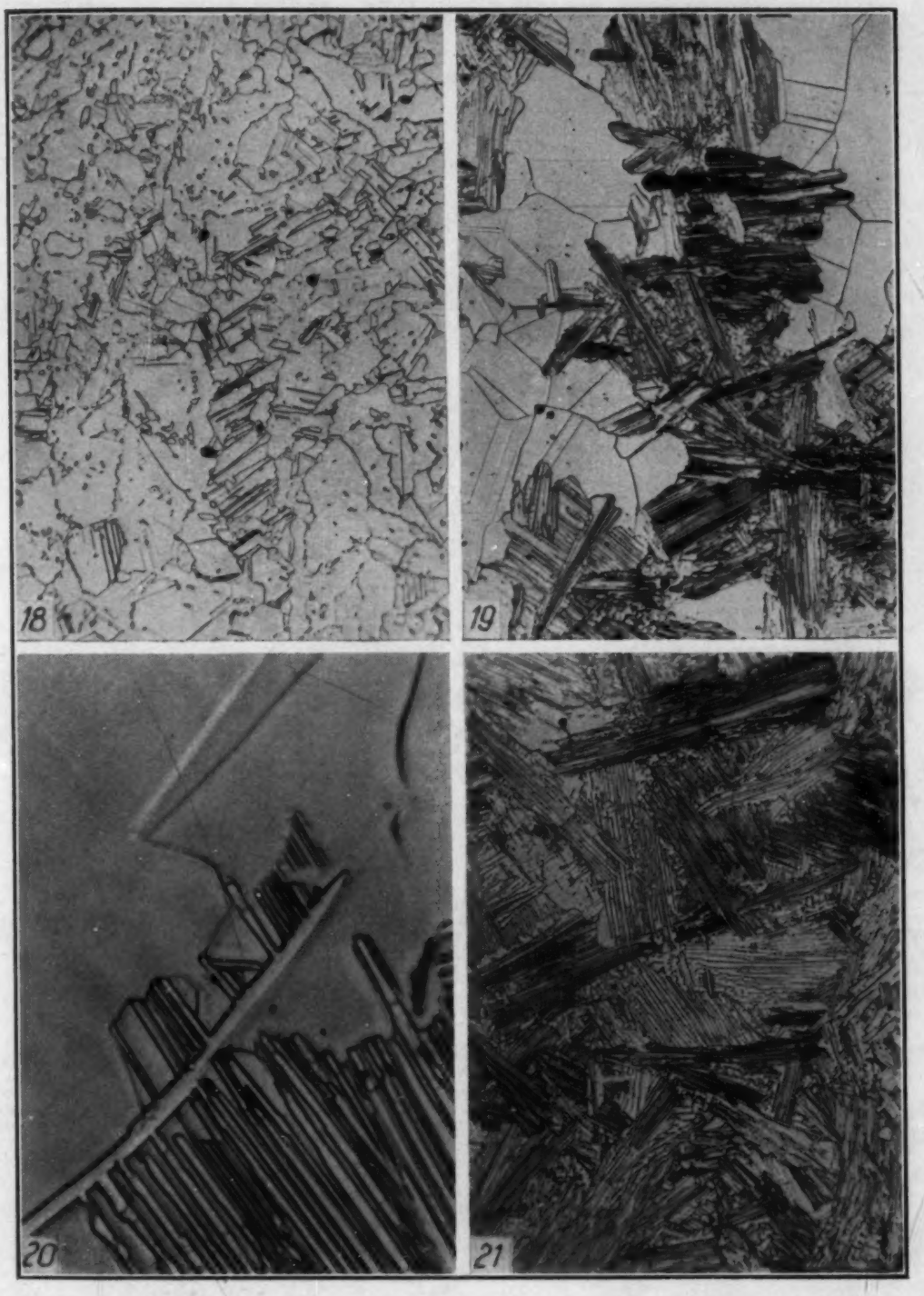

Fig. 18—Structure of Fig. 15 After Heating 20 Hours at 1100 Degrees Cent. Hydrochloric Etch. Recrystallized Alpha Plus Small Particles of Delta. × 200.

Fig. 19—30 Per Cent Molybdenum. Rolled, Heated 1300 Degrees Cent.—1 Hour, Transferred to 875 Degrees Cent. and Held 50 Hours. Hydrochloric Etch. Alpha Plus Banded Grains of Alpha Plus Gamma. × 200.

Fig. 20—Same Specimen Shown in Fig. 19. × 1500.

Fig. 21—33 Per Cent Molybdenum. Treated the Same as Specimen Shown in Fig. 19. Hydrochloric Etch. Banded Grains of Alpha Plus Gamma. × 200.

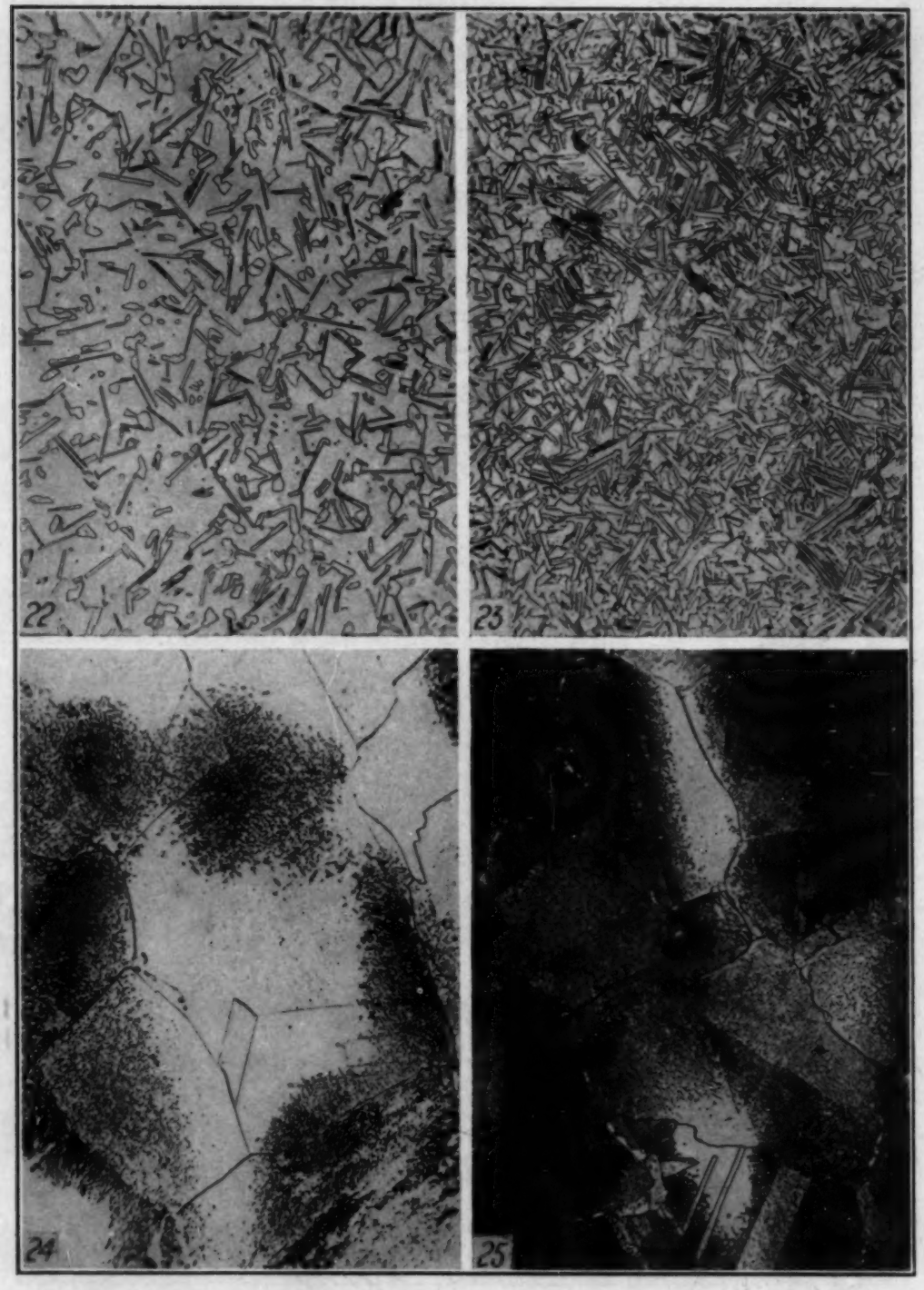

Fig. 22—30 Per Cent Molybdenum. Ingot Homogenized at 1300 Degrees Cent. and Cold Rolled. Heated at 875 Degrees Cent. for 300 Hours. Sulphuric Etch. Uniform Precipitation of Gamma in Alpha Matrix. × 200.

Fig. 23—32 Fer Cent Molybdenum. Treated the Same as Specimen Shown in Fig. 22. Sulphuric Etch. Gamma in Alpha Groundmass. × 200.

Fig. 24—23 Per Cent Molybdenum. Rolled, Heated 1300 Degrees Cent.—1 Hour and Quenched, Reheated 800 Degrees Cent.—1200 Hours. Hydrochloric Etch. Fine Precipitate of Beta. × 200.

Fig. 25—25 Per Cent Molybdenum. Same Treatment as Specimen Shown in Fig. 24. Hydrochloric Etch. Alpha Groundmass Darkened by Beta Precipitate. × 200.

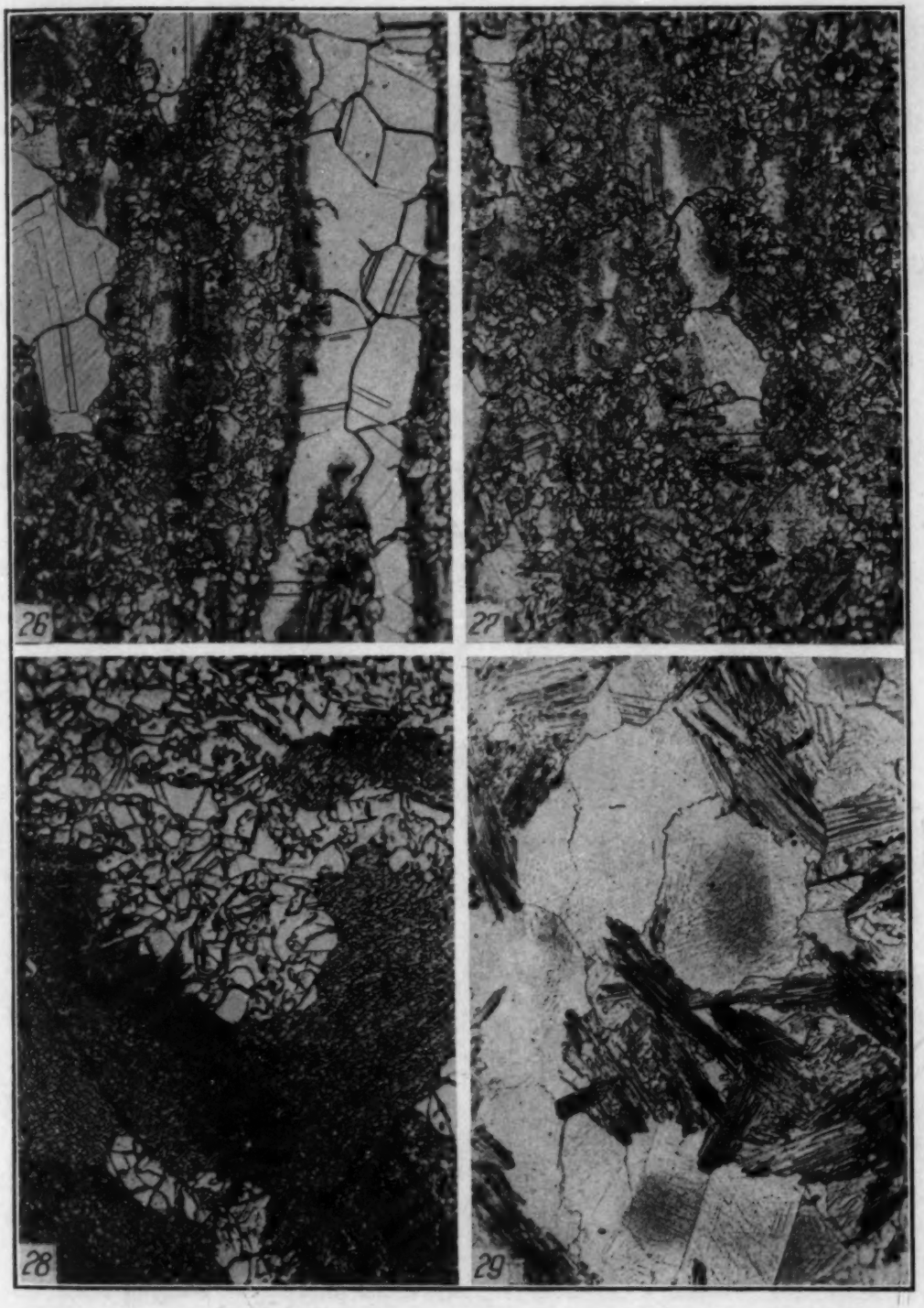

Fig. 26—26 Per Cent Molybdenum. Hot Rolled, Heated 1300 Degrees Cent.—1 Hour and Quenched. Cold Rolled, Heated 1000 Degrees Cent.—1 Hour, Transferred to 800 Degrees Cent. and Held 300 Hours. Hydrochloric Etch. Massive Beta Forming Within Darkened Areas of Beta Precipitate. × 200.

Fig. 27—28 Per Cent Molybdenum. Same Treatment as Specimen Shown in Fig. 26. Hydrochloric Etch. × 200.

Fig. 28—27 Per Cent Molybdenum. Aged 800 Degrees Cent. for 1200 Hours Subsequent to a Solution Treatment of 1 Hour at 1300 Degrees Cent. Hydrochloric Etch. Shows Massive Beta Formed About a Rockwell Brale Indentation. × 500.

Fig. 29—30 Per Cent Molybdenum. Structure of Fig. 19 After Additional 25 Hours at 800 Degrees Cent. Hydrochloric Etch. Alpha Decomposing to Beta. × 200.

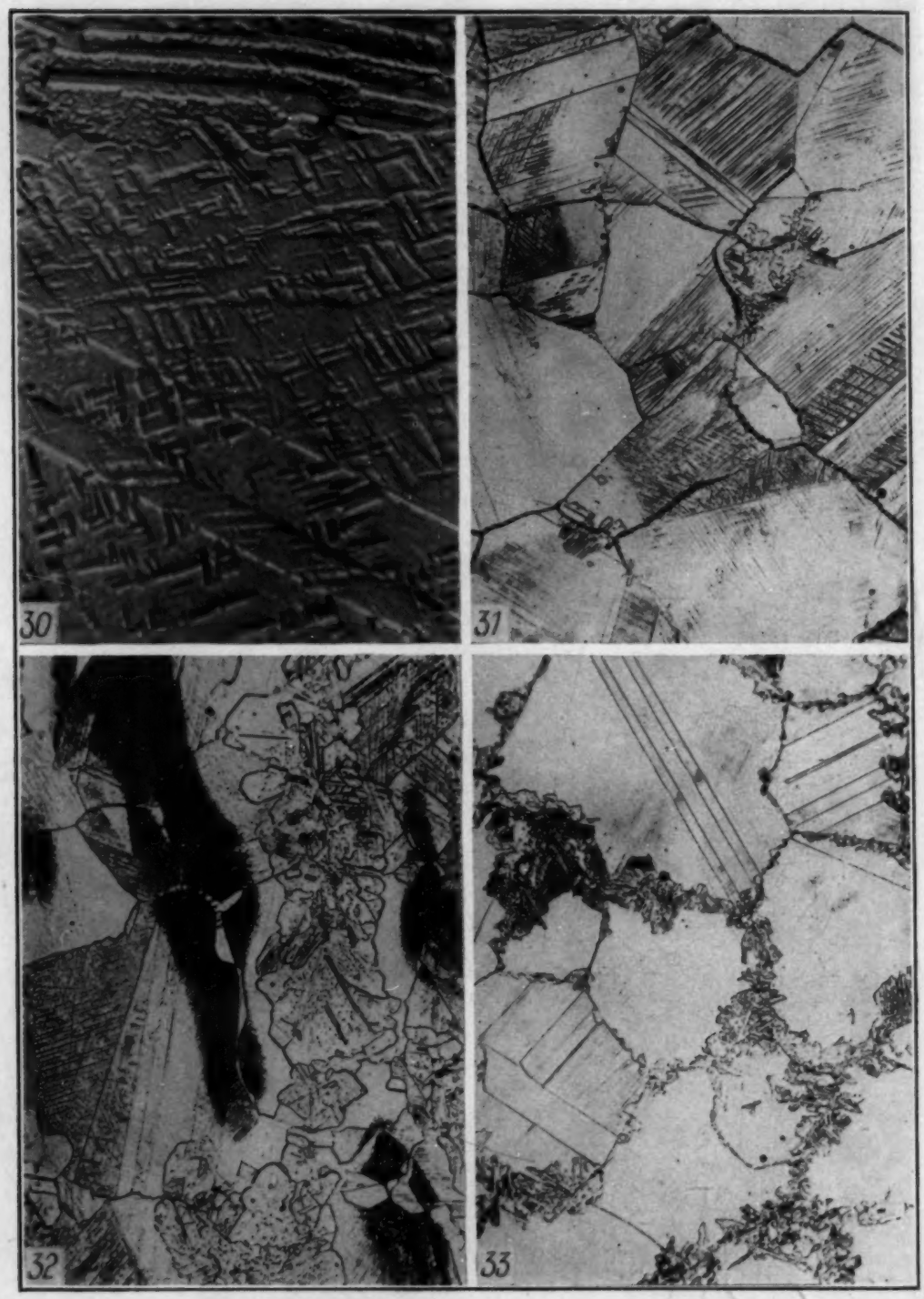

Fig. 30—Same Specimen Shown in Fig. 29. × 1500.

Fig. 31—29 Per Cent Molybdenum. Aged at 800 Degrees Cent. for 25 Hours Subsequent to Quenching from 1300 Degrees Cent. Hydrochloric Etch. × 200.

Fig. 32—29 Per Cent Molybdenum. Aged at 800 Degrees Cent. for 1200 Hours Subsequent to Quenching from 1300 Degrees Cent. Hydrochloric Etch. × 200.

Fig. 33—31 Per Cent Molybdenum. Same Treatment as Specimen Shown in Fig. 31. Hydrochloric Etch. Alpha Decomposing at Grain Boundaries. × 200.

develop in alpha grains upon heating below the beta peritectoid horizontal. In Fig. 29 and at a higher magnification in Fig. 30 is shown the appearance of the markings produced by cooling the alpha plus gamma structure of Fig. 19 to 800 degrees Cent. (1470 degrees Fahr.) and holding for 25 hours.

In Fig. 31 are shown striated grains produced by aging a 29 per cent molybdenum specimen at 800 degrees Cent. (1470 degrees Fahr.) for 25 hours subsequent to a solution treatment of 1 hour at 1300 degrees Cent. (2370 degrees Fahr.). Decomposition, beginning at the grain boundaries, is also evident which, with continued treatment at 800 degrees Cent. (1470 degrees Fahr.) for a total of 1200 hours, results in the heterogeneous structure of Fig. 32. Here is seen, on order of decreasing molybdenum concentration, areas composed of beta plus gamma with a few particles of delta distributed within them, the intermediate striated grains and finally alpha cores darkened by fine beta precipitate. Similar decomposition of a 31 per cent molybdenum alpha solution after 25 and 1200 hours is shown in Figs. 33 and 34 respectively; however, this composition has decomposed entirely to an aggregate of beta plus gamma with again the formation of some fine delta particles.

The severely cored nature of the alpha solid solution is believed to be the cause of this nonequilibrium structure. Prolonged heat treatment of these alloys would not produce equilibrium; however, by cold working such a structure as shown in Fig. 34 and then heating at 800 degrees Cent. (1470 degrees Fahr.) for 500 hours, the entire structure could be made to recrystallize and a uniform mixture of beta plus gamma produced with the absence of the delta. Such a structure is shown in Fig. 35 and at a higher magnification in Fig. 36 of a 30 per cent molybdenum alloy wherein the beta grains are easily recognized by their roughened, striated appearance in contrast to the smooth gamma particles.

For structural evidence of the reaction, alpha + gamma → beta, attempts were made to produce reaction rims around grains of gamma. A specimen consisting of alpha plus gamma of 30 per cent molybdenum (Fig. 22) was heated in the beta plus gamma field at 800 degrees Cent. (1470 degrees Fahr.) for 425 hours, producing the structure seen in Fig. 37. Close observation of the edges of the gamma particles shows very little effect of any reaction. It is believed that the gamma phase must be very stable at this relatively low temperature, thus greatly retarding the reaction.

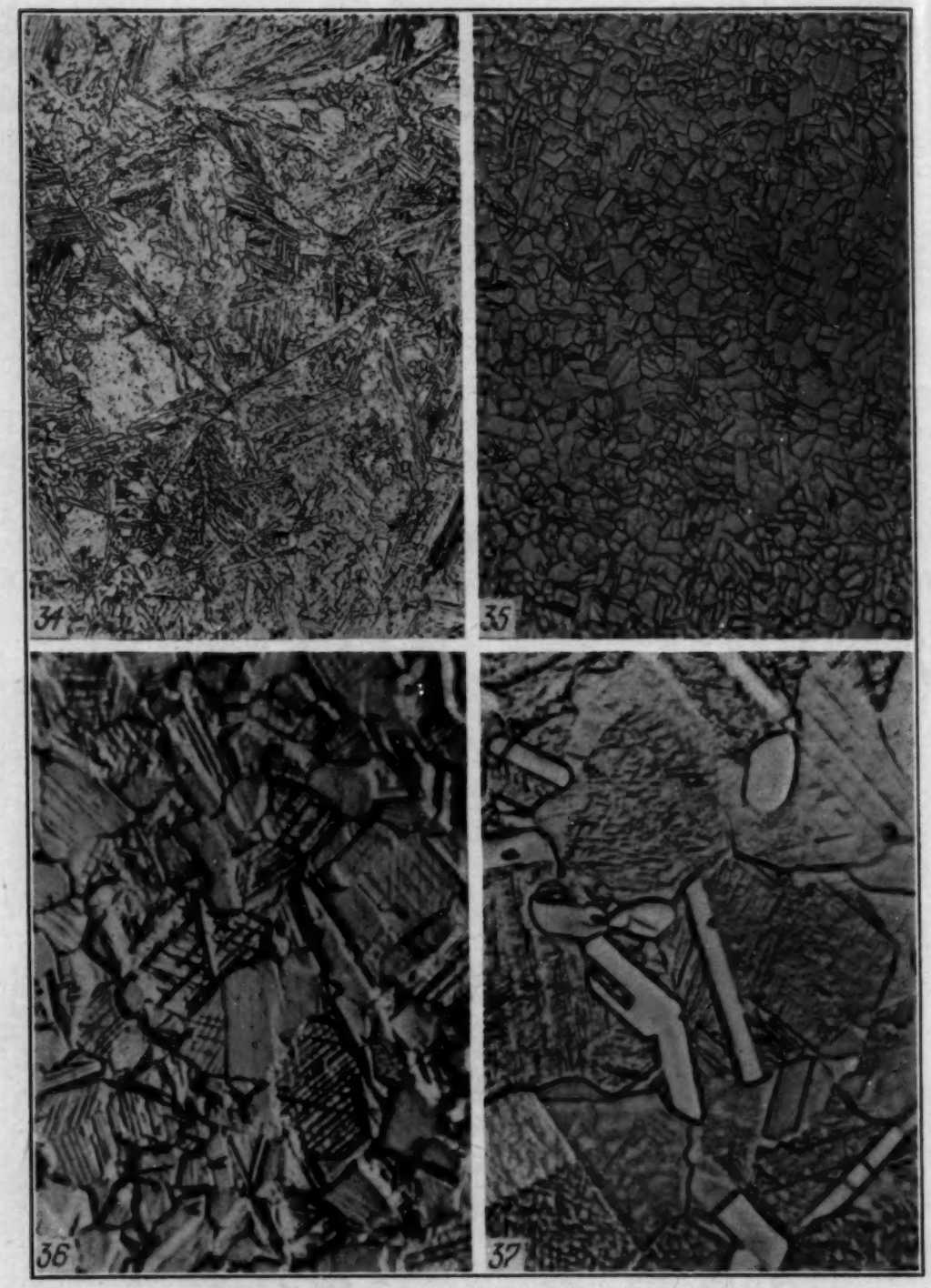

Fig. 34—31 Per Cent Molybdenum. Same Treatment as Specimen Shown in Fig. 32. Hydrochloric Etch. Alpha Completely Decomposed. × 200.

Fig. 35—30 Per Cent Molybdenum. Ingot Homogenized at 1300 Degrees Cent. and Cold Rolled. Heated at 800 Degrees Cent.—120 Hours, Cold Rolled and Reheated at 800 Degrees Cent. for 500 Hours. Hydrochloric Etch. Beta Plus Gamma. × 500.

Fig. 36—Same Specimen Shown in Fig. 35. × 1500.

Fig. 37—30 Per Cent Molybdenum. Ingot Homogenized at 1300 Degrees Cent. and Cold Rolled. Heated Successively at 875 Degrees Cent. for 300 Hours and 800 Degrees Cent. for 425 Hours. Sulphuric Etch. Beta Plus Gamma. × 1500.

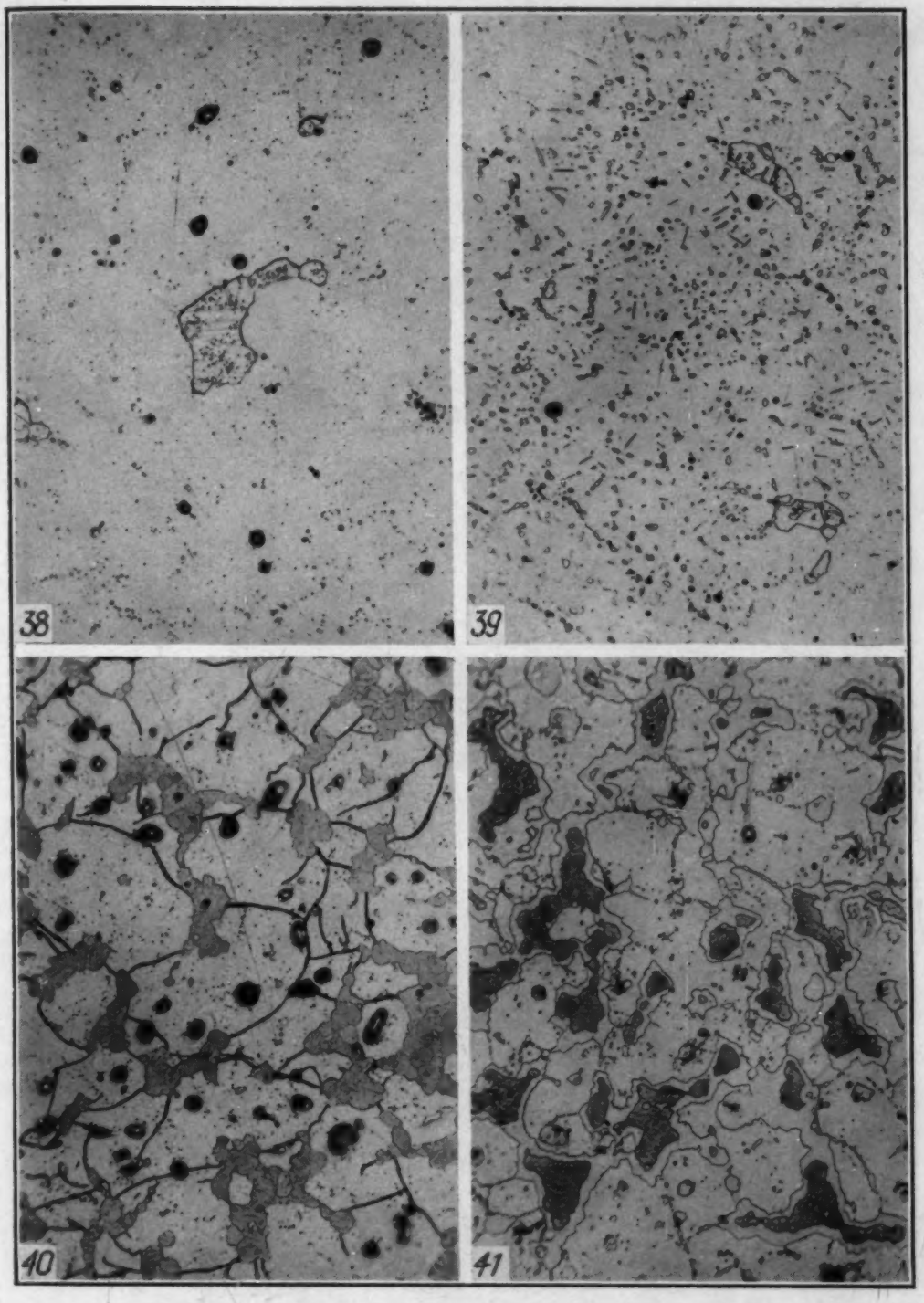

Fig. 38—60 Per Cent Molybdenum. Sintered at 1300 Degrees Cent. for 65 Hours. Hydrochloric Etch. Delta Plus Slight Amount of Alpha. × 200.

Fig. 39—Same Composition and Treatment of Fig. 38 After Additional 120 Hours at 1000 Degrees Cent. Phosphoric Etch. Shows Precipitation of Alpha in Delta Matrix. × 200.

Fig. 40—70 Per Cent Molybdenum. Sintered at 1300 Degrees Cent. for 65 Hours. Caustic and Hydrochloric Etches. Epsilon (Dark) Plus Delta. × 200.

Fig. 41—Same Composition and Treatment of Fig. 40 After Additional 110 Hours at 1000 Degrees Cent. Caustic and Hydrochloric Etches. Rims of Newly Formed Delta Around the Epsilon Particles. × 200.

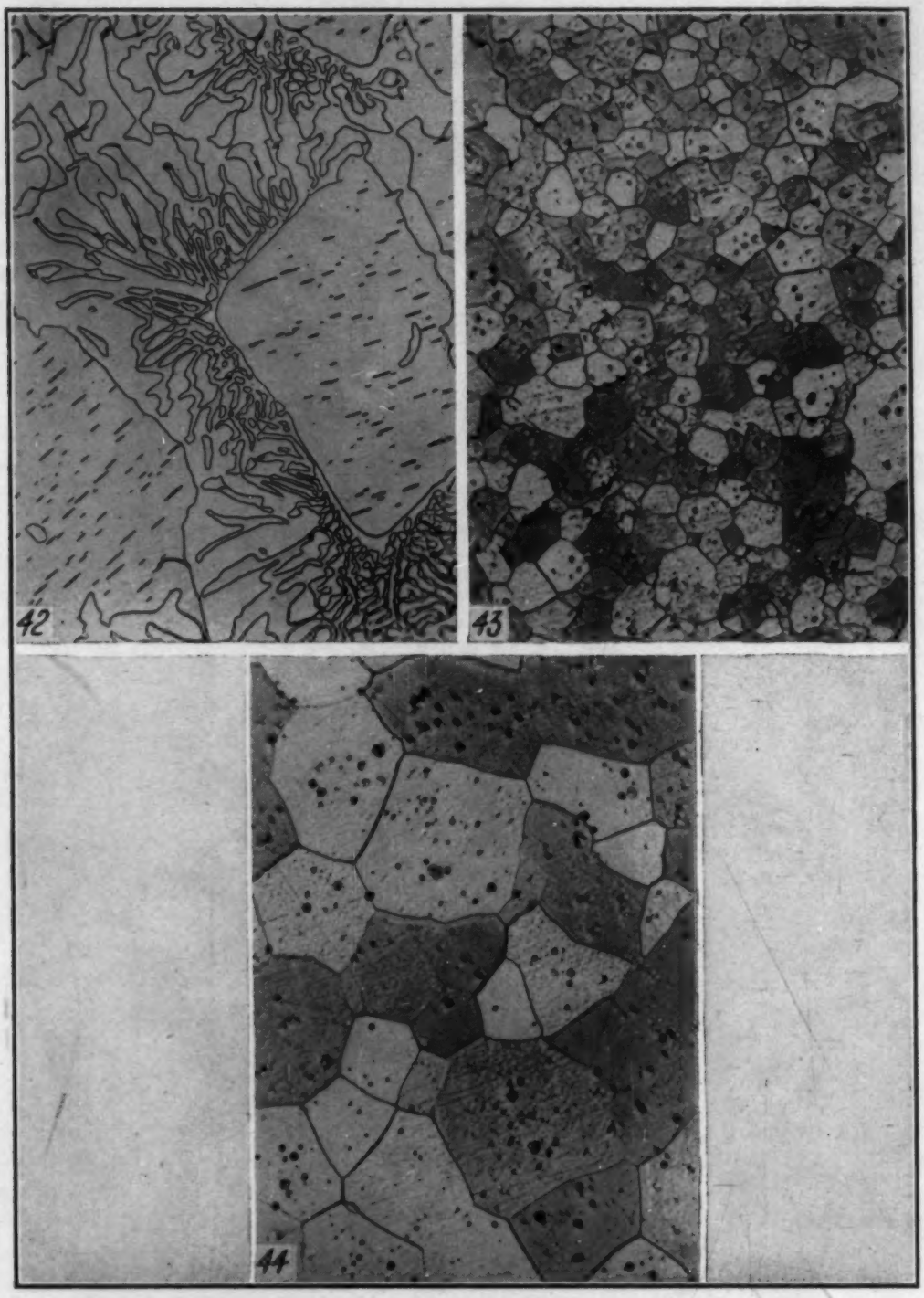

Fig. 42—52 Per Cent Molybdenum. As Solidified Slowly from Melt. Phosphoric Etch. Primary Delta Plus Eutectic. × 200.

Fig. 43—Molybdenum Plus 0.5 Per Cent Nickel. Sintered at 1370 Degrees Cent. for 65 Hours. Sodium Picrate Etch. Epsilon Phase. × 200.

Fig. 44—Molybdenum Plus 0.8 Per Cent Nickel. Sintered 1375 Degrees Cent. for 65 Hours. Sodium Picrate Etch. Epsilon Phase. × 200.

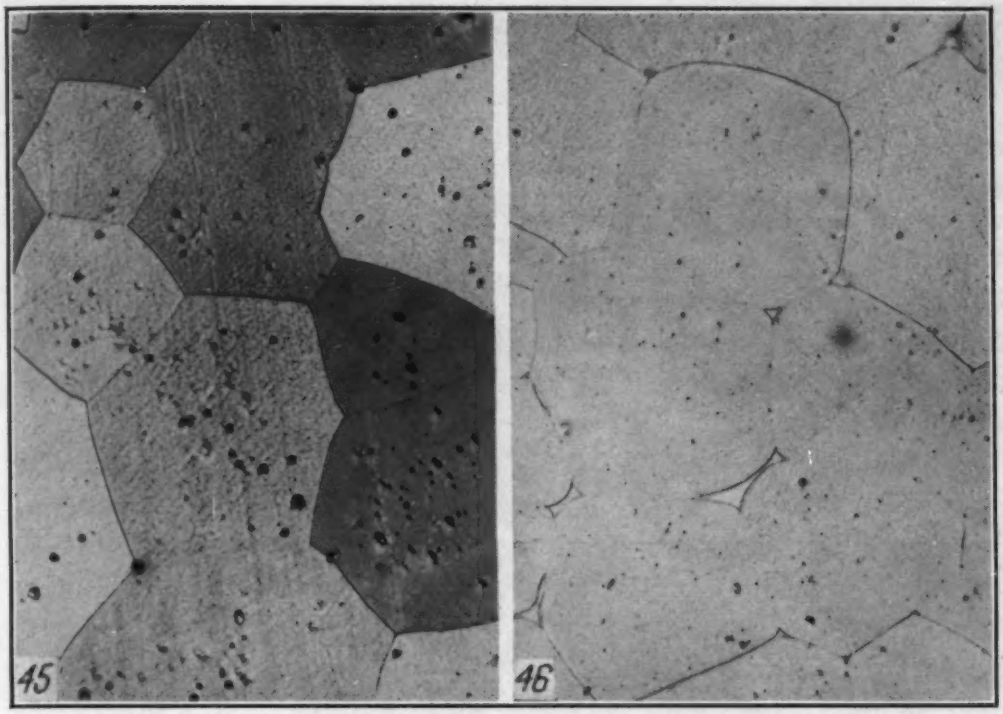

Fig. 45—Molybdenum Plus 0.9 Per Cent Nickel. Sintered 1375 Degrees Cent. for 55 Hours. Sodium Picrate Etch. Epsilon Phase. × 200.
Fig. 46—Molybdenum Plus 1.0 Per Cent Nickel. Sintered 1375 Degrees Cent. for 65 Hours. Sodium Picrate Etch. Epsilon Plus Liquid. × 200.

Delta Phase—The delta phase, corresponding to the ratio Ni-Mo, forms as a result of the peritectic reaction, epsilon plus liquid yields delta. This compound exists as 100 per cent of the structure over the range from 61 to 63 per cent molybdenum as can be produced by sintering the pressed powder mixtures at 1300 degrees Cent. (2370 degrees Fahr.) for 65 hours followed by 100 hours at 1325 to 1350 degrees Cent. (2415 to 2460 degrees Fahr.).

Fig. 38 shows the structure of massive delta in a 60 per cent molybdenum specimen which also contains a few islands of alpha. Reheating this specimen at 1000 degrees Cent. (1830 degrees Fahr.) for 100 hours results in the precipitation of small particles of alpha as shown in Fig. 39.

A 70 per cent molybdenum specimen sintered in the same manner as the specimen shown in Fig. 38 produces the delta plus epsilon (dark) structure shown in Fig. 40. Upon reheating this specimen at 1000 degrees Cent. (1830 degrees Fahr.) for 100 hours there is no precipitation of epsilon in the delta matrix but rather an increase in the amount of delta due to the decreased solubility of nickel in epsilon at the lower temperature. This is evident by the

rims of delta which have formed about the epsilon particles as shown in Fig. 41.

Massive primary delta crystals, as formed from the melt on slow cooling, contain a series of oval shaped particles of constant orientation within any single grain. These are shown in Fig. 42 which at 200 magnification appear as a series of dashes. Etching with caustic solution proved them to be molybdenum-rich or the epsilon phase. They are probably the result of nonequilibrium conditions in the alloy during solidification, for after a homogenizing treatment at or above 1000 degrees Cent. (1830 degrees Fahr.) they are no longer visible.

Molybdenum-Rich Phase (Epsilon)—The solubility of nickel in molybdenum was placed at 0.9 per cent nickel at the peritectic temperature. This was determined by examining alloys containing 0.5 to 1.0 per cent nickel for the presence of a second phase subsequent to sintering the pressed mixtures a few degrees above the peritectic temperature for 65 hours. These alloys were made by slurrying molybdenum oxide with nickel acetate solution and reducing the dried mixtures in hydrogen at 1050 degrees Cent. (1920 degrees Fahr.).

Figs. 43, 44, 45 and 46 show the sintered structures of the 0.5, 0.8, 0.9, and 1.0 per cent nickel alloys respectively. A second phase may be seen in the 1.0 per cent nickel alloy but none in the 0.9 per cent nickel specimen. An interesting characteristic of these specimens is the grain size which seems to depend on the nickel content. It is seen that the grain size increases with nickel content until a maximum has been reached at 0.9 per cent nickel. The fact that the grain size of the 0.9 per cent nickel specimen has reached that of the 1.0 per cent nickel specimen may be further evidence of the maximum solubility of nickel in molybdenum.

X-Ray Diffraction Patterns

X-ray photograms were obtained for confirmation of the microscopic data and for identification of the phases by their crystal structure. Metallographic specimens, prepared either from sintered or from melted and rolled alloys, were also used for X-ray specimens. The patterns were prepared by the powder method by means of directing the X-ray beam through a sharp edge of the specimen.

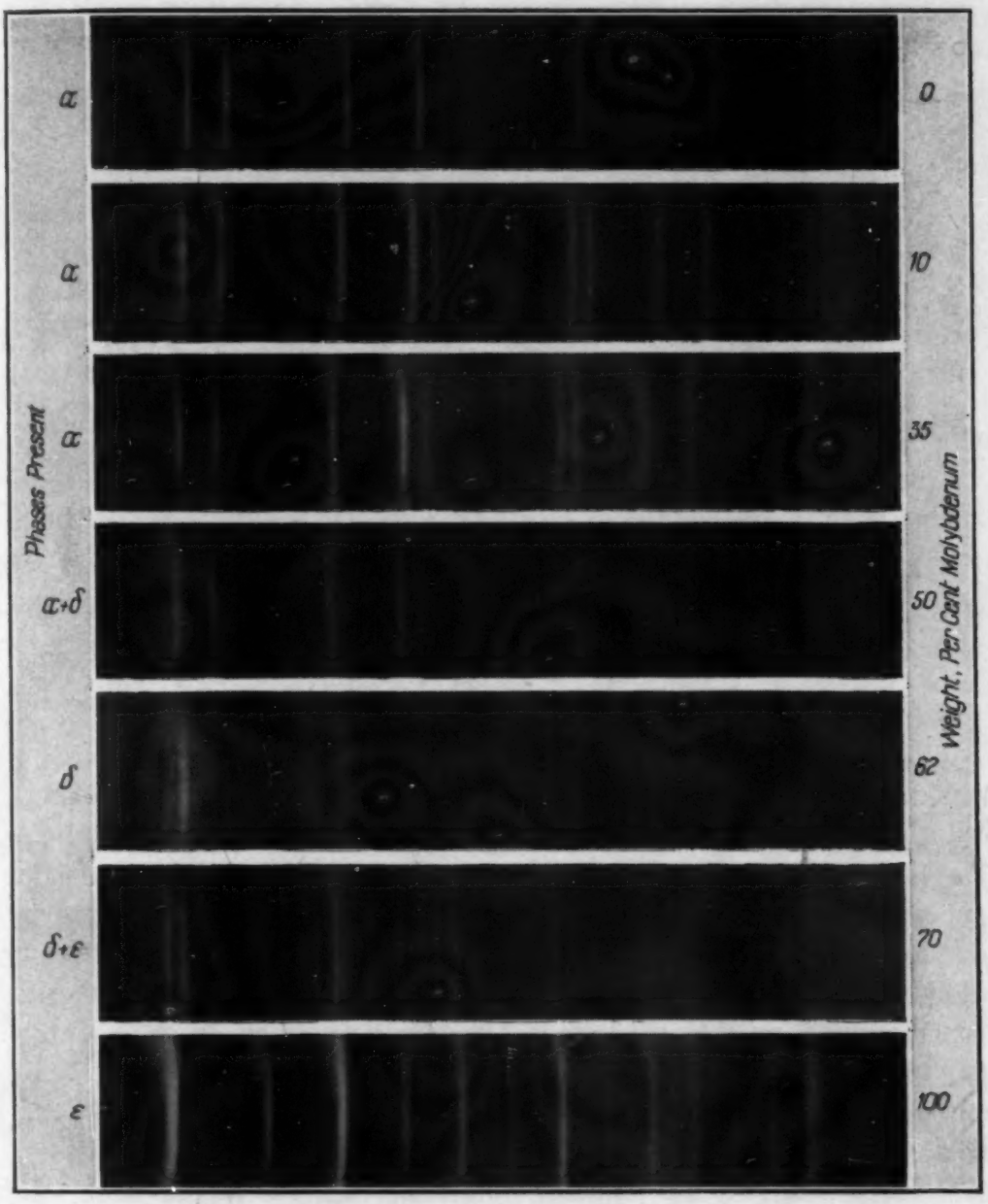

Fig. 47—Photograms of Nickel-Molybdenum Alloys as They Exist in the Upper Temperature Levels.

The wave length of the X-rays was 0.712 A.U. as produced with a molybdenum target and a zirconium filter. The radius of the cassette was 10.34 cm.

Diffraction patterns of the phases and combination of phases existing in the nickel-molybdenum alloys in the upper temperature levels from pure nickel to pure molybdenum are shown in Fig. 47. Pure nickel and alpha solid solution crystallize in the face-centered

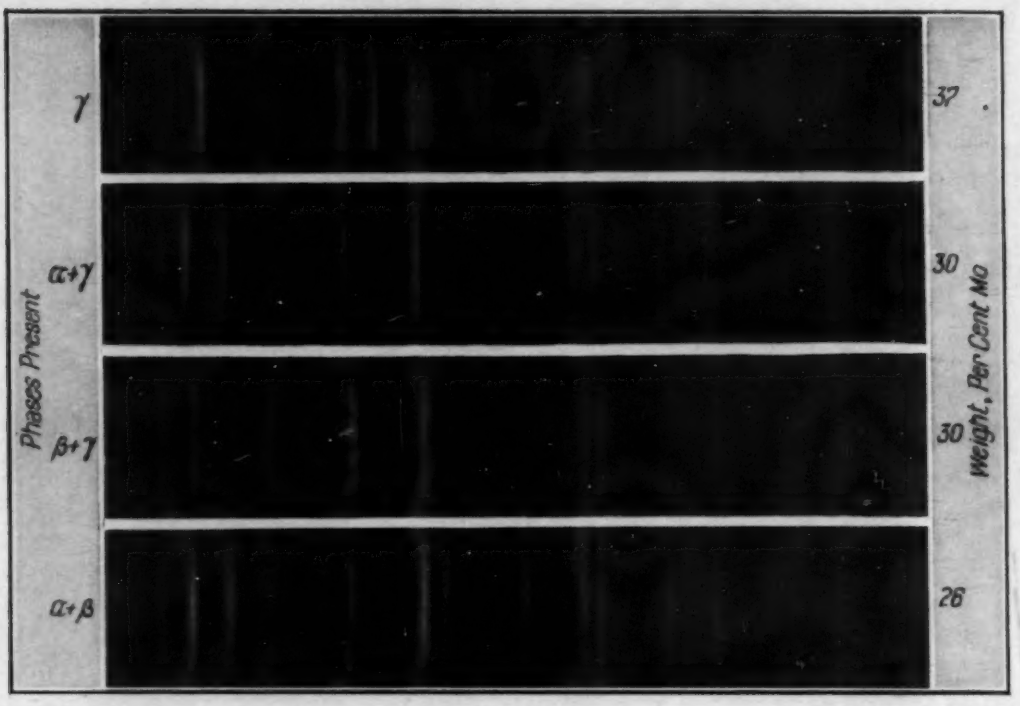

Fig. 48—Photograms of the Beta and Gamma Phases in the Nickel-Molybdenum System.

cubic system. The expansion in lattice parameter with increasing solution of molybdenum up to the saturation limit is evident by the shifting of the lines. The 50 per cent molybdenum alloy reveals the superimposed patterns of alpha and delta. The 62 per cent molybdenum alloy shows the complex pattern of delta; and at 70 per cent molybdenum the body-centered cubic pattern of the epsilon phase is superimposed on that of delta. The epsilon pattern appears identical to that of pure molybdenum since the X-ray equipment used was not sufficiently precise to reveal such slight differences in composition.

Fig. 48 shows the patterns obtained from the alpha, beta, and gamma phases and combinations of these phases. In the upper pattern is seen the close packed hexagonal pattern of the gamma phase. Calculation of the interplanar distances and matching the plotted values to a Davey chart showed the axial ratio (c/a) to be between 1.64 and 1.66. In the second pattern from the top, that of a 30 per cent molybdenum alloy, some of the stronger gamma lines are superimposed on the alpha pattern. Immediately below this is the pattern of an alloy of the same molybdenum concentration but now consisting of beta plus gamma. It is seen that there is very

little difference in the patterns except for the diffuseness of the former alpha lines. The bottom photogram shows the pattern produced from a mixture of alpha plus beta and here, again, only diffuse alpha lines are present.

It is evident that the beta phase cannot be identified with certainty from these diffraction patterns. However, by using a more precise X-ray technique, Grube and Schlecht (1) obtained a pattern of the beta phase, in which, besides the intense alpha lines, very weak extra lines appeared. They interpreted the pattern as being that of a face-centered tetragonal lattice with an axial ratio $\left(\frac{c}{a}\right)$ of 0.98 and possessing a superlattice which produced the weak reflections.

A comparison may be drawn between the beta phase of the nickel-molybdenum system and the beta phase of the nickel-tungsten system (3), both of which correspond to the ratio Ni_4X. Both phases exhibit structural and age-hardening characteristics of a similar nature. The diffraction patterns, as obtained with the same equipment, are similar in that both reveal strong, diffuse alpha lines, but the nickel-tungsten beta shows additional weak reflections which are absent in the pattern of Ni_4Mo. It is believed that the X-ray equipment used was suitable for revealing the weak reflections of Ni_4W due to the high density of tungsten (19.3) but not those of Ni_4Mo as molybdenum has a comparably low density (10.2).

Age Hardening Data

The phase diagram, shown in Fig. 1, indicates that alloys above 21 per cent molybdenum which solidify as alpha solid solution should respond to age hardening treatments. It is seen, however, that these alloys fall into two groups, (1) those that would harden by precipitation of the beta phase, and (2) those that would harden by the decomposition of the supersaturated solid solution into two new phases, beta and gamma.

The hardness changes of alloys from 21 to 35 per cent molybdenum, inclusive, at intervals of 2 per cent molybdenum were determined after aging at 600, 700, and 800 degrees Cent. (1110, 1290, and 1470 degrees Fahr.) subsequent to a solution treatment of 1 hour at 1300 degrees Cent. (2370 degrees Fahr.) and water quenching. Since some of the hardness values of this series of alloys fall

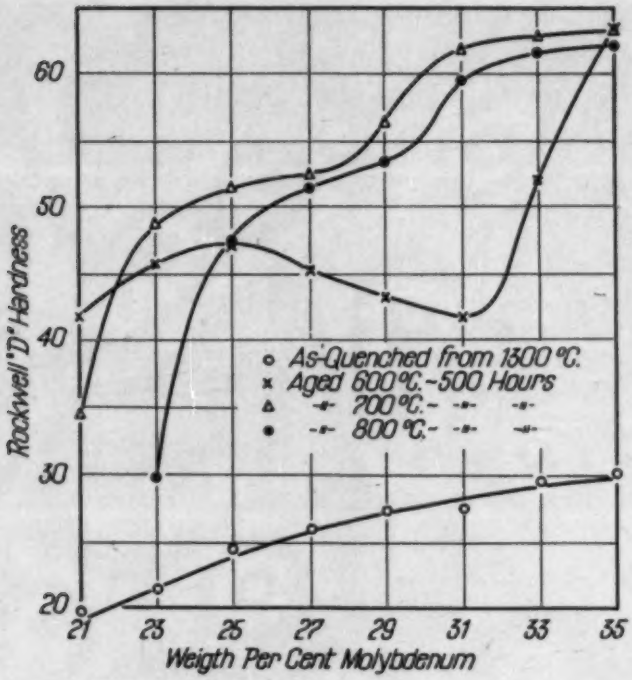

Fig. 49—Hardness vs. Molybdenum Concentration in Nickel-Molybdenum Alloys.

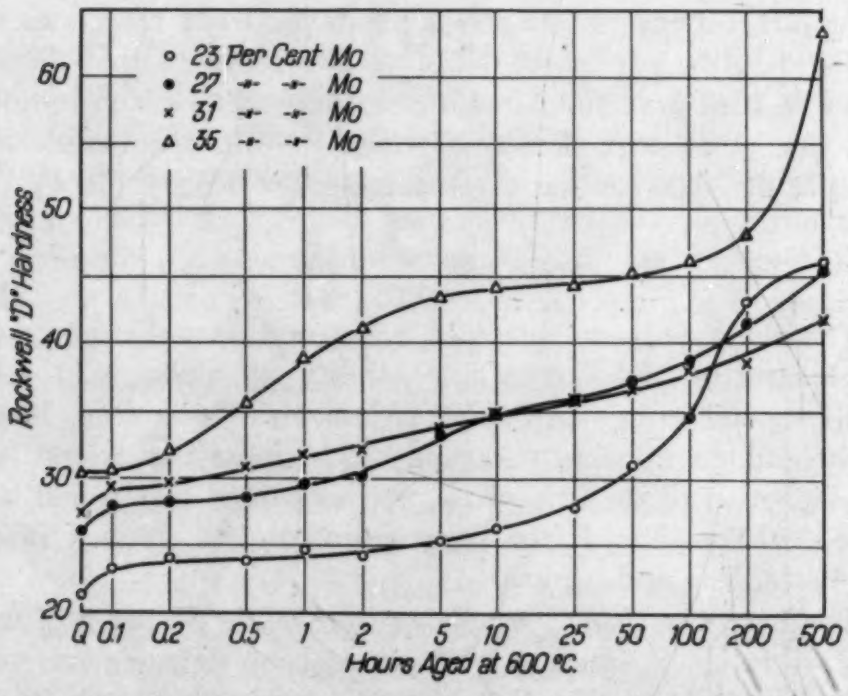

Fig. 50—Nickel-Molybdenum Alloys of Various Concentrations. Rolled, Solution Treated at 1300 Degrees Cent. for 1 Hour and Aged at 600 Degrees Cent.

within the "B" range of the Rockwell scale and others within the "C" range, the Rockwell "D" scale (diamond penetrator, 100 kilo-

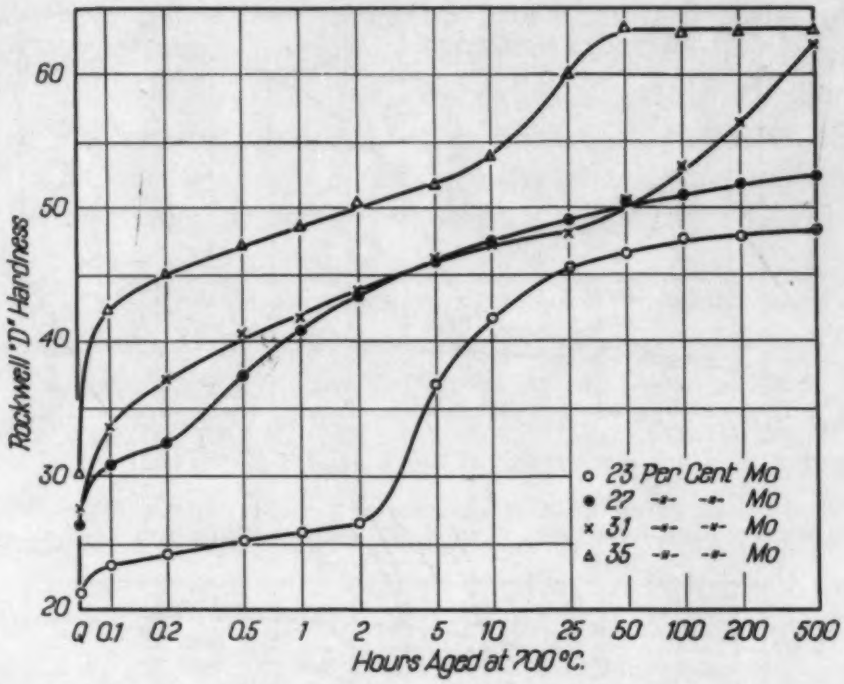

Fig. 51—Nickel-Molybdenum Alloys of Various Concentrations. Rolled Solution Treated at 1300 Degrees Cent. for 1 Hour and Aged at 700 Degrees Cent.

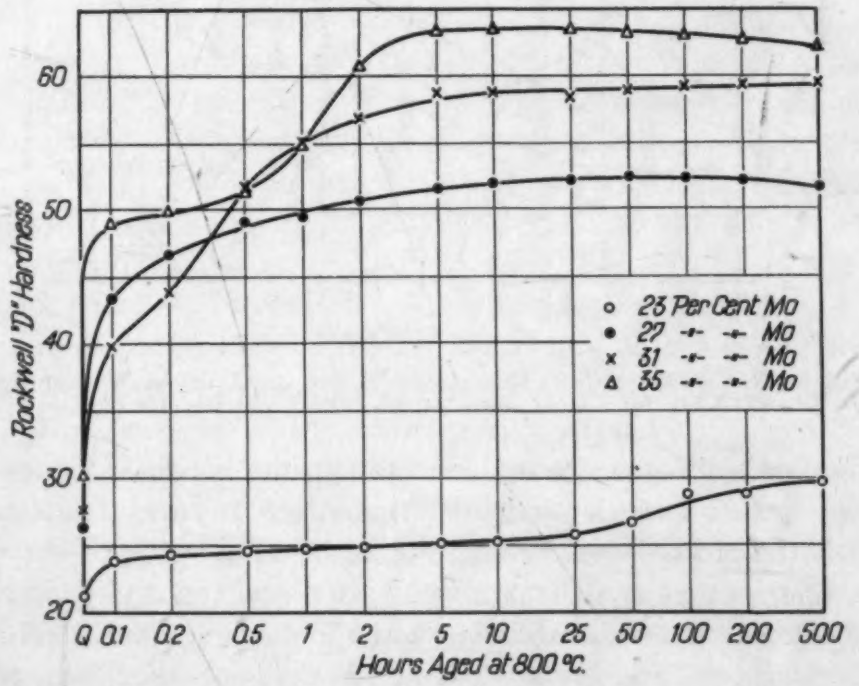

Fig. 52—Nickel-Molybdenum Alloys of Various Concentrations. Rolled, Solution Treated at 1300 Degrees Cent. for 1 Hour and Aged at 800 Degrees Cent.

gram load) was used so that the results would all be directly comparable.

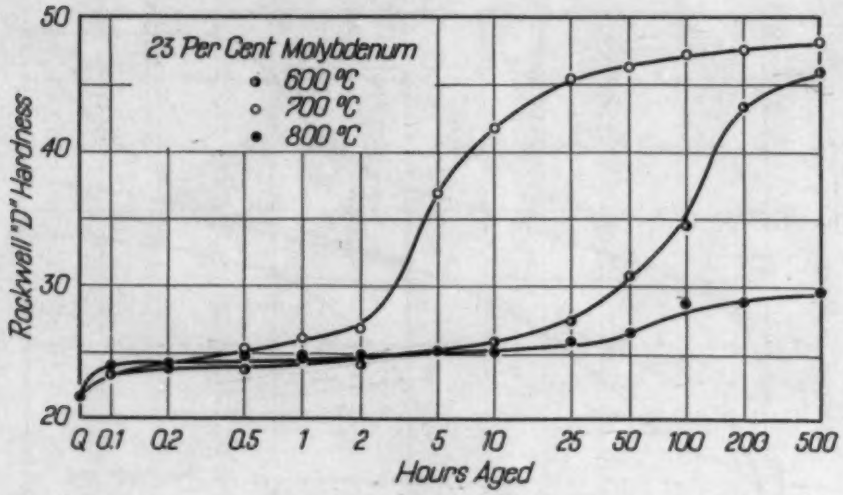

Fig. 53—Nickel 77 Per Cent, Molybdenum 23 Per Cent. Rolled, Solution Treated at 1300 Degrees Cent. for 1 Hour, Aged at 600, 700, and 800 Degrees Cent.

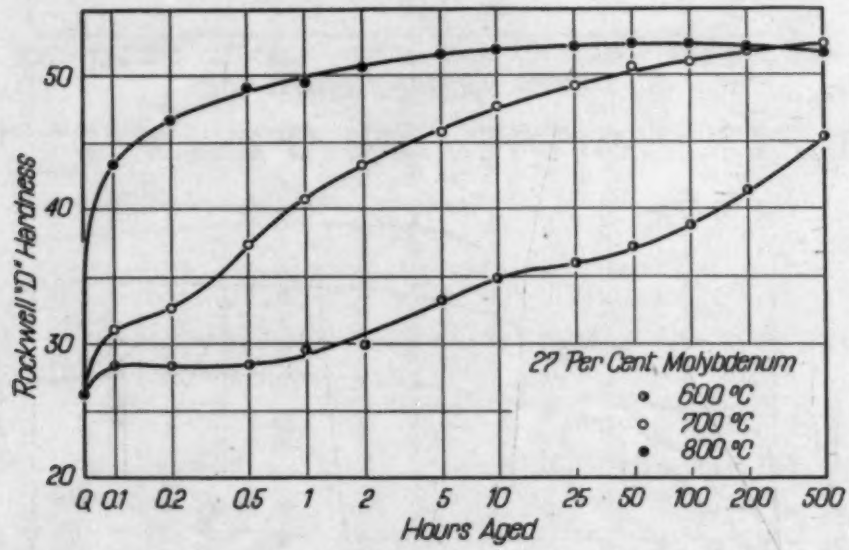

Fig. 54—Nickel 73 Per Cent, Molybdenum 27 Per Cent. Rolled, Solution Treated at 1300 Degrees Cent. for 1 Hour, Aged at 600, 700 and 800 Degrees Cent.

For each time-hardness curve plotted, the hardness values were the average of three separate determinations at each time interval. A total of six hardness readings, three on either side of the specimens (sections of a slab) and read to the nearest ½ point, were taken after each period of aging and their average value recorded. The raised portion of the Rockwell brale impression was always ground off before measuring the hardness on the reverse side of the specimen.

After measuring the hardness of the quenched specimens, the procedure was to place six specimens of a single composition into

the furnace and then remove one of them after each period of 0.1, 0.2, 0.5, 1, 2 and 5 hours respectively. After measuring the hardness of each specimen they were replaced in the furnace and one removed in the same order as before after each period of 10, 25, 50, 100, 200 and 500 hours, which included the time of the first aging period for each respective specimen. Again the hardness of each specimen was measured.

In Fig. 49 the as-quenched hardness of the alpha solid solutions from 21 to 35 per cent molybdenum inclusive is plotted in the lower line. In the upper lines is plotted the hardness of these alloys after aging 500 hours at each temperature of 600, 700, and 800 degrees Cent. (1110, 1290, and 1470 degrees Fahr.). It must be noted, however, that only the 800 degrees Cent. (1470 degrees Fahr.) curve represents the maximum hardness of the alloys after aging at each temperature. Most of the hardness values of the 600 and 700 degrees Cent. (1110 and 1290 degrees Fahr.) curves after 500 hours aging have not reached their maximum value.

Of particular interest in this series of curves are the irregularities, especially marked in the 600 degrees Cent. (1110 degrees Fahr.) curve, which occur at those compositions representing the transition range between the alpha plus beta field and the beta plus gamma field. It must be remembered that severe coring with consequently large concentration gradients exist in these alloys so that, upon aging, compositions between 27 and 31 per cent molybdenum are affected both by the precipitation of beta and by the decomposition of alpha into beta and gamma.

The effect of increased molybdenum concentration on the hardening characteristics of the 23, 27, 31 and 35 per cent molybdenum alloys may be compared at 600, 700, and 800 degrees Cent. (1110, 1290, and 1470 degrees Fahr.) in Figs. 50, 51, and 52 respectively. While it is seen that, in general, the ultimate hardness of the alloys becomes greater with increased molybdenum content, the rate of hardening, especially in the 27 and 31 per cent molybdenum compositions, varies considerably and shows no common relationship as to molybdenum content. Fig. 51 shows this condition clearly wherein the curves of the 27 and 31 per cent molybdenum alloys are practically coincident between 1 and 50 hours at 700 degrees Cent. (1290 degrees Fahr.). After 50 hours, the hardness of the 31 per cent molybdenum alloy increases rapidly to a value considerably higher than that of the 27 per cent molybdenum alloy.

Another example of this variation in the hardening rate is seen in Fig. 52, wherein the 27 per cent molybdenum alloy hardens more rapidly than the 31 per cent molybdenum alloy during the early stages of aging at 800 degrees Cent.

Time-hardness curves at 600, 700, and 800 degrees Cent. (1110, 1290, and 1470 degrees Fahr.) for the 23, 27, 31, and 35 per cent molybdenum alloys are shown in Figs. 53, 54, 55, and 56 respectively. In Fig. 53 the 23 per cent molybdenum alloy is seen to harden more rapidly and to reach a higher hardness value at 600 and 700 degrees Cent. (1110 and 1290 degrees Fahr.) than at 800 degrees

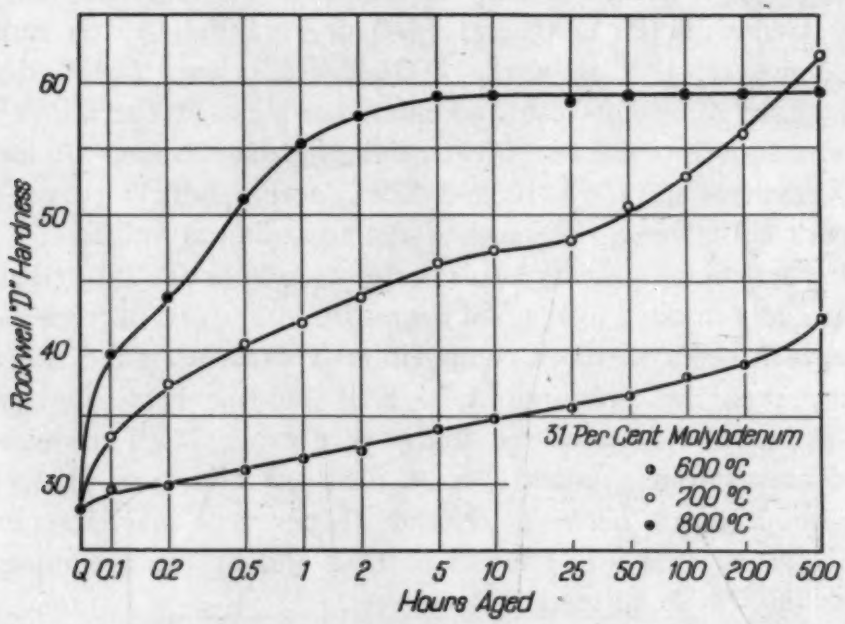

Fig. 55—Nickel 69 Per Cent, Molybdenum 31 Per Cent. Rolled, Solution Treated at 1300 Degrees Cent. for 1 Hour, Aged at 600, 700 and 800 Degrees Cent.

Cent. (1470 degrees Fahr.). This same condition also occurs in the 21 per cent molybdenum alloy but in this case the difference is noted between 700 and 600 degrees Cent. (1290 and 1110 degrees Fahr.). It is believed that the diminished solute content of the supersaturated solid solution at the higher aging temperature may account for this behavior.

An interesting feature of the 27, 31 and 35 per cent molybdenum alloys is the two hardness peaks on levels which occur in the curves, with two exceptions. One of these is the 800 degrees Cent. (1470 degrees Fahr.) curve of the 27 per cent molybdenum alloy wherein the hardening occurs so rapidly that the first peak is eliminated. The other is the 600 degrees Cent. (1110 degrees Fahr.)

curve of the 31 per cent alloy which is just rising to its first peak after aging 500 hours. Otherwise all the curves exhibit an intermediate rate of hardening which shifts to a shorter period of time with higher aging temperature.

An unusual characteristic of these alloys is the absence of any overaging after 500 hours, even at 800 degrees Cent. (1470 degrees Fahr.) where the maximum hardness is reached in a relatively short

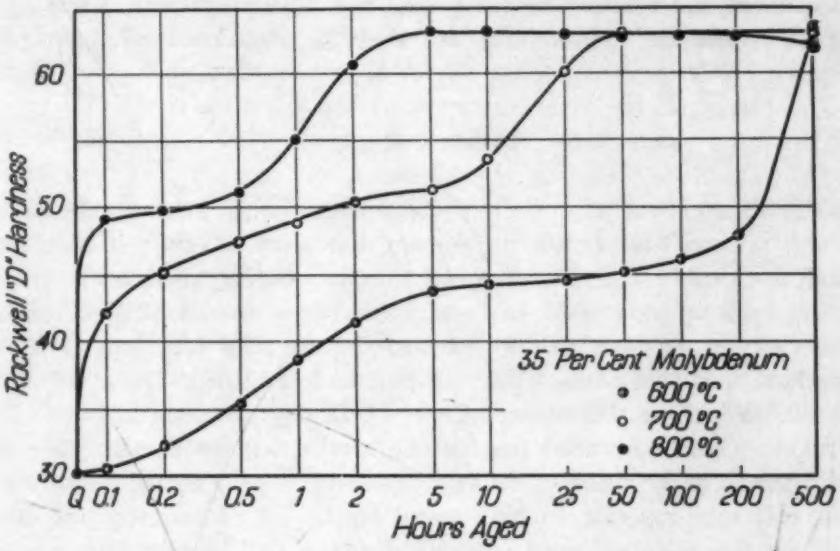

Fig. 56—Nickel 65 Per Cent, Molybdenum 35 Per Cent. Rolled, Solution Treated at 1300 Degrees Cent. for 1 Hour, Aged at 600, 700 and 800 Degrees Cent.

time. In an attempt to produce overaging, one set of specimens was aged at 800 degrees Cent. (1470 degrees Fahr.) for 1200 hours, but still there was no appreciable decrease in hardness.

Acknowledgment

The author is indebted to Mr. A. B. Gladding for the X-ray photograms prepared in the course of this work and to Dr. W. P. Sykes for many helpful discussions.

References

1. G. Grube and H. Schlecht, "Elektrische Leitfähigkeit and Zustandsdiagramm bei Binären Legierungen; Das System Nickel-Molybdän," *Z. Elektrochem.*, Vol. 44, 1938, p. 413.
2. G. Grube and O. Winkler, "Magnetische Suszeptibilität and Zustandsdiagramm von Binären Legierungen; Das System Nickel-Molybdän," *Z. Elektrochem.*, Vol. 44, 1938, p. 423.
3. F. H. Ellinger and W. P. Sykes, "The Nickel-Tungsten System," TRANSACTIONS, American Society for Metals, Vol. 28, 1940, p. 619.

ORAL DISCUSSION

T. H. WICKENDEN:[1] This work on developing information for constitutional diagrams is fundamental in its nature and extremely interesting. However, the properties of the materials, I think, appeal to many of us.

I was wondering whether Mr. Ellinger could give us a few words about some of the characteristics of the compositions that he worked with. I think we might all be interested in hearing something along that line.

W. L. HARBRECHT:[2] I would like to ask Mr. Ellinger if he would tell us something about the relative working qualities of these alloys, from 25 to 30 per cent molybdenum. How hard are they to work and what temperature is used?

Author's Reply

As Mr. Wickenden says: the chief purpose of this investigation was of a fundamental nature. So far, a nickel-tungsten alloy of 40 per cent tungsten has found a valuable use for swaging dies. Swaging dies made from this composition hold up very well, in fact, much better than any high speed steel ever used for this purpose. "Hot Hardness" tests made at Battelle Memorial Institute show that this composition, as cast and hardened, has a hot hardness figure of 300 Brinell at 800 degrees Cent. (1470 degrees Fahr.).

A nickel-molybdenum alloy has also been tried out for use as swaging dies. The molybdenum alloy was found not to hold up as well as the nickel-tungsten alloy, but still was superior to high speed steel. So, if tungsten becomes unobtainable for this purpose, good swaging dies can still be made by substituting molybdenum for the tungsten.

All the alloys used in this investigation were prepared from hydrogen reduced metal powders and were melted in a hydrogen atmosphere, thus hydrogen may have been an important factor in the workability of these alloys. However, ingots of all compositions up to 35 per cent molybdenum were rolled into slabs successfully but not into bars suitable for drawing into wire. The best rolling temperature was between 1100 and 1200 degrees Cent. (2010 and 2190 degrees Fahr.). My experience is that if cracking can be prevented during the first stages of rolling or while the cast structure of the ingot is being broken up, the alloy can be worked easily thereon.

---

[1]Assistant manager, International Nickel Co., New York.

[2]Union Carbide and Carbon Research Laboratories, Inc., Niagara Falls, New York.

PROBLEMS IN THE DRAWABILITY OF DEEP DRAWING SHEETS

By M. Asimow and J. N. Crombie

Abstract

The subject of "drawability" is reviewed in some detail. Questions of multiaxial stressing, the Bauschinger Effect, and plastic strain are discussed. Certain postulations concerning strain hardening and rupture strength are proposed. Various factors involved in drawing cylindrical shells are reviewed. The customary laboratory testing procedures fail to evaluate "drawability" adequately because the loading conditions of such tests, whether uniaxial or multiaxial, do not duplicate the wide variety of multiaxial loading conditions encountered in commercial deep drawing. While certain deep drawing tests involve reversed stresses, the effect of such reversed stresses has been neglected and is practically unknown. Frictional forces in drawing large shapes of relatively thin materials are shown to be of much larger magnitude than in small scale tests, thus vitiating interpretation of laboratory tests.

Part I

Introduction

In mass production the importance of deep drawing sheet metals is so generally recognized that it is surprising to find a very meager volume of American metallurgical literature which relates to the deep drawing problem proper, although considerable attention has been devoted to the problem of testing for drawing quality, as well as the production of drawing steels and other metals. Many tests have been devised in efforts to evaluate the deep drawing qualities of metals. Among these may be mentioned the customary tensile test (123), (155), (160), (182), (184),[1] hardness tests, Erichsen

[1]The figures appearing in parentheses refer to the bibliography appended to this paper.

A paper presented before the Twenty-third Annual Convention of the Society held in Philadelphia, October 20 to 24, 1941. Of the authors, M. Asimow is associated with the Central Metal Products Co., Los Angeles, and J. N. Crombie is manager, Tin Plate Bureau, Carnegie-Illinois Steel Corp., Chicago. Manuscript received June 25, 1941.

(107), (111), (137), (140), (142), (143), (149), (154), (157), (176), (197), Olsen (111), (196), Avery (174), Guillery (122), (149), (180), A. E. G. (175), (177), K. W. I. (173), Wazau (95), (150), (178), Sachs (164), the wedge cupping test (103), (114), (120), (145), cylindrical cupping tests (92), (94), (101), (133) and others (139), (146), (166), but in spite of every effort in development and refinement of these tests, it is nevertheless a matter of common knowledge that results of these laboratory tests either cannot be well correlated (98), (108), (109), (111), (116), (121), (131), (134), (146), (147), (162) or do not predict the results, which may be expected in practical drawing with a real degree of certainty. A review of the literature of the deep drawing problem reveals that it has been attacked in three ways: (a) development of testing procedures, (b) investigations in developing suitable metals generally, although this may be somewhat qualified, in an effort to obtain the softest material possible, and (c) the mathematical analysis of the type of deformation, extent of displacement, amount of strain undergone, and the forces involved. In the latter case, efforts were often made to correlate such factors with the ultimate tensile strength, without paying attention to the "flowability" of the metal, this quality being assumed inherent in the material. It is the purpose of this paper to review the problem of deep drawing and to clarify certain aspects which mitigate against the reliability of test procedures. Attention is drawn to certain factors affecting drawability which have received very little or no consideration and certain theories and postulations relating to rupture are proposed.

The term "drawability", as herein used, may be defined as the ability of steel or other metals to withstand cold pressing or stamping operations without rupture. In reality, there are several different properties of a metal which determine its drawability. The first is its ability to flow under various conditions of stress (and temperature); the second is its rate of strain hardening, i.e., the coincidental increase in resistance which the metal offers to deformation as plastic flow proceeds; the third is its rupture strength which represents the quantitative limit of the process that occurs when the increased stresses, in proper combination, have exceeded the limit at which the metal will break. This rupture strength must not be confused with the ultimate strength as determined by the conventional tensile test. An external factor also influences the final result, namely the

increased stress which must be applied to overcome the increased resistance that occurs upon strain hardening.

Deformation in Drawing of a Cylindrical Shell

The simplest deep drawing operation is that involved in shaping a cylindrical shell and nearly all investigators in this field have confined their theoretical considerations to this problem as it is the one most readily amenable to mathematical consideration, since the stresses at any given circumference must be uniform.

The first action of the downward movement (Fig. 1) of the punch bends the blank around the radius of the die (r_d) and the punch (r_p). The relation between the punch movement and the

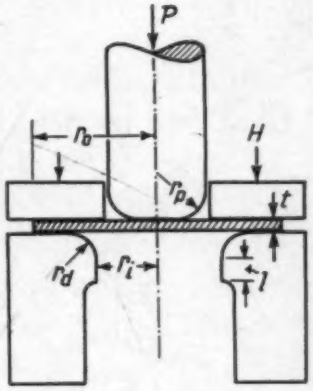

Fig. 1—Cross Section of Cylindrical Punch and Die.

movement of any cross section of the blank between r_d and r_p has been evaluated by Sommer (190), Asimow (135) and Fukui (118). The principal stresses during this first movement of the punch are those of bending around the nose of the punch and the radius of the die, although there must also be a certain amount of circumferential compression at the same time.

Coincidentally with the movement of the blank around the radius of the punch and die, there begins the movement of the metal under the blank hold-down, inward toward the center. The metal under the hold-down is subject to various stresses, as follows (Fig. 2):

1. Tension radially caused by the movement of the blank inward under the action of the punch while at the same time this

movement is retarded by the hold-down and the plastic resistance of the blank.

2. Compression circumferentially is set up as the circumference of the blank is reduced.
3. Compression vertically due to the pressure of the hold-down.

As the blank is bent around the radius of the die and downward along the land, i.e., that portion of die below drawing edge, the metal is rebent into the straight cylindrical side. At the same time there is an accompanying tensile stress downward, caused directly

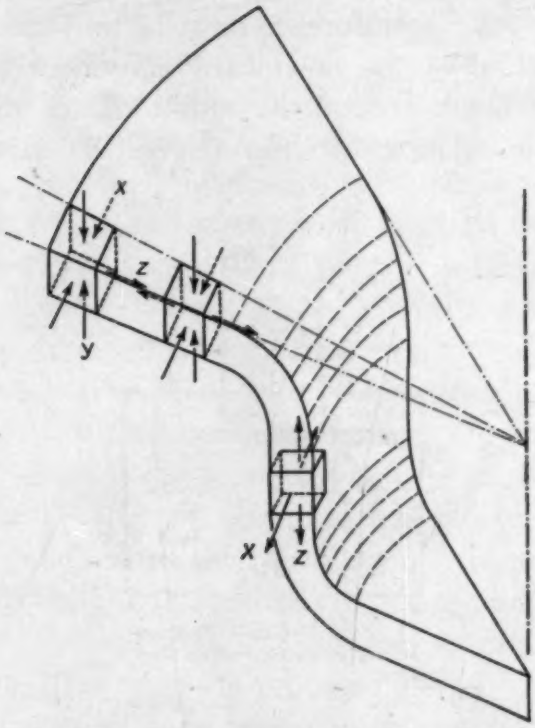

Fig. 2—Section of Partially Drawn Cylindrical Shell, Showing Stresses at Various Locations.

by the pressure of the punch on the bottom of the shell. Tensile stresses also occur circumferentially since the shell wall is restrained from contracting by the punch. There is therefore a change in direction of the circumferential stresses as the blank passes from the hold-down into the die. The tensile stress downward is partly balanced by the friction between the hold-down and the die, which results from the pressure applied to the hold-down, together with the friction of the blank as it passes over the edge of the die, and the plastic resistance of the flat portion of blank to further deformation.

Part II gives a more detailed review of the various factors in-

volved in drawing cylindrical shells and summarizes briefly the conclusions of various investigators.

Multiaxial Stressing

The foregoing sketchy analysis of the stresses arising during drawing of a cylindrical shell raises the question of our knowledge concerning multiaxial loading. For many years, engineers and mathematicians have developed numerous laws and formulae relating to the behavior of metals, etc., when subject to elastic loading. Elastic failure is usually considered to occur when plastic deformation begins. Various theories, including (a) the maximum stress theory, (b) the maximum strain theory, (c) the maximum shear or stress difference theory, (d) Mohr's theory and (e) the maximum strain energy theory, have been advanced to define the conditions under which the limit of elasticity occurs. It has only been within recent years that certain of these theories have been applied to the problem of plasticity and a mathematical basis established which may be used in analyzing the plastic flow processes.

The loading of metal in simple tension and compression has been subject to considerable study and need not be discussed in detail here. The writers know of no case on record where a metal has been subject to uniform tension in all directions but it would seem in such case there could be no yielding or elongation in any direction except for elastic elongation and that the metal would simply be pulled apart when subject to sufficiently high forces. In other words, the metal would act entirely as though it were brittle. These remarks should not be passed without reference to a proposal of Haigh and the researches of Kunze. Haigh (57), (74) suggested that cracking of ductile materials in general was commonly due to "triple tensile" stress. Kunze (64) investigated the tensile strength of specimens, having notches of various angles and also having varying ratios of the area of the test specimen to the reduced area at the notch, and by extrapolation ascertained the "technical cohesive strength" or the strength under triaxial stressing. Gensamer (9) also determined "the technical cohesive strength" by tensile testing notched specimens in which a slight fatigue crack had been developed. Triaxial compression has been investigated by Howard (88) and Bridgeman (39p151), who proved that metals can be compressed elastically and will withstand high hydrostatic pressures but sustain no permanent

effects, that is, of course, provided there is no porosity in the metal.

It is well known that metals can withstand simple tension up to a certain limit without failure, but in the study of deep drawing, one is faced with the problem of ascertaining what happens when the metal is subjected to a wide variety of combinations of both tension and compression, as illustrated by the following typical cases. Fig. 3 represents the forces involved in the portion of the blank

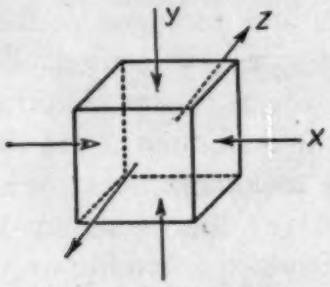

Fig. 3—Stresses Under Hold-Down.

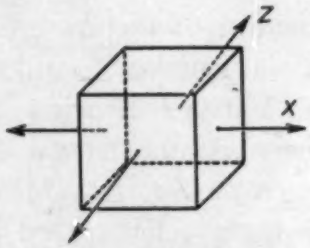

Fig. 4—Stresses in Side Wall of Shell.

under the hold-down as it moves inward toward the punch. Compressive forces (circumferential) in the X-plane are undoubtedly very high, Sachs (144), (164), Siebel (153). Compressive forces in the Y-plane arise from the hold-down pressure. Tensile forces (radially) in the Z-plane arise by the force of the punch drawing the blank inward. A recent analysis of the relative magnitude of these forces is given by Swift (92). Fig. 4 represents the forces involved after the blank has passed down into the die and has formed the cylindrical side of the shell. Tensile forces occur in the Z-plane; also tensile forces occur circumferentially (X-plane) because the punch prevents any reduction in diameter of the cylindrical portion of the shell which otherwise would occur in a manner analogous to the necking down of an ordinary tensile specimen. There is no stress on the Y-plane provided sufficient clearance is allowed.

There is comparatively little published in regard to the physical properties of metals subjected to multiaxial loading. Batson and Hyde (81p242) detailed some of the earlier work which was performed in investigating the resistance of metals to combined stresses.

One of the early investigators in this field was A. J. Becker (86). He subjected tubes to biaxial loading in varying degrees and took stress-strain measurements of tubes subjected to hydraulic pressure. Combinations of axial tension and axial compression with circumferential tension were investigated. Johnson's apparent elastic

limit in axial tension was found to be raised, when the tube was subjected to circumferential tension. Becker obtained values of 43,000 pounds per square inch in simple tension which approached a maximum of 50,000 pounds per square inch as the ratio of circumferential tension to axial tension reached one-half. In axial compression and circumferential tension, the limit decreased in one experiment from about 25,000 to about 16,000 pounds per square inch.

Other researches in this field have been made by Westergaard (82), Koenig, Linicus and Sachs (60), Siebel, and others (48), (52), Maier (44), Austin (29), Lode (79), Taylor and Quinney (71). All of these investigators used somewhat similar methods of approach in that stresses in different planes were obtained by the use of tubes and all have shown the condition of yielding and rupture is dependent upon the varying combination of stresses to which the tubes were subjected. The applicability of such tests with tubes to the deep drawing problem will be discussed later.

The Bauschinger Effect

The foregoing considers briefly the effect of simultaneous loading with various stresses. In the drawing of a shell there undoubtedly is an additional phenomenon which bears upon the question. It will be noted that the initial preponderant deformation on that portion of the blank under the hold-down is compressive, while as the wall is drawn down in the die, the strain is more largely tensile. There is therefore an alternation of stress from compression to tension.

Long ago Bauschinger (89) showed the elastic limit was altered by cyclical variations of stress. He proved that, when a metal is subjected to tension beyond the yield point and the elastic limit is thus raised and thereafter the same metal is compressed, the elastic limit in compression will be found to have a lower value than would be obtained on initial compression. After plastic flow and reversal of direction of loading from tension to compression, or vice versa, comparatively large plastic deformations are produced by relatively small loads. The Bauschinger Effect was confirmed by Bairstow (87), later by Sachs and Shoji (78). It was discussed by Elam (39p90) and treated mathematically by Prager (40). It is interesting that the method used by Becker (86) in loading his specimens was in progressive alternate steps and a very decided lowering of the

yield point was observed for axial compression-radial tension.

Swift (12) considered the effect of reversed torsion. Bars were reverse-twisted back through the same angle, to which originally subjected, and then tested in tension. The return shear did not continue the effect of the initial shear. Up to a certain point the effect was negligible. Beyond this point conditions fundamentally changed. In retwisted bars, the stress at incipient necking was not changed, but the reduction of area restored to its full value. The form of fracture was a perfect cone and cup in contrast to the wolf's ear which was found on bars merely twisted in one direction and then pulled in tension. Very significantly, photomicrographs showed that negative torsion apparently returned the structure to the original equiaxed condition. The grain structure was predominately unaltered by the twist and retwist, although the illustrations show some evidence of straining. Furthermore, the indentation hardness was not appreciably affected by the return twist. Swift did not relate his findings to the Bauschinger Effect but did offer in one explanation that the reversal of shear stress may in some measure effect a repair of the damage caused by initial overstrain. Essentially this is the same explanation which Asimow (135) advanced to explain the Bauschinger Effect. Reversal of flow relieves the obstructing effects, caused by the initial straining, and enables slip to take place again more readily along favorably oriented crystallographic planes.

To the best of our knowledge, the Bauschinger Effect has never been taken into consideration in the drawing problem, except briefly by Asimow (135p264) and it would seem this effect may play a not inconsiderable part in certain stages of deep drawing. Returning to the previous illustration (Fig. 2), it will be recalled that the circumferential compressive stress of any unit under the hold-down is reversed as it passes down into the die and a circumferential tensile stress then occurs. Here the Bauschinger Effect would be in effect if this circumferential tensile stress reaches a value at which the particular unit will yield following the combined compression and tension effects that occurred under the hold-down. The Bauschinger Effect would seem effective in redrawing operations. During the second draw of a cylindrical shell, the direction of the circumferential tensile stress in the shell wall which occurs during the first draw is again changed. Compression is in operation, since the circumference of the shell is reduced in diameter.

Theories of Plastic Strain

Most theoretical considerations of the deep drawing problem have been based upon the maximum shear theory—Sommer (190), Sachs (164), Siebel (153), Fukui (118), although Asimow (135) used the maximum strain-energy theory. Experimental tests involving combined stress, such as the work done by Lode (79) and Taylor and Quinney (71) indicate the strain energy theory agrees best with experimental data, although Swift (12) is not entirely in agreement with this.

The maximum shear theory defines elastic failure as occurring when the maximum shear stress reaches the elastic limit in shear while the maximum strain-energy theory postulates that inelastic action in a body, due to any combination of stresses, begins when the energy per unit volume at the point is equal to the energy absorbed per unit volume by a bar stressed to the elastic limit in tension. In the application of the strain-energy theory to plastic flow two expressions are derived, one of which defines the interdependence of the principal stresses in relation to the yield stress while the other defines the interdependence of the corresponding principal strains under the assumption that the density of the material remains constant. The interconnection between the expressions for stress and for strain is defined by the true stress-strain diagram for the material.

It is a matter of experience that the yield strength of a material in a given direction of loading is profoundly affected by the stresses applied in other directions. Whatever the stress system existing at a particular location in a material body undergoing plastic flow the stresses can be completely resolved into three mutually perpendicular directions. These directions are unique for that stress system and in fact establish the direction of principal stresses. If these three directions are denoted by x, y and z, the corresponding stresses may be indicated as S_x, S_y and S_z. To facilitate application of the theory it is assumed that the material is isotropic, that is to say it does not exhibit directional properties. Yielding or plastic flow according to the strain-energy theory will occur whenever the following condition is fulfilled

$$S = \frac{1}{\sqrt{2}}\left[(S_x - S_y)^2 + (S_y - S_z)^2 + (S_z - S_x)^2 \right]^{1/2}$$

that is, whenever the principal stresses collectively in accordance with

the expression above become equal to the yield stress in simple tension. In order to extend the application of the theory into the realm of plastic flow, the yield stress must be considered to increase as deformation occurs and this increase resulting from work hardening must correspond with the dictates of the true stress-strain diagram.

It is of interest to compare results from this formula with the preceding qualitative discussion of several cases of multiaxial stressing. If all three of the principal stresses are equal and in the same direction so that the material is subject to hydrostatic compression or tension, each of the three terms under the radical vanishes and it becomes impossible to raise the combination of stress to a value high enough to produce plastic flow. This is in accord with experience, since under such circumstances dense metallic materials will not take a permanent set. If two of the principal stresses vanish, for example S_y and S_z, the equation becomes simply $S = S_x$ which merely states that S_x must always equal the yield stress in order to maintain plastic flow. If S_z vanishes and S_x in tension is equal to S_y in compression $S = \sqrt{3}\, S_x$ which defines the relationship between yield stress in shear and yield stress in tension. These examples illustrate under what circumstances yielding will begin and subsequently be maintained when various conditions of multiaxial stressing are applied. The composite of stress calculated in accordance with the formula is often referred to as the "generalized intensity of stress".

The counterpart of the "intensity of stress" is the "intensity of strain". It is derived by calculating the work of deformation from a consideration of the strains in tension and compression when a material is subjected to pure shear and by equating to the work of deformation calculated directly from the shear strains, Asimow (135). The resulting expression for intensity of strain is

$$\bar{e} = \sqrt{\tfrac{2}{3}} \cdot \sqrt{e^2_x + e^2_y + e^2_z}$$

The strains in this formula are the logarithmic strains and are defined as the logarithms of the unit extensions in the three principal directions. The relationship between the intensity of stress and the intensity of strain is defined by the true stress-strain diagram. As shown in the formula above intensity of both stress and strain can be calculated if the component principal stresses and strains are known. In many problems of plastic flow the stress system is not known but the strains, because they are associated with the changing shape of the material body, are quite often actually known or can be estimated by

simple experimental expedients. It is therefore oftentimes necessary to infer from the principal strains the corresponding principal stresses which operated during the plastic flow of the material. In doing so three formulae are available, namely:

$$\tfrac{1}{2}\ (S_x - S_y) = Q\ (e_x - e_y)$$
$$\tfrac{1}{2}\ (S_y - S_z) = Q\ (e_y - e_z)$$
$$\tfrac{1}{2}\ (S_z - S_x) = Q\ (e_z - e_x)$$

From the known strains the procedure in calculating the stress system is as follows:

The strain intensity is calculated according to the formula in the preceding paragraph. This locates a point on the logarithmic true stress-strain diagram. The stress corresponding to this point is the intensity of strain. The slope from the origin to the point thus located on the stress-strain diagram is the coefficient Q in the preceding formula, Fig. 5. With three equations and three unknowns it is

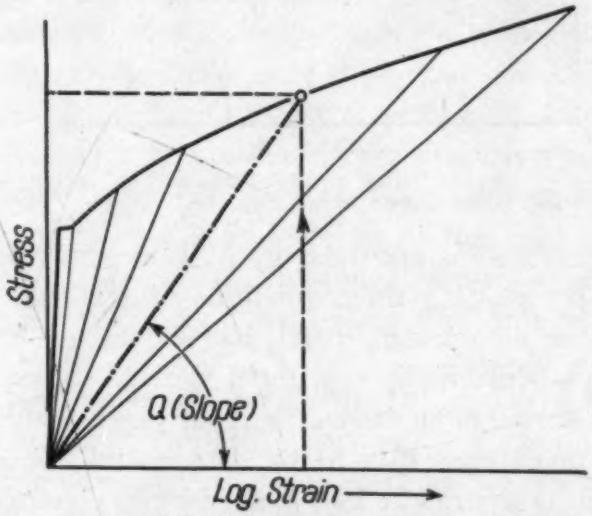

Fig. 5—Relationship Between Stress and Strain and Physical Significance of the Modulus "Q."

possible to calculate the individual values of stress. It is interesting to note that the plastic coefficient "Q" is similar to the modulus of elasticity inasmuch as it is defined as a ratio of a stress to a strain. Its magnitude varies continuously with increasing strain. The three formulae above are tantamount to saying that the amount of shear strain in each of the principal directions is proportional to the magnitude of the corresponding shear stress. The factor of proportionality, namely the plastic coefficient "Q", depends on the amount of strain. If desired the stress-strain relationship could be characterized by a plot of strain versus "Q" value. It would appear as

shown in Fig. 6. The initial value is equal to the modulus of elasticity.

Strain Hardening

It is evident from the discussion in the foregoing section that the true stress-strain diagram plays an important role in the analytical treatment of plastic flow. Very little data are available in literature on true stress-strain diagrams for the materials commonly used in deep drawing; perhaps the most complete recent discussion of true

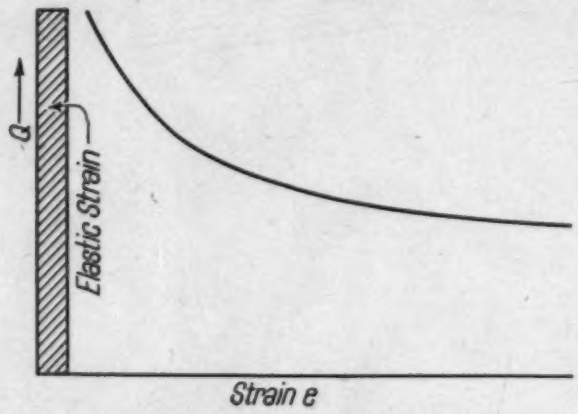

Fig. 6—Value of the Modulus "Q" with Increasing Strain Rate.

stress-strain relationships are those by MacGregor (4), (22) and by Norris (38). By plotting the logarithms of true stress against the logarithms of true elongation, Norris has shown that the plastic flow of a metal, which is originally free from internal stresses, follows one continuous law throughout the range from yield point up to rupture under tension, with constants to be determined for each material. The relationship is a straight line given by the equation

$$S = KE^m$$

in which S is the true stress, E is the true strain, K is a strength index (the stress which would correspond to 100 per cent elongation assuming the metal can support that much strain) and m indicates the rate of work strengthening. K and m are constants readily calculated from the stress-strain plot on logarithmic co-ordinates.

In the true stress-strain diagrams, there is frequently shown an upward hook in the region of necking up to the point of rupture. This deviation from the straight line is usually explained by difficulties in measurements during necking, as well as due to the fact that the last measurement of cross sectional area must necessarily be taken after fracture. It has been also customarily overlooked

that, during the necking period, the stresses occurring in necking are not simple longitudinal tensile stresses but are, in fact, a complex combination of multiaxial stresses. Haigh and Jones (153) have discussed this in the case of lead alloys and pointed out that transverse compression maintains the static equilibrium at the convex profile of the section, while that at the concave location is maintained by transverse tensile stresses. They suggested that transverse stresses in the neck may rise so high in a strong metal with a concave neck that the core of the mid-section breaks by "triple tensile" stress, leaving marginal zones to shear off as the final stage of fracture. Therefore, the upward hook of the true stress-strain diagram may not be entirely due to experimental errors but the result of lack of consideration of the actual stresses which occur during necking. See MacGregor (4) for a recent review on the subject of the tension test.

The question naturally arises whether a given effect of strain hardening results if the metal is cold-worked a definite amount in tension, in compression, or in a corresponding amount by any combination of tension and compression in varying degrees. It is usually considered throughout the literature that the manner in which strain hardening is accomplished is immaterial to the final effects. Crane (204), (223)—see also Sachs (3)—reported tests which show that a given metal will always strain harden at the same rate and to the same extent whether it is cold-worked in tension or compression. There are however occasional comments that would seem to indicate such is not the case with combined tension and compression. Kenyon and Mehl (11p453) reported that wire drawing produces a greater change in tensile properties for the same amount of reduction than does rolling. Eicken and Heidenhain (30) and Bonzel (43) have given values of the properties of steel wire reduced from one diameter to another by a varying number of passes. Both showed heavy drafts increase the yield point and tensile strength more than light passes for the same total reduction. It seems this may be due to a different amount of strain hardening occasioned by different compression and tension relationships which are brought into play with the various conditions of processing. Sachs and Linicus (see MacGregor 2) and Davis (see Templin 72p479) also gave some additional comments to indicate such may be the case.

Although it seems established that the amount of strain hardening is the same for a given material, whether it is cold-worked in tension

or compression, it does not necessarily follow that the same amount of strain hardening will result from an equivalent multiaxial stressing or from alternate tensile and compressive stressing. From the viewpoint that strain hardening is caused by fragmentation of crystallites which interrupt the continuity of slip planes and to mechanical obstructions resulting from adjacent grains with different orientations of slip planes, it would seem entirely logical that strain hardening is independent of the mechanical method by which it is accomplished and is fundamentally related to the microstructural effects which are induced by the plastic flow. The Bauschinger Effect (Asimow 135, also Hoyt 1) may be explained by the reversal of flow, which relieves the obstructing effect and enables slip to take place along new favorably oriented surfaces. It appears logical that the degree of crystallite fragmentation within the grains and at the grain boundaries depends solely upon the amount of work required for such deformation, no matter in what manner the deformation is accomplished. The amount of work actually expended to produce the deformation should therefore be a truer criterion of work hardening than the amount of strain or the amount of stress applied to the material.

Thus, if 10,000 inch-pounds of actual work are expended in deforming 1 cubic inch of a metal, a certain amount of fragmentation will occur. This certain amount of fragmentation is responsible for the apparent work hardening of the material. The preceding hypothesis implies that regardless of how the given material is deformed or by what steps the stress is applied in expending the 10,000 inch-pounds of work, the total amount of fragmentation will be the same. Consequently it is further implied that the work of deformation is under all circumstances uniquely related to the work hardening of a metal, in contrast to either stress or strain, which only under certain simple circumstances are directly related to work hardening. This hypothesis takes no account of precipitation hardening effects which may occur concurrently with the work hardening.

Evaluation of Rupture Strength

While the rupture strength of certain nonmetallic substances has been calculated theoretically (75), (76) and found in reasonable agreement with experimentally determined values, in the case of metals, experimental values of breakage strength are much below those obtained by theoretical calculations. This problem has been the subject of various theories (7), (21), (35), (46) and while it

properly belongs to the field of atomic physics, nevertheless it may not be amiss to consider certain aspects of rupturing which appear to be applicable to the deep drawing process. The following speculations are advanced which, while purely hypothetical, would seem to offer a partial explanation of various types of rupturing.

The rupture of metals involves an actual separation which may mean either a pulling apart of grains or an actual tearing of the lattice structure within the grains. It is generally considered that metals fail by shear but in the final analysis the atomic bonds would seem in some manner to be pulled apart. On this basis, it seems logical to assume that to some degree the rupture strength is independent of the amount of plastic flow which precedes the failure. According to this view, failure occurs when a tensile stress on any plane exceeds the cohesive strength. This condition may occur either due to an unfavorable arrangement of stresses or when strain hardening has proceeded to such a degree as to require tensile stresses greater than the cohesive strength to produce further fragmentation. An unfavorable stress condition would be exemplified by subjecting the metal to three equal and mutually perpendicular stresses, under which condition elongation could not occur, and the breakage would occur without prior strain hardening, provided sufficiently high stress could be imposed.

The extent to which a metal can be deformed depends largely upon whether the strain producing stresses are predominantly tensile or compressive. Subject to compressive stresses, or proper combination of tensile and compressive stresses (as in commercial cold reduction), steel can be elongated to an almost unlimited extent. However, in much commercial deep drawing, the preponderant stress is of necessity tensile and failures are invariably tensile failures. It becomes necessary therefore to consider the circumstances in which tensile failures occur in sections which must transmit pulling loads to other parts of the material if plastic flow is to be accomplished. This, for example, occurs in a deep drawn cylindrical vessel where the lower portion of the cylindrical wall must withstand all of the tensile load required to draw a shell. In this instance the material which fails is subjected only to a small amount of plastic deformation. In other instances, such as obtained in the drawing of fenders, failure occurs in sections which must not only transmit heavy tensile forces but have themselves been subjected to a great deal of prior plastic deformation.

To amplify these conjectures somewhat, it may be useful to consider some hypothetical stress diagrams in which the stress is related to the work of deformation instead of being related to the strain. These diagrams are based upon the postulations previously set forth.

(a) The critical limiting tensile stress at which rupture occurs is substantially constant regardless of the amount of plastic flow which proceeds failure. It depends solely on the inherent cohesive strength of the metal.

(b) The amount of fragmentation which occurs during plastic flow is, for a given material in a given initial condition, uniquely

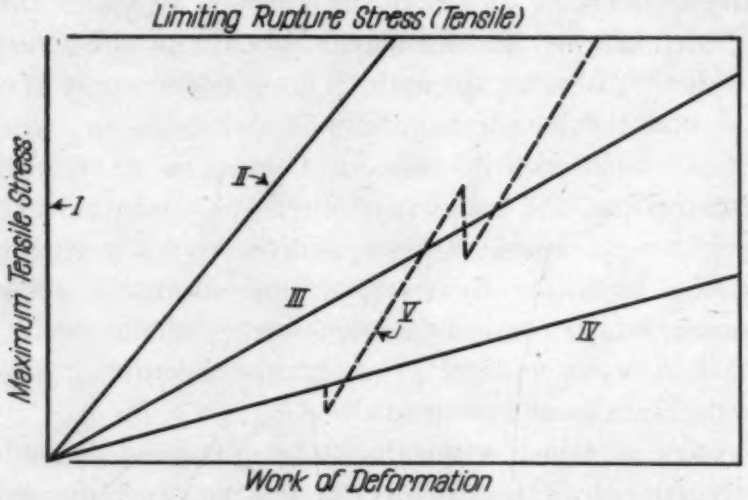

Fig. 7—Approximate Relationship Between Maximum Tensile Stress and Work of Deformation.
Curve I. Triaxial Stress. No Plastic Strain Occurs and Hence No Work of Deformation is Performed.
Curve II. Deformation With Biaxial Stress. Rupture Occurs When Limiting Stress Is Required to Produce Further Deformation.
Curves III and IV. Behavior with Simpler Stress (Uniaxial). Usually Limiting Rupture Stress is Induced Only After Necking Has Begun Which Alters the Simple Stress System to a Multiaxial Stress System.
Curve V. Behavior When Stress System Changed During the Course of Deformation. The Lowering of the Stress Upon Changing the Direction of the Stress System Is Due to the Bauschinger Effect.

related to the unit work of deformation. That is to say, a given amount of energy expended in deforming a unit volume of the material always results in the same amount of fragmentation and is therefore the appropriate measure of work hardening. When the deformation is wrought by stresses which are predominantly tensile, which is merely to say that the maximum stress in the particular system is a tensile rather than a compressive one, the amount of

deformation which the deforming element can absorb is definitely limited and that subsequent attempts to produce additional plastic flow are associated with a rapidly increasing tensile stress which promotes an immediate failure.

Such a hypothetical diagram is shown in Fig. 7. It is bound at the top by a limiting rupture stress value. The limiting rupture stress value applies only to tension, since the material can sustain compressive forces much greater than this limiting tensile value. Assuming that an element of material is subjected to some combination of stress, a curve will result on the diagram as the stresses are made progressively greater and deformation proceeds.

To illustrate, several instances will be considered. If the material is subjected to triaxial tension, no deformation can occur since the material cannot deform expansively in all three directions. Consequently the stress will rise, although no actual work of plastic deformation is involved. The curve (I) rises vertically until it meets the limiting stress value where rupture occurs.

If the material is subjected to biaxial tension wherein the tensile stress in one direction is half the tensile stress in the other direction, then the stress will rise at a relatively rapid rate as the material is deformed. (Curve II.) Usually the metal fails with little or no necking at the point of breaking.

In the case of uniaxial tension, the usual experience indicates that a considerable amount of necking of the material will occur before the limiting rupture stress value is obtained, as illustrated in Curve III.

Where compression in one direction is combined with somewhat larger tension in a perpendicular direction, the curve will be somewhat flatter. Curve IV.

When the Bauschinger Effect is called into play, the resulting graph will be a discontinuous curve (V), the stress values are always reduced when this change is operating, the amount of reduction depending on the amount of change in stress. It is even possible and may indeed often be the case, that the Bauschinger Effect may be continuously operating because of changing proportionality of the stresses involved, in which case some plot could result departing considerably from any of the more simple foregoing examples. Whenever this effect is called into play the work of deformation no longer becomes a unique function of the strain. It would seem that the total amount of strain, neglecting sign, may always be greater

in this event. When the stresses are predominantly compressive the possibility of necking is obviated and the resulting plot may extend considerably toward the right. If in conjunction with the compressive stresses there are also somewhat smaller tensile stresses, as may be the case in a cold reduction mill, then failure can occur if the tensile stress exceeds the limiting stress value regardless of the amount of work of deformation or the size of the compressive stresses.

Part II

Variables in Drawing a Cylindrical Shell

As previously mentioned, nearly all investigations of deep drawing have been confined to cylindrical shells, owing to the relative simplicity as compared with other draws, and because the geometrical configurations and the forces involved in such a draw are uniform around any given circumference. A few experiments have been made with irregular shapes, as well as the redrawing process, but information obtained from such tests is very meager.

Virtually all research workers have studied deep drawing phenomena in small scale. This means that the thickness of the test blanks were relatively great, compared to the more important range of commercial sizes. In these researches the thickness of the test blanks was in the order of 1.5 to 2.5 per cent of the diameter, whereas in industry most interest centers around conditions where the thickness is in the order of 0.1 to 0.3 per cent. The significance of such small scale tests consequently is clouded, because some factors of great importance in commercial deep drawing operations appear to have little significance in these small scale tests. Surface phenomena, such as friction, lubrication and hold-down pressures, become increasingly important as the amount of surface of the blank increases in relation to its thickness.

However, a brief review of the results of such investigations seems warranted, since much of the information is not readily available.

Increase in Thickness of Blank During Drawing

Linicus and Sachs (159) have shown the compressive forces, acting upon the blank area under the hold-down in the tangential direction, cause an increase in thickness of the outer edge of the

blank which may be calculated according to the equation:

$$t_i = t_o \sqrt{\frac{r_o}{r_i}}$$

when t_o—is thickness of blank originally
r_o—is radius of blank
t_i—is thickness of blank after drawing to radius r_i
r_i—is radius of flange after drawing

The calculation is based on the assumption that the compression is accomplished without friction and without blank holder pressure.

This calculated increase in thickness is greater than actually takes place in drawing for three reasons: (a) radial strains, resulting from the drawing, on all elements except the outside edge; (b) high normal compressive stresses exerted by the hold-down; and (c) radial frictional forces exerted as the blank moves inward. The equation therefore applies with accuracy only at the outer edge where radial tensile forces are nil. Elements near the circle of radius r_i tend to become thinner since the compressive forces are relatively low at this location. Asimow (135) has given an empirical formula, determined by actual measurements, which takes into account these factors.

If the blank hold-down is rigid, it is quite evident that the hold-down pressure increases as the blank thickens and, to overcome this, an increase in pressure with consequent increase in drawing force is required. Linicus and Sachs suggested that the blank hold-down be tapered, allowing greater clearance toward the drawing edge, and show that the drawing force decreases if the hold-down is tapered inward in varying ratio of 1/50 to $\frac{1}{10}$. These tests were made with a Wazau (178) testing machine using brass. In American practice the rigid type of blank holder, which is attached to the die, is seldom used. The type most frequently found for large stampings is the toggle press hold-down, which, while adjusted to a definite position, nevertheless may permit some vertical displacement. This vertical displacement may be attributed to the spring of the press and dies or to wear of the moving parts. American shop practice in tapering dies or hold-down varies according to the press and dies. With particularly rigid set-ups the taper may allow for thickening of the blank at the drawing edge, while in cases where there is appreciable spring it is customary to taper outward, giving more clearance on the outside of die. Either hold-down or die may be tapered, seldom both. One figure, given by a practical operator

for the amount of such taper, is ½ of 1 degree. Taper is not necessary with presses equipped with pneumatic hold-downs and in this case dies and hold-downs are usually flat.

With spring hold-downs or those having a rubber cushion or the pneumatic type, it is evident this increase in thickness does not have such a pronounced effect either on the momentary hold-down pressure or upon the drawing force itself. Fukui (118) has measured this increase in hold-down pressure in the cases of rigid, spring and rubber hold-down. In the case of rigid holding, the hold-down pressure increases more or less gradually until it increases very rapidly and in his experiments reached a maximum of over 100 per cent more than the original hold-down pressure, then falling suddenly as the partial pressing is drawn from beneath the pad. With helical spring holding he found (contrary to what might be expected) that the hold-down pressure increased, although it did not show any sharp maximum as is the case with rigid holding. This would, of course, depend upon the stiffness of the springs. When a rubber ring was used the hold-down pressure became larger but the rate of increase was far smaller than either of the former.

The Formation and Prevention of Wrinkles

The tangential compressive stresses causing the metal beneath the hold-down to rearrange and thicken has the additional effect of causing the blank beneath the hold-down to wrinkle. Crane (204) explains this tendency to wrinkle by comparing the condition set up in the flange with that of a structural column which is loaded beyond its elastic limit and is gradually being squeezed down plastically. Certainly this column effect must explain the formation of the wrinkles, and since the primary function of the hold-down is to prevent the formation of these wrinkles, there must be a balance of forces between the pressure exerted by the hold-down and the circumferential compressive forces. Nadai (66) gave some theoretical consideration on the subject of buckling after the yield point is exceeded and mentioned that a peculiarity of buckling under this condition is the decrease in the axial compressive forces during bending.

Fischer (181) was apparently the first to investigate the problem. For aluminum blanks of 0.8 millimeter (0.032 inch) thickness and 166 millimeters (6.54 inches) diameter, Fischer gave a value of 180 pounds per square inch which would prevent wrinkles. In 1928,

Goekeler (179) analyzed them mathematically. Herman and Sachs (152) made a report of investigation with brass and Sachs (144) stated that drawing capacity depends to a considerable extent on the form imparted to the blank hold-down and the manner in which it is pressed on the flange, the greater the pressure -H- the higher the force necessary for drawing and the smaller the drawing capacity. They stated that the most favorable hold-down pressure (i.e., the minimum hold-down pressure necessary to prevent wrinkle formation) increases rapidly as the curvature of the die increases and the blank thickness decreases. Sachs stated that 10 to 20 kilograms per square centimeter (142 to 284 pounds per square inch) hold-down pressure is favorable for steel and is sufficient to prevent wrinkles. Where sheets are thicker than 3 per cent of punch diameter, such hold-down pressures have little effect on drawing capacity.

Fukui (118) investigated the limiting force necessary and sufficient to prevent wrinkles with small diameters. As previously noted, the holding pressure increased moderately (about 20 per cent) when a rubber ring was used and no wrinkling occurred but when wrinkling did occur, the pressure of the hold-down, as would be expected, increased very materially. The initial start of wrinkle formation was very gradual and it was difficult to tell exactly the point where wrinkling began. In the case of aluminum, he found the limiting hold-down pressure increased with decreasing thickness, but contrary to expectation this same situation did not appear to hold true with steel. He also found that the tendency to wrinkle is affected considerably by the clearance between punch and die.

Fukui did not find any apparent effect on the limiting hold-down pressure by changing the radius of the corner of the punch. With constant diameter, his experiments showed that the necessary hold-down pressure decreased as the radius of the die corner increased, this being the result of decreased area under the hold-down. Of especial interest are his experiments with increasing blank diameter. Here he found that the hold-down pressure increased almost lineally with aluminum, but strange to say this was not the case with steel.

Swift (92) also did not give any exact lower limit for blank holder pressure but his results showed that this limit falls within the range suggested by Herman and Sachs (152). He stated the limiting blank hold-down pressure will be smaller with blanks of larger diameter than those of smaller diameter because the actual rupture strength of the shell wall will be less.

Mijon (128) investigated the limits of wrinkle formation in the case of a conical shaped die where no blank holder was used, but this procedure seems only possible with small sized drawings.

Force Required for Drawing

In drawing of a cylindrical shell, the tensile stress must not exceed the rupture strength; otherwise the shell will break at the base. As has been explained previously, this rupture strength is not the value given by the ultimate strength of the tensile test. The efforts of various investigators have been directed toward solving the problem of the total stresses involved in drawing, both by calculation of such stresses and by measurement of the force required for drawing and to determine various factors which affect the drawing force. Consideration of the various factors affecting the drawing force is given in succeeding paragraphs.

The actual results of these researches are all more or less empirical and none have completely solved the problem. However, certain of these researches have thrown some light on the problem of rupture strength of cylindrical shells. Among these are the investigations by Sommer (151), (190), Siebel (153), Herman and Sachs (152), Sachs (144), (164), Fukui (118) and Asimow (135).

Sommer wrote—

$$P = \pi d t s_{max} \geqq C^{\mu_1 \alpha} (2 \mu H + 2 \pi S_{max})$$

where t is the thickness of the material
$\pi d t$ is the cross section of the shell wall
s_{max} is the nominal ultimate tensile strength
α is the angle of bending around the drawing edge (close to 90 degrees)
C is the natural logarithm
μ_1 is the mean coefficient of friction around the drawing edge
μ is the coefficient of friction under the hold-down.
H is the hold-down pressure
S_{max} is the unit compressive stress
P is the drawing force

Siebel, using the maximum shear theory as the condition of plasticity, developed the following formula:

$$P = 2 \pi r_1 \cdot t K_f \cdot \log_e \frac{r_o}{r_1}$$

where K_f—is the average stress difference and is a function of the deformation occurring in the sheet at the outer edge and at the drawing edge.

r_o—is the radius of the blank

r_1—is the radius of the shell

Herman and Sachs gave an approximate empirical formula, obtained from experimental data, relating the breaking strength to tensile strength, thickness of metal, radius and diameter of punch.

Sachs (144) stated that the breaking strength is increased as the sheet thickness decreases and the die curvature decreases, until it becomes 1.14 times the value of the tensile strength. This increase of breaking strength he explained as follows: The shell is a tube subjected to tensile stress, any reduction of its diameter being prevented by the punch. If the same conditions are set up by hydraulic pressure, then the yield point and also the tensile strength of such tube are roughly 1.16 times as great as those of a solid bar or a tube of the same material without internal pressure. This was determined by Lode (79). It is also interesting to compare these results with those of Becker (86), who previously obtained similar results in the case of Johnson's elastic limit. Nadai (15) has calculated theoretically that the "constrained yield strength" in tension is 1.155 times the yield in simple tension. This is the tensile yield stress of a bar which is allowed to contract freely in one of the lateral directions, while it is constrained not to deform in the other lateral direction.

Fukui developed a theoretical formula for the drawing force but some terms were indeterminate and he concluded the drawing force could not be calculated but must be determined experimentally.

In the research conducted by Asimow (135), the total force required for drawing a shell was determined. This total force was then separated into the work of friction and the work of deformation. It was brought out in this paper that in drawing operations it is far easier to determine the amount of strain at any location than it is to determine the stress. By the use of the "strain intensity" function which he developed from the theory of strain-energy, the stress was calculated. The work of deformation was then ascertained and this theoretical work of deformation was in good agreement with experimentally determined values. Although no consideration was given to rupture strength, it is possible to apply the methods to such determination.

Effect of Hold-Down Pressure on Drawing Force

Sommer (190) and Sachs (164) showed that a linear relationship exists between the drawing force and the initial hold-down pressure for copper and brass, while Swift (92) confirms these results with steel. However, it is quite evident that this hold-down pressure in most cases increases as the draw proceeds and this rate of increase is dependent not only upon the rate of increase of thickness of flange but also is dependent upon the type of hold-down used for the draw.

Effect of Thickness of Blank on Drawing Force

Fukui (118) showed experimentally that the maximum drawing force was approximately proportional to the thickness of the blank when the same punch and die were used for drawing. This agrees fairly well with the results of Sommer (151), Siebel and Pomp (172) and is in accordance with theoretical considerations, Asimow (135).

Effect of Blank Diameter on Drawing Force

It is, of course, obvious that greater force is necessary to draw blanks of increasing blank diameter to die (punch) diameter ratio. Blume (193) found the permissible deformation depends primarily on volume displaced and this was later confirmed by W. Sellin (191), Schmidt (175), Sachs (164), Oehler (116) and Fukui (118); all have shown that an approximately linear relationship exists between this ratio and the drawing force. Fukui also plotted the total area of the blank and the area of the blank which is moved (total area minus area of die) and found a linear relation in both these cases. As the drawing force increases with the diameter, it finally reaches a value where the cylindrical rupture strength is reached and the blank tears off. Oehler (116) stated that the assumption that punch pressure increases with ratio of blank to die diameter holds true for brass and aluminum but is only approximately true for iron, while Swift (92) in his recent paper, obtained an approximately linear relationship with steel.

Effect of Form of Punch on Drawing Force

In his experiments Fukui showed that increasing the radius of

the nose of the punch has no effect on the maximum drawing force and his results agree with those of Herman and Sachs (152) with brass. Herman and Sachs report an increase in drawing capacity with punch radius up to 0.3 diameter.

However, it is known that this radius is of considerable importance in commercial practice. As Crane (204) stated there is an unsupported area of blank, in the initial stages of the drawing operation, from the outside edge of the die to the inside edge of the radius of the punch. If the radius of the nose of the punch is considerable and the metal relatively thin, wrinkles may result. (See below.) Crane also said the nose of the punch should have a radius four to six times the thickness of the blank in order not to cause thinning of the metal as it is bent over the edge of the punch. Swift (92) found that the punch load is not greatly affected by the punch radius but that greater blank diameters may be drawn successfully with a larger punch radius.

Effect of Radius of Drawing Edge Upon Drawing Force

It is well known that the results obtained in drawing practice are very much dependent upon the radius of the die; that when this radius is small, breakage frequently occurs, while if the radius is too large wrinkles are more apt to take place. Draeger (171) first measured the effect of changes in the radius on the drawing forces in drawing brass and tin plate and showed the force decreased with increasing radius at least up to a certain amount. In his tests with about 2-inch diameter dies, the decrease was not pronounced above the die radius of about $\frac{1}{8}$ inch. Ackerman (165) found the influence even more pronounced than did Draeger, decreasing in the case of brass, and in some instances, approximately 100 per cent by increasing the radius from 0.05 to 0.20 inch. Herman and Sachs (152) also found that increase in radius decreases the drawing force and Fukui (118) gave further data on this point. In drawing small blanks 0.02 inch thick, 1.54 inch diameter, an increase in radius from about $\frac{1}{16}$ to $\frac{1}{4}$ inch decreased the maximum force about 20 per cent and with smaller blank diameter the decrease was even greater. Swift confirmed these results and attributes the ability to draw larger blanks with increased die radius to the lessened amount of thinning which occurs with larger die radius.

Effect of Clearance Between Punch and Die on Drawing Force

Ironing takes place when the clearance between the punch and the land of the die is less than the thickness of the metal passing between. Under these circumstances a modified process of extrusion takes place since the thickness of the metal must be reduced to approximately the clearance space. If the initial thickness of the blank is more than the clearance, ironing occurs throughout the draw. In other cases, the initial thickness of the blank may be smaller than the clearance but if the clearance is insufficient to allow for the increase in thickness of that portion of the blank under the hold-down, ironing will also occur in the latter part of the draw to an extent dependent upon the increase in thickness and the actual clearance. As may be shown by the formula of Linicus and Sachs, the maximum probable increase in thickness is 41.4 per cent when the ratio of blank diameter to shell diameter is 2:1.

Fukui (118) experimented with the effect of clearance ranging between 115 and 200 per cent and a blank to shell diameter ratio of 1.94. Maximum force did not vary much with clearance of 115, 125 and 140 per cent (ironing must have taken place with 115 and 125 per cent since thickness at outer edge increases to close to 40 per cent with this ratio) but it is of interest that the peak of his force curves were of larger duration with each decrease in clearance. Between 140 and 200 per cent the maximum force decreased until at 200 per cent clearance the maximum was 16.8 per cent lower. This decrease was attributed to geometrical effects in the initial stages of drawing as the clearance increased. In this connection it seems logical to believe that this effect does not apply with larger blanks after the punch nose is considerably past the radius of the die. It seems doubtful whether this holds true with larger draws when the die clearance in practical operations is very often 150 to 200 per cent.

In the drawing trade, ironing is frequently practiced when it is desired to decrease the thickness of the shell. However, ironing is frequently spoken of as "ironing out the wrinkles". Ironing in this connection may not necessarily involve a decrease in thickness. Incipient wrinkles and even fairly large ones are flattened out or "ironed out" by the very act of passing over the drawing edge. This effect is generally considered to be more pronounced the smaller the radius of the drawing edge and it is the necessity of flattening out these wrinkles that limits, at least to a certain extent, the maxi-

mum allowable radius of drawing edge. As Swift (92) pointed out a small amount of ironing at the end of the draw is not objectionable as it produces a more perfect shell while the punch load is not affected at the critical portion of the draw.

Effect of Friction

Sommer (151, 190), Siebel (153), Asimow (135) and Fukui (118) devoted some attention to analyzing the effects of friction in drawing cylindrical shells. It is possible to obtain an approximation of the frictional forces, notwithstanding the difficulties attendant to determine the coefficient of friction under drawing conditions. The following considerations are drawn largely from these investigators although elaborated somewhat.

The frictional forces arise from the—

1. *Friction Between Blank and Blank Holder*—The force of friction acts radially in the outward direction and, of course, applies on both sides of the blank. This may be written—

$$F_{HD} = 2\mu_1 H$$

where H is the hold-down pressure and μ_1 is the coefficient of friction between the blank and the top surface of the die and the hold-down. This frictional stress acts upon the circumferential rim area of the partly drawn shell and unit frictional stress is, therefore—

$$S_{FHD} = \frac{\mu_1 F_{HD}}{\pi r_1 t}$$

It is frequently assumed that μ_1 does not vary during the draw but this is not necessarily true since H as previously explained increases as the draw proceeds, due to the thickening of the blank. In fact, Sommer (190) gives curves showing the effect of pad pressure on the coefficient of friction of steel.

Pad Pressure Pounds Per Square Inch	Coefficient of Friction	
	Dry	Lubricated (Grease)
36	.14	.10
72	.15	.13
144	.17	.14
288	.18	.16
432	.19	.17
576	.20	.17

It is readily seen that

$$S_{FHD} = \frac{\mu_1 p (r_o^2 - r_i^2)}{r_1 t}$$

where p is the unit hold-down pressure.

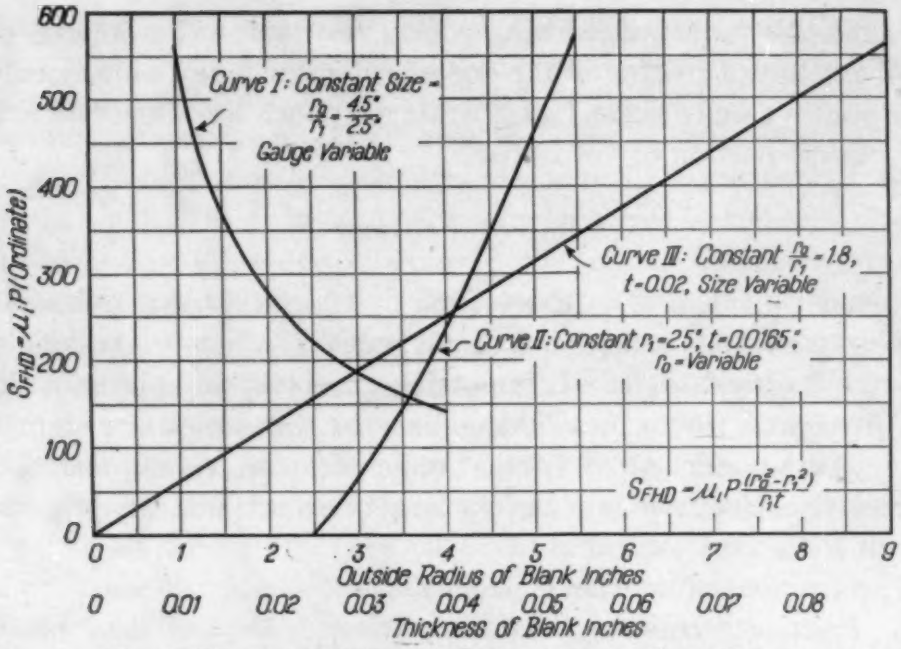
600
500
400
300
200
100
0
$S_{FHD} = \mu_1 P$ (Ordinate)
Curve I: Constant Size - $\frac{r_0}{r_1} = \frac{4.5"}{2.5"}$ Gauge Variable
Curve III: Constant $\frac{r_0}{r_1} = 1.8$, t-0.02, Size Variable
Curve II: Constant $r_1 = 2.5"$, t-0.0165"; r_0 - Variable
$S_{FHD} = \mu_1 P \frac{(r_0^2 - r_1^2)}{r_1 t}$
0 1 2 3 4 5 6 7 8 9
Outside Radius of Blank Inches
0 0.01 0.02 0.03 0.04 0.05 0.06 0.07 0.08
Thickness of Blank Inches

Fig. 8—Effect of Hold-Down Frictional Forces Upon Unit Stress in the Side Wall of Cylindrical Shells.

The curves (Fig. 8) give the relative values of the unit stress for some typical cases, exerted upon the side wall of the shell arising from the hold-down frictional forces. Curve I shows the effect of changing gage, curve II illustrates the effect of increasing the outside blank diameter for a given gage and diameter of the shell, while curve III shows the effect of increasing the size of the shell for a given ratio of outside to inside diameter. From curve III it will be readily seen that the frictional forces in the case of larger size commercial draws exert a distinctly greater unit stress upon the side wall of a shell than is the case with small sized shells, such as have been customarily used in researches on the drawing problem. For example, assuming $\mu_1 = 0.15$ and $p = 100$ pounds per square inch, the unit stress in the case of a 2-inch diameter blank is 900 pounds per square inch and in the case of a 12-inch diameter blank is 5625 pounds per square inch. Many similar illustrations could be made comparing these frictional forces in small scale tests, such as Fukui's and Swift's, with commercial draws but it is sufficient to state that the differences between this hold-down frictional force in small scale tests and larger commercial sizes will range in the order of 4000 to 8000 pounds per square inch. The magnitude of these values is such as to throw considerable doubt upon the value of small scale cylindrical cupping tests in interpreting commercial drawing performance.

2. *Friction Around Drawing Edge*—Siebel (153) stated that the total forces and the work of drawing are increased by a factor $e^{\mu_2 \frac{\pi}{2}}$ because of friction at the drawing edge. If μ_2 (the coefficient of friction at the drawing edge) is 0.1 then $e^{\mu_2 \frac{\pi}{2}} = 1.17$ and if $\mu_2 = 0.2$ then $e^{\mu_2 \frac{\pi}{2}} = 1.37$. That is, the losses at the drawing edge in the latter case amount to 37 per cent of the useful work. These comparatively high values show that the greatest consideration must be given to frictional losses at the drawing edge. Sommer (190) apparently was the first to evaluate the frictional forces at the drawing edge by this method, which is similar to the formula for the friction of belts (Kent, Mechanical Engineers Pocket Book) where

$$T_2 = e^{\mu \beta} T_1$$

where T_1 is the tension on the drawing side
T_2 is the tension on the slack side
μ is the coefficient of friction (Kinetic friction if the belt is sliding)
β is the angle in radians through which the belt is acting

From this formula it will be seen that theoretically the radius of the drawing edge has no effect upon the frictional force at the edge of the die, although practically it would seem probable that decreasing the radius might make it more difficult to have proper lubrication around the drawing edge. Actually this is somewhat difficult to harmonize with various tests of the effect of decreasing the radius of the drawing edge as well as with practical experience, since it is usually considered that the greater difficulty in drawing with a small radius of drawing edge is the result of increased friction. Swift attributes this to more thinning at the base with smaller radius.

Decreasing the angle β should effect considerable reduction in frictional forces. This is in agreement with experimental tests as Fukui (118) finds that the maximum drawing force is reduced 10 per cent by the use of a conical die tapered 30 degrees. Mijon (128) also obtained similar results with a 30-degree tapered conical die. In the case of the 30-degree conical die, the friction amounts to $e^{\mu_2 \frac{\pi}{6}}$ and if $\mu_2 = 0.1$, then $e^{\mu_2 \frac{\pi}{6}} = 1.056$, and if $\mu_2 = 0.2$, the value is 1.11. With one-draw operations in commercial practice, except possibly with small sized blanks, any appreciable change in β is not practical, but in the case of multiple draws, β can be changed and,

in commercial practice, considerable benefit is obtained by sloping the die and hold-down for the second or succeeding draws. It may also be mentioned that this effect must have considerable bearing upon the action of drawing beads.

3. *Friction Between the Shell and the Land of the Die Below the Drawing Radius*—This effect will depend upon the normal pressure between the land and the piece, and this normal pressure will largely depend on the thickness of the piece, clearance and ironing effect. The normal pressure will certainly be greater than the yield point in compression, if any actual ironing (thinning) occurs. If a coefficient of friction of the order of 0.1 is assumed, the additional frictional force of something greater than 3000 pounds per square inch may be anticipated. The area involved is the bearing area on the inside of the die, i.e., the die circumference times the height of the land. An estimation of the magnitude of the forces may be obtained in this manner.

Crane (204) gave the results of some tests which determine the combined frictional load and the load of bending around the drawing edge. He prepared star-shaped blanks, having segments cut out to eliminate the crowding of the metal under the hold-down and these star blanks were then drawn into shells. Without using any hold-down pressure the load was measured and this load was assumed to represent the stress due to bending over the drawing edge only. Pressure was applied to the hold-down and the load then measured. The increase in load was considered to represent the frictional resistance by the blank holder pressure.

Sommer (190) using the same procedure and putting

$$P = 2\mu e^{\mu \frac{\pi}{2}} H$$

and using a linear relation between P and H obtained under various values of H, evaluated μ for brass, copper and aluminum. The rise in the coefficient of friction, quoted above, was attributed to the fact that the lubricant may have been squeezed out in the case of the star blanks and this may not occur to the same extent with solid disks. Sachs (164) also evaluated μ from a linear relationship between P max and H.

Fukui (118) considers Sommer's results unreliable for the reason mentioned, while Sachs' were believed unreliable because of spring holding. Fukui, using instantaneous experimental values for the drawing force and hold-down pressures, calculated the coefficient

of friction from a relationship which he developed and obtained the figures for μ with steel ranging from 0.19 to 0.26. He estimated that if μ is changed 20 per cent by the lubricant, the maximum drawing force is changed about 8 per cent at the most. Fukui did not distinguish between the friction beneath the hold-down and around the drawing edge.

Asimow (135) used a pneumatic hold-down in his experimental investigation and did not attempt to determine the coefficient of friction directly, but was able to separate the work of friction and the work of deformation from the total work of drawing by graphical methods.

Lubrication

In considering the question of lubrication of the blank and dies it is first well to review some fundamentals of this question, especially in view of the newer conception of friction and lubrication. Formerly the force of friction was viewed as being the result of a sort of interlocking of minute asperities at the points of friction. The modern theory (Pye 244) considers the resistance to motion as due to the cohesive forces between molecules acting across the interface of the surface and that these forces are of the same kind as the cohesive forces between molecules of a solid on which its strength depends. In the present state of knowledge, sliding motion is accomplished by a very rapid succession of weldings together and tearings apart between groups of molecules.

Bowden and Ridler (245) measured experimentally the temperatures produced by friction by using a rotating cylinder with a pencil of dissimilar metal pressing down on it and found the temperatures astonishingly high. They also proved that these temperatures were confined to exceedingly thin surface layers of the metal. Using a constantan pencil on a steel track, a temperature of 1000 degrees Cent. (1830 degrees Fahr.) was measured at a speed of 11 meters per second. Using low melting metals, they found that the speed-temperature curve, which is at first a straight line, flattens off at the melting point of the metal in every case, while at the same time, however, there was no apparent melting of the metal. With lubricants, temperatures were also found to be quite high. With constantan at 8 meters per second, 750 degrees Cent. (1380 degrees Fahr.) was recorded without lubrication and 500 degrees Cent. (930 degrees Fahr.) lubricated with oil.

The significance of the work of Bowden and Ridler lies in the fact that the measured temperatures are well above the decomposition temperature of the lubricant and there is danger of local breakdown of the film and that, when boundary conditions persist for any length of time, the primary film of lubricant on the metal surfaces does not remain intact, but is continuously being destroyed and repaired as sliding proceeds.

The condition known as "boundary lubrication" occurs when there is no free oil between the surfaces and friction depends not upon the viscosity of the oil but upon the interaction of a few layers of oil molecules associated closely with metal surfaces. It seems entirely logical to suppose that this type of friction prevails during a great many drawing operations or at least during a certain portion of the draw. It is probable this is the reason why there are a great variety of drawing compounds in use, each no doubt being best suited for the type of draw being made, aside from the questions of removal subsequent to the draw. The circumstance of boundary lubrication undoubtedly explains many cases of die scoring.

Fukui (118) obtained some very interesting results in testing the drawing force with different lubricants. Machine oil, motor oil, rape oil, whale oil, transformer oil, water and soap water of various concentration were used. There was comparatively little difference between the maximum value of the drawing force with all these materials. The minimum value in one set of experiments was obtained with 2 per cent soap solution (about 2110 pounds) and the maximum with water (about 2270 pounds). It was of interest that 2 per cent soap solution gave lower values than the higher concentrations of 4 and 5 per cent.

Jevons (129) attributed some of the differences in performance as observed between laboratory tests and the press shop as due to the possibility that adequate lubrication may not be maintained at the high speeds of drawing while at slow speeds it is relatively easy to maintain proper lubrication. This idea is exactly the opposite to that found experimentally by Swift. The film of grease lubricant is expelled, in part at least, during the drawing action, and the more complete expulsion occurs at slower drawing speeds due to the time effect. In other words the lubrication is more efficient at high speeds. Swift (92) gave considerable data of the maximum punch loads with various lubricants. Graphite in oil or tallow was found to be the most efficient. The time effect for graphite was found

to be nil, this lubricant maintaining a film regardless of speed. In conformity with the aforementioned functional considerations, Swift showed that lubrication is really only essential around the drawing edge and that, when the side of the blank toward the drawing edge is lubricated in a definite manner, the punch load is independent of the condition of the upper surface.

Poorly polished or ground dies are frequently observed in commercial operations and it is of interest that Mijon (128) recorded that the polish of the die has considerably more influence upon the drawing force than does lubrication. The required force was greatly increased when poorly polished dies were used, although the influence decreases with increased blank thickness.

The Effect of Speed on Drawability

The effect of speed on the results of commercial drawing is shadowed by conflicting results. Many instances are known where draws are successful at low speeds whereas breakage occurs at higher speeds. On the other hand, many commercial drawing operations are successful at quite high speeds. Crane (204) attributed breakage at higher speed to inertia, or specifically, a sudden start as the punch hits the blank in mid-stroke combined with high resistance to the start of movement of the metal.

The effect of speed on the tensile test is well known and has been subject to numerous investigations. Elam (17), Davis (20). The markedly increased yield point elongation with increased speed is of special significance in deep drawing.

It is of interest that Asimow (135) suggested the possibility that ductile materials might best be drawn rapidly while brittle materials should be drawn slowly. This was based on the notion that very plastic materials have a rather flat stress-strain diagram and that therefore an increase in speed would have the effect of increasing the apparent rate of strain hardening and consequently might delay necking down of the material. In the case of brittle material the reverse would be desired. The possibility may account for some anomalous performances in actual practice. Just where the dividing line may lie between a "ductile" and a "brittle" material was not considered and may not enter the picture with steel but the reasoning would seem to apply in the case of lead. This is more or less confirmed by

the results of Mathewson, Trewin and Finkeldy (195), who showed that increased speed has much less influence on the dynamic ductility of dead soft zinc than it has upon hard rolled zinc. For example, at a speed of 0.034 inch per minute of cupping, dead soft zinc gave 0.341 inch depth of cup while hard rolled zinc gave 0.415 inch. At a speed of 163 inches per minute, the same soft zinc showed 0.286 inch depth of cup while the hard zinc gave only 0.150 inch.

Comparatively little consideration has been given to the effect of speed in theoretical considerations of the drawing process. Sommer (190) stated that maximum drawing force was not affected by changes in speed from 0.1 to 2.0 millimeters per second (2.36 to 4.7 inches per minute) in case of brass, copper and aluminum. Fukui did not find speed had any effect on drawing small shells of iron between the speed range of 2 to 10 millimeters per second (4.7 to 23.6 inches per minute). Asimow (135) used the formula—

$$S_0 - S_m = \text{Const. } \log_{10} \frac{V_m}{V_0}$$

which was established by Deutler (63) and corrected the values of yield stress for varying punch press speeds but gave no experimental data to confirm the results.

Swift (92) found that the greater the drawing speed (up to 50 feet per minute) the greater the blank diameter which could be drawn successfully. At higher speeds the punch load was found to have a somewhat greater maximum value which endures for a rather shorter period. In more than one instance, blanks failed at a certain punch load during a slow draw, but similar blanks carried a considerably higher load and drew successfully at higher speeds. This was considered to be because the actual process of necking did not have time to develop at higher speeds, while at slower speeds there was a greater opportunity to such effect leading to fracture. Of especial interest is the effect of speed upon lubrication as advanced by Swift.

Andrews and co-workers (93) obtained some anomalous results in finding that increased speed decreased the drawability within a certain range while a further increase improved the drawability.

As the speed of commercial drawing operations is increased, the temperature of the dies and drawn part is of course increased and consideration of the effect of speed is not complete without taking into account the effect of increased temperature prevailing during the draw. Mijon (128) found that a lower drawing force was required

with each of the second and third succeeding blanks drawn, which he attributed to heating of the die. Increased temperature affects the dimensions of the die, the effectiveness of the lubricant and also the cold working properties of the metal. Usually, though not always, it is observed the operations are more satisfactory when the dies are warmed up. Generally speaking, increase in temperature will increase the clearances somewhat, though here again the reverse may be true, particularly with irregular shapes. The cold working properties of the metal at slightly increased temperature (150 to 200 degrees Fahr.) are seldom considered in drawing problems. Nevertheless it is known that certain metals will strain harden more rapidly if cold worked at the slightly increased temperatures often prevailing during drawing operations, and it seems possible some of the conflicting observations of speed and temperature may be explained on this basis. In such case, particularly if successive draws are involved, it seems reasonable to conclude that more successful results might be obtained by drawing at room temperatures. This is in direct contrast with the suggestion of Jevons (141) and Swift (92) that drawing be conducted at 212 degrees Fahr., but, however, these considerations suggest that water cooled dies might be desirable for use with such type metals, provided due consideration is given to the design of the die and proper lubrication. Here again it seems no definite conclusion can be drawn without due consideration of various factors involved.

Summary and Conclusions

1. A review has been made of many factors involved in deep drawing, a subject which has received comparatively little attention in the American literature.

2. The various testing procedures ordinarily employed by which attempts have been made to evaluate drawing qualities fail to predict results of commercial drawing operations for one or more of the following reasons:

(a) The customary tensile test provides information on uniaxial loading, whereas the loading conditions encountered in deep drawing are multiaxial.

(b) Test procedures, involving multiaxial stressing, do not duplicate the wide variety of multiaxial loading conditions encountered in commercial deep drawing except incidentally.

(c) Most laboratory testing procedures do not take into account

the high rate of straining of commercial drawing operations.

(d) No testing procedures furnish any adequate information of the effect on plastic behavior of changing (reversing) direction of stress. In particular, the so-called Bauschinger Effect has been almost completely ignored in discussions of deep drawing. Beyond question further knowledge of this phenomenon must be gained before complete understanding of the deep drawing process can be fully accomplished.

(e) Frictional forces exert a much greater stress per unit area in large scale commercial deep drawing than in laboratory test procedures and interpretation of the latter is vitiated on this account.

3. Much information is needed concerning the true stress-strain relationship of deep drawing metals as well as a better interpretation of the tensile test.

4. Fracture in drawing is dependent upon the relative multiaxial stress conditions as well as the amount of strain hardening which the metal undergoes. A hypothesis is advanced which suggests the general conditions under which rupture may be expected to occur.

5. A review is included of the effect of different variables upon deep drawing.

6. A bibliography of literature pertinent to the deep drawing problem is submitted.

ACKNOWLEDGMENTS

The authors wish to express appreciation to Messrs. R. K. Bowden, Manager, Metallurgical Division, Chicago District, Carnegie-Illinois Steel Corporation; L. J. Rohl, Assistant Manager, Metallurgical Division, Chicago District, Carnegie-Illinois Steel Corporation, and Dr. M. A. Grossmann, Director of Research, Carnegie-Illinois Steel Corporation, for their encouragement and suggestions in the preparation of this paper.

Since this paper was originally prepared, three publications have appeared, which deal in part or in whole with this subject.

Practical Metallurgy, Sachs and Van Horn, A.S.M., 1940.
The Metallurgy of Deep Drawing and Pressing, Jevons, Wiley, 1940.
Strength of Metals Under Combined Stresses, Gensamer, A.S.M., 1941.

Bibliography

Plasticity and Cold Deformation

1. S. L. Hoyt, "Plastic Deformation in Metals," METAL PROGRESS, Vol. 38, 1940, p. 659.
Critique of theories of slip.

2. H. W. Swift, "Plastic Flow in Metals," *Metal Industry,* Vol. 56, 1940, p. 127, 149, 173.
Survey of present position.
3. G. Sachs, "Flow of Metals," *Iron Age,* February 1 and 8, 1940, p. 36.
Strain hardening same in tension and compression.
4. C. W. MacGregor, "The Tension Test," *Proceedings,* American Society for Testing Matrials, Vol. 40, 1940, p. 508.
Review; true stress strain diagrams; true strain and true local necking strain proposed to define ductility; true stress at fracture is more a material constant than value of maximum load.
5. M. Manjoine and A. Nadai, "High Speed Tension Tests at Elevated Temperatures," *Proceedings,* American Society for Testing Materials, Vol. 40, 1940, p. 822.
Review of speed effect in tension tests. New high speed test machine. Copper.
6. P. G. Jones and H. E. Moore, "Investigation of the Effect of Rate of Strain on the Results of Tension Tests of Metals," *Proceedings,* American Society for Testing Materials, Vol. 40, 1940, p. 610.
7. Symposium, "Report of a Conference of Internal Strains in Solids," *Proceedings,* Physical Society of London, Vol. 52, 1940, p. 1.
8. E. A. Davis, "Combined Tension-Torsion Loadings," *Transactions,* American Society of Mechanical Engineers, Vol. 62, 1940, p. 577. *Steel,* Vol. 107, July 29, 1940.
Amount of axial strain and ultimate strength in tension reduced by superimposed torque. Angle of twist at rupture reduced in torsion test by superimposed tensile stresses.
9. M. Gensamer, E. B. Pearsall and G. V. Smith, "Mechanical Properties of the Isothermal Decomposition Products of Austenite," TRANSACTIONS, American Society for Metals, Vol. 28, 1940, p. 380.
Technical Cohesive Strength.
10. H. Carpenter and J. M. Robertson, "Metals," Oxford University Press 1939.
11. "Metals Handbook," American Society for Metals 1939.
12. H. W. Swift, "Tensional Effects of Torsional Overstrain in Mild Steel," *Journal,* Iron and Steel Institute, Vol. 140, 1939, p. 180.
Reversed torsional results of especial interest.
13. J. Winlock and R. W. E. Leiter, "Some Observations on the Yield Point of Low Carbon Steel," *Transactions,* American Society of Mechanical Engineers, Vol. 61, 1939, p. 581.
Transition from elastic to plastic state considered.
14. C. W. MacGregor, "The Plastic Flow of Metals," *Metals Technology,* 1939 TP 1036.
Photographic device for observing plastic flow.
15. A. Nadai, "The Forces Required for Rolling Steel Strip Under Tension," *Transactions,* American Society of Mechanical Engineers, Vol. 61, 1939, A54.
Mathematical relationships of rolling pressures with varying front and back tension.
16. Y. Nakagawa, "Fundamental Equations of Plasticity and Their Applications," Society Mechanical Engineers, Vol. 5, February 1939, Japan. English abstract p. S-7-8; *Engineering Index* 39-15423.
Theoretical development with object to eliminate certain assumptions of Nadai's theory.
17. C. F. Elam, "Influence of Rate of Deformation on Tensile Test with Special Reference to Yield Point of Iron and Steel," *Proceedings,* Royal Society of London, Vol. 165, 1938, p. 568.
18. G. Welter and S. Gockowski, "Some Fundamental Factors Regarding the Stress-Strain Diagram of Mild Steel," *Metallurgia,* Vol. 18, 1938, p. 99.
Spring of test machine has definite influence on formation of stress strain diagram.

19. M. Gensamer, "Yield Point of Mild Steel," *Metals Technology,* Vol. 5, February 1938, TP-894.
Transition between homogeneous and heterogeneous flow discussed.
20. E. A. Davis, "Effect of Speed of Straining and Rate of Loading on the Yielding of Mild Steel," *Transactions,* American Society of Mechanical Engineers, Vol. 60, 1938, A-137.
Discussion of stress concentration on presence upper yield point.
21. H. J. Gough and W. A. Wood, "Deformation and Fracture of Metals," *Journal,* Institution of Civil Engineers, Vol. 8, March 1938, No. 5, 249-84.
Effect of deformation on X-ray spectra. Fracture stage appears to be condition of extreme fragmentation into a mass of crystallites of a definite critical size.
22. C. W. MacGregor, "Relations between Stress and Reduction in Area for Tensile Tests of Metals," *Metals Technology,* Vol. 4, 1937, No. 805.
Critical discussion of methods of plotting stress-strain and stress reduction of area curves. Reference to difference in strain hardening under different conditions of stress.
23. A. Nadai and E. A. Davis, "Plastic Behavior of Metals in the Strain Hardening Range, Parts I and II," *Journal,* Applied Physics, Vol. 8, 1937, p. 205.
Mathematical treatment of strain energy theory. Comparison of strain hardening copper bars in tension, compression and torsion. Cold working of a metal may be described by the curve connecting octohedral shearing stress with the corresponding shear.
24. E. Siebel, "Plastic Deformation," International Association of Testing Materials, London Congress, April 1937, p. 131.
Short discussion.
25. E. W. Fell, "Yielding Phenomena and Distortion of Iron, Steel, Aluminum Alloys and Other Metals Under Stress," Iron and Steel Institute, *Carnegie Scholarship Memoirs,* Vol. 26, 1937, p. 123.
Luder's lines occur nearer 50° angle than 45° due to stress concentration. X-ray studies.
26. E. N. Da C. Andrade, "The Flow of Metals," *Journal,* Institute of Metals, Vol. 60, 1937, p. 427.
General discussion.
27. M. Nakahara and C. Han, "On the Compression of Mild Steel, *Transactions,* Society of Mechanical Engineers, Vol. 3, p. 220, Japan 1937.
Effect of ratio of dimensions.
28. Y. Tuani, "Plastic Deformation of Metals and True Ultimate Tensile Strength," *Metals & Alloys,* Vol. 8, Abstracts, 1937, p. 140.
True ultimate stress expressed as function of melting point constant and testing temperature of metal.
29. G. W. Austin, "Stress in Steel," *Journal,* West Scotland Iron and Steel Institute, Vol. 44, 1937, p. 63.
G. W. Austin, "Flow and Fracture in Steel," *Mechanical World and Engineering Record,* Vol. 102, 1937, p. 171.
Behavior of various metals under complex stresses. Bursting pressure of tubes.
30. F. T. Sisco, "Alloys of Iron and Steel," McGraw Hill, Vol. II, 1937, p. 128.
31. G. Sachs, "The Plastic Working of Metals," *Metal Industry,* Vol. 48, 1936, p. 51.
Short Discussion.
32. H. Quinney, "Further Tests on Effect of Time in Testing," *Engineering,* Vol. 161, 1936, p. 669.
Tension and Torsion tests.
33. A. Nadai, "Review of Recent Research Work in Plasticity," *Transactions,* American Society of Mechanical Engineers, Vol. 58, 1936, A-104.
Short discussion of theories of plastic flow.

34. E. N. Da C. Andrade, "The Ultimate Strength of Metals," *Science Progress,* Vol. 30, 1936, p. 593.
General Discussion.
35. H. J. Gough and W. A. Wood, "The Strength of Metals in the Light of Modern Physics," *Journal,* Royal Aeronautical Society, Vol. 40, 1936, p. 586.
Review and results of X-ray examination.
36. H. Schlectweg, "Review of Physical Principles of Metal Plasticity," *Krupp Technische Mitteilungen,* Vol. 4, 1936, p. 29.
Review of atomic theory and theory of Taylor.
37. G. Wassermann, "Plasticity of Metal Crystals and Its Effect on the Properties of Material," *Zeitschrift des Vereins deutscher Ingenieure,* Vol. 80, 1936, p. 283.
Discussion.
38. E. B. Norris, "The Plastic Flow of Metals," *Bulletin,* Virginia Polytechnic Institute, Vol. 30, 1936, Bulletin 27.
Straight line relationship of logarithmic true stress-strain tensile curves.
39. C. F. Elam, "Distortion of Metal Crystals," Oxford University Press, 1935.
40. W. Prager, "Effect of Previous Deformation on Yield Point of Tough Plastic Material," *Zeitschrift angewandte Mathematik and Mechanik,* Vol. 15, 1935, p. 76-80.
Mathematical treatment of theory of plasticity; effect of strain hardening; Bauschinger effect.
41. A. Burkhardt and G. Sachs, "Mechanical-Technical Properties of Pure Metals," Berlin 1935.
42. P. W. Bridgeman, "Effect of High Shearing Stress Combined with High Hydrostatic Pressure," *Physical Review,* Vol. 48, 1935, p. 825.
43. M. Bonzel, "Steel Wire, Manufacture and Properties," *Engineers Book Shop,* New York, 1935.
Translation by K. B. Lewis.
44. A. F. Maier, "Influence of the State of Stress on the Plasticity of Metallic Materials," *Zeitschrift des Vereins deutscher Ingenieure,* Vol. 80, 1936, p. 484. V.D.I. Verlag 1935.
Tension and compression tests of tubes and cylinders under hydrostatic pressure. Limiting deformation appreciably reduced in biaxial stressing in comparison with simple tension.
45. E. Siebel and H. F. Vieregge, "Dependence of Beginning of Flow on Stress Distribution and Material," *Mitteilungen, Kaiser Wilhelm Institut für Eisenforschung,* Vol. 16, 1934, p. 225.
Effect of nonuniform stress distribution on the upper yield point.
46. G. I. Taylor, "Mechanism of Plastic Deformation in Crystals," *Proceedings,* Royal Society of London, Vol. 145A, 1934, p. 362, 388.
Theory of Taylor.
47. G. I. Taylor, "Faults in Materials which Yield to Shear Stress," *Proceedings,* Royal Society of London, Vol. 145A, 1934, p. 1.
Calculations of stress distribution caused by hollows.
48. E. Siebel and E. Kopf, "Strength Properties of Metal Tubes Under Internal Pressure," *Zeitschrift für Metallkunde,* Vol. 26, 1934, p. 169.
Mathematical treatment. With steel elastic limit and ultimate strength lowered slightly while elongation is markedly lowered when tubes tested under internal pressure.
49. G. Cook, "Stresses in Thick Walled Metal Cylinders of Mild Steel Overstrained by Internal Pressures," *Proceedings,* Institute Mechanical Engineers, Vol. 126, 1934, p. 407.
Stress distribution across walls.
50. C. H. Johansson, "Deformation and Fracture Mechanism," *Teknisk Tidskrift Mekanik,* Vol. 64, 1934, p. 13.
Review of plasticity by studying tensile strength of single crystals.

51. G. Baranski, "Breaking Tests Under Planar Plastic Deformation," *Zeitschrift für Metallkunde,* Vol. 26, 1934, p. 173.
Mathematical treatment using theory of Hencky.

52. E. Siebel and A. Maier, "Influence of Multiaxial States of Stress on Deformability of Metallic Materials," *Zeitschrift des Verein deutscher Ingenieure,* Vol. 77, 1933, p. 1345.
Simultaneous tension and internal pressure tests of non-ferrous hollow cylinders.

53. A. Reuss, "Simplified Evaluation of Plastic Deformation Speeds under Assumption of Shear Stress Stipulation," *Zeitschrift angewandte Mathematik und Mechanik,* Vol. 13, 1933, p. 356.
Mathematical treatment.

54. F. K. G. Odquist, "Strain Hardening of Bodies Resembling Mild Steel," *Zeitschrift angewandte Mathematik und Mechanik,* Vol. 13, 1933, p. 360.
Derivations compared with those of Nadai, Hencky, Taylor. Cylindrical rods in torsion and thin walled tubes in torsion and tension.

55. H. Hencky, "New Theory of Plasticity, Strain Hardening, Creep and the Testing of Inelastic Behavior of Metals," *Transactions,* American Society of Mechanical Engineers, APM55-18, 1933.
Mathematical treatment of strain energy theory.

56. A. Nadai, "Theories of Strength," *Transactions,* American Society of Mechanical Engineers, APM55-15, 1933.
Mathematical treatment of strain energy theory.

57. B. P. Haigh and B. Jones, "Interpretation of the Tensile Test (With Reference to Lead Alloys)", *Journal,* Institute of Metals, Vol. 51, 1933, p. 49.
Mathematical principles which govern distribution of plastic strain in tensile test. "Ductility" or true stress-strain diagrams. Discussion of complex longitudinal and transverse stresses which occur during necking.

58. F. Korber, "Plastic Deformation of Metals," *Journal,* Institute of Metals, Vol. 48, 1932, p. 317.
General discussion of mechanism of deformation.

59. O. Manfred, "Plastic Deformation and Its Underlying Law," *Zeitschrift für Physikalische Chemie,* Vol. B15, 1932, p. 383.
Summary and discussion.

60. W. Jung Koenig, W. Linicus and G. Sachs, "Experiments in Tube Drawing," *Metallwirtschaft,* Vol. 11, 1932, p. 395.
Brass Tubes.

61. L. Weiss, "Velocities of Flow in Plastic Deformation and Their Reference Quantities," *Zeitschrift Metallkunde,* Vol. 24, 1932, p. 131.
Calculation of velocity of flow in cold drawing through dies.

62. K. Przibraum, "Empirical Law Governing the Behavior of Some Plastic Bodies Under Compression," *Sitzungsberichte Akademie Wissenschaften im Wien Klasse, Abteilung* II, Vol. 141, 1932, No. 1-2, p. 63.
Reduction expressed by function of pressure and slenderness ratio Nonferrous.

63. H. Deutler, "Experimental Researches on Dependence of the Tension Test on Speed," *Physikalische Zeitschrift,* Vol. 33, 1932, p. 247-59.

64. W. Kuntze, "Cohesion Strength" *(Kohäsionsfestigkeit),* Published by J Springer, Berlin 1932.

65. G. Cook, "Yield Point and Initial Stages of Plastic Strain in Mild Steel Subjected to Uniform and Nonuniform Stress Distributions," *Philosophical Transactions,* Royal Society of London, Vol. A-230, 1931, p. 103.
Maximum shear stress at yield point of mild steel higher in nonuniform stress distribution than in tension with thick-walled metal cylinders.

66. A. Nadai, "Plasticity," United Engineering Trustees 1931, McGraw-Hill, New York.
67. C. W. MacGregor, "Yield Point of Mild Steel," *Transactions,* American Society Mechanical Engineers, Vol. 53, 1931, APM 53-15-187.
Effect of stress concentration on localized yielding.
68. Z. Jeffries, "Plasticity of Metals," *Scientific Monthly,* 1931, Vol. 33, p. 235. *Mechanical Engineering,* Vol. 53, 1931, p. 262.
General Discussion.
69. A. Nadai, "Phenomena of Slip in Plastic Materials," *Proceedings,* American Society for Testing Materials, Vol. 31, 1931, p. 11.
General discussion of slip lines under various conditions of stress application.
70. K. Hohennemmser, "Recent Testing Results on the Plastic Behavior of Metals," *Zeitschrift angewandte Mathematik and Mechanik,* Vol. 11, 1931, p. 423.
Summarizes mathematical interpretation of plastic deformation.
71. G. I. Taylor and H. Quinney, "Plastic Distortion of Metals," *Philosophical Transactions,* Royal Society of London, Vol. 230A, 1931, p. 323.
Thin-walled tubes subject to torsion and tension. Considers Lode's tube experiments. Results confirm strain energy theory.
72. R. L. Templin, "Effect of Cold Working on the Physical Properties of Metals," *Transactions,* American Institute of Mining and Metallurgical Engineers, Vol. 89, 1930, p. 466.
Character of work done on a metal appears to have comparatively little effect on mechanical properties obtained. Exception taken to this by Davis, p. 479, in instance of cold reduction under tension compared with ordinary cold rolling.
73. W. Schwinning and E. Strobel, "Strengthening by Reversals of Stress," *Zeitschrift für Metallkunde,* Vol. 22, 1930, p. 378, 412.
Strength, changes in structure, recrystallization of steel and brass wires by bending and rebending.
74. B. P. Haigh, "Relative Safety of Mild and High Tensile Alloy Steels Under Alternating and Pulsating Stresses," *Proceedings,* Institution of Automobile Engineers, Vol. 24, 1929-1930, p. 356.
Triple Tensile stress.
75. F. Zwicky, "On the Imperfections of Crystals," *Proceedings,* National Academy of Science, Vol. 15, 1929, p. 253.
76. A. F. Joffe, "Physics of Crystals," McGraw-Hill, New York, 1928.
77. E. Siebel and A. Pomp, "Determination of Work of Deformation of Metals by Compression Test," *Mitteilungen, Kaiser Wilhelm Institut für Eisenforschung,* Vol. 9, 1927, p. 157.
Conical compression test and fracture of steel, copper, aluminum.
Work of deformation in technical shaping.
78. G. Sachs and H. Shoji, "Tension-Compression Tests with Brass (Bauschinger Effect)," *Zeitschrift für Physik,* Vol. 45, 1927, p. 776.
79. W. Lode, "Researches on the Influence of the Ratio of Principal Stress on the Straining of Metals, Iron, Nickel and Copper," *Zeitschrift für Physik,* Vol. 36, 1926, p. 913.
Tubes subjected to direct tension and internal pressure.
80. Z. Jeffries and R. S. Archer, "The Science of Metals," McGraw-Hill Book Co., New York, 1924, 1st Edition.
81. R. G. Batson and H. Hyde, "Mechanical Testing," New York, Vol. 1, 1st Edition, 1922, p. 242, E. F. Dutton & Co., New York.
82. H. M. Westergaard, "On the Resistance of Ductile Materials to Combined Stresses in Two or Three Directions Perpendicular to One Another," *Journal,* Franklin Institute, Vol. 189, 1920, p. 627.
Maximum stress and maximum strain theories.
83. F. B. Seeley and W. J. Putnam, "Relation Between Elastic Strength of Steel in Tension, Compression and Shear," University of Illinois Bulletin 115, Engineering Experiment Station, 1919.

84. J. A. Van den Brock, "The Effects of Cold Working on the Elastic Properties of Steel," Iron & Steel Institute, *Carnegie Scholarship Memoirs*, Vol. 9, 1918, p. 125.
Studies of prior effect of compression, tension and torsion, as well as aging on elastic properties in tension and compression. Bauschinger effect.

85. W. E. Alkins, "The Effect of Progressive Cold Work Upon the Tensile Properties of Pure Copper," *Journal*, Institute of Metals, Vol. 20, 1918, p. 33.
In certain case of wire drawing, no change in tensile strength occurred, although reduction of area was about 10 per cent.

86. A. J. Becker, "The Strength and Stiffness of Steel Under Biaxial Loading," University of Illinois Bulletin 85, Engineering Experiment Station, 1916.
Tubes subject to axial tension and compression with varying internal pressures.

87. L. Bairstow, "Elastic Limits of Iron and Steel Under Cyclical Variations of Stress," *Philosophical Transactions*, Royal Society of London, Vol. 210A, 1910, p. 35.

88. J. E. Howard, "Notes on the Cubic Compression and Cold Flow and Crushing Strength of Iron, Steel and Other Metals," *Iron Age*, Vol. 46, 1890, p. 692.
Cubic compression does not change physical properties when unaccompanied by flow.

89. Bauschinger, "Title Not Known," *Mitteilungen aus dem Mechanisch-Technischen Laboratorium der Polytechnischen Hochschule in München*, Vol. 13, 1886, p. 31.

Deep Drawing and Testing

90. J. D. Jevons, "The Metallurgy of Deep Drawing and Pressing," Chapman and Hall, London, 1940.

91. W. Pungel, "Testing of Deep Drawing Materials by the Wedge-Draw Cupping Test," *Stahl und Eisen*, Vol. 60, 1940, p. 570.

92. H. W. Swift, "Drawing Tests for Sheet Metal," *Journal*, Institution of Automobile Engineers, Vol. 8, 1940, p. 361-431; *Sheet Metal Industries*, Vol. 14, 1940, p. 389, 505.
Testing machine devised for drawing cylindrical cups.

93. J. H. Andrews, J. W. Rodgers, H. A. Wainwright and J. N. Blackhurst, "The Quench Aging, Strain Aging and Cold Working of Steel," *Journal*, Institution of Automobile Engineers, Vol. 8, 1940, p. 433-76.
Drawing cylindrical shells in commercial press.

94. C. A. Edwards, R. Higgins and T. D. Rees, "A Study of Deep Drawing Characteristics and Testing of Sheet Steel," *Journal*, Institution of Automobile Engineers, Vol. 8, 1940, p. 477-516.
Erichsen machine modified to draw cylindrical cup.

95. H. Guth and H. Schmidtke, "Deformation Phenomena in Deep Drawing and Suitability of Aluminum Alloys for Deep Drawing Work," *Metallwirtschaft*, Vol. 19, 1940, p. 193.
Influence of hold drawn pressure, die and punch radii, wrinkling studied with Wazau machine.

96. P. Mabb, "Deep Drawing of Mild Steel," *Metal Treatment*, London, Vol. 6, 1940, p. 72.
General Discussion.

97. J. R. Low, Jr., "Mechanical Tests for Deep Drawing Sheets," Modern Industrial Press, November, 1940.

98. A. Pomp and A. Krisch, "Deep Drawing Experiments with Sheets and Strips of Alloy Steels," *Mitteilungen, Kaiser Wilhelm Institut für Eisenforschung*, Vol. 22, 1940, p. 19-34.

Methods included: Siebel and Pomp, Erichsen, wedge drawing and A.E.G. cup. Best agreement between Erichsen and cup tests. Test at elevated temperatures gave erratic results with various alloy steels.

99. E. Mohr, "The Bending Tensile Test," *Zeitschrift des Vereins deutscher Ingenieure,* Vol. 84, 1940, p. 49.
Review of the bend tensile tests. Test of magnesium alloys.

100. G. Sachs, "Deep Drawing and Related Processes," Modern Industrial Press, March, 1940.
General Discussion.

101. A. G. C. Gwyer and P. C. Varley, "Deep Drawing of Aluminum," *The Metal Industry,* London, Vol. 55, 1939, p. 465.
Revision of previously developed cup test. Reductions in drawing small cylindrical cups. Best results obtained with warm dies.

102. L. J. Weber and J. T. Weinzierl, "Drawing of Aluminum," TRANSACTIONS, American Society for Metals, Vol. 27, 1939, p. 1052-71.
Factors affecting drawing of aluminum.

103. W. Pungel and H. Karpeler, "Modern Testing of Thin Sheets," *Technisches Zentralblatt,* Praktische Metallbearbeitung, Vol. 49, 1939, p. 37; Kalt-Walz-Welt, January and February, 1939.
Wedge drawing-cupping tests. New device developed for true bending number by applying a special guide on bending roll to keep sample adhering tightly to bending surfaces.

104. E. Goehre, "The Deformation Phenomena in Deep Drawing from Cylindrical Hollow Body to Irregular Shaped Parts of a Car Body," *Werkstattstechnik und Werksleiter,* Vol. 33, 1939, p. 5, 105.
Cylindrical, conical, square drawing, draw rings and shoulders, uneven drawing flanges, irregular parts, form and size of holding areas.

105. H. Guth, "A New Method of Bend Testing," *Metallwirtschaft,* Vol. 18, 1939, p. 188.
Radius of bend varies over known range and radius at point of fracture can be determined with accuracy.

106. C. S. Atchinson and L. B. Tuckerman, "The Pack Method of Compressive Tests of Thin Specimens of Materials Used in Thin Walled Structure," United States National Advisory Committee for Aeronautics, Report 649, 1939.

107. H. Barbier and K. Lohberg, "Influence of Rate of Deformation on the Strength and Capacity of Some Zinc Alloys," *Metallwirtschaft,* Vol. 18, 1939, p. 735.
Erichsen test.

108. J. D. Jevons, "The Testing of Sheet Metal Destined for Deep Drawing and Pressing," *Sheet Metal Industries,* Vol. 13, 1939, p. 775, 901, 1019, 1145, 1362, 1462, 1467.
General discussion of various tests.

109. G. Oehler, "Study of Several Standard Deep Drawing Test Methods," *Zeitschrift Vereins deutscher Ingenieure,* Vol. 83, 1939, p. 411.
Short review.

110. H. Unckel, "Experiments in Mode of Deformation in the Deep Drawing of Shells of Various Profiles," *Metallwirtschaft,* Vol. 18, 1939, p. 567.
Brass, Copper and Aluminum. Round, oval and rectangular shapes.

111. Report of Committee El, "Report on Study of Cup Testing of Sheet Steel," *Proceedings,* American Society for Testing Materials, Vol. 38 (1), 1938, p. 490.
Comparison of Erichsen and Olsen tests by different laboratories.

112. E. Erlinger, "An Alternating Bend Testing Machine," *Archiv für das Eisenhüttenwesen,* Vol. 11, 1938, 455.

113. M. Mijon, "Results of Some Tests on Deep Drawing of Aluminum Sheets," *Revue de L'Aluminum,* Vol. 15, 1938, p. 1481—Vol. 16, 1939, p. 1669.
Effect of punch and die radii, lubrication on stresses in drawing.

114. A. J. Stelljes and O. Weiler, "Deep Drawing Test on Light Metals by the Wedge Tensile Cupping Method," *Aluminum*, Vol. 20, 1938, p. 109.

115. H. H. Stanley, "A Survey of Recent Work on Mild Steel," *Iron Steel Industry*, Vol. 11, 1938, p. 273, 483.
Short review of properties mild steel sheets.

116. G. Oehler, "The Significance of Deep Drawing Testing Procedure in Practice," *Werkstattstechnik und Werksleiter*, Vol. 32, 1938, p. 5.
Review. Results of Erichsen, A.E.G. and Siebel tests.

117. H. Yamanouti, "Studies in Die Shape for Metal Drawing," *Transactions*, Society of Mechanical Engineers, Vol. 4, Japan 1938.
Drawing tests with conical tapered dies. Drawing force at various stages in reduction.

118. S. Fukui, "Researches on the Deep Drawing Process," *Scientific Papers*, Institute of Physical and Chemical Research, Tokyo, Japan, Vol. 34, 1938, p. 1422.
Comprehensive tests of drawing small cylindrical shells with theoretical calculations.

119. P. Bastien, "A Study of Method of Fluid Pressure Cupping Recommended by C. Jovignot," *Revue de Metallurgie*, Vol. 34, 1937, p. 339; *Iron Age*, Vol. 140, 1937, p. 51; *Sheet Metal Industry*, Vol. 11, 1937, p. 730.

120. J. T. Kayseler and W. Pungel, "Draw Wedge Impression Method of Testing Sheets for Deep Drawing," *Technisches Zeutrablatt*, Praktische Metallbearbeitung, Vol. 47, 1937, p. 228.
Drawn wedge followed by cup test.

121. O. Andrieu, "Present Status of Testing Deep Drawing Sheets," *Kalt-Walz-Welt*, 1937, April p. 23, May p. 29, July p. 45.
Comprehensive review.

122. M. Marchand, "Elimination of the Influence of Gage in Cupping Tests of Thin Metals," *Revue de Metallurgie*, 1937, Vol. 34, p. 472-4; *Sheet Metal Industry*, Vol. 11, 1937, p. 898 and 903-4.
Mathematical consideration of Guillery Test.

123. J. Winlock and R. W. E. Leiter, "Some Factors Affecting the Plastic Deformation of Sheet and Strip Steel and Their Relation to the Deep Drawing Process," TRANSACTIONS, American Society for Metals, Vol. 25, 1937, p. 163.
Yield point elongation discussed.

124. G. Oehler, "Elimination of Scrap in Drawing Hollow Bodies of Thin Sheets with Special Reference to Available Deep Drawing Testing," *Beiträge zur Wirtschaft, Wissenschaft u. Technik d. Metallen ihre Legierungen*, Vol. 5, 1938, p. 1-81; *Metallwirt.*, Vol. 16, 1930, p. 1059.
Detailed account various drawing factors. Tests with brass, aluminum, tin plate, steel. Critical review of various cupping test methods. Practical drawing tests best agree with elongation in tensile test.

125. C. H. Marshall, "Report on the Usefulness and Limitations of Various Tests Applied to Sheet Metals," *Proceedings*, American Society for Testing Materials, Vol. 37, 1937, (1), p. 518.
Reports of various laboratories.

126. P. Tongas, "On the Graphical Interpretation of Results of the Jovignot Test," *Revue de Metallurgie*, Vol. 34, 1937, p. 702.

127. G. Sachs, "New Experimental Results on Deep Drawing Cylindrical Vessels," *Teknisk Tidskrift*, Vol. 67, 1937, 33 Section Mekanik.
Comprehensive Review.

128. M. Mijon, "Contribution to the Study of Drawing Sheet Metal," *Arts and Metiers*, Vol. 91, 1937, p. 86; *Sheet Metal Industries*, Vol. 11, 1937, p. 535 and p. 561.
Discussion of factors governing limits of depth of draw, including blank diameter, punch and die diameters, lubrication, condition of die, especially with conical die without blank holder.

129. J. D. Jevons, "Properties of Sheet Metal," "Behavior of Metal During Deep Drawing," *Metal Industry,* Vol. 51, 1937, p. 127, 157, 181, 335.
Review.

130. J. D. Jevons, "Effect of Stress Strain Curve on Blanking Properties of Mild Steel," *Sheet Metal Industries,* Vol. 11, 1937, p. 547.

131. R. L. Templin, "Ductility Testing of Aluminum and Aluminum Alloys," *Proceedings,* American Society for Testing Materials, Vol. 36, 1936, (II), 239.
Comparison tensile, Erichsen and bend test reveal nothing definite for determining slight difference in workability.

132. H. C. Mann, "High Velocity Tension Impact Test," *Proceedings,* American Society for Testing Materials, Vol. 36, 1936, (II), p. 85.
"Transition" velocity or tension rate of straining found above which impact energy decreases with increasing strain rate.

133. A. G. C. Gwyer and P. C. Varley, "A Deep Drawing Test for Aluminum," *Journal,* Institute of Metals, Vol. 58, 1936, p. 83.
Cylindrical sheet drawn in two stages. Slight differences in results may be detected by performance on second draw, which not shown by Erichsen or ordinary properties.

134. F. Eisenkolb, "Deep Drawability of Steel Sheets," *Archiv für Eisenhüttenwesen,* Vol. 9, 1936, p. 575.
Comparison of Tests.

135. M. Asimow, "An Investigation of the Plastic Flow Processes Involved in Drawing Cylindrical Shells from Flat Cylindrical Blank," University of California Publications, Vol. 3, 1936, p. 235.
Theoretical calculations based on strain energy theory compared with results of work of deformation in drawing cylindrical shells. Results in agreement.

136. M. Fournier, "Determination of Qualities in Metals in Thin Sheet Form by Cupping Tests," *Bulletin de la Societe d'Encouragment L'Industrie Nationale,* Vol. 135, 1936, p. 585.

137. W. Helling, "Deep Drawing Capacity of Aluminum Sheets," *Metallwirtschaft,* Vol. 15, 1936, p. 388, 409.
Drawability could only be predicted by Erichsen value when tensile strength also known.

138. Meyer auf der Heyde, "Flow of Metal in Cold Drawn Hollow Ware," *Werkstatt und Betrieb,* Vol. 69, 1936, p. 132.
Practical examples show usefulness of formula developed for flow of material.

139. "Testing Thin Sheet Metals," National Physical Laboratory, *Engineering,* Vol. 142, 1936, p. 71.
Oil Pressure cup testing machine.

140. W. Busson, "Effect of Specimen Thickness and Width in Deep Drawing Tests," *Stahl und Eisen,* Vol. 56, p. 769.
Erichsen test.

141. J. D. Jevons, "Metallurgical Aspects of Deep Drawing," *Metal Industry,* Vol. 48, 1936, p. 67, 403, 459, 513, 563, 607; Vol. 49, p. 607; *Iron and Steel World,* Vol. 9, 1935, p. 54, 419, 483; Vol. 10, p. 135.
Review.

142. A. Vegesack, "Exclusion of Influence of Sheet Thickness in the Deep Drawing Test by the Erichsen Method," *Zeitschrift für Metallkunde,* Vol. 27, 1935, p. 227.
Formulae for gage conversion.

143. M. Schonzeller, "Deep Drawing Ability of Thin Sheets and Its Preservation During the Working Process," *Metallwaren Industrie und Galvano Technik,* May 1935.
Erichsen test—Stress-elongation curves.

144. G. Sachs, "New Researches on the Drawing of Cylindrical Shells," *Proceedings,* Institution of Automobile Engineers, 1935, Vol. 29, p. 588.;

Sheet Metal Industry, Vol. 9, 1935, p. 196, 223.
Review of Sachs experimental results on effect of tool form, blank, holding, drawing force, stress and strains in drawing. Wedge drawing tests.

145. J. T. Kayseler, "Testing Deep Drawing Materials," *Zeitschrift Vereins deutscher Ingenieure,* 1935, Vol. 79, p. 1346.
Sachs wedge test and cup test on drawn wedge test.

146. H. J. Gough and G. A. Hankins, "A Research into Tests for Materials used in Cold Drawing Operations," *Proceedings,* Institution of Automobile Engineers, Vol. 29, 1935, p. 543.
Development of dome test machine by National Physical Laboratory. Comparison with Erichsen, Avery, Guillery, KWI and A.E.G. machines. No information concerning drawability not given by tensile test.

147. J. C. Arrowsmith, "Significance of Test of Auto Body Sheet," *Metal Treatment,* Vol. 1, 1935, p. 117.
Cup, tensile and wedge tests.

148. L. W. Schuster, "The Bend Test and Its Value as a Guide to Ductility," *Proceedings,* Institute of Mechanical Engineers, Vol. 129, 1935, p. 251
Correlation between bend and tensile tests. Calculation of stresses.

149. W. Tonn and W. Pungel, "Effect of Dimensions of Drawing Tools on Results of Drawability Tests of Sheet Steel," *Archiv für das Eisenhüttenwesen,* Vol. 8, 1935, p. 511.
Increased radius of punch or die increases depth Erichsen and Guillery test.

150. C. H. Desch, "Cold Pressing and Drawing," *Journal,* Royal Aeronautical Society, Vol. 39, 1935, p. 1077; *Journal,* Institution of Automobile Engineers, March 1935.
General discussion.

151. M. B. Sommer, "Relation between Plastic Deformation in Deep Drawing and Tensile Properties of Various Metals," *Transactions,* American Institute of Mining and Metallurgical Engineers, Vol. 113, 1934, p. 273; *Zeitschrift Vereins deutscher Ingenieure,* Vol. 78, 1934, p. 1195.
Forces in drawing cylindrical shell. Review of Sommer's previous work.

152. L. Herrmann and G. Sachs, "Investigations of Deep Drawing," *Metallwirtschaft,* Vol. 13, 1934, p. 687-92, 705-710.
Effects of form of punch and die upon drawing and holding forces to prevent wrinkles with brass.

153. E. Siebel, "The Plastic Forming of Metals," "Force Relationships in Deep Drawing," translated by J. H. Hitchcock, *Steel,* Oct. 16, 1933 to May 7, 1934.
Calculation of drawing force.

154. A. H. F. Goederetz, "The Pressure-Cup Drawing Diagram as Criterion of the Deep Drawing Process. New Researches with the Erichsen Sheet Testing Apparatus," *Zeitschrift Metallkunde,* Vol. 26, 1934, p. 49-55.
Curves connecting punch and blank holder pressures with depth of draw.

155. R. L. Kenyon and R. S. Burns, "Autographic Stress Strain Curves of Deep Drawing Steel," TRANSACTIONS, American Society for Steel Treating, Vol. 21, 1933, p. 577.
True stress-strain curves.

156. E. V. Crane, "Plastic Drawing of Sheet Steel into Shapes," TRANSACTIONS, American Society for Steel Treating, Vol. 21, 1933, p. 155.
General discussion, wrinkling, breakage, die construction.

157. F. Dorge, "A Study of the Deep Drawing Sheet by the Erichsen Method," *Zeitschrift Metallkunde,* Vol. 25, 1933, p. 165, 210.
Stress relationships in drawing Erichsen cup.

158. F. Eisenkolb, "Investigation on the Testing of Drawing Quality of Thin Sheets," *Stahl und Eisen,* Vol. 52, 1932, p. 357.
General studies of Erichsen and tensile test. Influence rolling direction. Deformation in a cylindrical shell.

159. W. Linicus and G. Sachs, "Importance of the Blank Holder in Deep Drawing Operation," *Werkstatts-Technik,* Vol. 26, 1932, p. 233.
Wazau testing machine used. Studies in tapering dies.

160. R. L. Kenyon, "Percentage Elongation in the Tensile Test as a Method of Measuring Ductility of Sheet Metals," *Metals and Alloys,* Vol. 3, 1932, p. 220.
Elongation a function of slenderness ratio.

161. W. Reim, "Studies in Deep Drawing," *Zeitschrift Metallkunde,* Vol. 24, 1932, p. 157.
Simple cup drawing tests with aluminum, copper with varying hold down pressures. Force versus displacement curves. Drawability expressed as Ro/Ri.

162. H. W. Gillette, "Testing of Deep Drawing Qualities of Sheet Metal," *Metals and Alloys,* Vol. 2, 1931, p. 214.
Review of various tests methods and many references.

163. E. V. Crane, "Metal Working in Power Presses," *Transactions,* American Institute of Mining and Metallurgical Engineers, 1931, Institution of Metals, p. 284.
Strain hardening in tension and compression equal.

164. G. Sachs, "Researches on Deep Drawing," *Mitteilungen, Deutsche Material-Prufüngs Anstalten,* Vol. 16, 1931, p. 11-38.
Blank dimensions, holding force, clearance of dies with copper, brass, aluminum and steel. Wedge-drawing test.

165. E. Ackerman, "Deep Drawing of Hollow Bodies from Thin Sheets with Particular Attention to the Influence of Holding Dies," *Stahl und Eisen,* Vol. 51, 1931, p. 619. Dissertation, Dresden, 1931.
Tests with brass and tin plate. Curves relating blank holder pressure, radius of die and drawing force.

166. C. Jovignot, "Fluid Pressure Cup Tester," *Revue de Metallurgie,* Vol. 27, 1930, p. 443.

167. J. Winlock and G. L. Kelley, "Sheet Steel and Strip Steel for Automobile Bodies," TRANSACTIONS, American Society for Steel Treating, Vol. 18, 1930, p. 241.
General discussion.

168. Fetschenko-Tshpiwski and M. Opalko, "Flow Phenomena in Deep Drawing Sheet Metal," *Metal Stampings,* Vol. 3, 1930, p. 1027, 1115.

169. Willi Sellin, "Influences of Rounding of Draw Ring and Draw Punch of the Drawing of Thin Hollow Bodies," *Berichte Betriebwissenschaftliche Arbeiten,* Vol. 3, 1930, p. 18-35.
Dissertation, München 1929.

170. G. Sachs, "Bearing of Present Day Knowledge of Plastic Deformation on the Testing of Materials." First Communication of New International Association for Testing Materials, Group A, Zürich 1930.

171. H. Draeger, "Influence of Rounding of Edges of Drawing Dies for Thin Sheets," *Berichte über Betriebswissenschaftliche Arbeiten,* Vol. 2, 1929; *Stahl und Eisen,* Vol. 49, 1929, p. 1731.
Tests with brass and tinplate in forming small cylindrical cups.

172. E. Siebel and A. Pomp, "On the Force Curve in Deep Drawing and Cupping Tests," *Mitteilungen, Kaiser Wilhelm Institut für Eisenforschung,* Vol. 11, 1929, p. 139-54; *Stahl und Eisen,* Vol. 49, 1929, p. 951.

173. E. Siebel and A. Pomp, "A New Method of Testing Thin Sheets," *Mitteilungen Kaiser Wilhelm Institut für Eisenforschung,* Vol. 11, 1929, p. 287; Vol. 12, 1930, p. 115.
Hole widening test.

174. Anonymous, "Avery Testing Machine," *Engineering,* Vol. 128, 1929, p. 497.
175. M. Schmidt-Kapfenberg, "Die Tests of Deep Drawing Thin Sheet," *Archiv für das Eisenhüttenwesen,* Vol. 3, 1929, p. 213.
A.E.G. cup test method. Mathematical evaluation.
176. H. Kummer, "The Erichsen Test of Sheets," *Maschienbau,* Vol. 6, 1927, p. 764.
177. G. Fischer, "Test Procedure of Value in Deep Drawing," *A.E.G. Tiefziehverfahren A.E.G. Mitteilungen,* 1929, p. 483, Vol. 1, 1927, p. 419.
Cylindrical cup test.
178. P. W. Dohmer, "The Deep Drawing Tester of the Wazau Type," *Maschinenbau,* Vol. 8, 1929, p. 772.
179. J. W. Geckler, "Plastic Buckling of the Walls of Hollow Cylinders and Some Other Phenomena upon Cups and Sheets," *Zeitschrift angewandte Mathematik und Mechanik,* Vol. 8, 1928, p. 341.
Short treatment of wrinkling during deep drawing.
180. R. Guillery, "Machine for Applying Cupping and Tensile Tests to Sheet Metals," *Bulletin de la Societe d'Encouragement L'Industrie Nationale,* Vol. 127, 1928, p. 483.
181. G. Fischer, "On the Surface Stretching, Formation of Folds and Prevention of Folds during Deep Drawing of Hollow Bodies."
Dissertation, Stuttgart 1927.
182. J. Winlock and G. L. Kelley, "Testing Automobile Body Sheet Steel," TRANSACTIONS, American Society for Steel Treating, Vol. 12. 1927, p. 635.
Tensile test as criterion of drawing is erratic.
183. R. L. Templin, "Methods for Determining Tensile Properties of Thin Sheet Metal," *Proceedings,* American Society for Testing Materials, Vol. 27, 1927, p. 235.
184. J. T. Nichols, E. S. Taylerson and J. C. Whetzel, "Tension Test Specimens of Sheet Metal," *Proceedings,* American Society for Testing Materials, Vol. 27, 1927, p. 259.
185. G. Sachs, "On the Theory of the Drawing Process," *Zeitschrift angewandte Mathematik und Mechanik,* Vol. 7, 1927, p. 235.
Drawing through dies.
186. W. S. Montgomery and E. R. Enders, "Some Attempts to Measure the Drawing Properties of Metals," *Mechanical Engineering,* Vol. 48, 1926, p. 119.
Comparison of Erichsen, Herbert, Rockwell results with Erichsen giving best results.
187. E. Ruhrmann, "Flanging and Drawing in Technology of Working Thin Sheets," V.D.I. Forschungsarbeiten, 1926, No. 277; *Iron and Steel World,* Vol. 1, 1927, p. 359.
188. G. G. Beard, "A Cupping Test for Determining the Drawing Qualities of Thin Sheet Metals," *Journal,* West Scotland Iron and Steel Institute, Vol. 34, 1926, p. 23.
189. C. L. Eksergian, "Plastic Behavior of Metal in Drawing," *Transactions,* American Society of Mechanical Engineers, Vol. 48, 1926, p. 609; *Metal Industry,* Vol. 30, 1927, p. 405, 433, 459, 483.
190. M. Sommer, "Researches on the Drawing of Hollow Bodies," *V.D.I. Forschungarbeiten,* 1926, No. 286; *Maschinenbau,* Vol. 4, 1925, p. 1171.
Theoretical. Calculation of drawing force. Determination of coefficient of friction.
191. Walter Sellin, "Calculation of the Work of Deep Drawing," *Maschinenbau,* Vol. 3, 1924, p. 229.
192. M. Guillery, "Cupping Tests of Thin Sheets," *Revue de Metallurgie,* Vol. 21, 1924, p. 303.
193. J. Blume, "Determination of Drawing Ability of Deep Stamping Sheets," *Metallborse,* Vol. 12, 1922, p. 1945; *Maschinenbau,* 1921, p. 187.
194. C. Fremont, "Cupping Tests of Thin Sheets," *Bulletin de la Societe d'Encouragement L'Industrie Nationale,* Vol. 133, 1921, p. 241.

195. C. H. Mathewson, C. S. Trewin and W. H. Finkeldy, "Some Properties and Application of Rolled Zinc Strip and Drawn Zinc Rod," *Transactions,* American Institute of Mining and Metallurgical Engineers, Vol. 64, 1920, p. 305.
Dynamic Cupping Test.
196. T. Y. Olsen, "Ductility Testing Machines," *Proceedings,* American Society for Testing Materials, Vol. 20, 1920, II, p. 398.
197. A. M. Erichsen, "A New Method for Testing Thin Sheets," *Stahl und Eisen,* Vol. 34, 1914, p. 879.

Technology of Deep Drawing

198. W. F. Burchfield, "The Perforating and Drawing of Nickel and High Nickel Non-Ferrous Alloys," Modern Industrial Press, January 1941.
199. S. D. Brootskoss, "The Press Handbook," The Dreyden Press, 103 Park Ave., N. Y., 1940.
200. C. W. Hinman, "Drawing and Redrawing Sheets without Wrinkles," Modern Industrial Press, December 1940, January 1941.
201. W. T. Forde and G. L. Reed, "Punches and Dies," American Society of Tool Engineers, March 7, 1940.
202. C. W. Hinman, "The 'Inside Out' Method for Redrawing Shells," Modern Industrial Press, August 1940.
203. J. D. Jevons, "Tools for Deep Drawing and Pressing," *Metal Industry,* Vol. 55, 1939, p. 3, 59, 105, 217, 309, 355, 425, 449, 485.
204. E. V. Crane, "Plastic Working of Metals," John Wiley & Sons, Inc., New York, 1939, 2nd Edition.
205. J. D. Jevons, "Progress in Deep Drawing and Pressing," *Metal Industry,* Vol. 54, 1939, p. 35.
Review.
206. J. D. Jevons, "New Applications for Press Work," *Metal Industry,* Vol. 53, 1938, p. 389, 467, 541, 565, 615.
Discusses drawing of alloys and alloy steels.
207. J. D. Jevons, "Presses for Deep Drawing," *Metal Industry,* Vol. 52, 1938, p. 331, 383, 429, 455.
Factors in press operation. Speed.
208. N. C. Wilson, "Design of Dies and Tools for Press Work," *Transactions,* Manchester Association of Engineers, 1936-7, p. 183.
209. G. L. Smith, "Modern Practice in Press Tool Design," *Metal Industry,* Vol. 51, 1937, p. 545, 575.
Development of blanks and drawn part.
210. E. C. Booth, "The Flow of Metals in Stamping," *Product Engineering,* New York, Vol. 7, 1936, p. 90.
211. Anonymous, "Modern Presses and Stamps," *Emaillwaren Industrie,* Vol. 13, 1936, p. 357.
212. J. H. Paull, "Industrial Sheet Metal Drawing," D. Van Nostrand & Co., New York, 1935.
213. C. W. Hinman, "How to Prevent Breakage in Drawn Shells," *Sheet Metal Industry,* Vol. 9, 1935, p. 27.
214. Anonymous, "Deep Drawing of Stainless Steel—Particulars of the Latest German Practice," *Machinery,* London, Vol. 46, 1935, p. 78.
215. M. Schonzeller, "Deep Drawing Ability of Thin Sheets and Its Preservation During the Working Process," *Metallwaren Industrie und Galvano Technick,* Vol. 33, 1935, p. 184, 218.
216. L. B. Hunt, "Deep Drawing of Sheet Metal," *Sheet Metal Industry,* Vol. 9, 1935, p. 101, 154.
217. K. M. Dolezalek, "Technology of Stamping," *Zeitschrift des Vereins deutscher Ingenieure,* Vol. 78, 1934, p. 871.
Measurements showing direction and magnitude of forces. Die is shown to be stationary while parts of press are deformed.

218. C. F. Henderson, "Tool for Deep Drawing in a Single Action Press," *American Machinist,* Vol. 77, 1933, p. 87.
Combination blanking and drawing tool.
219. R. Dale, "Die for Deep Drawing," *Iron Age,* Vol. 130, 1932, p. 213.
220. R. Wake, "Power and Hand Press Production," *Mechanical World and Engineering Record,* Vol. 91, 1932, p. 248.
Shop problems.
221. E. Ackerman, "Deep Drawing with Blank Holder Operated by Air Pressure," *Werkstattstechnik,* Vol. 26, 1932, p. 4.
222. Walter Selling, "Handbook of Drawing Technique," J. Springer, Berlin 1931.
223. E. V. Crane, "Plastic Working of Metals," Various Articles in American Institute of Mining and Metallurgical Engineers, Feb. 1931; *Metal Stamping* during years 1929, 1930, 1931; *Iron Age,* Vol. 128, July, Aug., Sept., Oct. 1931.
224. E. V. Crane, "Drawing Attachments Employed on Single Action Presses," Cam Drawing Presses. *Metal Stampings,* Vol. 4, 1931, p. 309, 497.
Movement of punch. Blank holding pressures.
225. E. V. Crane, "Operating Problems Involved in Drawing Metals," *Metal Stampings,* Vol. 3, 1930, p. 29.
Discussion of speed in practical drawing.
226. E. E. Clark, "Metal Stamping Dies," *Metal Stampings,* Vol. 3, 1930, p. 153, 323, 737.
227. O. Kuhner, "Application of Air Pressure in Stopping Wrinkles in the Working of Nonferrous Metals," *Zeitschrift Metallkunde,* Vol. 22, 1930, p. 190.
Press described.
228. O. Kuhner, "Modern Air Press Drawing," *Werkstattstechnik,* Vol. 23, 1929, p. 556.
229. M. Kurrein, "Tools and Working Methods of Presses," J. Springer, Berlin, 1926.
230. E. Kaczmarek, "The Modern Stamping Plant," *Maschinenbau,* Vol. 6, 1927, p. 764; J. Springer, Berlin, 1925.
231. G. Schlesinger, "Drawing Lowered with Air Operations," *Werkstattstechnik,* Vol. 19, 1925, p. 831.
232. F. D. Jones, "Die Design and Diemaking Practice," Industrial Press, New York, 1930.
233. K. Musiol, "Mathematical and Graphic Methods of Lay Out Determination in Draw Pressing," Leipsig, 1908.
234. K. Musiol, "Calibration of Draw Press Apparatus," *Stahl und Eisen,* Vol. 27, 1907, p. 477, 513, 551.
235. K. Musiol, "Drawing and Pressing in Theory and Practice," Dingler's Polytechnic Journal, Vol. 315, 1900, p. 428, 440.

Lubrication and Deep Drawing

236. F. P. Bowden, L. Leben and D. Tabor, "The Sliding of Metals, Frictional Fluctuations and Vibration of Moving Parts." *The Engineer,* Aug. 1939, p. 214.
237. F. P. Bowden and L. Leben, 'The Nature of Sliding and Analysis of Friction," *Proceedings,* Royal Society of London, Vol. 169A, 1939, p. 371.
Friction apparently due to actual welding at points of contact. Nature and extent of slipping depends on melting point of metal.
238. F. Ohl, "Modern Additions to High Grade Drawing Press Lubricants," *Kalt-Walz-Welt,* 1939, p. 49.
239. R. Saxton, "Lubrication in Bar and Tube Drawing," *Wire Industry,* Vol. 4, 1937, p. 584.
240. J. C. Arrowsmith, "Lubricants in Cold Pressing of Sheet Metal," Institu-

tion of Mechanical Engineers, Lubrication Symposium, Oct. 1937.
Short general discussion.

241. Anonymous, "Lubrication in the Cold Working of Metals," *Metal Industry*, Vol. 50, 1937, p. 383.
Short discussion.

242. Anonymous, "Cooling and Lubrication in Working of Metals," *Illustrierte Zeitung für Blechindustrie*, Vol. 66, 1937, p. 1346.

243. J. D. Jevons, "Lubricants Employed in Deep Drawing," *Metal Industry*, Vol. 49, 1936, p. 577, 607, 629; Vol. 50,1937, p. 9.
Discussion.

244. D. R. Pye, "Surface Films and Lubrication," *Journal*, Royal Aeronautical Society, Vol. 40, 1936, p. 754.
Present view of lubrication. "Boundary lubrication."

245. F. P. Bowden and K. E. W. Ridler, "Surface Temperatures of Sliding Metals and the Temperature of Lubricated Surfaces," *Proceedings*, Royal Society of London, Vol. 154, 1936 A, p. 640.
Exceedingly high temperatures recorded.

246. E. E. Halls, "Lubrication for Deep Drawing," *Machinery* (London), Vol. 42, 1933, p. 453.
Characteristics of compounds.

247. H. A. Montgomery, "Lubrication in Cold Drawing Sheet Steels," TRANSACTIONS, American Society for Steel Treating, Vol. 21, 1933, p. 557.

248. M. Restwick, "Lubricants Used in Deep Drawing of Sheet Steel," TRANSACTIONS, American Society for Steel Treating, Vol. 21, 1933, p. 181.
Characteristics and composition of drawing compounds.

DISCUSSION

Written Discussion: By R. L. Templin and R. G. Sturm, Aluminum Company of America, Research Laboratories, New Kensington, Pa.

The authors are to be commended for the comprehensive discussion of deep drawing of sheets. This paper is of real value in that it points out the essential factors involved in deep drawing. The bibliography is particularly useful, not only because of the great number of references but because of the organization and scope of the presentation.

The authors have effectively emphasized the great need for further information regarding the behavior of metals subjected to large strains in more than one direction. Certainly the ordinary tensile test is quite inadequate to determine the deep drawing characteristics of metals. The writers agree with the authors that thus far no single test has been devised which is adequate to indicate the drawability of metals, except an actual drawing operation.

In order to enhance the value of this paper, the writers believe that a few constructive suggestions might be made.

Bauschinger's work which was done in the early 1880's was limited to relatively small deformations and to specimens subjected to unidirectional deformation. Recent tests[1] indicate that the Bauschinger Effect is generally applicable to most metals for relatively small amounts of unidirectional strain, comparable to those studied by Bauschinger, but when larger amounts of such strains are used on aluminum alloys at least, both the tensile and compressive yield strengths in the direction of straining may be increased. For polydirectional deformation, both tensile and compressive strengths are increased by

[1]R. L. Templin and R. G. Sturm, "Some Stress-Strain Studies of Metals," *Journal of the Aeronautical Sciences*, Vol. 7, No. 5, March 1940.

about the same percentage which is proportional to the per cent reduction in area.[3] Perhaps most deep drawing operations involve sufficient strain to increase both the tensile and compressive properties of the material.

The writers have encountered considerable difficulty in following the use of the plastic modulus, Q, because for widely different strains in the three principal directions the value of Q would certainly not be a constant. Perhaps more explanation is all that is needed.

Unidirectional deformation may cause slipping on planes which are not brought into play by subsequent tests on the material. Tensile tests in directions at 45 to 90 degrees, with the direction of previous stretching, do not show the same effect of stretching as tests in the direction of stretching. As the authors point out, if a bar is twisted, then untwisted, the tensile properties are not significantly changed although a considerable amount of work has been expended in deforming the metal. Nevertheless the work done on a given volume of the material is the same regardless of the direction of test. Consequently one would hesitate to conclude that a given amount of work expended in deforming 1 cubic inch of metal will cause the same strain hardening regardless of how the work is done. We wish to strengthen the authors' conclusion that a great amount of investigation and study is necessary before an adequate understanding of the deformation of metals during drawing can be reached.

In the authors' discussion of the effect of speed on drawability, the flow characteristics of the metal are considered from the point of view of constant temperature. It has been found that high instantaneous temperatures at points of localized working occur at higher drawing speeds. The high temperature might materially change resultant strain hardening at those points. It is altogether possible that a consideration of these high local temperatures will help to explain some of the phenomena mentioned by the authors.

Written Discussion: By F. B. Dahle and Francis W. Boulger, Battelle Memorial Institute, Columbus, Ohio.

Messrs. Asimow and Crombie are to be commended for the study and thought they have devoted to the problems of drawability. Their conclusions regarding the limitations of the standard tension test, Olsen, Erichsen, and other tests are substantiated by the fact that these standard tests give an incomplete and sometimes misleading estimate of probable success in drawing operations. However, the discussers believe that the authors' indictment of cylindrical cup-drawing tests for evaluating drawability is not substantiated by the references quoted or the theoretical treatment of the problem.

Drawing operations on sheet metal require the absorption and distribution of the applied forces by definite amounts of deformation and strain. In drawing operations, the stresses are tri-axial and result in the fabrication of the desired form by bending, stretching, and upsetting actions. Usually the bending actions present no problem, although they have been the object of some nonstandard tests. Stretching always occurs in drawing operations, and when a material fails it almost invariably fails in a region subject to stretching. This fact has led to the conception that the most satisfactory materials for deep drawing are those that show the maximum amount of elongation without frac-

[3]See Reference 72.

ture. Considerable emphasis in routine testing, therefore, has been laid mistakenly on elongation figures from tension tests and cupping values determined by tests of the Olsen type in classifying drawing materials.

Both of these methods are capable of differentiating between good and bad materials for deep drawing, probably because they show the behavior under simple stretching action. In some respects, cupping tests of the Olsen type or stretching tests have much to recommend them. They show up directional differences and indicate the ability for deformation under simple tension stresses, the grain size of the material, and the probable surface finish. It must be remembered, of course, that cupping values, and to a lesser extent the tensile elongation figures, are affected to a marked degree by the thickness of the material tested.

The failure of cupping, tension, and other standard tests to make close distinctions of drawing quality is due to the fact that the severity of stretching action is affected by other factors during drawing operations. As the authors mention, these factors include clearances, hold-down pressures, drawing forces, frictional forces, and other variables due to die practice. In addition to these mechanical variables, the properties of the material, such as strength, resistance to upsetting, work hardening, surface finish, and tendencies for local or uniform elongation, also affect the behavior in drawing operations.

The mechanical variables affecting the deep-drawing performance pointed out by the authors are of undoubted importance but must of necessity be minimized when measuring inherent drawability.

Cylindrical cup-drawing tests can be used to avoid the errors of the other tests mentioned in the paper and should then be expected to evaluate the drawability of materials, since they incorporate the effects involved in deep drawing. The Bauschinger Effect is operative in some cylindrical cup-drawing operations, and in cases where it is particularly important, redrawing operations can be included in the testing procedure

Frictional effects are present to a limited degree in laboratory cup tests and are integrated in the results to the extent to which they are affected by the properties of the material. In most actual operations, the effects of surface areas and stresses present are more important than surface finish in determining the magnitude of frictional forces. These factors are largely dependent on the specific operations and cannot be evaluated in laboratory tests. It should be noted that higher than normal frictional forces often enhance the drawing performance in certain operations by aiding in the distribution of stresses.

The problem of measuring drawability by cup-drawing tests is somewhat analogous to that of measuring machinability by simple tests. The machinability of metals depends upon a number of metallurgical factors that are not readily measurable by standard tests and also depends upon innumerable variables set up by differences in shop practices and the host of different machining operations. Yet for most purposes, a fairly accurate index of the machinability of materials can be obtained from standardized drill and saw tests which eliminate variables extraneous to the materials. In a like manner, the drawability of materials should be shown by their behavior in a standardized drawing test.

Because of these facts, we believe that a properly designed cup-drawing test will measure inherent drawability in a steel. The cup-drawing test should, therefore, not be condemned on hypothetical grounds without an attempt being made to compare its findings with actual performance.

Written Discussion: By E. L. Bartholomew, Jr., instructor, Massachusetts Institute of Technology, Cambridge, Mass.

The authors have succeeded in clearly establishing the factors to be considered in the problem of deep drawing. A noteworthy bibliography has also been presented.

Among other conclusions the authors state that, "much information is needed concerning the true stress-strain relationship of deep drawing metals as well as a better interpretation of the tensile test." This is one of the important factors to be developed if the "drawability" of the metal in question is to be accurately determined.

Work is being carried out along these lines at Massachusetts Institute of Technology.

A stress analysis of drawn cups at the "critical" section (location of fracture) has indicated reasonable correlation with the MacGregor s-q′ tensile plot.

A linear relationship between maximum punch force and blank diameter has been indicated for deep drawing steel with constant space hold-down. This is in agreement with the fact that punch force increases linearly with the initial hold-down pressure as stated in the paper, since, with a constant space pressure pad the hold-down force increases with blank diameter.

It has also been found possible to establish within close limits the maximum blank diameter which may be successfully drawn under a given set of conditions. This is in agreement with the work of Swift.

Sufficient tests will be completed shortly enabling the writer to present these data.

Authors' Reply

The authors wish to express their appreciation for the comments made on their paper.

In regard to the discussion by Messrs. Templin and Sturm, we wish to preface our remarks by expressing deep regret that we unfortunately missed their paper entitled, "Some Stress-Strain Studies of Metals," in the Journal of Aeronautical Sciences. The discussers point out that the Bauschinger Effect, at least in aluminum, appears to be not effective or operative when the strains are very large. In a general way, the authors agree with that. The point of view which the authors have taken is that the grain structure of the material is disorganized upon deformation; this disorganization is felt more strongly in some directions than in others, particularly in the direction of straining. There is various evidence to show that in ferrous metals at least considerable discrepancies in the yield strength in the several directions are brought about by deformation of the material.

One example which has come recently to our attention is contained in the paper by Franks and Binder, published by the American Society for Testing

Materials, June 23-27, 1941. Unfortunately, we cannot show the graphs, but in the case of 18-8 stainless steel, 0.035 inch thick, considerably cold reduced by cold rolling, the tensile strength in the direction of rolling is considerably enhanced. Likewise, the tensile strength and compressive strength in transverse direction is increased. However, the compressive strength in the direction of rolling, although it has been increased because of the great amount of general deformation, proportionately has not been increased nearly so much as the tensile strength.

There are many other similar examples which indicate that the Bauschinger Effect, at least in a modified form, does operate. If the strains are so large that the complete structure is disorganized, quite likely the yield strength in all directions will be increased. Even so the increase will not be the same in all directions.

In the case of the plastic modulus Q, we wish to state that it is never a constant. It always varies and its particular value depends on the amount of strain which the metal has undergone.

Referring to Fig. 5 of text, the plastic modulus Q is measured by referring to the true stress-strain diagram, the strain being plotted as a logarithmic strain. The value of Q on such a diagram is the slope from the origin to the particular point indicating the amount of strain which the material has undergone.

Thus, in the early stages of deformation, the plastic modulus Q has a higher value than it has at later stages of deformation, and the value of Q must therefore be determined after the amounts of strain have been measured and determined.

This is further illustrated on the next slide, which shows how the modulus Q varies with increasing strain. Naturally, the exact curve would depend upon the type of material which is being strained. At the early stages, that is, at the very beginning of change from the elastic condition to the plastic, the values are very high and are nearly the same as the modulus of elasticity.

Messrs. Templin and Sturm mentioned that unidirectional deformation may cause slipping on planes which are not brought into play by subsequent tests on material. They add that tensile tests at 45 to 90 degrees, with the direction of previous stretching, do not show the same effect on stretching as tests in the direction of stretching. In other words, applied in one direction apparently has a greater effect on the yield strength of material in the original direction than it has in other directions. This, to our mind, is another evidence of the Bauschinger Effect in its more generalized sense.

The authors have suggested that perhaps the only variable which can be reasonably well measured where directions of stress vary considerably during the deforming operations is the work of deformation, since that can be added up for each stage of the deformation operation. While the work of deformation by itself is one variable, it must be considered in relation to the changes in the direction of strain which may occur during the deforming process. This, we believe, will account for the fact that in stressing material in one direction, and then stressing it in the opposite direction, the yield strength does not rise continuously with the work of deformation, but is rather a discontinuous function of the work of deformation.

The authors have mentioned the possible effects of temperature, especially where lubrication may be faulty and where physical contact is established between the surfaces of the dies and the material being drawn and they fully agree with Messrs. Templin and Sturm's remarks relative to the instantaneous high temperatures at localized points.

In reply to the discussion of Mr. Dahle, our main objection to placing sole reliance on the cupping test is based on considerations which are somewhat analogous to the effect which is observed in testing tensile specimens of various gage length. With a short specimen, for example, the effect of necking is very considerable on the measured elongation. On the other hand, with specimens of long gage length, the effect of necking is relatively unimportant. Similar effects appear to be important in testing small cylindrical shells and comparing the results with large drawings.

It was not the intention of the authors to indict the cylindrical cupping test as not being a useful tool in the study of deep drawing. On the contrary, we consider that its lack of use in this country has probably retarded a more complete understanding of the deep drawing process. On the other hand, it is our opinion that the cylindrical cupping tests will not always reveal inherent drawability or always enable the tester to predict the results of commercial performance such as, for example, obtained in fender draws.

As has been discussed, the condition of yielding and rupture of metals has been shown to be dependent on the varying combinations of stresses and nowhere in the drawing of a cylindrical shell are such conditions of stressing the same, or closely the same, as exist in the drawing of a fender, for example. Scribed squares (1 inch) have shown that the elongations are as high as 30 per cent in the two directions at right angles to each other at certain critical locations in the cases of certain fender draws. This condition does not exist in the case of cylindrical shells wherein scribed areas have shown that elongation in one direction is always accompanied by compression at right angles. Furthermore, in the latter case failure almost always occurs at the base which is subject to very little prior work hardening, while in the case of the fender draw it is likely a great amount of work hardening has occurred at the critical locations prior to failure.

As noted by Messrs. Dahle and Boulger, we have also observed occasions where high frictional forces appear to enhance the drawing performance of certain commercial operations; one instance, by the way, in the case of a cylindrical shell where the distribution of stress was uniform.

We are much interested in Mr. Bartholomew's remarks and believe that true stress-strain relationships are of fundamental importance in "drawability." Such relationships should develop two of the fundamental properties governing drawability, namely, the rate of work strengthening and the rupture strength (or possibly technical cohesive strength). It may be of some interest to note the authors several years ago endeavored to develop an impact test upon tapered specimens, somewhat analogous to the two-load method used by DeForest, MacGregor, and Anderson, AIME TP-1393, whereby it was hoped to obtain a correlation in the case of deep drawing steels, but were unable to obtain satisfactory results.

THE CARBON-OXYGEN EQUILIBRIUM IN LIQUID IRON

By Shadburn Marshall and John Chipman

Abstract

An experimental method has been developed for the study of reactions of liquid metals with gases at pressures up to 20 atmospheres. The equilibria between carbon and oxygen in liquid iron and carbon monoxide and dioxide in the gas phase has been studied in the range 1540 to 1700 degrees Cent. (2805 to 3090 degrees Fahr.). Equilibrium constants have been determined for the following reactions:

$$C \text{ (in Fe)} + CO_2 \text{ (g)} = 2\ CO \text{ (g)} \qquad (1)$$
$$O \text{ (in Fe)} + CO \text{ (g)} = CO_2 \text{ (g)} \qquad (2)$$
$$C \text{ (in Fe)} + O \text{ (in Fe)} = CO \text{ (g)} \qquad (3)$$

When per cent by weight is substituted for activity of carbon and oxygen, the resulting constants (designated K'_1, etc.) are not constant but depend upon carbon content. The activity coefficient of carbon, defined as $f_c = a_c/$per cent carbon increases, the corresponding coefficient for oxygen decreases with increasing carbon content. Using these activity coefficients, the values of the constants at 1540 degrees Cent. (2805 degrees Fahr.) are, respectively, 430, 1.21 and 512.

Introduction

Of the many chemical reactions which occur during the making of a heat of steel, the one which it is most essential to control and which has therefore been most widely studied is that by which carbon and oxygen in the liquid metal react to form carbon oxide gases which are evolved from the bath. Since the product of the reaction is essentially carbon monoxide and since commercial furnaces are operated under nearly constant atmospheric pressure, it has been generally agreed that as the reaction approaches equilibrium the product of the percentages of carbon and oxygen should approach a

This paper is based upon a thesis submitted by Shadburn Marshall in partial fulfillment of the requirements for the degree of Doctor of Science at the Massachusetts Institute of Technology.

A paper presented before the Twenty-third Annual Convention of the Society held in Philadelphia, October 20 to 24, 1941. Of the authors, Shadburn Marshall is associated with the research department, Remington Arms Co., Bridgeport, Conn., and John Chipman is professor of metallurgy at the Massachusetts Institute of Technology, Cambridge, Mass. Manuscript received June 22, 1941.

constant value denoted by the symbol m. The fact that under operating conditions in the open hearth a nearly constant value of the product is found, at least at low carbon content, suggests that the reaction rate is sufficient to maintain a condition closely approximating equilibrium. Obviously any quantitative treatment of the rate of this reaction and indeed any understanding of the mechanism of the process as a whole will depend upon a knowledge of the state of equilibrium in this reaction.

Le Chatelier, in 1912, was probably the first to suggest a value for m. In a paper on the reduction of iron oxides (1)[1] he calculated

$$m = \% \text{ C} \times \% \text{ O} = 0.0020 \text{ at 1600 degrees Cent.}$$
(2910 degrees Fahr.)

The calculation was based on the application of the Carnot-Clapeyron equation for simple reactions and values for the maximum solubilities of carbon and oxygen in iron of 5.5 per cent and 0.244 per cent respectively. No references to the sources of the heat and solubility data were given; however, it is worthy of note that the solubility values are essentially those accepted today.

Styri (2), in 1919, pointed out Le Chatelier's calculation and recomputed the constant, using the same solubility data but more recent heat data and arrived at a value of 0.0022 at 1600 degrees Cent. (2910 degrees Fahr.). Later (3) he recalculated the constant using the Nernst theorem and obtained a value of 0.0005. He believed the latter to be the better value but admitted that actual measurement was necessary to settle the point.

Pierard (4) gave a mean value of 0.0019 at 1600 degrees Cent. (2910 degrees Fahr.) based on measurements made in an open hearth furnace. The carbon contents were observed while the oxygen contents were calculated from the solubility data of Tritton and Hansen (5).

In his work on the physical chemistry of steel-making, Herty (6) studied the rate of carbon elimination in the open hearth furnace. By plotting rate of carbon elimination against the product per cent carbon $\times$ per cent oxygen and extrapolating to zero rate, he obtained the values 0.0044 at 1600 degrees Cent. and 0.0033 at 1660 degrees Cent. (3020 degrees Fahr.) for the constant. Because of probable errors

[1]The figures appearing in parentheses refer to the bibliography appended to this paper.

in sampling technique and analysis for oxygen, he repeated his work and obtained the value 0.0022 for the product in the temperature range 1570 to 1600 degrees Cent. (2855 to 2910 degrees Fahr.). He believed this value to be correct because of the improved techniques of sampling and analysis for oxygen.

Feild (7) in attempting to arrive at a rate equation for the elimination of carbon in the open hearth found it necessary to assume a value of 0.0023 for the constant in order to obtain results that were not absurd.

In 1929 Kinzel and Egan (8) presented the first results obtained under laboratory conditions. In a series of experiments in which irons containing varying percentages of carbon and oxygen were melted under an atmosphere of pure CO, they found a value of 0.00011 at 1550 degrees Cent. (2820 degrees Fahr.). This result was very reproducible regardless of the approach to equilibrium. None of the melts contained more than 0.04 per cent carbon or 0.005 per cent oxygen.

Larsen (9) using the data of Eastman and Evans (10) for the reaction

$$Fe + H_2O = FeO + H_2$$

and of Eastman (11) for the reactions

$$CO_2 = CO + \tfrac{1}{2} O_2$$
$$H_2 + \tfrac{1}{2}O_2 = H_2O$$

calculated the value of the constant to be 0.00036.

In a round table discussion on the physical chemistry of steel-making (12), Herty disagreed with the results of Kinzel and Egan on the basis that if the constant were so low as 0.00011, it should be possible to remove all the carbon from iron in the steel-making process and yet leave the metal practically free of oxygen. Gaines suggested that the amounts of carbon and oxygen in the metal in the open hearth might be those which would be in equilibrium at a pressure of CO much higher than one atmosphere due to the difficulty of bubble formation, or other such reason, which would explain the difference between the results of Kinzel and Egan and those obtained in the open hearth furnace.

Jette (13) likewise postulated that the value of Kinzel and Egan

is correct and that the product observed in the open hearth corresponds to a pressure of 20 or more atmospheres.

Vacher and Hamilton (14) made laboratory studies using mixtures of CO and CO_2 and reported a value for m of 0.0025 at 1620 degrees Cent. (2950 degrees Fahr.) for a carbon range of 0.01 to 0.94 per cent. Due to difficulties in controlling the gas composition, no relations were established between the gas and the metal.

Because of the discrepancy in the results of Vacher and Hamilton and of Kinzel and Egan, which were the only two laboratory studies up to that time, Vacher (15) repeated his experiments under more carefully controlled conditions. He again established a value of 0.0025 at 1580 degrees Cent. (2875 degrees Fahr.). These two investigations by Vacher were the first experimental studies of the reaction in which actual equilibrium conditions were attained.

In a study of the gases evolved from a rimming steel ingot during solidification, McCutcheon and Chipman (16) found the product of the concentrations of the carbon and oxygen in the unsolidified portion of the ingot to remain approximately constant at a value of 0.0022 throughout the period of solidification. Chipman (17) reported a value of 0.0032 for the product as a result of measurements made in the open hearth furnace at about 0.05 per cent carbon. Individual heats ranged from 0.0026 to 0.0040 and the value was independent of the slag composition.

McCutcheon (18) reported values obtained in the open hearth using a special sampling method to prevent contamination of the sample by air which showed that the magnitude of the constant varies with the carbon content. He found that the product varied from 0.0032 at 0.04 per cent carbon to 0.0048 at 0.30 per cent carbon.

Leiber (39) reported a value of 0.0026 at 1620 degrees Cent. (2950 degrees Fahr.) in the range of 0.05 to 0.6 per cent carbon as a result of experiments carried out in the open hearth. His sampling method was good in that oxidization from the air was prevented.

The results of a statistical study on data obtained from eight steel companies as reported by Fetters and Chipman (19, 20) indicated that the value of the carbon-oxygen product increased with increasing carbon content from 0.0033 at 0.05 per cent carbon to 0.008 at 0.50 per cent carbon. The product was found not to be affected by the manganese content of the metal.

Schenck, Reiss and Bruggeman (21) gave a value of 0.0010 for the product taken from a smoothed curve of open hearth measure-

ments. They assumed that CO gas was liberated from the bath at a pressure of 1.1 atmospheres and the value was found to be constant up to carbon concentrations of 0.70 per cent. The magnitude of the value was not affected by furnace lining, temperature in the range 1500 to 1650 degrees Cent. (2730 to 3000 degrees Fahr.) and the ordinary impurities up to 0.70 per cent manganese, 0.09 per cent phosphorus, 0.06 per cent sulphur and 0.14 per cent silicon.

Kalling and Rudburg (22), using an evacuated sampling mold, found values in the open hearth furnace from 0.0025 at 0.10 per cent carbon to 0.01 at 2.0 per cent carbon.

A laboratory study under actual equilibrium conditions was reported by Phragmén and Kalling (43). They showed that the equilibrium constant is only slightly affected by temperature, being slightly larger at 1700 degrees Cent. (3090 degrees Fahr.) than at 1550 degrees Cent. (2820 degrees Fahr.) In the carbon range below 0.10 per cent their results agreed quite well with those of Vacher.

The above discussion has been limited to the data available in the literature for the value of the constant,

$$m = \% \text{ C} \times \% \text{ O}$$

in solution in an iron bath at one atmosphere pressure.

The carbon and oxygen contents of the bath are both dependent upon the composition of the gas phase. According to the phase rule, if the temperature and total pressure are fixed, the composition of the metal uniquely determines that of the equilibrium gas. Constants for the reaction of carbon or oxygen in the metal with CO and CO_2 gases can be obtained from some of the published works. A discussion of these equilibria will be deferred until our own experimental data have been presented.

Experimental Method

Because of the relatively low concentrations of oxygen in equilibrium with the higher percentages of carbon at or below atmospheric pressure, it was decided that the experimental work should be carried out at pressures up to 20 atmospheres. This should permit an evaluation of the effect of pressure upon the equilibrium and thus contribute materially to an understanding of the reaction.

A. Pressure Furnace—In order to carry out equilibrium meas-

urements at a maximum total pressure of 20 atmospheres, it was necessary to design and construct a furnace which would enclose a small induction coil in such a manner that the electrical, water and gas leads could be attached without the possibility of short circuits or gas leaks which might endanger the operator. Because of the difficulties involved in insulating electrical leads through a metal container, it was decided to use some sort of fiber material for the pressure vessel. There are several fiber materials available which might have been suitable for the purpose. Micarta, a pressed paper material, has been used in this laboratory for vacuum work with good success; however, it has a tendency to char and flake when overheated. Furthermore, higher pressures were planned than were covered by our experience with micarta. Of the materials considered, it was decided to use a linen impregnated material called "Phenolite". Grade CE_m has a tensile strength of 9000 pounds per square inch, is chemically inert and may be easily machined.

Fig. 1 shows a sketch of the assembled furnace. The Phenolite cylinder, K, is 9½ inches long and 5 inches inside diameter with a wall thickness of ½ inch. The ends of the cylinder are closed by ½-inch brass plates, U, V, which are grooved to fit the cylinder and to hold rubber gaskets to insure pressure-tight connections. Pressure is applied to the connections by means of 4 staybolts, F. In the first experiment at 20 atmospheres it was found that both plates bent due to the pressure, thereby making it impossible to keep the furnace tight. The circular reinforcing plates, L, were added to overcome this difficulty. The top reinforcing plate was made of iron because it was observed that most of the bending took place at the top. The bottom plate was of brass which was found to be sufficiently strong.

The top plate, V, is water cooled, G, since it is subjected to direct radiation from the crucible, and incorporates a brazed-in sight tube and ¼-inch Pyrex glass window, D, through which temperatures may be observed. In order to prevent overheating as well as fogging of the glass, a "butterfly" shutter, E, is built into the sight tube. By means of a magnet this shutter can be opened and closed as desired. The sight glass is pressed against a seated rubber gasket by means of a hollow screw.

The top plate likewise supports a thin copper radiation shield, J, which prevents overheating the fiber cylinder. This cylindrical screen is slotted in 2 places to prevent heating by induction. Passing through

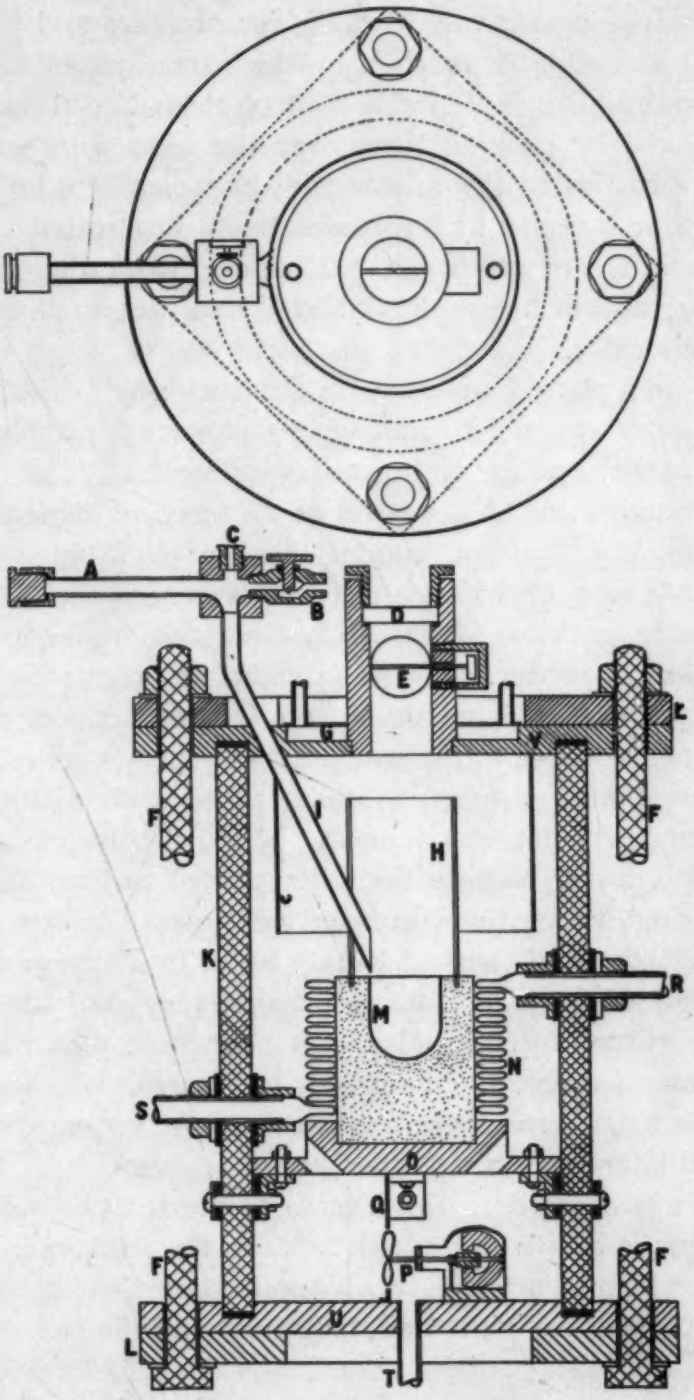

Fig. 1—Details of Furnace Construction.

the top plate is a ¼-inch brass tube, I, by means of which gas and vacuum may be applied to the furnace and gas samples removed for analysis. This tube extends to within ½ inch of the crucible. The outside end of the tube, I, terminates in a brass block to which are

threaded 2 Hoke needle valves, B, C, for pressure and vacuum and a horizontal ¼-inch brass tube, A, in which small pieces of aluminum may be stored until it is desirable to drop them into the melt. This is accomplished by pushing them over the edge with an iron slug which can be motivated from the outside by means of a magnet. The end of the tube is closed by a threaded brass plug seated on a rubber gasket. In order to remove a gas sample from the furnace for analysis, the vacuum line is disconnected and the sampling line connected to this valve.

The bottom plate, U, is likewise fitted with a ¼-inch brass tube and needle valve in order to remove gas samples for analysis and to release the pressure at the end of an experiment.

The induction coil, N, consists of 12 turns of flattened ⅜-inch copper tubing and is of conventional design. It is supported on an Albarene stone base, O, which is in turn fastened to the fiber cylinder by brass angle pieces. The bolts holding the angles are suitably gasketed with soft rubber. The water and power connections through the cylinder, at R and S, are made by means of brass nipples which screw into lugs soldered to the ends of the induction coil.

The inside of the induction coil is lined with a thin layer of magnesia cement. This was found to be much better than the conventional mica lining because the latter tended to give off a smoky gas when heated, which fogged up the sight glass.

The crucible, M, is packed loosely in 14 to 20-mesh electrically sintered magnesia in order that the charge may cool rapidly when the power is turned off. By placing it near the top of the coil, the charge was situated near the main body of the gas.

The small fan, P, was not used in the first few experiments but was installed later when a definite thermal segregation of the gas in the furnace was observed. The bottom of the furnace is baffled, Q, so that the gas is drawn in through holes in the Albarene stone base on one side and discharged through similar holes on the other side. In order to prevent circulation of the gas around the coil rather than over the top, the space between the coil and the cylinder was likewise baffled with sections of Pyrex tubing.

The radiation screen, H, consists of a piece of cylindrical refractory and is used for temperatures above 1540 degrees Cent. (2805 degrees Fahr.) to protect the fiber cylinder further. It was later found to be unnecessary for this reason but is used in dynamic experiments to assist in directing the incoming gas onto the melt.

B. Metal Charges—In order to approach the equilibrium from both the high carbon and the high oxygen sides, two materials were used as melting stock. One contained 0.95 per cent carbon and a small amount of oxygen while the other contained 0.006 per cent carbon and 0.195 per cent oxygen. Both were prepared in the large vacuum furnace; the ingots were forged to approximately 1¼ inches round and the oxidized surface was machined away. Solid sections weighing 75 to 100 grams were cut off as needed for charging. For charges of intermediate carbon content it was originally planned to use mixtures of the two. However, it was later found more convenient to use electrolytic iron and crushed graphite for this purpose.

C. Crucibles—All of the crucibles used in the investigation were made of electrically sintered magnesia and were manufactured by the slip casting technique of Thompson and Mallett (26). The crucibles were found to be of excellent quality. They were strong, dense and impervious to molten iron oxide at 1600 degrees Cent. (2910 degrees Fahr.) for periods of as long as 3 hours.

D. Gases and Their Analysis—In carrying out experiments in which gases are to be used under pressure, it is usually possible to obtain the highly compressed gas in cylinders. The cylinders may then be used as reservoirs to furnish the desired pressures by means of reducing valves. While CO_2 can be obtained in cylinders at a pressure of 3000 pounds per square inch, CO is not sold at all commercially due to its extreme toxicity and explosiveness. It is easily manufactured in the laboratory in small amounts, however, but investigation showed that the necessary compressing equipment for obtaining the pressures desired was not available and would require a considerable expenditure if purchased. The alternative then was to manufacture a large amount of CO or CO-CO_2 mixture and have it compressed into cylinders. The method used for the manufacture of CO was that whereby formic acid is decomposed to CO and water by the action of hot concentrated sulphuric acid.

From a survey of Vacher's work (15) it was decided that the first lot of gas should contain approximately 15 per cent of CO_2. The cylinder into which the CO was to be compressed was evacuated for several hours and filled with the proper amount of CO_2 from a commercial cylinder. The CO was then compressed from the gas holder through a drying tube of calcium chloride into the cylinder. CO was added to a pressure of 1600 pounds. The resulting mixture was later found to contain 23.2 per cent CO_2 and will be referred to

as Tank 1a. This amount of CO_2, greater than the anticipated amount, was probably due to the use of this gas in flushing out the gas holder. Some air leakage likewise occurred for the gas was found to contain 1.1 per cent of nitrogen.

A second lot of CO was generated to provide gas with lower CO_2 content. The system was again flushed out with CO_2 but none was added to the cylinder into which the gas was compressed. This gas later analyzed 2.75 per cent CO_2 and will be referred to as Tank 2. More CO was obtained than was required to fill one cylinder so the remainder was added to Tank 1a. The CO_2 content of the gas was reduced to approximately 15 per cent and this gas will be referred to as Tank 1b.

During compression of the second lot of CO some difficulty was encountered with the compressor so that Tank 2 contained 6.5 per cent of N_2 by contamination with air and the nitrogen content of Tank 1b was 4.5 per cent.

After the gas mixtures were prepared, the cylinders were allowed to stand for at least one month before any analysis was attempted. This was done in order to permit complete mixing.

A number of difficulties appeared in trying to analyze these gas mixtures by the ordinary Orsat method, because of the high CO content. Ordinarily, CO_2 is absorbed by potassium hydroxide, oxygen by alkaline pyrogallol, CO by acid cuprous chloride, and nitrogen is determined by difference. This method is successful for amounts of CO not exceeding 15 per cent, but for gas mixtures containing larger amounts it is recommended (27) that a combustion or expulsion method be used. An apparatus involving these refinements was not available and it was therefore necessary to devise a method for using the ordinary flue gas analyzer.

The first attempts showed that water could not be used as the fluid for moving the gases around because of the high solubility of CO_2 and mercury was therefore substituted. It was also necessary to dilute the gas sample with a substantial amount of nitrogen since practically everything in the gas was to be absorbed and the handling of very small amounts of gas in this type of analyzer leads to inaccuracies.

After these changes in technique were made, it was found that both potassium hydroxide and alkaline pyrogallic acid would absorb appreciable quantities of CO from a gas with such a high CO content. The results for both CO_2 and oxygen were consequently in

Table I
Analyses of Gas Mixtures

Constituent	Tank 1a Per Cent	Tank 2 Per Cent	Tank 1b Per Cent
CO_2	23.2	2.75	15.1
O_2	0.3	1.6	1.1
CO	75.3	89.15	79.3
N_2	1.2	6.5	4.5

error. No means of overcoming this was found and it was therefore concluded that the best procedure would be to absorb all the absorbable constituents, thereby determining nitrogen, and to determine the CO_2 by a weight method. The amount of oxygen in the gas could be assumed to be equivalent to the nitrogen content on the basis that the only source of both was air. The CO content could then be taken as the difference between the sum of the other quantities and 100 per cent.

The weight method used for determining carbon dioxide consisted in passing a known volume of gas through a weighed tube of "Ascarite" and determining the weight increase. The volume of gas passed through the tube was determined by collecting the exit gases over water. Observation of the barometric pressure and the water temperature allowed the calculation of the volume of gas equivalent to the amount of carbon dioxide collected in the weighed tube. This method was found to be accurately reproducible and was used for all experiments where it was necessary to know the gas analysis at equilibrium.

In all except the dynamic runs the analysis of the tank gas was relatively unimportant, except for nitrogen content, since the proportions of carbon monoxide and carbon dioxide usually changed to meet the conditions of equilibrium. In these static runs it was assumed that the nitrogen content of the gas remained constant and that all the oxygen present reacted with CO to form CO_2. This was the basis of the CO determination by difference.

The analysis of the three gas mixtures by the methods outlined above are given in Table I.

E. Freezing Trap—A freezing coil consisting of 6 turns of ½-inch thin wall copper tubing was installed in order to freeze out any water vapor or carbonyls that might be present in the gas. Although mixtures of dry ice and acetone were used for several runs, nothing was ever condensed and the practice was discontinued. Each

tank of gas was tested for water vapor content by passing several liters through weighed phosphorus pentoxide tubes, but no indication of water vapor greater than 0.04 per cent was ever found. This degree of dryness was no doubt due to the fact that the gas was compressed into the cylinders through calcium chloride.

F. Pressure Measurement—Pressures were measured on a 6-inch Bourdon tube type test gage calibrated in 2-pound divisions over the range 0 to 300 pounds per square inch. The gage was calibrated before use against a dead-weight tester.

G. Temperature Measurement—Temperatures were measured with a new type Leeds and Northrup disappearing filament type optical pyrometer. Because liquid iron in the open is not a black body and because of the absorption of part of the radiation by the sight glass and prism, it was necessary to calibrate the pyrometer to the conditions of use. This was done by observing the melting point of electrolytic iron under a gas containing 7 per cent hydrogen and 93 per cent nitrogen. The observed melting point was found to be quite reproducible at 1335 degrees Cent. (2435 degrees Fahr.). Assuming the melting point of electrolytic iron to be 1535 degrees Cent. (2795 degrees Fahr.), there is a correction of 200 degrees Cent. (390 degrees Fahr.) at this temperature.

The relationship between the temperature of a source at T° absolute and the temperature, S° absolute, observed with absorbing glasses or screens interposed, is (24)

$$\frac{1}{T} - \frac{1}{S} = K$$

where for all practical purposes K is a constant. Applying this expression to the above observation we find

$$K = -0.0000688$$

This value of K was used for correcting all observed temperatures above the melting point of iron. For the lower temperatures used on the heats made in graphite crucibles, the pyrometer was again calibrated in a similar manner by observing the eutectic temperature of the iron-carbon system. For this calibration the eutectic temperature was taken as 1130 degrees Cent. (2065 degrees Fahr.) and the value of K for melts saturated with carbon was found to be — 0.000054.

H. Furnace Operation—It was originally planned that the ex-

periments should be "dynamic", that is, that gas should be passed through the furnace continually during the run until equilibrium was indicated by a constant analysis of the exit gas. As will be pointed out later, this method proved inapplicable and the experiments were carried out in a closed system. The first few "static" runs were made by simply isolating the furnace, allowing the charge to remain at constant temperature and pressure for 2 hours, and then sampling the gas and allowing the metal to freeze. Due to thermal separation of the gases in the cold parts of the furnace, a small fan was installed to keep the gases mixed, but otherwise the conditions were static. The majority of the runs were made in this manner by the following procedure:

A weighed amount of charge of the desired carbon content was placed in the crucible and the furnace was closed and sealed by tightening the staybolts. Aluminum was placed in the holder to be added if desired at the end of the experiment, and the vacuum, water and pressure lines were connected. The furnace was then evacuated through the vacuum connection. The purpose of this evacuation was simply to remove the air from the furnace. In order to flush out the connecting tubing between the gas cylinder and the furnace, the furnace was allowed to fill to a pressure of 5 to 10 pounds per square inch with gas from the cylinder. This gas was then pumped away with the vacuum pump. The furnace was then allowed to fill to approximately 1 atmosphere pressure with gas from the cylinder at which time the power was turned on. As soon as the charge was melted, the pressure was slowly raised to the desired point and the fan was started. When the pressure was approximately adjusted, the furnace was isolated by closing the needle valve between the pressure gage and the cylinder.

For the next 20 to 30 minutes the power input was adjusted so as to hold the metal at constant temperature. At the end of this time the pressure, which had been slowly increasing due to heating up of the gas by the charge, was adjusted by either adding gas from the cylinder or by releasing it at the bottom of the furnace. For the next 1½ hours minor variations in power input were required to hold the temperature constant. Pressure and temperature readings were made every 10 to 15 minutes.

When the experiment was completed, the gas was sampled by disconnecting the vacuum connection and connecting a rubber hose leading to the Ascarite bulb. Approximately 500 cubic centimeters

of gas were allowed to flush through the tubing and drying bulb (which preceded the Ascarite bulb) in order to remove air or gas from a previous experiment. The weighed Ascarite bulb was then connected into the line. The amount of gas passed through the bulb was determined by collecting the exit gas over water. The barometric pressure and water temperature were observed so that the gas analysis could be calculated.

When the gas analysis was completed, the power was turned off unless aluminum was to be added. In this case, the aluminum was dropped in and allowed to mix for approximately 30 seconds before shutting off the power.

As soon as the charge had cooled it was removed from the furnace for sampling. In some runs small bits of the crucible tended to stick to the surface. In order to remove these, the samples were ground on a wheel over the entire surface and pickled lightly in hydrochloric acid. Chips for the carbon determination and for oxygen analysis by chemical methods were obtained by machining a complete cross section of the piece starting at the edge and finishing at the center. In this way exactly half of the material was machined up and errors due to segregation were eliminated. The remaining half of the piece was either stored or used for the determination of oxygen by the vacuum fusion method.

When aluminum was added to the melts, it was necessary to determine the oxygen content by chemical methods because excess aluminum interferes with oxygen determinations by vacuum fusion. The chemical methods for the determination of oxygen are based on the assumption that all the iron oxide in a melt is converted to alumina upon addition of aluminum and that this alumina is retained by the metal provided the melt is cooled rapidly. Determination of the alumina then allows the calculation of the oxygen content of the metal.

I. The Experiments—The first experiment performed was the melting of a charge in an atmosphere of nitrogen at 20 atmospheres pressure in order to test the furnace and other equipment. The furnace was found to operate quite satisfactorily at this pressure and the temperature was raised to more than 1800 degrees Cent. (3270 degrees Fahr.) without difficulty or apparent harm.

From the analysis of the gas in Tank 1a, which had considerably more CO_2 than had been anticipated, it was realized that the carbon contents of the melts made with it would be very low and the

Table II
Dynamic Runs

Run	Temp. Degrees Cent.*	Pressures, Atm. P	p_{CO_2}	p_{CO}	Per Cent C	Per Cent O	K'_1	K'_2	K'_3	Per Cent C × Per Cent O	Remarks
2	1605	0.993	0.172	0.796	0.010	0.220	368	0.98	362	0.0022	Unkilled, OK
3	1675	11.26	1.69	9.29	0.037	.....	1380	....	...	.....	Porous
4	1545	11.23	2.20	8.75	0.054	.....	646	....	...	.....	Porous
5	1525	21.11	3.99	16.60	0.167	0.212	414	1.14	469	0.0354	Killed, OK
6	1525	0.991	0.204	0.762	0.017	0.171	167	1.57	264	0.0029	Unkilled, OK

*True temperatures observed after obtaining suitable calibration.

oxygen contents very high. Accordingly the first few runs were made as feeler runs using the high oxygen material for charges. Runs 2 to 6 were made as planned, that is, dynamically, at pressures of 1, 10 and 20 atmospheres. On analyzing the gas leaving the furnace to determine the state of equilibrium, it was found that it eventually reached a fairly constant analysis, but considerably lower in CO_2 than the incoming gas. Temperature readings were made with difficulty because of the continual streakiness of the surface of the bath due to oxidation. Attempts to observe the melting point of oxygen-saturated iron as a calibration for the pyrometer proved unsuccessful due to the scumming over of the surface by oxide thrown out of solution as the metal cooled. It was also noted that the length of the run had a definite effect on the amount of oxide formed as a separate phase. The only conclusion to be drawn was that the gas contained too much CO_2 to ever reach equilibrium with the metal, and the result of an extended run would simply be the conversion of all the iron to iron oxide. From the data obtained, shown in Table II, it was evident however, that increasing the pressure increased the amount of carbon to be found in the resulting ingot, although in all cases the metal was probably saturated with oxygen. The oxygen analyses proved quite erratic as might be expected from the fact that iron oxide was observed to come out of solution on cooling in the case of the unkilled runs. All the runs in this series at pressures greater than 1 atmosphere were killed with aluminum after it was found in Run 3 that the metal would not solidify without gas evolution when the carbon content was more than about 0.02 per cent.

On the basis of these results it was decided to repeat the experiments, except that the furnace should be isolated and no gas allowed to enter. It was assumed that the CO_2 content of the gas would

Table III
Static Runs, No Fan. Temperature 1530 ± 10 Degrees Cent.

Run	Pressure, Atm. P	p_{CO_2}	p_{CO}	Per Cent C	Per Cent O	K'_1	K'_2	K'_3	Per Cent C × Per Cent O	Remarks
7	11.03	1.98	8.79	0.097	0.185	402	1.22	491	0.0179	Killed, OK
8	3.0	0.41	2.51	0.014	0.23 ±0.01	1098	0.71	784	0.0032	Unkilled
9	20.74	3.08	17.15	0.145	0.22+	659	0.82	538	0.0319	Killed, OK for carbon
10	20.56	3.30	16.73	0.119	.....	713	....	...	.....	Porous
11	11.35	1.73	9.33	0.104	0.230	484	0.80	391	0.0239	Killed, OK
12	6.04	0.89	5.00	0.063	0.134	446	1.33	595	0.0084	Killed, OK
13	2.56	0.383	2.11	0.026	0.184	447	0.99	440	0.0048	Killed, OK

lower itself by reaction with the iron to form iron oxide, but that the reaction would eventually stop, allowing equilibrium to be established. In order to sample the gas directly over the melt, a silica extension tube was fastened to the gas inlet tube. It extended to within ¼ inch of the metal surface. Runs 7 to 13 were made by this procedure, using the high oxygen material for charge. So much trouble was encountered in setting up the furnace and dropping the aluminum into the melt with the silica extension tube in place that it was removed after Run 10.

The results of these runs are shown in Table III in which are also included the corresponding values of the equilibrium constants, K'_1, K'_2 and K'_3, to be defined later by Equations 4, 5 and 6. On the first of these runs it was again difficult to obtain accurate temperature measurement due to the formation of oxide, but for the remainder of the runs temperatures could be read quite readily after the initial oxidation was over. At the beginning of Run 10 a charge of electrolytic iron was melted under an atmosphere of nitrogen and hydrogen and a satisfactory calibration of the pyrometer was obtained.

During these runs the gas samples were removed from the top of the furnace through the vacuum connection. Samples taken at 1½ hour and at 2 hours after starting the run gave check analyses and it was concluded that 2 hours was sufficient to establish equilibrium.

On Runs 10 and 11 samples were taken also from the bottom of the furnace. It was found that although the top gas analysis was constant, the bottom gas analysis was higher in CO_2. The series was completed with Runs 12 and 13 and in all calculations the analysis of the gas taken from the top was used.

Table IV

Killed vs. Unkilled Runs. Temperature 1540 ± 10 Degrees Cent.

Run	Pressure, Atm. P	p_{CO_2}	p_{CO}	Per Cent C	Per Cent O	K'_1	K'_2	K'_3	Per Cent C × Per Cent O	Remarks
				High Carbon Charge, Unkilled						
14	7.56	1.11	6.26	0.082	0.180	431	0.99	423	0.0148	Porous
16	10.25	1.50	8.49	0.133	.....	361	....	...	.....	Blown
21	20.46	3.34	16.61	0.102	0.253	810	0.80	644	0.0258	Blown
24	5.31	0.28	4.90	0.140	0.122	613	0.47	287	0.0171	Porous
29	2.81	0.12	2.62	0.080	0.126	715	0.36	260	0.0101	Blown
				High Carbon Charge, Killed						
15	9.84	1.47	8.25	0.108	0.129	429	1.38	593	0.0139	OK
17	20.18	3.22	16.72	0.191	0.153	455	1.26	573	0.0292	OK
25	5.25	0.61	4.58	0.083	0.108	414	1.23	509	0.0090	OK
28	2.97	0.17	2.76	0.097	0.048	462	1.28	587	0.0047	OK
				High Oxygen Charge, Unkilled						
18	21.00	3.59	16.88	0.096	.....	827	....	...	.....	Blown
23	10.63	1.59	8.78	0.083	.....	584	....	...	.....	Blown
27	4.99	0.72	4.15	0.026	0.148	920	1.17	1079	0.0038	Blown
				High Oxygen Charge, Killed						
19	20.60	3.49	16.86	0.163	0.157	500	1.32	658	0.0256	OK
22	10.66	1.62	8.91	0.102	0.146	480	1.24	598	0.0149	OK
26	5.23	0.75	4.42	0.046	0.172	566	0.99	560	0.0079	OK
30	2.83	0.39	2.40	0.035	0.155	422	1.05	445	0.0054	OK

The results, Table III, indicate that equilibrium was more nearly approached than in the dynamic runs. but the results are considerably erratic and open to the criticism of possible thermal segregation of the gas. They also indicate that the values of K'_1, which involves per cent carbon only and not per cent oxygen, are more consistent when the samples were killed with aluminum. The possibility of carbon and oxygen reacting as the metal cools and giving erroneous results may have been overcome by adding aluminum.

Since melts made with the high CO_2 gas will necessarily contain large amounts of oxygen and small amounts of carbon, it is conceivable that oxygen results obtained on unkilled samples may be very little in error and may be compared with carbon results obtained on duplicate heats which are killed with aluminum. The difference in carbon contents may then be used to calculate the loss in oxygen due to the reaction. This would allow the determination of oxygen by the more accurate vacuum fusion method (for large amounts of oxygen).

Accordingly a new series of runs was planned. In order to prevent thermal diffusion and separation of the gases, the small fan mentioned in the description of the furnace was installed. Killed and unkilled heats were made starting with both the high carbon and the high oxygen material at pressures of 3, 5, 10 and 20 atmos-

Table V

Runs at Low Carbon to Determine Effect of Temperature on K_2

Run*	Pressure, Atm. P	p_{CO_2}	p_{CO}	Per Cent C	Per Cent O	K'_1	K'_2	K'_3	Per Cent C × Per Cent O	Remarks
					1540 ± 10 Degrees Cent.					
31	1.40	0.22	1.16	0.013	0.198	471	0.96	448	0.0026	OK, Vacuum fusion
32	1.27	0.22	1.04	0.015	0.151	328	1.40	459	0.0023	OK " "
33	1.28	0.146	1.12	0.020	0.109	429	1.20	514	0.0022	OK " "
34	1.28	0.188	1.08	0.016	0.140	388	1.24	482	0.0022	OK " "
35	1.34	0.202	1.12	0.016	0.151	388	1.20	464	0.0024	OK " "
69	1.54	0.0795	1.36	0.048	0.055	485	1.06	515	0.0026	OK, Killed
					1600 ± 10 Degrees Cent.*					
36	1.33	0.189	1.135	0.017	0.165	394	1.02	406	0.0028	OK, Vacuum fusion
37	1.34	0.185	1.13	0.015	0.172	460	0.95	435	0.0026	OK " "
40	1.28	0.153	1.11	0.012	0.197	670	0.70	463	0.0024	OK " "
67	1.41	0.121	1.22	0.016	0.099	770	1.00	762	0.0016	OK " "

*See also Runs 2 and 62.

Run	Pressure, Atm. P	p_{CO_2}	p_{CO}	Per Cent C	Per Cent O	K'_1	K'_2	K'_3	Per Cent C × Per Cent O	Remarks
					1650 ± 10 Degrees Cent.					
68	1.54	0.165	1.31	0.022	0.150	473	0.84	397	0.0033	Killed, OK
83	1.53	0.137	1.32	0.019	.....	670	....	...	.....	Killed, Erratic oxygen results
					1700 ± 10 Degrees Cent.*					
38	1.27	0.142	1.11	0.011	0.243	788	0.53	415	0.0027	OK
39	1.26	0.126	1.14	0.011	0.251	938	0.44	413	0.0028	OK
75	1.53	0.118	1.34	0.025	0.151	609	0.58	352	0.0038	OK, Killed

*See also Runs 63 and 65.

pheres, at a temperature of 1540 degrees Cent. (2805 degrees Fahr.)

The results of these runs are shown in Table IV. The data again indicate that more uniform values for the constants are obtained when the sample is killed with aluminum. Reaction between carbon and oxygen was evidenced by the porosity of the samples which were not killed and the erratic results obtained upon analysis by vacuum fusion. Any attempt to calculate oxygen values for the unkilled samples based on the difference in carbon contents of the killed and unkilled melts lead to absurd figures. Furthermore, the "duplicate runs" were not sufficiently alike to allow the calculation. Compared on the basis of the starting material, the results indicate that equilibrium was not quite attained since the average value of K'_1 starting with high carbon material is lower than the average value when low carbon material was used as the charge material.

At this point it was decided that a gas, less rich in CO_2, thereby giving ingots of a higher carbon content, might lead to greater accuracy since the analytical error in determining carbon would have more weight in the low carbon samples. On the other hand, a more

Table VI
First Runs with Tank 2, High Carbon Charge. 1540 ± 10 Degrees Cent.

Run	Pressure, Atm. P	p_{CO_2}	p_{CO}	Per Cent C	Per Cent O	K'_1	K'_2	K'_3	Per Cent C × Per Cent O	Remarks
41	1.35†	.....	1.25	0.71	0.0059	...	....	298	0.0042	Sample only fair
42	1.55	0.0067	1.44	0.75	0.006	415	0.78	320	0.0045	Killed, OK
43*	19.99	1.06	17.63	0.66	.....	445	....	...	.....	Unkilled, porous
44*	20.12	0.936	17.87	0.65	0.064	524	0.82	430	0.0416	Killed, OK
45	10.27	0.372	9.24	0.52	0.035	442	1.15	508	0.0182	Killed, OK
46*	5.11	0.089	4.68	0.62	0.031	397	0.61	244	0.0192	Killed, OK
47	3.05	0.028	2.82	0.75	0.008	379	1.24	470	0.0060	Killed, OK

*Gas analysis changed after power was off.
†Estimated.

Table VII
30-Minute Runs, 1540 ± 10 Degrees Cent.

Run	Pressure, Atm. P	p_{CO_2}	p_{CO}	Per Cent C	Per Cent O	K'_1	K'_2	K'_3	Per Cent C × Per Cent O	Remarks
48	10.36	0.281	9.40	0.66	0.029	477	1.03	490	0.0192	Killed, OK
50	5.18	0.090	4.75	0.74	0.014	339	1.35	457	0.0104	Killed, OK
52	20.14	0.934	17.90	0.71	0.061	483	0.86	413	0.0433	Killed, OK

Table VIII
Runs with Mixed Charges, 1540 ± 10 Degrees Cent.

Run	Pressure, Atm. P	p_{CO_2}	p_{CO}	Per Cent C	Per Cent O	K'_1	K'_2	K'_3	Per Cent C × Per Cent O	Remarks
49	10.17	0.534	8.98	0.36	0.062	420	0.96	403	0.0223	Killed, OK
51	5.10	0.167	4.60	0.29	0.032	437	1.13	495	0.0093	Killed, OK

accurate value for K'_2, the oxygen constant, could probably be obtained with the high CO_2 gas provided the carbon were kept so low that there would be no reaction between carbon and oxygen on cooling. During the interval of manufacturing more CO, compressing it into cylinders and allowing it to mix thoroughly, Runs 31 to 40 were made with Tank 1a in order to establish a value for K'_2. The temperatures used were 1540, 1600 and 1700 degress Cent. (2805, 2910 and 3090 degrees Fahr.) in order to establish a temperature coefficient. By charging the high oxygen material and confining the pressures to slightly over 1 atmosphere, the carbon contents were kept below 0.02 per cent and no reaction occurred on cooling. Excellent checks for oxygen by vacuum fusion method were obtained.

Using the gas of lower CO_2 content in Tank 2, runs were made at 1+, 3, 5, 10, 20 atmospheres and 1540 degrees Cent. (2805 degrees Fahr.) using the high carbon material for charging. The ingots resulting from Runs 41 to 47 all contained 0.50 to 0.75 per cent carbon. Run 41 was not killed in order to observe whether or not the reaction between carbon and oxygen would occur on cooling in this carbon range. The resulting ingot was porous. The results of these runs are shown in Table VI.

Three short runs were made at this time in order to determine whether or not the usual time of 2 hours was sufficient to establish equilibrium. Runs 48, 50 and 52 were made at 1540 degrees Cent. (2805 degrees Fahr.) at pressures of 5, 10 and 20 atmospheres for 30 minutes each. The high carbon charge material was used with the gas from Tank 2. The results, Table VII, indicate that 30 minutes was a sufficient time to establish equilibrium with the possible exception of Run 50.

In order to obtain values for the constants at intermediate carbon contents between the previous results of 0.10 per cent to about 0.75 per cent, Runs 49 and 51 were made using mixtures of the high and low carbon material. The resulting ingots analyzed 0.36 and 0.29 per cent carbon respectively and the results are given in Table VIII. The temperature was 1540 degrees Cent. (2805 degrees Fahr.) and the pressures used were 10 and 5 atmospheres.

The next series of runs, 53 to 61, were made with charges of electrolytic iron and crushed graphite to determine values for the constant at higher, 1 to 2 per cent, carbon contents. All of the runs were made at pressures of 10 and 20 atmospheres in order that the concentration of CO_2 would be sufficiently high for accurate gas analysis. Temperatures used were 1410, 1445, 1540 and 1600 degrees Cent. (2570, 2635, 2805 and 2910 degrees Fahr.). Runs 60 and 61 were made at 20 atmospheres and temperatures of 1135 and 1400 degrees Cent. (2075 and 2550 degrees Fahr.) respectively in graphite crucibles. The pyrometer was again calibrated by observing the eutectic point of the iron-carbon system in order to eliminate any errors which might arise in using the calibration obtained on relatively carbon-free iron. The purpose of the runs in graphite crucibles was to establish a value for the reaction

$$C\ (gr) + CO_2\ (g) = 2CO\ (g)$$

for comparison with the established values for this reaction and

Table IX
High Carbon Runs at Various Temperatures

Run	Temp. Degrees Cent.	Pressures, Atm. P	p_{CO_2}	p_{CO}	Per Cent C	Per Cent O	K'_1	K'_2	K'_3	Per Cent C × Per Cent O	Remarks
53*	1540	10.17	0.068	9.44	2.27	0.016	577	0.45	260	0.0363	Killed, OK
54*	1446	20.15	0.165	18.68	3.78	0.009	559	0.98	547	0.0341	Killed,OK
55*	1446	20.23	0.135	18.76	4.13	0.0043	630	1.67	1057	0.0165	Unkilled, OK
56	1414	19.75	0.535	17.92	1.85	0.051	325	0.59	190	0.0388	Unkilled, OK
57*	1600	5.15	0.307	4.51	0.10	0.095	661	0.72	474	0.0095	Killed, OK
58*	1540	10.18	0.070	9.45	1.83	0.008	696	0.93	647	0.0146	Unkilled, Faulty Sampling
59*	1600	10.26	0.078	9.52	1.62	0.013	717	0.63	451	0.0211	Unkilled, Faulty Sampling
					Graphite Crucibles						
60	1135	19.96	0.72	17.94	4.33	0.004	103	10.1	1038	0.0173	Unkilled, Erratic Oxygen Results
61*	1400	19.97	0.210	18.46	4.73	0.018	343	0.632	217	0.0850	Unkilled, OK

*Gas analysis changed after power was off.

Table X
Dynamic Runs After Altering Furnace

Run	Temp. Degrees Cent.*	Pressures, Atm. P	p_{CO_2}	p_{CO}	Per Cent C	Per Cent O	K'_1	K'_2	K'_3	Per Cent C × Per Cent O	Remarks
62	1600	0.997	0.174	0.777	0.012	0.231	289	0.97	280	0.0028	Unkilled, OK
63	1700	0.996	0.174	0.777	0.010	0.27 ±0.02	347	0.83	288	0.0027	Unkilled, Oxygen Erratic
64*	1600	0.995	0.060	0.869	0.30	0.012	420	5.76	241	0.0036	Killed
65*	1700	0.994	0.060	0.868	0.41	0.010	306	6.91	212	0.0041	Killed
66*	1540	0.994	0.060	0.868	0.32	0.010	393	6.28	248	0.0035	Killed

*On Runs 64, 65, 66 the gas cracked badly.

Table XI
Carbon Recovery from Charge

Run	Charged	Recovered	Per Cent O	Per Cent C × Per Cent O	Gas	Remarks
70A	0.20	0.058	0.043	0.0025	Tank 2	Killed
70B	0.40	0.281	0.012	0.0034	Tank 2	Killed
70C	0.60	0.488	0.007	0.0034	Tank 2	Killed
70D	0.20	0.091	0.028	0.0025	Tank 1b	Killed
70E	0.40	0.259	0.010	0.0026	Tank 1b	Killed
70F	0.60	0.51	0.006	0.0031	Tank 1b	Killed

with the data obtained at the same time for iron saturated with carbon. The results are given in Table IX. The results for the above mentioned reaction did not agree with the established values for the reason that the graphite and metal were observed to be at different

temperatures and the temperature of the metal only could be read accurately.

As mentioned earlier, during the preparation of the Tank 2 gas enough CO was available to add some to the original Tank 1a which contained too much CO_2. The CO_2 content was reduced from 23.5 per cent to 15 per cent. After this gas had become thoroughly mixed in the cylinders, Runs 62 to 66 were made in order to determine if dynamic runs could be carried out as was originally planned. Gas was passed through the furnace in the manner previously described for 1 hour at 1 atmosphere pressure and at temperatures of 1540, 1600 and 1700 degrees Cent. (2805, 2910 and 3090 degrees Fahr.). Runs 62 and 63 were made with the high oxygen charge material and gas from Tank 1b while Runs 64, 65 and 66 were made with high carbon charge material and gas from Tank 2. In order to calculate p_{CO_2} and p_{CO} the analysis of the tank gas was used. This procedure was satisfactory for the runs made with Tank 1a but with the low CO_2 gas, Tank 2, CO "cracked" badly depositing carbon in the furnace so that the calculations based on the tank gas analysis are probably considerably in error. The results of these runs are shown in Table X.

At the conclusion of Run 66, some alterations were made in the furnace arrangement in order to improve the circulation of the gas. The copper radiation shield, J (Fig. 1), was folded back towards the fiber cylinder in such a way that it prevented circulation of the gas into the top part of the furnace and directed it across the melt. The refractory radiation shield, H (Fig. 1), was removed entirely and the holes through which the gases circulated to and from the fan were widened into slots. Runs 67, 68 and 69 were made to obtain checks on the oxygen constant, K_2. Gas from Tank 1b and high oxygen charge material were used. The pressure was 1+ atmosphere and the temperatures were 1600, 1650 and 1540 degrees Cent. (2910, 3000 and 2805 degrees Fahr.) respectively. The results of these runs are shown in Table V with the other runs of this type.

A survey of the data on which analytical results had been obtained to this point indicates that there was considerable spread in the values for the constants. One reason for this could be non-attainment of equilibrium due to charging material whose carbon content was considerably above or below that at equilibrium and not allowing sufficient time for equilibrium to be attained. It was pos-

Table XII
Runs with Charges Near Equilibrium Carbon Content, 1540 ± 10 Degrees Cent.

Run	Pressures, Atm. P	p_{CO_2}	p_{CO}	Per Cent Carbon Charged	Per Cent Carbon Recovered	Per Cent O	K'_1	K'_2	K'_3	Per Cent C × Per Cent O	Remarks
71	1.56	0.147	1.33	0.02	0.03	0.090	402	1.23	492	0.0027	Killed, OK
76	1.53	0.107	1.36	0.04	0.038	0.074	452	1.06	486	0.0028	Killed, Erratic Oxygen
72	10.22	1.38	8.38	0.10	0.122	0.130	417	1.27	527	0.0159	Killed, OK
77	10.18	1.37	8.35	0.15	0.113	0.177	449	0.93	418	0.0200	Killed, OK
73	1.54	0.0645	1.38	0.05	0.064	0.042	461	1.11	511	0.0027	Killed, OK
78	1.53	0.042	1.39	0.08	0.077	0.026	598	1.16	695	0.0020	Killed, OK
74	10.18	0.653	8.86	0.15	0.275	0.085	437	0.87	379	0.0234	Killed, Erratic Oxygen
79	10.25	0.725	8.86	0.30	0.224	0.064	483	1.28	620	0.0143	Killed, OK

sible, on the basis of the results at hand, to estimate fairly closely the probable carbon content at equilibrium with a given gas, and it was therefore planned to make a series of runs in which the amount of carbon present immediately after melting would be first slightly above the equilibrium amount and then slightly below the equilibrium amount. In order to do this it was necessary to determine the amount of carbon that would be recovered immediately after melting for a given amount charged. Runs 70, —A, —B, —C, etc., were made by charging varying amounts of carbon and electrolytic iron and melting them under the two gases. As soon as the metal was melted, it was killed and the power turned off. The results showing the amount of carbon charged and the amount recovered under a given gas are shown in Table XI.

From the results of Run 70, Runs 71, 72, 73 and 74 were charged so as to melt at what should be the equilibrium carbon content from the data so far obtained. The temperature used was 1540 degrees Cent. (2805 degrees Fahr.) and the pressures were 1 and 10 atmospheres for each tank of gas. It was found that in each of these runs the carbon increased slightly in coming to equilibrium and therefore Runs 76, 77, 78 and 79 were made by charging slightly more carbon than was present at equilibrium in Runs 71, 72, 73 and 74. In these runs it was found that the carbon content at equilibrium was slightly less than the amount of carbon recovered on melting. In other respects the runs were duplicate and the equilibrium had therefore been approached from both sides from very near the equilibrium carbon content. The results of these runs are given in Table XII. The intermediate experiment, Run 75, was made in an effort to

Table XIII
High Carbon Runs, 1540 ± 10 Degrees Cent.

Run	Pressure, Atm. P	p_{CO_2}	p_{CO}	Per Cent C	Per Cent O	K'_1	K'_2	K'_3	Per Cent C × Per Cent O	Remarks
81	10.17	0.138	9.36	1.21	0.027	525	0.55	287	0.0326	Killed, OK
84	1.54	.....	1.44	2.31	0.009	...	....	69	0.0208	Killed, OK
85	5.10	0.0602	4.71	1.66	0.026	222	0.49	109	0.0432	Killed, OK
86	10.18	0.211	9.30	0.88	0.039	466	0.58	271	0.0343	Killed, OK
87	18.3	.....	....	1.30	0.047	...	....	...	0.0611	Killed. Furnace Leaked. Short Time
88	19.81	1.14	17.38	0.50	0.087	530	0.75	400	0.0435	Killed, OK
89	10.18	0.620	8.89	0.24	0.057	530	1.22	649	0.0137	Killed, OK

obtain another value for the oxygen constant at 1700 degrees Cent. (3090 degrees Fahr.). The results of this run are shown in Table V with the other similar runs.

In order to obtain more data in the high carbon range at 1540 degrees Cent. (2805 degrees Fahr.), Runs 80 and 81 were made. Run 80 was made with the low CO_2 gas from Tank 2 and a charge of the 1 per cent carbon charging material with the addition of 1 per cent of crushed graphite. The pressure was 10 atmospheres. This melt was not killed because of difficulty in dropping the aluminum and the reaction was so great on turning off the power that no results are reported. Run 81 was a duplicate of Run 80 except that aluminum was added. The results are shown in Table XIII with the other high carbon data.

Runs 82 and 83 were made with the high oxygen material and the high CO_2 gas from Tank 1b at 1 atmosphere pressure and 1650 degrees Cent. (3000 degrees Fahr.) in order to check the value of the oxygen constant, K'_2, previously obtained at this temperature. Run 82 was not killed and there was considerable reaction on cooling so that the results were considered worthless. Run 83 was a duplicate run in which the melt was killed. The results of Run 83 are shown in Table V with the other comparable data.

Runs 84 to 89 constitute a series of runs made at 1540 degrees Cent. (2805 degrees Fahr.) and various pressures in an attempt to obtain further data for the constants over a considerable range of carbon content and to fill in the gaps in the data already obtained. All charges were electrolytic iron with various amounts of crushed graphite added and the runs were made with the low CO_2 gas in Tank 2. The results of this series are given in Table XIII.

Sources of Error

Before drawing any conclusions from the data obtained in the experimental work, it is necessary to consider the possible sources of error in the individual runs or groups of runs and weigh the values of the constants accordingly.

Errors in Pressure Measurement—No difficulty was encountered in any run in keeping the pressure at the desired value after the first 20 to 30 minutes, and, since the gage calibration showed that the gage error was less than 1 per cent over the entire range, it is believed that the errors in pressure measurement may be neglected.

Errors in Temperature Measurement—The calibration of the pyrometer was quite satisfactory and was checked several times during the experimental work. In the first dynamic runs, Table II, observations were difficult due to the formation of oxide which continually streaked the surface and these temperatures are probably the most inaccurate. Because of the difficulty of measuring the temperature, the melts, with the exception of Runs 2 and 3, were held as near the melting point as could be determined by observation and several times solidified during the course of the experiments.

In the experiments at 1700 degrees Cent. (3090 degrees Fahr.) to establish a temperature coefficient for K'_2, Table V, the formation of soot from the decomposition of CO tended to fog the sight glass and these temperatures are probably higher than recorded. With these exceptions it is thought that the temperatures are accurate to $\pm$ 10 degrees Cent. Observations were quite reproducible and no difficulty was encountered in holding the temperature constant to within $\pm$ 5 degrees during an experiment.

Errors in Gas Analysis—The gravimetric method gave very reproducible results and checked the modified Orsat method used to analyze the tank gases. On Runs 41 and 84 the amount of CO_2 in the gas was very small and negative weight gains were obtained when the gas was analyzed. Investigation showed this to be due to the fact that the U-tube containing the Ascarite had not been flushed out with the gas being analyzed before the first weight was made. For the type of gas being analyzed, it is believed that the method used was beyond a doubt the best available.

For the earlier runs where consecutive samples were taken ½ hour apart to determine if equilibrium had been attained, the results always checked within 2 or 3 per cent and, after it was established

that 2 hours was a sufficiently long time, only one sample was taken in order that the pressure should not be lowered too much by taking gas from the furnace.

On some of the high carbon experiments where the pressure was necessarily high in order that the CO_2 content of the gas be high enough for accurate analysis, samples were taken after the power had been turned off and the melt was cold in order to check the analysis obtained before shutting off the power. These determinations sometimes failed to check the first determination by considerable amounts. The CO_2 content was usually considerably higher in the sample taken after the power was turned off. The reason for this is not known unless it could be due to some change that occurs in the gas during cooling. It is not likely that there could be enough gas dissolved in the metal or even enough carbon and oxygen present in such small charges to change the analysis of the amount of gas in the furnace appreciably. In all these cases the analyses of the gas obtained before the power was turned off were used in the calculations since they should represent more nearly the gas analysis at equilibrium. The runs in which this phenomenon occurred are marked with asterisks in the tables.

Errors in Carbon and Oxygen Analyses—The possible errors in the analytical results for carbon and oxygen are by far the most important and the results must be examined critically from this standpoint. These errors may not necessarily arise from the actual chemical analysis for these elements but rather from the fact that the analysis must be carried out on the samples after being cooled from a high temperature to a low one. In order to know the carbon and oxygen contents of the metal in the molten state it is necessary that the melt be cooled in such a manner that no carbon nor oxygen is gained nor lost during the cooling.

One source of loss of carbon and oxygen is in the reaction that may occur between the two during cooling. This reaction was observed in all samples containing between 0.02 and 2.0 per cent carbon that were not killed with aluminum. On samples containing less than 0.02 and more than 2.0 per cent carbon no reaction occurred as evidenced by soundness of the ingots. The oxygen contents of these samples were determined by the vacuum fusion method which is considered to be the most reliable when it can be used. The results for oxygen so obtained were found to be quite consistent and check determinations were obtained. On the other hand, samples very

low in carbon content contain very large amounts of oxygen, amounts that may exceed the solubility of oxygen in iron at the freezing point. In this case it might be conceivable that some loss of oxygen could occur by being thrown out of solution as ferrous oxide on cooling to the freezing temperature.

In the case of samples killed with aluminum it is necessary that the oxygen content be determined by chemical analysis for alumina. In order to be sure that all the iron oxide in the melt is converted to aluminum oxide an excess of aluminum must be added. This excess interferes with the analysis as carried out by vacuum fusion leading to low results. Since the possibility of the reaction between carbon and iron oxide on cooling is eliminated in a sample treated with aluminum, it is likely that the results for carbon on these samples are quite accurate. However, the oxygen results are open to several sources of error. First, is all the iron oxide converted to aluminum oxide? Whether or not this is true can be estimated by the appearance of the residue obtained on solution of the sample in acid as the first step in the analysis. Samples in which the oxygen is not completely converted to alumina in general show a brown or red colored residue due to the presence of iron oxide. Of the several analytical methods for alumina, the one which gives the whitest residue is considered best. Both the nitric acid and hydrochloric acid solution methods were used in this study and it was found that cleaner looking residues were obtained by the hydrochloric acid method. The results checked each other better by this method and were in most cases lower than those obtained by the nitric acid method. The results reported for killed steels were all obtained by the hydrochloric acid method.

Another possible source of oxygen loss may occur if alumina particles float out of the melt between the time aluminum is added and the time the melt solidifies. It is thought that error from this source is not likely since alumina particles do not have a tendency to collect together in large pieces and since the melts were usually solid in 20 to 30 seconds after the power was turned off.

A source of high oxygen results is the oxidation of the aluminum added by the gas. This oxidation was observed to occur to some extent at the surface of the bath where the aluminum melted. The thin film of aluminum oxide formed, however, tended to remain on the surface and was later ground off before taking samples for analysis.

On the basis of these sources of error, a number of runs were

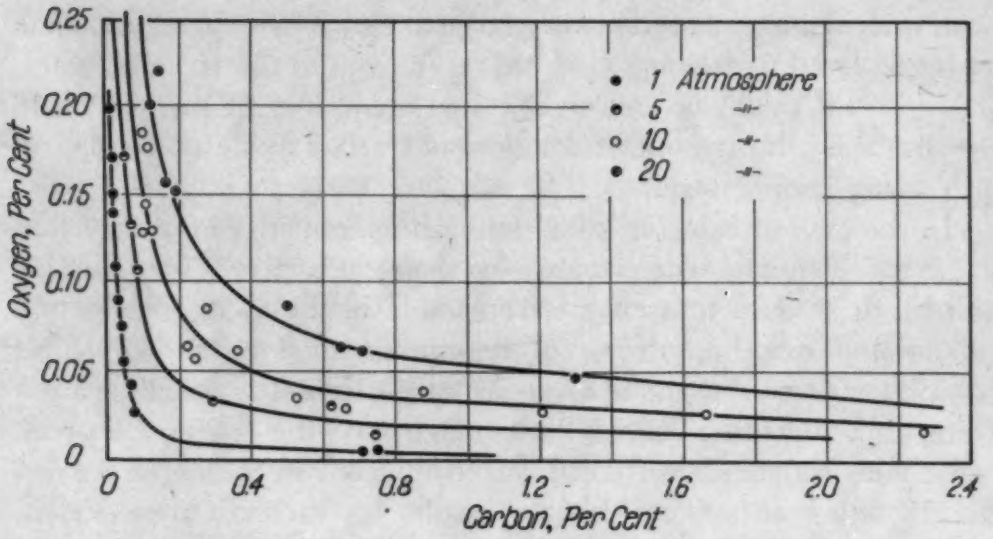

Fig. 2—Effect of Carbon on the Oxygen Content at 1540 Degrees Cent.

discarded entirely and not included in the presentation of the data. They are included in the tables, however, and, if not used, the reason for not doing so is indicated in the "Remarks" column. All samples marked "OK" are considered good runs in which reproducible carbon and oxygen results were obtained and no source of major error was apparent.

Since all the sources of error mentioned above would tend to make the analytical results for carbon and oxygen low and the corresponding values for the constants high (carbon and oxygen always appear in the denominator of the ratios), the low values of the constants have been given more weight.

Presentation of the Data

The variation of the oxygen content of the ingots obtained with their carbon contents at total pressures of 1, 5, 10 and 20 atmospheres is shown in Fig. 2. This plot shows that the oxygen content of the metal falls off in a quite regular manner as the carbon content increases. The greater the pressure, the larger the amounts of carbon and oxygen that can exist together in liquid iron. These curves bear a striking resemblance to those found in studies of the oxygen content of metal in the open hearth (18, 20). The open-hearth data fall between our curves for 1 and 5 atmospheres pressure.

The product per cent carbon $\times$ per cent oxygen at equilibrium is not a constant as was formerly assumed but increases with in-

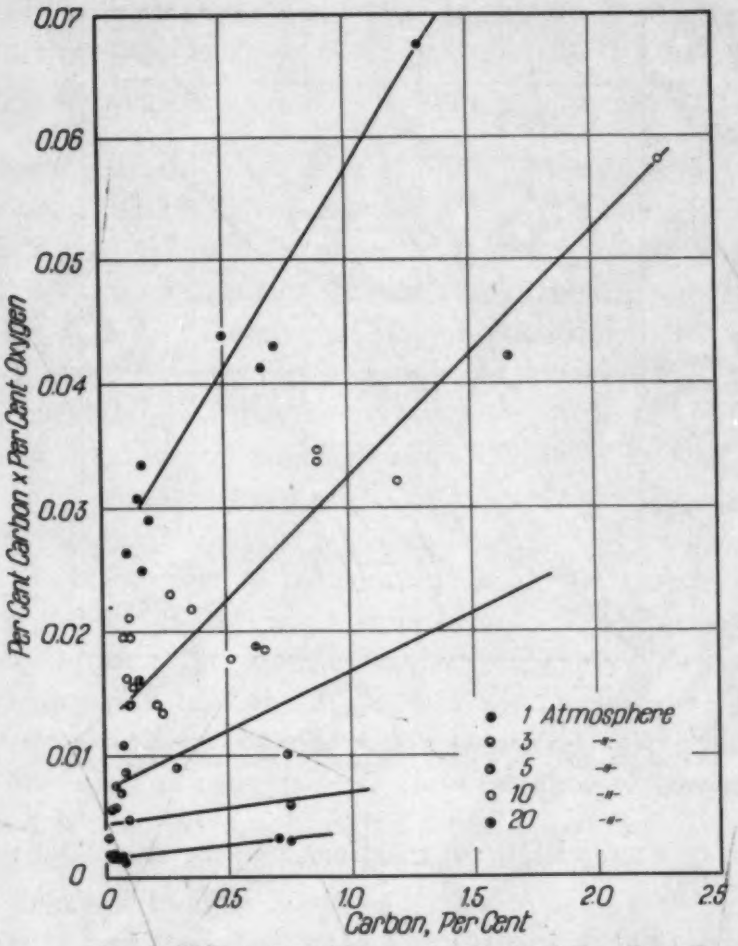

Fig. 3—Effect of Carbon on the Product, Per Cent Carbon × Per Cent Oxygen, at 1540 Degrees Cent. and Indicated Total Pressures.

creasing carbon content as shown in Fig. 3. The points shown in this plot include all of the data obtained at 1540 degrees Cent. (2805 degrees Fahr.). Since the experiments were not carried out at exactly 20, 10, etc. atmospheres pressure, the values of the product have been corrected slightly to these pressures by multiplying the observed products by 20/P, 10/P, etc. The result is a family of straight lines each showing at constant pressure a marked increase in the product with increasing carbon content.

The effect of pressure on the carbon-oxygen product is shown in Fig. 4. The product increases linearly with carbon monoxide pressure but the rate of increase is much greater at higher percentages of carbon.

Equilibrium Constants of the Reactions at 1540 Degrees Cent. (2805 Degrees Fahr.)—From the data that have been obtained the

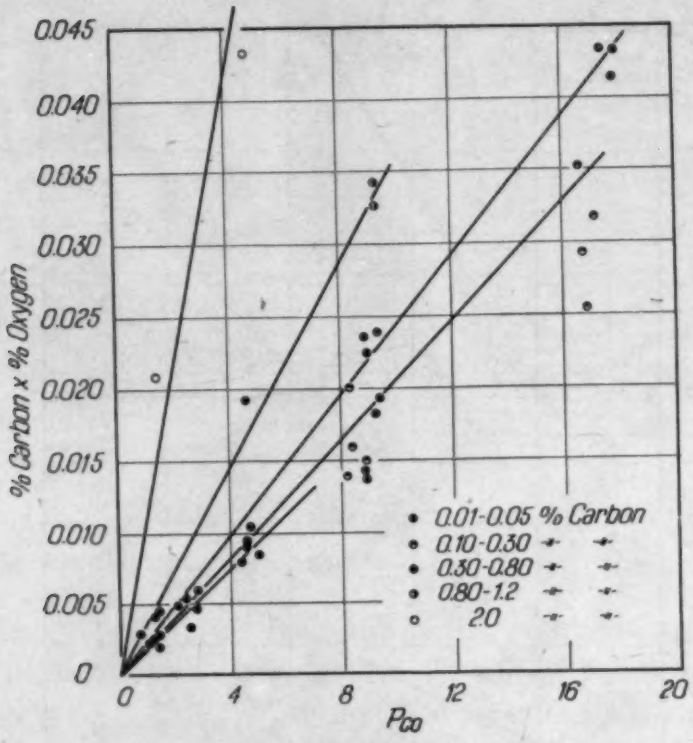

Fig. 4—Effect of Carbon Monoxide Pressures on the Product, Per Cent Carbon × Per Cent Oxygen, at 1540 Degrees Cent.

equilibrium constants of three reactions may be calculated:

$$C\ (\text{in Fe}) + CO_2\ (g) = 2\ CO\ (g) \qquad K_1 = \frac{p_{CO}^2}{p_{CO_2} \times a_C} \qquad [1]$$

$$CO\ (g) + O\ (\text{in Fe}) = CO_2\ (g) \qquad K_2 = \frac{p_{CO_2}}{p_{CO} \times a_O} \qquad [2]$$

$$C\ (\text{in Fe}) + O\ (\text{in Fe}) = CO\ (g) \qquad K_3 = \frac{p_{CO}}{a_C \times a_O} \qquad [3]$$

No data are available as to the activities of carbon and oxygen in solution in iron simultaneously, and for lack of these data we may assume as a first approximation that their activities are proportional to their weight per cents. On this basis the following approximation constants are defined; their numerical values are included in the tables of data.

$$K_1' = \frac{p_{CO}^2}{p_{CO_2} \times \%\,C} \qquad [4]$$

$$K_2' = \frac{p_{CO_2}}{p_{CO} \times \%\,O} \qquad [5]$$

$$K_3' = \frac{p_{CO}}{\%\,C \times \%\,O} \qquad [6]$$

It will be convenient to consider the constants individually. If the assumption regarding the proportionality of the activity of carbon and its weight per cent is true, then a plot of $\frac{p_{co}^2}{p_{co_2}}$ against the carbon content should result in a straight line whose slope is equal to K_1'. Such a plot is shown for 1540 degrees Cent. (2805 degrees Fahr.) in Fig. 5. It will be observed that the line begins to curve after a concentration of about 0.5 per cent carbon is reached indicating that the activity of carbon is not proportional to its weight per cent above about 0.5 per cent carbon. At lower carbon concentrations, however, the data may be adequately represented by a straight line and the slope in this range gives a value of $K_1' = 430$.

In Fig. 6 are plotted the values of K_2' against the carbon content for a temperature of 1540 degrees Cent. (2805 degrees Fahr.). It is evident that K_2' is not at all constant and that carbon drastically affects the activity of oxygen in liquid iron. At zero carbon content the curve intersects the axis at a value of $K_2' = 1.2$. In drawing the line the lower values of the constant have been favored (for the reasons previously stated). There is no apparent correlation between the pressures used and the value of the constant. Statistical analysis of the data plotted gives a standard deviation of 0.22 K_2' units or a probable error of 0.032 K_2' units in the line as drawn.

The calculated values for K_3' are plotted against the carbon content in Fig. 7 and again the line is drawn to favor the low values of the constant because of possible carbon or oxygen losses. The plot shows that K_3' is likewise drastically affected by the carbon concentration. Statistical analysis of these data gives a standard deviation from the line drawn of 82 K_3' units or a probable error of the line of 12.4 K_3' units.

When per cent carbon $\times$ per cent oxygen is plotted against p_{co} a straight line should result whose slope is equal in value to K_3'. The result of such a plot is shown in Fig. 4. The fact that K_3' is not a true constant as defined is shown by the fact that a series of lines can be drawn for different carbon ranges. The lines are straight for a given carbon content indicating that the value of K_3' is determined only by the carbon concentration.

Activity of Carbon and Oxygen in Liquid Steel—From the foregoing it is evident that the constants, as defined, are not true equilibrium constants. Their variation with the carbon content indicates that the assumption that the activities of carbon and oxygen are pro-

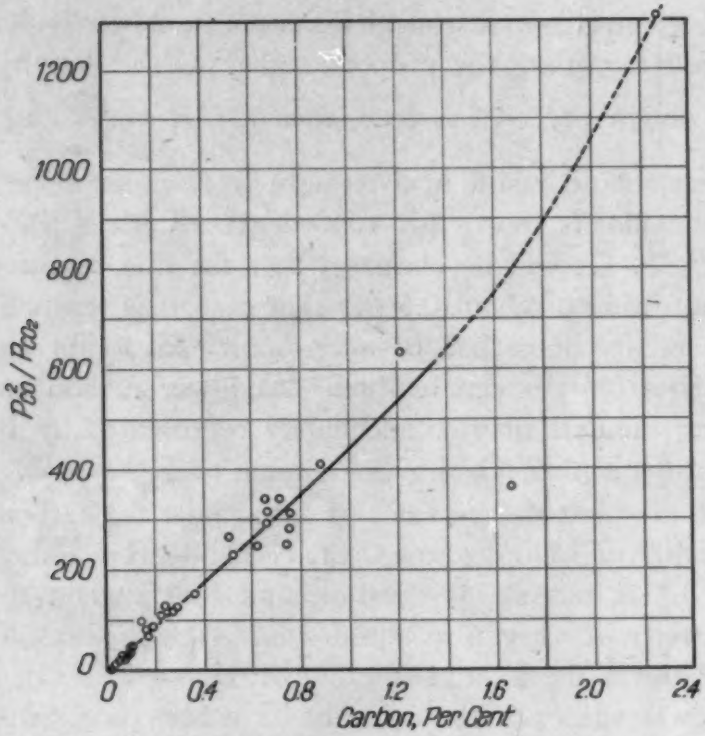

Fig. 5—Relation Between Carbon Content and the Ratio p^2_{CO}/p_{CO_2} at 1540 Degrees Cent.

portional to their weight per cents is erroneous. The determination of the true equilibrium constants is simplified by introducing activity coefficients defined as $f_c = a_c/\%\ C$ and $f_o = a_o/\%\ O$. Equations 1, 2 and 3 may then be rewritten:

$$K_1 = \frac{p^2_{CO}}{p_{CO_2} \times (f_c \times \%\ C)} \qquad [7]$$

$$K_2 = \frac{p_{CO_2}}{p_{CO} \times (f_o \times \%\ O)} \qquad [8]$$

$$K_3 = \frac{p_{CO}}{(f_c \times \%\ C)\ (f_o \times \%\ O)} \qquad [9]$$

It is possible to determine the values of these activity coefficients in the following manner. By means of Fig. 5 in which $\frac{p^2_{CO}}{p_{CO_2}}$ was plotted against per cent carbon, it was shown that up to about 0.5 per cent carbon a straight line was obtained indicating that the expression $\frac{p^2_{CO}}{p_{CO_2} \times \%\ C}$ is a true constant at low carbon concentrations with a value of 430 at 1540 degrees Cent. Then at any carbon content

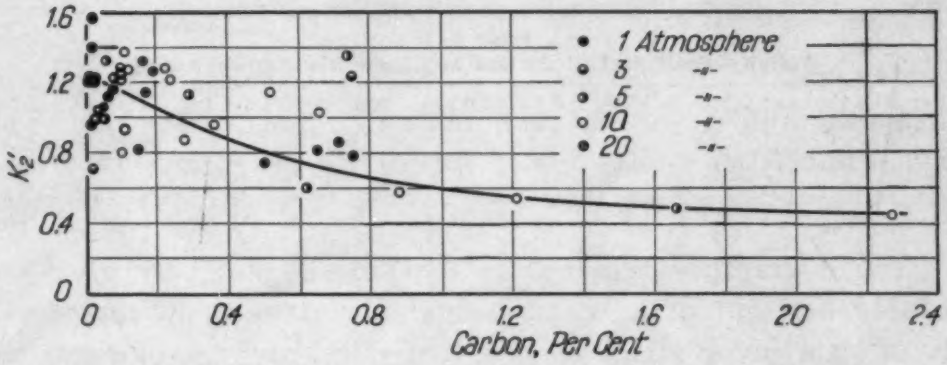

Fig. 6—Effect of Carbon on $K'_2 = p_{CO_2}/p_{CO} \times \%$ O at 1540 Degrees Cent.

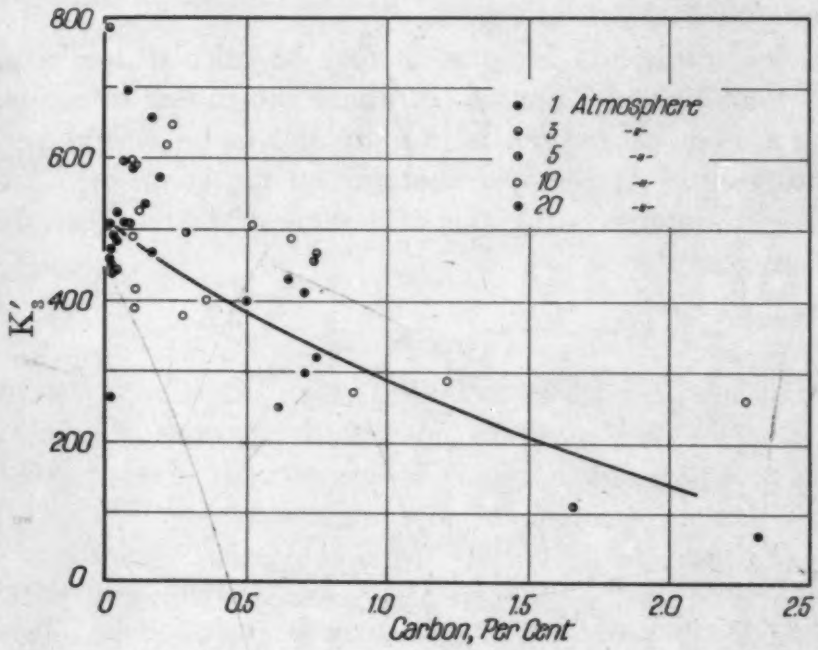

Fig. 7—Effect of Carbon on $K'_3 = p_{CO}/\%$ C $\times$ % O at 1540 Degrees Cent.

$$K_1 = \frac{p^2_{CO}}{p_{CO_2} \times (f_c \times \% C)} = 430 = \frac{K'_1}{f_c}$$

$$f_c = \frac{K'_1}{430}$$

By taking values of K'_1 at different carbon contents from the curve, the activity coefficients shown in Table XIV may be calculated. The second set of f_c values were calculated for the sake of comparison from the equations which Darken (30) derived from a theoretical study of the available equilibrium data on the reaction

$$C \text{ (in Fe)} + 3 \text{ Fe (l)} = Fe_3C \text{ (in Fe)} \qquad [10]$$

Table XIV
Activity Coefficient of Carbon in Liquid Iron-Carbon Alloys

Per cent Carbon	0.0	0.1	0.2	0.5	0.75	1.0	1.5	2.0
f_c (from K'_1)	1.0	1.0	1.0	1.0	1.01	1.03	1.08	1.23
f_c (from Darken (30))	1.0	1.02	1.04	1.12	1.19	1.27	1.46	1.73

The discrepancy between the two lines is not very great and probably lies within the experimental uncertainties in the several sets of data involved. The fact that our activity coefficients are greater than unity is regarded as at least a partial confirmation of Darken's methods. A plot of the two sets of values for f_c against carbon content is shown in Fig. 8.

Activity coefficients for oxygen may be calculated in a similar manner. Fontana and Chipman (31) have shown that in carbon-free melts the activity of oxygen is proportional to its weight per cent up to saturation. At zero per cent carbon the curve of K'_2 versus carbon, Fig. 6, intersects the axis at a value of 1.21. Therefore, at low carbon contents

$$K_2 = \frac{p_{CO_2}}{p_{CO} \times (f_o \times \% O)} = 1.21$$

and at higher carbon concentrations

$$K_2 = 1.21 = \frac{K'_2}{f_o}$$

$$f_o = \frac{K'_2}{1.21} \qquad [11]$$

By taking values of K'_2 from the curve at different carbon contents the activity coefficients for oxygen may be calculated. These are shown in Table XV.

Table XV
Activity Coefficient of Oxygen in Liquid Iron-Carbon-Oxygen Alloys

Per cent Carbon	0.0	0.1	0.2	0.3	0.4	0.5	1.0	1.5	2.0
f_o (from K'_2)	1.0	0.93	0.86	0.79	0.73	0.67	0.50	0.42	0.39
f_o (from K'_3)	1.0	0.94	0.89	0.84	0.79	0.75	0.55	0.41	0.30

By considering the data for K'_3 in a similar manner and using the activity coefficients already calculated for carbon, an additional set of activity coefficients for oxygen may be calculated. At low carbon concentrations, from Fig. 7, K'_3 has a value of 512. Then

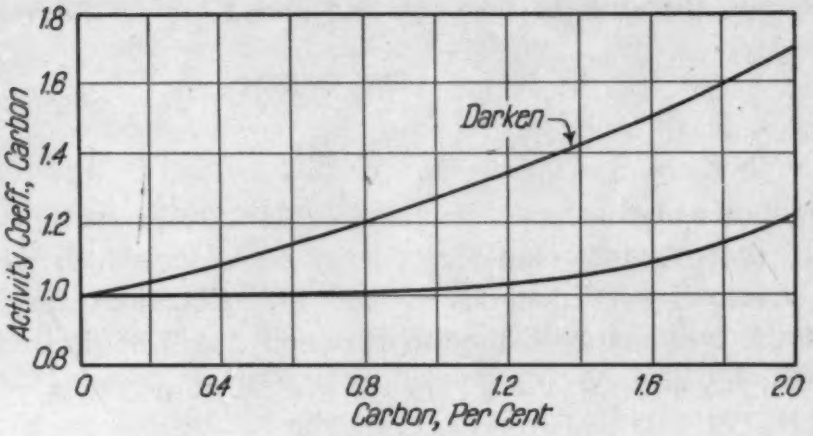

Fig. 8—Activity Coefficients for Carbon, 1540 Degrees Cent.

$$K_3 = \frac{p_{CO}}{(f_c \times \%\,C)\ (f_o \times \%\,O)} = 512$$

And at higher carbon contents

$$K_3 = 512 = \frac{K_3'}{f_c \times f_o}$$

$$f_o = \frac{K_3'}{512\, f_c} \qquad [12]$$

By taking values of K_3' from the curve at different carbon contents the values of f_o shown in the last line of Table XV may be calculated. The comparison of the two sets of values is shown in Fig. 9.

Effect of Temperature Upon the Reactions—From the data collected in Table V it is possible to determine temperature coefficients for the equilibrium constants at low carbon contents. These results were obtained on runs made at temperatures of 1540, 1600, 1650 and 1700 degrees Cent. (2805, 2910, 3000 and 3090 degrees Fahr.) and at slightly more than 1 atmosphere pressure. The resulting ingots contained less than 0.02 per cent carbon and were all sound, showing no evidence of gas evolution even though no aluminum was added to the melts. The oxygen contents were determined by vacuum fusion and checks were obtained on duplicate analyses. In Figs. 10, 11 and 12 the logarithms of K_1', K_2' and K_3' respectively, are plotted against the reciprocal of absolute temperature. The results of Vacher (15) at 1580 degrees Cent. (2875 degrees Fahr.) and of Phragmén and Kalling (43) at 1550 and 1700 degrees Cent. (2820 and 3090 degrees Fahr.) are included for purposes of comparison. The data for K_2' are most adequately represented by a curved line while the

equations of the straight lines for K'_1 and K'_3 give the following expressions:

$$\log K'_1 = -\frac{5778}{T} + 5.784 \quad [13]$$

$$\log K'_3 = \frac{1860}{T} + 1.643 \quad [14]$$

The heats of these two reactions ($\triangle H$) are given by the first terms of the two following free energy equations which were obtained directly from Equations 13 and 14. Equations for log K_2 and for the free energy change in Reaction 2 will be derived later.

$$C \text{ (in Fe)} + CO_2 \text{ (g)} = 2\ CO \text{ (g)};\ \triangle F^\circ = 26400 - 26.45\ T \quad [15]$$

$$C \text{ (in Fe)} + O \text{ (in Fe)} = CO \text{ (g)};\ \triangle F^\circ = -8510 - 7.52\ T \quad [16]$$

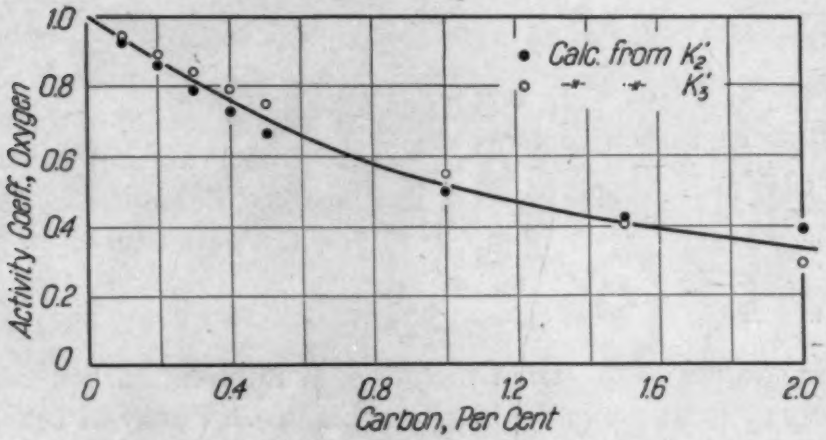

Fig. 9—Activity of Coefficients for Oxygen, 1540 Degrees Cent.

It should be pointed out that Equations 13 and 14 were derived by the method of least squares from our data at or below 0.02 per cent carbon. The equations yield the following values at 1540 degrees Cent. (2805 degrees Fahr.): $K'_1 = 400$; $K'_3 = 470$. Both of these are lower than the corresponding values of K obtained by extrapolating the data of Figs. 5 and 7 to very low carbon content. It seems probable that the discrepancy is due to an effect of the very high oxygen content of the low carbon melts upon the activity of carbon, analogous to the effect of high carbon upon the activity of oxygen.

Comparison With Other Investigations—In order to establish the accuracy of the results that have been presented it is desirable to compare them where possible with the results of other investigations. Two previous studies of the same system have been mentioned. Vacher's experiments were carried out at 1580 degrees Cent.

(2875 degrees Fahr.) and a comparison of his work with the results of this investigation has been shown in Figs. 10, 11 and 12. Phragmén and Kalling (43) devoted most of their effort to determining the carbon-oxygen product at 1550 and 1700 degrees Cent. (2820 and 3090 degrees Fahr.). Excluding certain of their results which showed rather wide deviations, average values at these temperatures of $m = 0.0019$ and $m = 0.0025$ are obtained. The corresponding values of K'_3 shown in Fig. 12 are in excellent agreement with our results. From their published gas and metal analyses, average values of K'_1 have been included in Fig. 10. The points are above our curve but the discrepancy is not serious in view of the rather wide scatter. Their data were at somewhat higher carbon content than our points of Fig. 10 and the possibility that K'_1 is diminished by the high oxygen associated with very low carbon has already been mentioned. In both Figs. 10 and 12 our line lies between the data of Vacher and the average of Phragmén and Kalling. The discrepancy between our results and Vacher's in Fig. 12 corresponds to a difference in carbon analysis of 0.002 per cent.

Fontana and Chipman (31) and Chipman and Samarin (32) have studied the following reaction at temperatures of 1600 to 1750 degrees Cent. (2910 to 3180 degrees Fahr.):

$$H_2\,(g) + O\,(\text{in Fe}) = H_2O\,(g);\ K_H = \frac{p_{H_2O}}{p_{H_2} \times \%\ O} \qquad [17]$$

Their data may be calculated to the system under investigation by means of the accurately known equilibrium of the water gas reaction:

$$CO_2\,(g) + H_2\,(g) = CO\,(g) + H_2O\,(g);\ K_{WG} = \frac{p_{H_2O} \times p_{CO}}{p_{H_2} \times p_{CO_2}} \qquad [18]$$

Subtracting Equation 18 from Equation 17 we have

$$CO\,(g) + O\,(\text{in Fe}) = CO_2\,(g);\ K_2 = \frac{p_{CO_2}}{p_{CO} \times \%\ O} \qquad [19]$$

A very accurate expression for the equilibrium constant of the water gas reaction has been calculated from the spectroscopic free energy data of Gordon (33), Kassel (34), Johnson and Davis (35) and Davis and Johnson (36), equilibrium data of Neumann and Kohler (28) and of Emmett and Shultz (29) and the thermal data of Rossini (37) and leads to the following expression which is

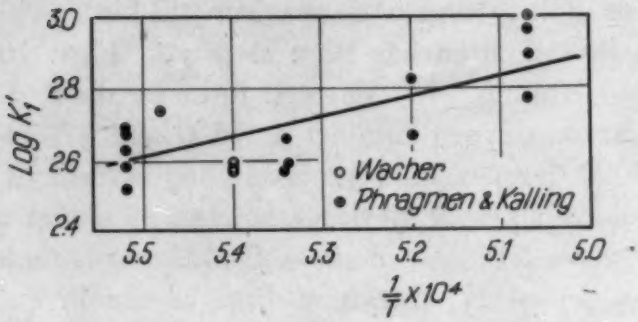

Fig. 10—Effect of Temperature on $K'_1 = \frac{p^2_{CO}}{p_{CO_2} \times \% C}$ at 1 Atmosphere Pressure in the Range Below 0.02 Per Cent Carbon.

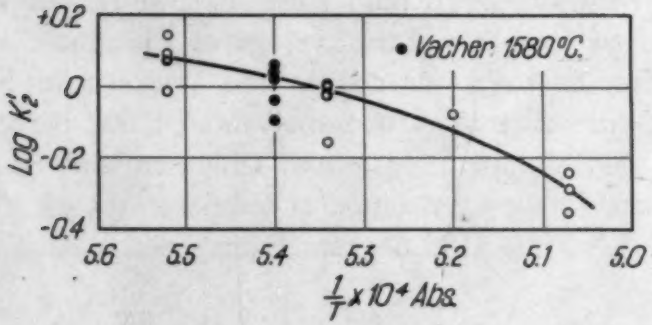

Fig. 11—Effect of Temperature on $K'_2 = \frac{p_{CO_2}}{p_{CO} \times \% O}$ at 1 Atmosphere Pressure in the Range Below 0.02 Per Cent Carbon.

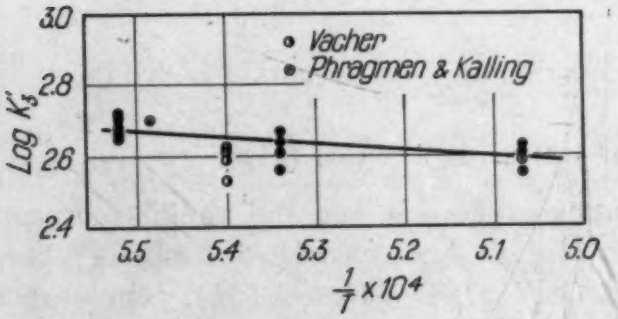

Fig. 12—Effect of Temperature on $K'_3 = \frac{p_{CO}}{\% C \times \% O}$ at 1 Atmosphere Pressure in the Range Below 0.02 Per Cent Carbon.

probably accurate to 3 per cent within the range 1700 to 2100 degrees Kelvin.

$$CO_2\,(g) + H_2\,(g) = CO\,(g) + H_2O\,(g)\,;\ \log K_{wg} = \frac{-1386}{T} + 1.350 \quad [20]$$

By means of this expression each of the experimental points of the above mentioned investigators has been calculated from the Fe-H-O system to the Fe-C-O system and the results are shown graphically in Fig. 13 together with all of the direct data on the Fe-C-O system at or below 0.02 per cent carbon.

Ordinarily when the logarithm of an equilibrium constant is plotted against reciprocal temperature, the result is a straight line. In the present case, however, a curved line is required. This same peculiarity was observed in constructing Fig. 11 and at first was attributed to experimental errors. The very close agreement between results from the Fe-H-O system and from the Fe-C-O system indicate either that the relationship is actually curvilinear or that a reproducible source of error has affected both series of results. Since temperatures were measured optically in all cases, it is very possible that this is the source of error. Observations at higher temperatures are more subject to smoke errors and the emissivity of liquid iron may change enough at higher temperatures to account for the departure from linearity. It should be noted, however, that if the results up to 1600 degrees Cent. (2910 degrees Fahr.) are considered correct, the temperature correction at 1700 degrees Cent. (3090 degrees Fahr.) (observed) required to straighten out the plot would be about 150 degrees Cent. (300 degrees Fahr.). Since this seems most improbable the results will be represented by the curve of Fig. 13 whose equation is:

$$\log K'_2 = 7200/T - 3.855 - 9 \times 10^{-6}\,(T - 1873)^2 \quad [21]$$

For approximate calculations the straight dotted line seems to be the best linear representation of the data. Its equation is:

$$\log K'_2 = 7320/T - 3.960 \quad [22]$$

Oxygen Pressure of Oxygen-Saturated Iron—When metallic iron and an iron oxide phase co-exist at equilibrium, the oxygen pressure of the system is determined by the temperature. This oxygen pressure of the saturated solution is an important feature of the iron-oxygen system and the data here reported permit a more accurate calculation at temperatures above the melting point than has been possible in the past. It will be interesting to compare the newly

calculated values with those formerly obtained from the Fe-H-O system both above and below the melting point of iron.

These calculations involve a number of subsidiary data, including the free energies of the reacting gases which are now quite accurately known. From the sources cited above in deriving Equation 20 we find for the free energy of water vapor and the corre-

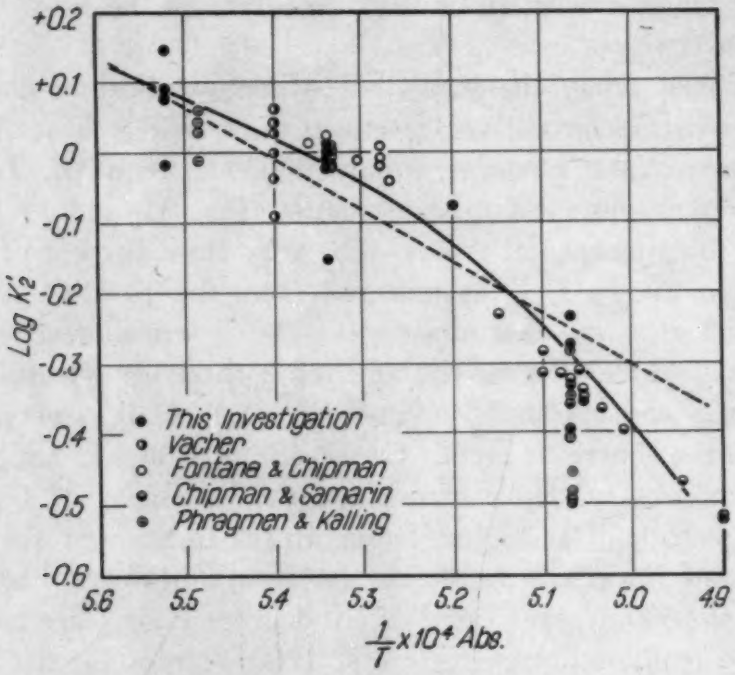

Fig. 13—Comparison of Values of $K'_2 = p_{CO_2}/p_{CO} \times \%\ O$ at Low Carbon Contents With Results of Other Investigators, Including Calculations From the Iron-Hydrogen-Oxygen System.

sponding dissociation constant in the range 1700 to 2100 degrees Kelvin

$$H_2\ (g) + \tfrac{1}{2}\ O_2\ (g) = H_2O\ (g);\ \Delta F^\circ = -60{,}200 + 13.97T \quad [23]$$
$$K = p_{H_2O} / (p_{H_2} \times p\tfrac{1}{2}O_2);\ \log K = +13{,}160 - 3.053/T$$

Similarly for carbon dioxide

$$CO\ (g) + \tfrac{1}{2}\ O_2\ (g) = CO_2\ (g);\ \Delta F^\circ = -66{,}550 + 20.14T \quad [24]$$
$$\log K = 14{,}546/T - 4.403$$

The equilibrium of solid iron, liquid iron oxide, steam and hydrogen was studied by the authors (38) at temperatures up to the melting point of iron. Their results were expressed as follows:

$$FeO\ (l) + H_2\ (g) = Fe\ (s) + H_2O\ (g);\ \log K = \frac{1583}{T} - 1.021 \quad [25]$$

The result of combining this expression with Equation 23 is shown in the solid portion of line IV in Fig. 14. The dotted portion of this

line represents an extrapolation to higher temperatures obtained by increasing the slope to include the heat of fusion of iron. This represents the best estimate from low temperature data that is possible at the present time. Line I shows the result of a similar estimate made by Chipman and Murphy (41) in 1933.

A calculation based upon equilibrium measurements on liquid iron, steam and hydrogen was also published (23), (42) in 1933. This is represented by line II and the then existing discrepancy is indicated by the offset A. This calculation involved a knowledge of the solubility of iron oxide in liquid iron and for this purpose the data of Herty (6) and co-workers and of Körber (40) were combined in the equation

$$FeO\ (1) = Fe\ (1) + O\ (\text{in Fe});\ \log \%\ O = -\ 5750/T + 2.548 \qquad [26]$$

When this is combined with the steam-hydrogen-liquid iron equilibrium data of Chipman and Samarin, and simultaneously with Equation 23, the result is the following expression:

$$FeO\ (1) = Fe\ (1) + \tfrac{1}{2}\ O_2\ (g);\ \log K = -\ 8708/T + 0.751 \qquad [27]$$

from which the oxygen pressures plotted in line III are obtained.

The data represented in Fig. 13 may now be used to recalculate the oxygen pressure of the saturated metal. The combination of Equations 22, 24 and 26 gives us the following equation which is plotted as line V:

$$FeO\ (1) = Fe\ (1) + \tfrac{1}{2}\ O_2;\ \log K = -\ 12976/T + 2.991 \qquad [28]$$

All of the above calculations have involved the older data on the solubility of iron oxide in liquid iron. More recently a new series of solubility measurements has been carried out by Fetters and Chipman (25) whose results are expressed as follows:

$$FeO\ (1) = Fe\ (1) + O\ (\text{in Fe});\ \log \%\ O = -\ 4860/T + 1.935 \qquad [29]$$

This equation, combined with Equations 21 and 24, provides the best estimate of the oxygen pressure that can be made at the present time. This is shown by the curved line VI of Fig. 14. The reasons for the curvature and for the deviation from line IV must be left as questions to be answered by future, more precise investigations.

Solubility of Carbon Monoxide in Liquid Iron—From the purely thermodynamic viewpoint the foregoing equations and graphs representing equilibrium constants and activity coefficients adequately summarize the available information on the system liquid iron-carbon oxides. They provide no insight into the molecular nature of the molten iron solution and are independent of any assumptions regarding it. No explanation has been offered to account for the large effect

of carbon upon the activity of oxygen and thermodynamics requires no explanation. It may be shown, however, that the simple assumption that carbon monoxide is soluble as such in the liquid metal provides at once the explanation of the low activity coefficient of oxygen and of the variability of K_2' and K_3' and at the same time permits a considerable simplification in the thermodynamic treatment of the results.

In most of the literature on the chemistry of steelmaking, the assumption has been made, explicitly or tacitly, that all of the oxygen in unkilled steel is in solution as FeO. In the following discussion, however, it will be considered that part of it is CO, and the rest

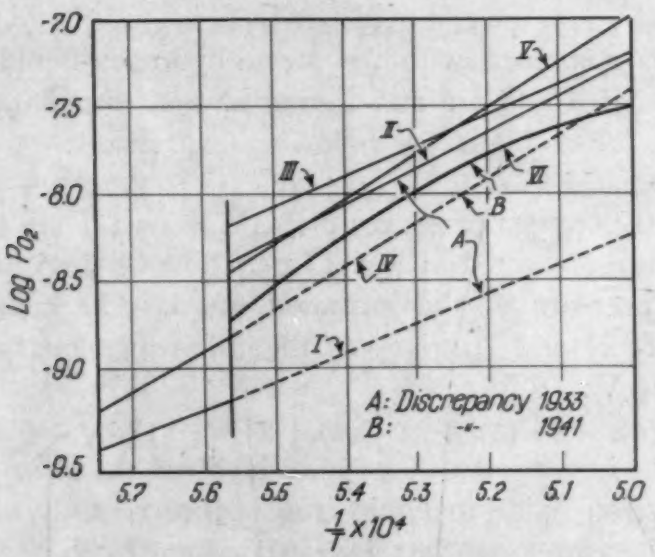

Fig. 14—Oxygen Pressure of Liquid Iron Oxide in Equilibrium With Iron: I. Chipman and Murphy, 1933 (Low Temperature); II. Chipman, 1933; III. Chipman and Samarin, 1937; IV. Chipman and Marshall, 1940 (Low Temperature); V. Data of This Paper (Eq. 22) Combined With Older Solubility Data; VI. Data of This Paper (Eq. 21) Combined With Solubility Data of Chipman and Fetters.

either simple O or dissolved FeO, there being no method of distinguishing between these two. Similarly carbon is in part CO, in part C, and in part Fe_3C or other carbides. The carbon-carbide equilibrium has been studied by Darken whose work was mentioned in connection with Fig. 8. Our data are not considered sufficiently precise to offer any improvement over his calculations but for concentrations up to 1 per cent carbon it will be considered unnecessary to distinguish between C and Fe_3C. For our purposes, then, carbon is in solution as C and as CO, the latter being much smaller than

the former except at low carbon contents where it has already been noted that the activity of carbon is depressed.

The experimental data have provided material for much calculation on the actual solubility of carbon monoxide. Without burdening the reader with the details of these computations, it may be reported simply that in all cases the result at 1 atmosphere pressure of CO fell between 0.002 and 0.004 per cent. A convenient average was found to be 0.0028 per cent, corresponding to 0.0012 per cent carbon and 0.0016 per cent oxygen at 1540 degrees Cent. (2805 degrees Fahr.) and 1 atmosphere. Like other simple gas solubilities, this one is directly proportional to the partial pressure of carbon monoxide.

The carbon and oxygen which are dissolved as such or as carbide or oxide are, respectively, per cent carbon — .0012 p_{co} and per cent oxygen — .0016 p_{co}. New equilibrium constants may now be written involving only these portions of the carbon and oxygen, for example:

$$K_3^o = \frac{p_{co}}{(\%\,C - .0012\,p_{co})\,(\%\,O - .0016\,p_{co})}$$

The data of Fig. 7 lead to an average value of $K_3^o = 540$ at 1540 degrees Cent. (2805 degrees Fahr.). From this constant it is now possible to compute the oxygen content of the metal at any specified values of total carbon and partial pressure of carbon monoxide. The results of this calculation for carbon contents up to 1 per cent and for 1, 5, 10 and 20 atmospheres total pressure are shown in the "calculated" columns of Table XVI. The "observed" columns contain the product % C × % O × 10^4 as obtained directly from the curve of Fig. 7 which is used simply as a method for smoothing and interpolating the experimental results. Values of K_3' corresponding to the "calculated" total oxygen are also included in the table. Comparison with Fig. 7 shows excellent agreement but the calculated values demonstrate additionally that K_3' passes through a maximum at about 0.03 to 0.04 per cent carbon, falling to substantially lower values below 0.03 per cent. The explanation of this effect, which was suspected also in connection with K_1', is now apparent. The lower the carbon content the greater the fraction of it which is tied up as CO and it is only at higher percentages, where this fraction becomes inappreciable, that the activity coefficient can approach unity. The curve of Fig. 8 is therefore not strictly accurate when the metal

contains oxygen but should bend downward at the low carbon end. As we have remarked before, however, the precision of our data is not sufficient to determine the exact form of this line.

Summary

An experimental method has been developed for the study of reactions of liquid metals with gases at pressures up to 20 atmospheres. The equilibria between carbon and oxygen in liquid iron and carbon monoxide and dioxide in the gas phase has been studied in the range 1540 to 1700 degrees Cent. (2805 to 3090 degrees Fahr.).

Equilibrium constants have been determined for the following reactions:

$$C\ (\text{in Fe}) + CO_2\ (g) = 2\ CO\ (g);\ K_1 = p^2_{CO}/(p_{CO_2} \times a_C) \quad (1)$$

$$O\ (\text{in Fe}) + CO\ (g) = CO_2\ (g);\ K_2 = p_{CO_2}/(p_{CO} \times a_O) \quad (2)$$

$$C\ (\text{in Fe}) + O\ (\text{in Fe}) = CO\ (g);\ K_3 = p_{CO}/(a_C \times a_O) \quad (3)$$

When per cent by weight is substituted for activity of carbon and oxygen, the resulting constants (designated K'_1, etc.) are not constant but depend upon carbon content. The activity coefficient of carbon, defined as $f_c = a_c/\%$ C increases, the corresponding coefficient for oxygen decreases with increasing carbon content. (Figs. 8 and 9.)

Using these activity coefficients, the values of the constants at 1540 degrees Cent. (2805 degrees Fahr.) are, respectively, 430, 1.21 and 512.

The effect of temperature upon the constants at low percentages of carbon (below 0.02 per cent) is given by the following equations:

$$\log K'_1 = -5778/T + 5.784$$

$$\log K'_2 = 7200/T - 3.855 - 9 \times 10^{-6}\ (T - 1873)^2$$

$$\log K'_3 = 1860/T + 1.643$$

Table XVI

Comparison of Observed and Calculated Carbon-Oxygen Product at 1540 Degrees Cent.

Observed values are from K_3' in Fig. 7; calculated values are based on assumed CO solubility. Values % C × % O × 10^4

$p_{CO} + p_{CO_2} =$		1 Atm.		5 Atm.		10 Atm.		20 Atm.	
Per Cent C	K_3'	Obs.	Calc.	Obs.	Calc.	Obs.	Calc.	Obs.	Calc.
0.02	500	18	18.0	...	...	...	...	...	...
0.03	508	18	18.3	76	75	...	...	...	...
0.05	504	19	19.0	84	82	149	...	...	...
0.10	493	20	19.8	94	91	173	168	307	296
0.20	458	22	21.6	104	106	199	200	368	358
0.50	382	26	26.0	127	129	249	252	479	480
1.0	293	34	34.0	172	170	340	335	665	660

Table XVII

Summary of Experimental Results at 1540 Degrees Cent.

Gas and metal compositions at indicated pressures of CO + CO_2, obtained from K_1 and K_3

$p_{CO} + p_{CO_2} = 1$ Atm.		5 Atm.		10 Atm.		20 Atm.	
Per Cent C	Per Cent CO_2	Per Cent O	Per Cent CO_2	Per Cent O	Per Cent CO_2	Per Cent O	Per Cent CO_2	Per Cent O
0.02	10.0	0.090	....	.....	....	.....	....	.....
0.05	4.3	0.038	16.3	0.168	....	.....	....	.....
0.10	2.25	0.020	9.6	0.094	16.5	0.173	....	.....
0.20	1.15	0.011	5.28	0.051	9.6	0.100	16.5	0.184
0.50	0.46	0.0052	2.24	0.025	4.3	0.050	8.0	0.096
1.00	0.23	0.0035	1.13	0.017	2.2	0.034	4.25	0.066
1.5	0.14	0.003	0.71	0.015	1.43	0.029	2.75	0.057
2.0	0.10	0.0026	0.48	0.013	0.94	0.026	1.85	0.052

Values of the constants compare rather closely with results of other investigators and, in the case of K'_2, they correlate well with data on the iron-hydrogen-oxygen system.

The product, per cent carbon × per cent oxygen, depends upon temperature, pressure and carbon content. At 1 atmosphere pressure of CO plus CO_2 and 1540 degrees Cent. (2805 degrees Fahr.), it increases from 0.0018 at 0.02 per cent to 0.0034 at 1 per cent carbon.

The effects of pressure and of carbon content may be accounted for by the assumption that carbon monoxide is soluble as such to the extent of about 0.0028 per cent.

A general summary of the experimental results, interpolated to round percentages of carbon, is given in Table XVII.

Acknowledgments

The authors wish to express their thanks to Mr. D. L. Guernsey for carrying out a large number of the chemical analyses.

To Professor E. R. Gilliland and his associates for their assistance and the use of their equipment in the preparation of carbon monoxide.

To the National Open Hearth Committee for its award of the Open Hearth Fellowship for the year 1940-41.

Bibliography

1. Le Chatelier, "The Reduction of Iron Oxides," *Revue de Met.* Vol. 9, 1912, p. 513.
2. Styri, "Flaky Fractures and Their Possible Elimination," *Chemistry and Metallurgy,* Vol. 20, 1919, p. 478.

3. Styri, "Theory and Practice of Steel Refining," *Journal,* Iron and Steel Institute, Vol. 108, 1923, p. 189.
4. Pierard, "Physical Chemistry of Steel Refining," *Revue de Met.,* Vol. 24, 1927, p. 41.
5. Tritton and Hansen, "Iron and Oxygen," *Journal,* Iron and Steel Institute, Vol. 110, No. 2, 1924, p. 70.
6. Herty and Associates, (a) "Solubility of FeO in Liquid Iron," Mining and Metallurgy Investigations, Carnegie Institute of Technology, Bulletin 34, 1927; (b) "Elimination of Metalloids in the Basic Open Hearth Furnace," *Transactions,* American Institute of Mining and Metallurgical Engineers, Vol. 73, 1926, p. 1079; (c) "Control of Iron Oxide in the Open Hearth," Mining and Metallurgical Investigations, Carnegie Institute of Technology, Bulletin 68, 1934; (d) "Chemical Equilibrium of Manganese, Carbon and Phosphorus in the Basic Open Hearth Process," *Transactions,* American Institute of Mining and Metallurgical Engineers, Vol. 73, 1926, p. 1107.
7. Feild, "The Rate of Carbon Elimination and Degree of Oxidization of the Metal Bath in the Basic Open Hearth," *Transactions,* American Institute of Mining and Metallurgical Engineers, Iron and Steel Division, 114, 1928.
8. Kinzel and Egan, "Experimental Data on the Equilibrium of the System Iron Oxide-Carbon in Molten Iron," *Transactions,* American Institute of Mining and Metallurgical Engineers, Iron & Steel Division, 304, 1929.
9. Larsen, "Origin and Effect of Inclusions in Steel," *Metals and Alloys,* Vol. 1, 1930, p. 763.
10. Eastman and Evans, "Equilibria Involving Oxides of Iron," *Journal,* American Chemical Society, Vol. 46, 1924, p. 888.
11. Eastman, "The Free Energy of Water, Carbon Monoxide and Carbon Dioxide," U. S. Bureau of Mines Circular 6125, 1929.
12. Round Table, "The Physical Chemistry of Steel Making", *Transactions.* American Institute of Mining and Metallurgical Engineers, Iron and Steel Division, Vol. 84, 1929, p. 233.
13. Jette, "The Open Hearth Process as a Problem in Chemical Kinetics," *Transactions,* American Institute of Mining and Metallurgical Engineers, Vol. 95, 1931, p. 80.
14. Vacher and Hamilton, "The Carbon-Oxygen Equilibrium in Liquid Iron," *Transactions,* American Institute of Mining and Metallurgical Engineers, Vol. 95, 1931, p. 124.
15. Vacher, "The System Liquid Iron-Carbon Oxides," Bureau of Standards, *Journal of Research,* Vol. 11, 1933. p. 541.
16. McCutcheon and Chipman, "Evolution of Gases from Rimming Steel Ingots," *Transactions,* American Institute of Mining and Metallurgical Engineers, Iron and Steel Division, 1938, p. 206.
17. Chipman, "Effect of Slag Composition on Oxygen, Carbon and Sulphur in the Bath," American Institute of Mining and Metallurgical Engineers, *Open Hearth Proceedings,* 1937, p. 110.
18. McCutcheon, "Bath Samples for Oxygen Determination," American Institute of Mining and Metallurgical Engineering, *Open Hearth Proceedings,* 1938, p. 143; *Transactions,* American Institute of Mining and Metallurgical Engineers, Iron and Steel Division, 1940, p. 133.
19. Chipman, "Studies on Slag Equilibria," American Institute of Mining and Metallurgical Engineers, *Open Hearth Proceedings,* 1939.
20. Fetters and Chipman, "Correlation with Oxygen Content in Slag-Metal Studies," American Institute of Mining and Metallurgical Engineers, *Open Hearth Proceedings,* 1940, p. 208-215.
21. Schenck, Reiss and Bruggeman, "Velocity and Equilibrium Constants of Carbon Reduction, *"Zeit. Elektrochem.,* Vol. 38, 1932, p. 562.

22. Kalling and Rudburg, "Refining Process in the Acid Open Hearth Furnace," *Jernkontorets,* Vol. 121, 1937, p. 93.
23. Chipman, "Equilibrium and the Reaction of Water Vapor with Liquid Iron," *Journal,* American Chemical Society, Vol. 55, 1933, p. 313.
24. "Pyrometric Practice," Bureau of Standards Technical Paper 170, 1921.
25. Chipman and Fetters, "Solubility of Iron Oxide in Liquid Iron," American Society for Metals, 1941, Preprint 54.
26. Thompson and Mallett, "Preparation of Crucibles of Special Refractories by Slip-Casting," Bureau of Standards, *Journal of Research,* Vol. 23, 1939, p. 319.
27. Gas Engineer's Handbook, McGraw-Hill, 1st Edition, 1934.
28. Neumann and Kohler, *Zeit. Elektrochem.,* Vol. 34, 1928, p. 218.
29. Emmett and Shultz, *Journal,* American Chemical Society, Vol. 52, 1930, p. 1782 and 4268.
30. Darken, "Equilibrium in Liquid Iron with Carbon and Silicon," *Transactions,* American Institute of Mining and Metallurgical Engineers, Vol. 140, 1940, p. 204.
31. Fontana and Chipman, "Equilibrium in the Reaction of Hydrogen with Iron Oxide in Liquid Iron at 1600 Degrees Cent." TRANSACTIONS, American Society for Metals, Vol. 24, 1936, p. 313.
32. Chipman and Samarin, "Effect of Temperature on the Interaction of Gases with Liquid Steel," *Transactions,* American Institute of Mining and Metallurgical Engineers, Iron and Steel Division, 1937, p. 331.
33. Gordon, "The Free Energy, Entropy and Heat Capacity of Steam," *Journal of Chemical Physics,* Vol. 2, 1934, p. 65.
34. Kassel: "Thermodynamic Functions of Nitrous Oxide and Carbon Dioxide," *Journal,* American Chemical Society, Vol. 56, 1934, p. 1838.
35. Johnson and Davis, "Entropy and Heat Capacity of Carbon Monoxide and Nitrogen from Near 0 to 5000° K," *Journal,* American Chemical Society, Vol. 56, 1934, p. 271.
36. Davis and Johnson, "The Heat Capacity, Entropy and Total Energy of Hydrogen at High Temperatures," *Journal,* American Chemical Society, Vol. 56, 1934, p. 1045.
37. Rossini, "Heat and Free Energy of Formation of Water and Carbon Monoxide," Bureau of Standards, *Journal of Research,* Vol. 22, 1939, p. 407.
38. Chipman and Marshall, "The Equilibrium $FeO + H_2 = Fe + H_2O$ at Temperatures up to the Melting Point of Iron," *Journal,* American Chemical Society, Vol. 62, 1940, p. 299.
39. Leiber "Reactions of the Basic Open Hearth Furnace," *Mitt.,* Kaiser Wilhelm Inst. für Eisenforschung, Vol. 18, 1936, p. 135.
40. Körber, "Investigations on the Behavior of Manganese in the Steel Making Process," *Stahl und Eisen,* Vol. 52, 1932, p. 133.
41. Chipman and Murphy, "The Free Energy of Iron Oxides," *Industrial and Engineering Chemistry,* Vol. 25, 1933, p. 319.
42. Chipman, "Application of Thermodynamics to the Deoxidation of Liquid Steel," TRANSACTIONS, American Society for Metals, Vol. 22, 1934, p. 385.
43. Phragmén and Kalling, "Influence of Temperature on the Equilibrium Between Carbon and Oxygen in Steel and in a Gas Phase," *Jernkontorets Annaler,* Vol. 123, 1939, p. 199.

DISCUSSION

Written Discussion: By H. A. Schwartz, manager of research, National Malleable and Steel Castings Co., Cleveland.

For the sake of clarifying his own understanding, one is prompted to ask

a question concerning the interpretation which Messrs. Marshall and Chipman place upon their own publication.

In the last two paragraphs of their summary the authors apparently decide that it is unnecessary to consider the possibility that the carbon in solution in iron may be iron carbide, partially dissociated into its elements. Earlier in the paper they have alluded to Darken's conclusions on the latter subject and say that their own data are not such as to warrant any particular criticism of Darken's conclusions. Is one incorrect in believing that their final conclusion with regard to the change in the equilibrium product with change in carbon is that there is no evidence of dissolved iron carbide participating in the explanation?

This writer would appreciate as explicit a statement as possible on this particular portion of the paper.

Written Discussion: By Frank G. Norris, metallurgist, Wheeling Steel Corp., Steubenville, Ohio.

The authors, the A. S. M. and the Open-Hearth Committee of the American Institute of Mining and Metallurgical Engineers are to be congratulated for the excellent results of this investigation and for the co-operation which made possible the determination and publication of these results. The first part of the paper is the modest account of how one obstacle after another was overcome. The pioneer work in the preparation and analysis of the gas and in the construction of a furnace in which the atmosphere can be controlled at high pressures may be looked to as the forerunner of many more investigations along similar lines. It is fitting that the presentation of the results is in a manner that is worthy of their importance and the American Society for Metals deserves special thanks for publishing the numerous figures and for including derived as well as original data in the many tables. The results are given in mathematical form, which is called for because of their theoretical importance, and in figures and derived tables, the clarity of which is justified by their practical importance. It appears that this is a difficult piece of work well done and that there is no question of the results within the conditions of the experiment. The possible application to other conditions remains to be done.

In view of their investigation on the effect of pressure, I would like to have the authors' comment on the suppression of gas evolution in keyed and capped steel in bottlenecked molds. Knowing (or for purposes of calculation assuming) the carbon, oxygen and temperature of the steel going into the molds is it possible to estimate the pressure required to stop gas evolution, and can such pressures reasonably be expected?

Does the total oxygen content of the metal as determined from the alumina content of aluminum-killed samples taken in a covered mold include oxygen present as CO? If so it seems that the results of this method are more properly reported as oxygen as is done in this paper than as FeO.

Several years ago one of the authors stated that he had never obtained any data of sufficient accuracy that the method of least squares yielded any better representation of the relation than any of several other lines that could be guessed in. Therefore in this respect also can this paper be regarded as a milestone indicating progress in the use of precise methods in studying data on ferrous solutions.

Written Discussion: By Karl Fetters, assistant professor of metallurgy, Carnegie Institute of Technology, Pittsburgh.

The authors are to be commended for a valuable contribution to our understanding of the scientific aspects of steelmaking processes and on the manner in which they solved their laboratory difficulties. The basic reaction between carbon and oxygen is fundamental to all steelmaking processes and up to the present time had not been subjected to careful laboratory study over a wide

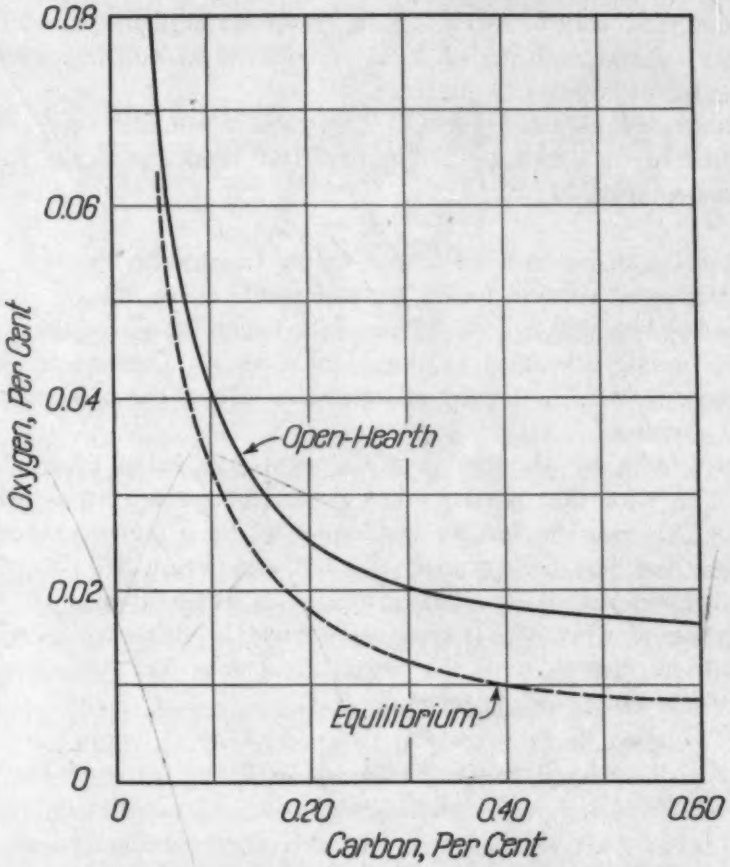

Fig. 1A—Comparison of Open-Hearth Carbon-Oxygen Relations with Equilibrium Values.

range of compositions, temperatures, and processes. The present findings will aid greatly in further studies of steelmaking reactions.

Mention might be made at this time of a few points which are of interest in connection with this work:

Previous work by Fetters and Chipman[1] based on a statistical study of open-hearth slag and metal samples showed that the carbon-oxygen relation in the open-hearth could be expressed by the equation

$$C \times O = 0.00111\ C + 0.00276$$

This line would be situated about midway between the lines for 1 and for 3 atmospheres shown by Marshall and Chipman's Fig. 3 where they show a plot

[1]K. Fetters and J. Chipman, *Transactions*, American Institute of Mining and Metallurgical Engineers, Vol. 140, 1940, p. 170-203.

of the carbon oxygen product vs. the per cent carbon. Fig. 1A shows the carbon-oxygen relation for the open-hearth data for comparison with the equilibrium data. In this figure a correction has been made to bring the equilibrium relation to 1600 degrees Cent. (2910 degrees Fahr.) and to about 1.5 atmospheres pressure of CO which would correspond to the pressure existing near the bottom of the bath in the open-hearth—a position which Larsen[2] has postulated as that at which bubbles of CO are formed. The open hearth results are somewhat higher than the equilibrium values. This higher value of the constant than the equilibrium may be ascribed to two causes: first, the transfer of oxygen from the slag, and second, the physical restrictions of bubble formation which result in higher apparent CO pressure.

The authors mention a lower CO/CO_2 ratio when their gas samples were taken after the furnace cooled. Might this have been due to the shift in equilibrium of the reaction (1)

$$C + CO_2 = 2CO$$

with deposit of small amounts of carbon in the furnace cavity.

A few fractional vacuum fusion samples would be of interest to answer the authors' question regarding the aluminum-killed samples where they ask, "First, is all the iron oxide converted to aluminum oxide?" Data to be published in the near future by Dr. G. Derge indicates that all of the oxygen may not be converted to alumina.

These new data by Marshall and Chipman now bring the carbon-oxygen reaction in line with that of the other deoxidation reactions which are also exothermic. This may be further confirmed by the common experience with rimming steel that has been poured too hot and which fails to rim, but as soon as the temperature drops rimming begins in usual fashion.

Continuation of work of the type represented by this carbon-oxygen paper will eventually furnish us with the fundamental data for a complete scientific knowledge of the reactions of steelmaking.

Oral Discussion

L. S. DARKEN:[3] It seems to me that this very excellent paper answers a great number of questions which have been in our minds concerning the fundamentals of the chemistry of the open-hearth.

The outstanding feature is the change of the equilibrium carbon-oxygen product with per cent carbon. It is surprising to find such marked departure from the behavior of ideal and dilute solutions. The authors have shown clearly that it is mainly the oxygen rather than the carbon which is responsible for this departure.

In this connection it is of interest to note that carbon has the opposite effect on sulphur in iron—i.e., carbon markedly decreases the activity of oxygen but increases even more markedly the activity of sulphur. Clearly the effect of carbon in increasing the activity of sulphur cannot be interpreted in terms of compound formation. Thus, although the hypothesis of compound molecules

[2]B. M. Larsen, *Transactions*, American Institute of Mining and Metallurgical Engineers, Vol. 141, 1941, p. 67-83.

[3]United States Steel Corp., Research Laboratory, Kearny, N. J.

(such as CO in this case) in molten steel is useful in some cases, this method of attack is not of universal applicability to the physical chemistry of molten iron and steel.

There appears to be a slight inconsistency in the interpretation of the data relative to the three "constants" K'_1, K'_2 and K'_3. From the definitions (Equations 4, 5, and 6), it is apparent that K'_3 is identically equal to the product of K'_1 and K'_2. It is shown (Figs. 11 and 13) that the plot log K'_2 vs. $\frac{1}{T}$ is not linear. Yet in Figs. 10 and 12 and Equations 13 and 14, log K'_1 and log K'_2 are represented as linear functions of $\frac{1}{T}$ (all at low per cent carbon). Clearly at least one of these must also be a curved function of $\frac{1}{T}$. In other words the given relations do not exactly satisfy the necessary condition log K'_1 + log K'_2 = log K'_3.

Authors' Reply

This work, of course, is all directed toward a better understanding of the open hearth process and other processes of steelmaking, so I am very glad to have Dr. Fetters' comparison with the open-hearth data. I noticed in the comparison that whereas the curves appear to depart farther from each other as the carbon content increases, nevertheless, they are essentially displaced by a constant amount vertically.

It appears that in the open hearth there is more or less constant excess of oxygen in the metal. Dr. Fetters' curves appear to depart further, but if you compare vertically, you find an offset of slightly less than 0.01 per cent oxygen at all carbon levels. There is a constant, rather than an increasing difference between the two curves.

Regarding the difference between the effect of carbon on the activity of sulphur and its effect on the activity of oxygen, I think possibly that is associated with the fact that you can get a lot more sulphur into iron than you can oxygen. We are very limited as to the amount of oxygen in solution, especially in the presence of carbon. Carbon, of course, has much less effect on the amount of sulphur held in the iron than it has in the case of oxygen. If carbon affects the activity of sulphur in an upward direction, it may also have a similar tendency to increase the activity of that part of the oxygen which is present as other than CO. The fact that we get an over-all effect in the downward direction may require that instead of 0.0028 for the solubility of CO we raise the estimate to a slightly higher figure; that is, we have two effects working in opposite directions. If there is a raising effect similar to that of sulphur, the lowering effect due to CO must be even slightly greater than we had calculated.

The inconsistency which Dr. Darken mentions would be removed by drawing a slightly curved line in Fig. 10 (concave upward). It is doubtful if the precision warrants anything more than the straight line but a curved line would actually fit the data better than the "least squares" line drawn.

In reply to Mr. Norris' question regarding capped and keyed steel, it may be pointed out that the pressure developed during solidification may exceed

greatly the equilibrium pressure due to carbon and oxygen in the liquid metal at the time of casting. Both carbon and oxygen have a strong tendency to segregate and if evolution is prevented their concentration in the molten interior of the ingot increases greatly, especially near the solidifying interface. A study of segregation phenomena in ingots of this type might make it possible to estimate the pressures developed.

All the evidence we have seen indicates that the alumina content of aluminum-killed samples represents the total oxygen content of the bath including FeO, CO, and the oxides of manganese and silicon if present. The practice of reporting this as FeO was based upon the assumption that other oxides in solution were negligible. Since this assumption can no longer be held, it is suggested that oxygen analyses be reported in terms of percentage of oxygen, using subscripts if necessary to distinguish between various oxides, as O_{FeO} and O_{CO}. Attention is also called to the common error of calling oxygen "O_2"; this symbol correctly denotes only gaseous oxygen.

Dr. Schwartz has requested a more explicit statement regarding carbon and carbide in the liquid iron. It should be pointed out that in order to draw any distinction between carbon and a partly dissociated carbide in low or medium-carbon melts, a far greater experimental precision would be required than we were able to obtain. The general trend of the data is in the direction required by the presence of some dissolved carbide but quantitative conclusions cannot be drawn. Our data are not considered sufficiently precise to offer any improvement over Darken's calculations but for concentrations up to 1 per cent carbon it is considered unnecessary to distinguish between C and Fe_3C.

APPLICATION OF OSCILLOGRAPH TO DETERMINATION OF COOLING RATES OF QUENCHED STEELS

By Charles R. Austin, R. M. Allen and W. G. Van Note

Abstract

A method is described for recording rapid cooling rates of quenched steels by use of an oscillograph, operated by a thermocouple e.m.f. through a cascade connected two-stage direct current amplifier. The complete assembly includes a gas quenching unit, a thermocouple amplifier circuit, a low frequency oscillograph and a recording camera.

A brief description is given of the basic principles and calibration of the oscillograph in terms of millivoltage (or temperature) and time, and hence of the method of obtaining the cooling curve of a quenched sample. The application to the determination of the critical cooling velocity of a steel is then outlined.

Since the procedures differ markedly from any of those employed by other investigators, and because of the special technique and problems involved in the application of a direct current amplifier oscillograph unit, precise information is given in an appendix on the exact modus operandi followed.

MUCH attention has been given in recent years to the development and study of various tests which permit an evaluation of the hardenability of carbon and alloy steels. These tests have been discussed with a view to the formulation of some concept which may serve as a relative measure of reaction to quenching. The terms for consideration of quenching results have included: quenching media; size and shape of test sample, hardness penetration as indicated by the shape of the hardness-distance from quenched surface curve as well as by the area under this curve, and by the distance of penetration to some arbitrarily chosen hardness value or to a limiting region where the microstructure reveals either complete suppression of the

A paper presented before the Twenty-third Annual Convention of the Society held in Philadelphia, October 20 to 24, 1941. Of the authors, C. R. Austin is professor of metallurgy, Pennsylvania State College, State College, Pa., R. M. Allen is metallurgist, metallurgical laboratory, Carnegie-Illinois Steel Corp., Homestead, Pa., and W. G. Van Note is associate professor of chemical engineering, North Carolina State College, Raleigh, N. C. Manuscript received May 26, 1940.

pearlite inversion or some arbitrarily chosen pearlite content in a martensitic matrix. Details of the viewpoints of several authorities may be found in recent additions to the technical literature on this subject (1).[1] A new wedge test which appears to have considerable merit has also been outlined by Luerssen (2). A similar test has been discussed by Spring and Desmond (3).

However, the fundamental basis of all hardenability tests is dependent on factors which control the "critical cooling velocity" of a steel, whether this velocity be defined as that rate of cooling which must be exceeded to completely suppress the formation of pearlite, or in a modified form so as to represent that cooling rate which will yield a structure consisting of 50 per cent pearlite and 50 per cent martensite. This latter state possibly is better suited to experimental investigation and is critical in terms of rate of elapsed time as brought out clearly in discussion of the subject by Grossmann (1a).

Accordingly, it seemed to the authors that the development of a simple tool merited consideration, whereby predetermined cooling rates could be applied to small steel samples, and the resultant time-temperature curves indicated and recorded. Furthermore, such an instrument was required in the authors' laboratory to permit a study of the factors controlling critical cooling velocities of a series of pure iron-carbon alloys containing varying small amounts of a third added element.

In 1904 Le Chatelier (4), recognizing the profound effect of rate of cooling on the resultant properties of steels, decided that time-temperature curves would be of value in studying the reactions of steels to quenching. He developed a method using a thermocouple in series with a string galvanometer and thereby recorded the rapid changes of e.m.f. during quenching. This method has been used since that time by many investigators (5), and satisfactory results have been reported in most cases. The response, sensitivity, and ease of operation of the string type galvanometer is, however, limited and an instrument, capable of improving any of these qualities, merits investigation. With this thought in mind it was decided that the cathode-ray oscillograph could be adapted to the problem of recording time-temperature curves. The response of this instrument to voltage changes is instantaneous, and its deflection per volt can be calibrated with a good degree of accuracy. Its main advantage over

[1]The figures appearing in parentheses refer to the bibliography appended to this paper.

the string galvanometer lies in the accurately controlled time axis which is an alternating current of suitable wave form having a wide range of frequencies and which is used to time the phenomenon being analyzed. However, the oscillograph will not respond to the small e.m.f. generated by a thermocouple and an amplifier is necessary to bring these minute voltages into the operating range of the instrument. An amplifier has been designed which adequately satisfies the requirements for the oscillograph used and a detailed description of the circuit and operation will be included in the report. Along with this information there will be outlined the method used to interpret the records, and an example of the correlation between various recorded cooling rates and the resultant microstructures will be discussed. Control of the cooling rates of the small steel specimens used was obtained by means of a gas quenching apparatus which was designed for the purpose. The equipment consists of:

1. A gas quenching unit which permits various but reproducible cooling rates of a metal specimen of suitable form and size. This equipment will be described in some detail.
2. A thermocouple amplifier circuit which permits the use of a cathode-ray oscillograph to follow the changes of an e.m.f. generated by a thermocouple.
3. An oscillograph which may indicate these changes on a fluorescent screen, in terms of time-voltage co-ordinates.
4. Suitable means of recording completely the changes observed on this fluorescent screen.

The Thermocouple Amplifier Circuit

The literature appears to afford little assistance in the development of a suitable stable circuit applicable to the amplification of thermocouple millivolts to voltages of the magnitude necessary to operate the standard type oscillograph, without changing from direct to alternating current. Ross Gunn (6) has recently described a regenerative direct current amplifier for the amplification of thermocouple electromotive forces but states that, in common with all amplifiers of this general type, it requires considerable attention. Accordingly, he concludes that this type of circuit is unsatisfactory.

The present authors, however, have somewhat simplified the problem by substituting a cascade connected two-stage direct current amplifier for the regenerative type described by Gunn. The circuit

affords simple and accurate control of the grid bias voltage in the first stage of the amplifier, which in turn permits the necessary control, in minute increments, of the grid voltage and hence of the output current. (See Fig. 1). This enables the initial amplification to be controlled accurately so that a reproducible starting current can be obtained for successive tests. With the input from the thermocouple varying from about 0 to 32 millivolts (0 to 770 degrees Cent.), it was observed that by starting with 0.5-milliampere output it was prac-

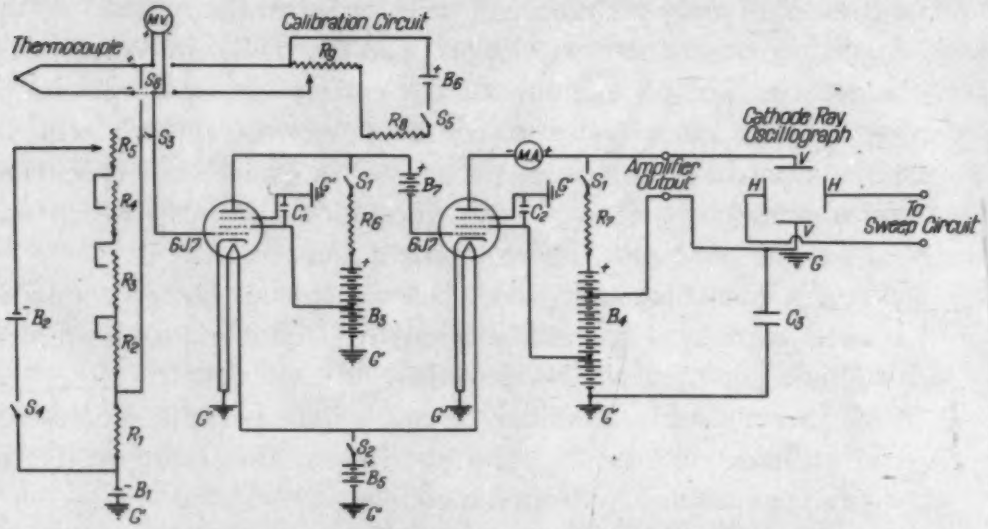

Fig. 1—Thermocouple Amplifier Circuit Diagram.

ticable to operate on the portion of the curve where the output current was approximately linear to the millivoltage input (Fig. 2).

The amplifier circuit designed for use in conjunction with a cathode-ray oscillograph is shown diagrammatically in Fig. 1. Instability of the output is the major difficulty encountered in using a vacuum tube circuit for direct amplification of a thermocouple e.m.f. This instability is related directly to the fundamental principle of the amplifier, namely, the high sensitivity of plate current to minute changes of e.m.f. on the control grid of the tube. If the thermocouple e.m.f. were the only voltage impressed on the grid of the tube the instability would tend to be small. However, another voltage must be impressed on the control grid along with that from the thermocouple. Disregarding any theoretical development of the operating characteristics of vacuum tubes, this additional voltage is necessary to bring the operation of the tube into the region of response where the output is approximately a linear function of the input. It is the small change or drift in this initial voltage on the

grid which causes the major portion of the instability. It is essential therefore that the grid be supplied with a voltage which will remain as close to a constant value as possible. The following method has been used to attain this condition.

A source which would give a nearly constant voltage was obtained by providing 2-volt storage cells at B_1 and B_2 in the grid control circuit (Fig. 1). The procedure which was then adopted for keeping the initial grid voltage constant is somewhat analogous to the standardization of a potentiometer. By shunting out the thermocouple circuit with S_3 the grid voltage will be made up of the components B_1 and the voltage drop across R_1, from battery B_2 which is controlled by the voltage dividers R_2 to R_5.

Using the output of the amplifier, measured by the milliammeter, as an indicator of the proper grid bias voltage and selecting 0.50 milliampere as a standard output current, the variable resistances R_2 to R_5 are adjusted to bring the output current to this value. If S_3 is now opened the voltage on the grid will consist of B_1 and the drop across R_1, in addition to whatever e.m.f. the thermocouple is generating. An equation for the grid voltage may be written

$$V_g = V_o + V_{TC} \quad \text{.....(I)}$$

where V_g is the total grid bias voltage consisting of the constant initial grid bias V_o and the added bias V_{TC} from the thermocouple. No difficulty has been encountered in maintaining V_o during required periods of tests, hence the recorded changes in the grid voltage V_g are dependent solely, and represent entirely, the changes in thermocouple e.m.f.

The selection of voltages and resistances in the plate circuits are dependent on the operating characteristics of the tubes. Accordingly the values of the battery voltages B_3 and B_4 and of the resistors R_6 and R_7 were chosen to provide the linear response already discussed in outlining the grid control circuit. A plot of the milliampere output of the amplifier and the millivolt input to the amplifier is shown in Fig. 2. It will be noted that the linearity, while not exact, is satisfactory for tracing thermocouple millivoltage changes from 0-32, or in terms of output, from 0.5 to 3.6 milliamperes. The relation might be stated only approximately by the following empirical equation.

$$\text{Output (milliamps)} = 0.5 + K.V_{TC} \quad \text{.....(II)}$$

However, on account of the apparent though small variance in K all data have been interpreted by use of the specific relationship shown in Fig. 2 and not by use of the approximate equation (II).

The Cathode Ray Oscillograph

The basic principle, on which the cathode-ray oscillograph is dependent, is that an electron beam will be deflected instantaneously when brought within the range of influence of an electrostatic field. Since the response is practically instantaneous and since the amount of deflection is dependent on the magnitude of the voltage drop between the plates, the characteristics of the instrument

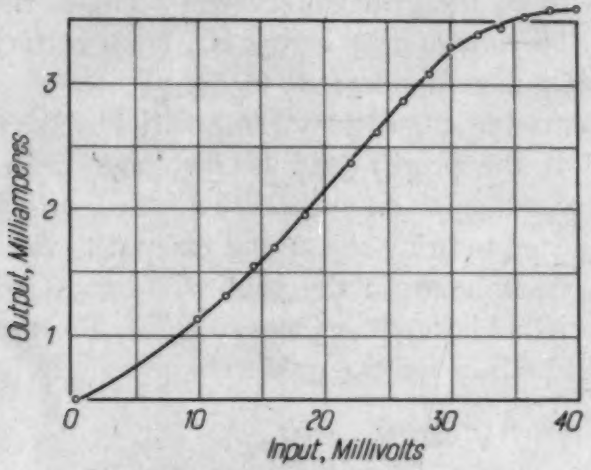

Fig. 2—Amplifier Input-Output Relationship.

immediately satisfy two criteria for recording rapid time-temperature curves: (a) rapidity of response to change in e.m.f., and (b) the calibration necessary for interpretation of the curves. The application of the cathode-ray oscillograph is further facilitated by the sweep circuit incorporated in the commercial instruments which provides a controllable oscillating voltage suitable for timing any voltage change phenomena. The wave form of this oscillating voltage is such that the beam moves across the screen at the controlled frequency, then instantly returns (in a time period less than 10^{-6} seconds) to the starting point, to begin the cycle anew. The pattern traced by the electron beam appears as a fluorescence on the screen. The procedure, therefore, consists of impressing the signal to be studied on the vertical plates and simultaneously impressing on the horizontal plates the sweep circuit voltage with the frequency controlled at the optimum value to give the most easily analyzed curve.

The signal to be studied in this problem originates across the resistor R_T in the amplifier circuit (Fig. 1). As shown in equation (II) a decrease in e.m.f. input will decrease the milliamperage output, that is, the voltage across the 70,000 ohm resistor R_T decreases as the e.m.f. decreases. The change in e.m.f. during the quench used is from 32 millivolts to 1 millivolt which causes a change from 3.6 to about 0.6 milliamperes output, under the particular grid

bias conditions previously outlined. This variation in current through R_7 results in a potential drop of about 200 volts, which provides a 4-inch vertical deflection of the electron beam over the screen. This voltage change is of course impressed on the vertical plates of the oscillograph. Concomitantly the sweep circuit output, impressed on the horizontal plates, is exerting a force which gives the horizontal component. The resultant of these two forces, which represents a complete cooling curve of the sample, is a series of lines traced on the screen, the number of which depends on the rate of change of e.m.f. as well as the frequency of the sweep circuit voltage.

A point particularly to be noted is the sensitivity of the circuit to extraneous alternating current fields in the laboratory. This may be observed by the presence of a 60-cycle A. C. ripple on the screen of the oscillograph, even though the amplifier output is theoretically direct current. These stray alternating current fields induce the ripple noted, and their effect may be rendered negligible by careful shielding of all equipment used in the operation of the amplifier, namely, by enclosing amplifier chassis and batteries in metal cases and by covering all leads with braided copper cable. When the shielding is connected to a common terminal G′ (Fig. 1) which is grounded through the condenser C_8, all extraneous A. C. effects are passed to earth. The condenser C_8 prevents shorting of about 290 volts from battery B_4 to the ground G while at the same time allowing alternating current to pass.

The thermocouple leads should be handled with care since they constitute a portion of the grid circuit, and it is desirable that the leads be shielded up to the bead or hot junction of the couple. Naturally all parts of the thermocouple must be insulated from this shielding material in order to prevent grounding. This precaution must be extended to the quenching medium and container, when liquid baths are used to control cooling rates.

With these necessary but relatively simple precautions the amplifier has been found to function quite satisfactorily, and the change of thermocouple e.m.f. can be impressed on the oscillograph, as an amplified voltage for analysis, to determine rate of cooling.

In order to record photographically the fast moving trace, a combination of high speed film and fairly fast camera lens is required. Since the characteristic radiation of the screen is essentially green, Eastman Ortho Portrait cut film, which has a high sensitivity for green radiation, was tried but gave poor results. Only moderate results were obtained on testing Eastman Ortho X film, despite the fact that this film has maximum green sensitivity of any commercial photographic emulsion. The film finally adopted was Eastman Super Panchro Press. This emulsion gave a relatively clear background whereby better contrast was obtained between the desired traces made by the electron beam during the quenching cycle, and the unavoidable fogging of the film from general light diffusion. An overdevelopment time of 3 or 4 minutes materially improved the contrast.

A camera having a f. 4.5 lens was used with 5 x 7 cut film for recording purposes, although a lens of lower f. value would have been markedly superior in terms of contrast.

Fig. 3 is a photograph which clearly shows the general arrangement of

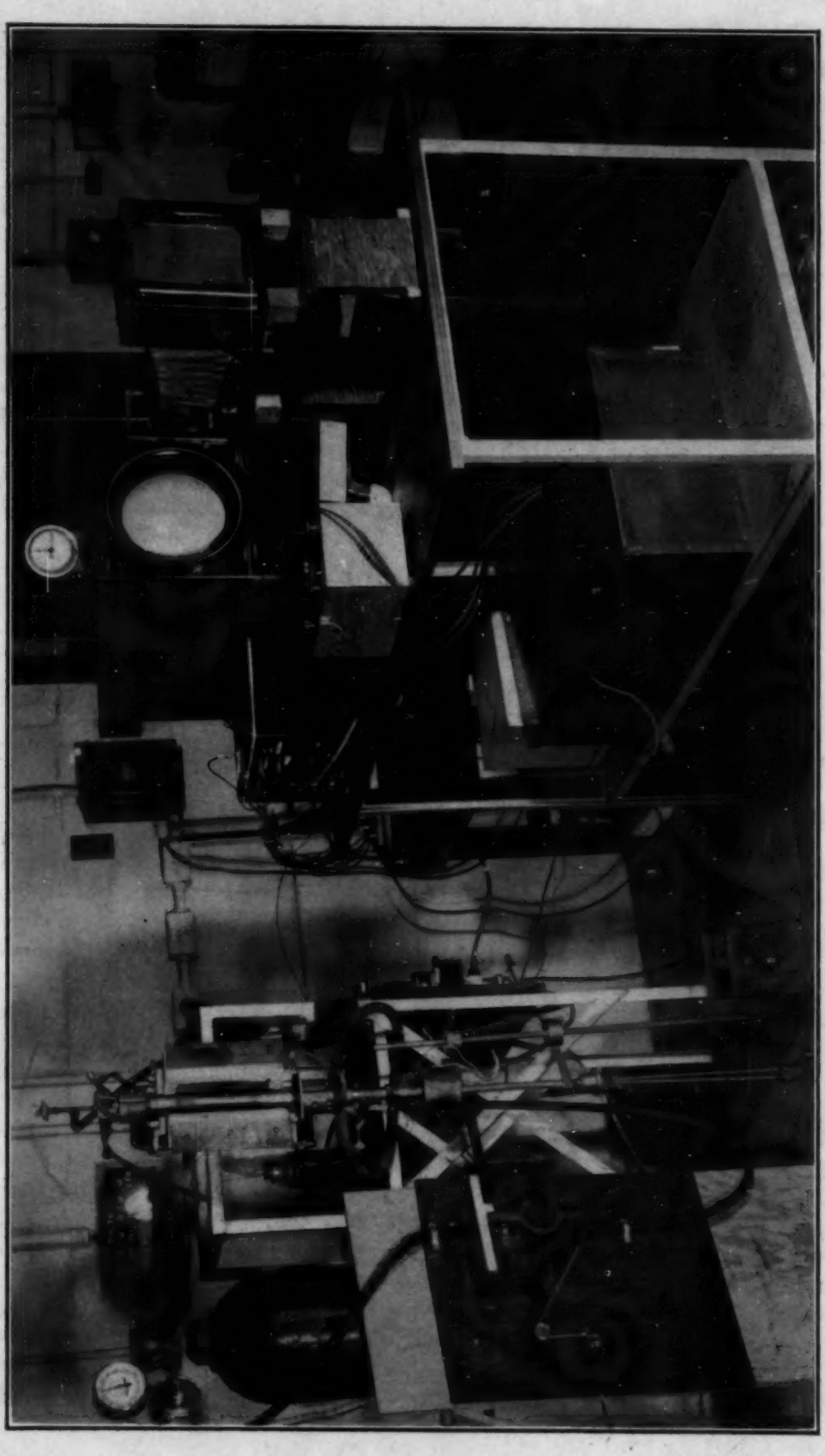

Fig. 3—Picture of the Complete Assembly, Showing the Camera and Oscillograph With Amplification Circuit, the Heating and Gas Quenching Chambers and Gas Cylinder With Tripper Control Mechanism.

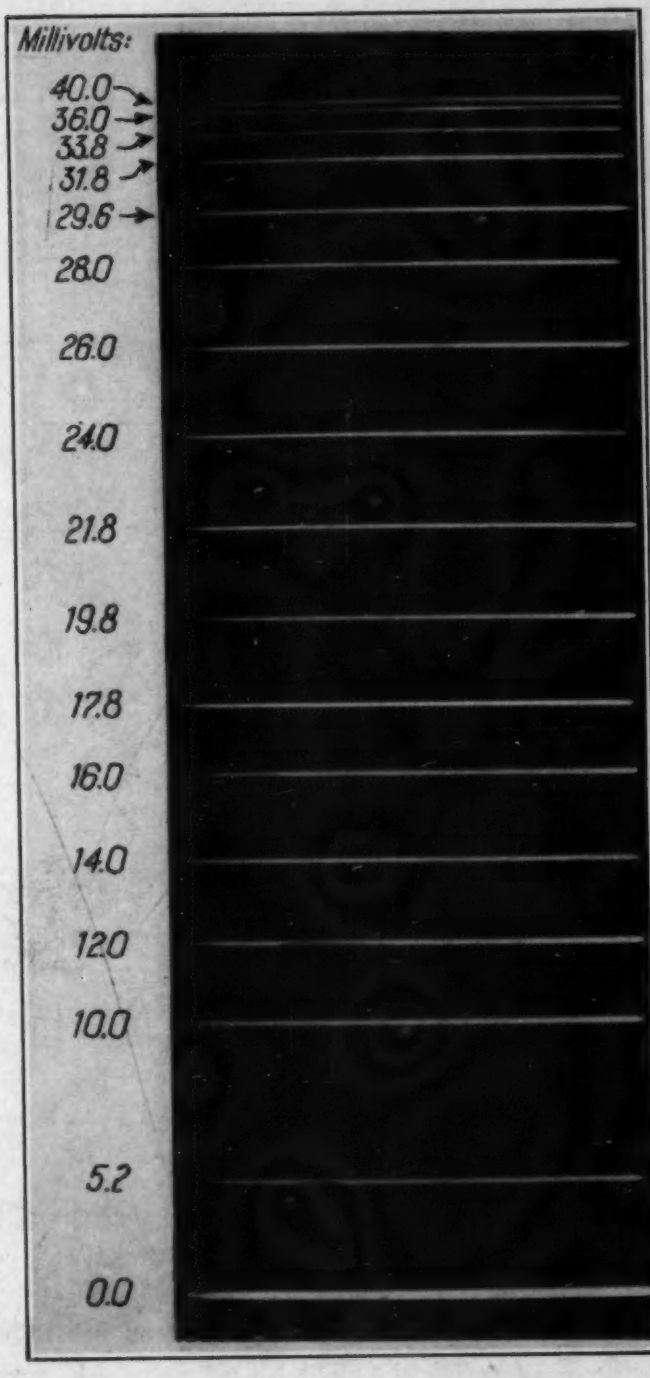

Fig. 4—Calibration Record Showing Position of Trace as a Function of Millivoltage Input.

the complete quenching, indicating and recording equipment. On the left is noticed the new gas quenching unit with the thermocouple leads passing from near the floor in the center of the equipment, to the shielded amplifier resting on the table adjacent to the oscillograph. The recording camera, box potentiometer and milliammeter may also be noted. The metal boxes under-

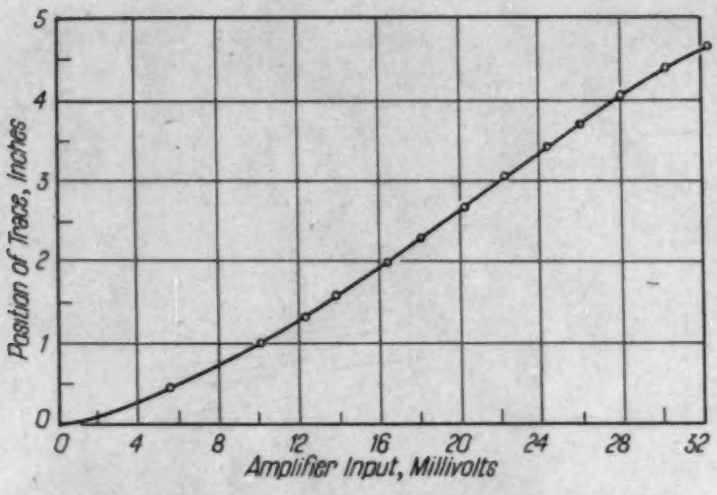

Fig. 5—Calibration Chart Showing Vertical Deplacement, in Inches, of the Trace in Terms of Millivoltage Input.

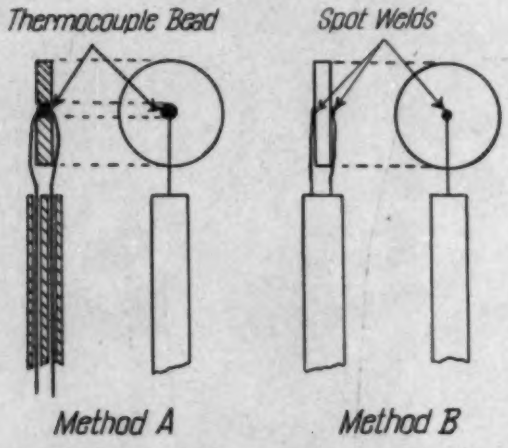

Fig. 6—Methods of Attaching Thermocouple to Test Sample.

neath the table serve as electrical shielding for the dry batteries and storage cell.

To make a record a light shield is set up between the camera lens and the oscillograph screen—appearing as a white disk in the picture.

Calibration of Oscillograph

In order to calibrate the deflection of the electron beam, for analysis of the cooling records, the calibration circuit shown in the upper part of Fig. 1 is used. The output of this circuit is substituted for the thermocouple e.m.f. by throwing switch S_6 toward the calibration circuit.

The operation of calibration commences with the grid bias adjusted so that the amplifier output is 0.5 milliampere, as described, and the electron trace, providing a reference line vibrating horizontally across the bottom of the screen, serves as an indication of zero millivoltage input so far as the thermocouple circuit is concerned. The position of this trace is photographi-

cally recorded. An increased e.m.f. can now be selected from the variable resistor R_6, and impressed on the amplifier circuit. This causes the oscillograph beam to deflect upwards to a new horizontal trace which is also recorded on the same film. By a series of similar procedures several different horizontal traces, corresponding to specific impressed millivoltages, can be thus recorded, as illustrated in Fig. 4, which is a print from the calibration film.

This record is then translated in terms of deflection versus millivoltage with the result obtained in Fig. 5. The mechanics of this operation are as follows: The film and graph paper for the plot are aligned so that the zero

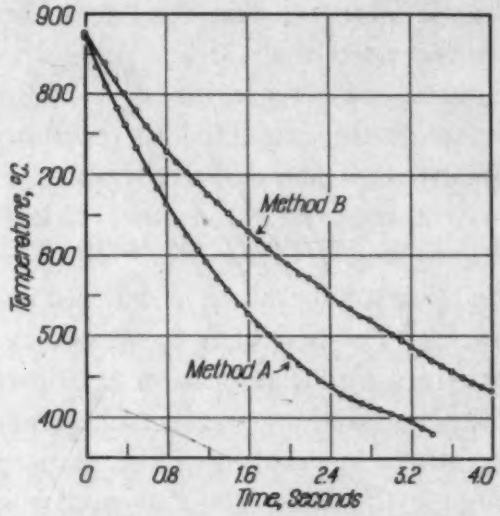

Fig. 7—Plot of Time-Temperature Relationships Obtained From the Methods of Thermocouple Mounting Illustrated in Fig. 6.

millivoltage trace is parallel to the zero ordinate of the graph. Using an arbitrary millivolt input abscissa, the other points are located by drawing parallel lines from the traces on the film to the corresponding millivoltages on the plot.

Determination of Rate of Cooling of a Steel Sample

The experimental procedures discussed were followed in order to permit a study of the details involved in an analysis of the correlation between microstructure and measured cooling rates, using the equipment described in the previous pages.

In order to obtain controlled and predetermined rates of cooling, specimens about ⅜ inch in diameter and 0.04 ± 0.001 inch thick were attached to a chromel-alumel thermocouple, heated in vacuum to 800 degrees Cent. (1470 degrees Fahr.) for 15 minutes, and then rapidly withdrawn to a cool portion of the chamber where a variable but controlled gas quenching rate was effected, using nitrogen.

In a preliminary series of quenching tests the thermocouple was attached to the specimen as shown in Method A, Fig. 6, the thermocouple bead being embedded, by light hammering, into a 0.03-inch hole. Inspection of results from quenching tests suggested that cooling rates of the steel specimens were less rapid than the figures calculated from the actual cooling rates of the thermocouple bead. To investigate this apparent discrepancy one wire of the thermocouple was spot welded on each side of the steel disk in the manner depicted in Method B, Fig. 6. The steel was then quenched in a manner identical to that used with Method A. In order to confirm that the quenching rates had been identical in both experiments, sections of the specimens were examined under the microscope after quenching. The presence in each sample of about 1 per cent pearlite in a martensitic matrix confirmed that the critical cooling velocity had been approximated in both tests.

A plot of the time-temperature relationships for these two samples is shown in Fig. 7, where it is suggested that the spot welding method (B) provides a true indication of the rate of cooling of the sample. The plot by Method A gives the cooling curve of the thermocouple bead, when inserted into the sample. Clearly, even though efforts are made to obtain good thermal contact by wedging the bead into a hole in the sample, it is apparently impracticable to obtain a true picture of sample quenching rate by this method. Calculations showed that Method A indicated a cooling rate of 150 degrees Cent. (300 degrees Fahr.) per second through the temperature range 600-500 degrees Cent. (1110-930 degrees Fahr.), whereas Method B indicated a rate of 100 degrees Cent. per second over the same temperature interval. Accordingly, all the results discussed in this paper were obtained from samples to which the thermocouple had been spot welded.

Quenching and Recording Procedure

A simple description of the actual procedure used to obtain the necessary photographic records, and of their interpretation in terms of the usual time-temperature cooling curve co-ordinates, now follows.

With the test sample at temperature and immediately prior to the quench, the amplifier output current was adjusted to 0.5 milliamps, with the thermocouple shunted out of the circuit as previously outlined, and the horizontal trace recorded on the photographic film.

This line gave the position on the film for zero millivoltage. A similar exposure of the trace obtained with the known quenching temperature millivoltage, impressed from the thermocouple, provided the position on the film of this co-ordinate. This was used merely as a check to ensure exact correlation with the standard calibration curve as shown (reduced in size) in Fig. 5.

With the sweep circuit frequency adjusted to 3 cycles per second, the lowest sweep rate attainable with the oscillograph available, and with the thermocouple in the circuit providing a horizontal sweep at the millivoltage corresponding to the temperature of the sample ready for quench, the camera shutter was opened. Immediately the test specimen was moved into the gas quenching zone, and when the temperature fell to about 200 degrees Cent. the shutter was closed.

Analysis of the Photographic Record

The method to obtain a time-temperature relation or direct cooling curve from the photographic record is the reverse of that outlined on page 757 in drawing the calibration record illustrated in Fig. 5. The record to be analyzed is aligned with the original calibration curve by use of the reference line for zero millivoltage, checked by the reference line for the quenching temperature millivoltage. Since the successive traces, representing 0.3-second time interval, form part of a continuous cooling curve, they are naturally inclined to the horizontal reference zero. An arbitrary reference point on each of the traces is selected from which to draw a parallel line, really a projection, to the point where it crosses the calibration curve. This point of intersection defines the millivoltage at the specific time interval represented by the particular trace considered. A tabulation of elapsed times since start of quench, and corresponding millivoltages are thus obtained, and the conversion of millivoltage to temperature provides all necessary data to permit the desired cooling curve to be drawn.

On account of slight changes in the zero position of the trace over periods of time, it has been found desirable to obtain a calibration curve at frequent periods of test.

Determination of Critical Cooling Velocity

In order to illustrate the application of the assembled equipment to the determination of critical cooling velocity, details of procedure

and results from studies on a 1 per cent carbon commercial steel will be outlined. By the item "critical cooling velocity" the authors refer to the rate of cooling required to provide a microstructure consisting of approximately 50 per cent martensite and 50 per cent pearlite and having a hardness of about 55 Rockwell C. This structure corresponds with that obtained by Grossmann and Stevenson (7) in their determination of "characteristic cooling time", and permits more accurate evaluation, in point of time or rate, than is practicable with small percentages of residual pearlite as used by Digges (8).

The steel selected has been designated as "Z" in previous researches (9) by one of the authors and had the following chemical analysis:

Carbon	Silicon	Manganese	Sulphur	Phosphorus
0.98	0.19	0.20	0.017	0.014
Chromium	**Nickel**	**Copper**	**Nitrogen**	**Aluminum**
0.04	0.04	0.04	0.0014	0.004

This steel, which is shallow hardening, was chosen because of its relatively high critical cooling velocity, and particular suitability for demonstrating the sensitivity of the method herein described.

Several 0.04-inch thick disks of the ⅜-inch bar stock were subjected to various rates of nitrogen quenching, after heating to 820 degrees Cent. (1510 degrees Fahr.) for 20 minutes. The hardness of the quenched samples was then taken, and cut sections were examined under the microscope. From this test five quenching rates were selected as providing examples of cooling rates which were—

(a) Sufficiently rapid to produce martensitic structure.

(c) Suitable to provide a structure approximately 50 per cent martensite and 50 per cent pearlite.

(e) Sufficiently slow to ensure the formation of 100 per cent pearlite.

(b) and (d) Intermediate rates resulting in the formation of small percentages of pearlite and martensite respectively.

The selected procedures were repeated and oscillograph records taken of the cooling curves.

Fig. 8 illustrates the oscillograph records for the above mentioned conditions. The most rapid rate of cooling (A) suggests absence of any critical point. Similarly no evidence of transformation can be obtained directly from trace B. Trace C at once shows evidence of thermal disturbance while the slower rates as typified by D and E clearly reveal the recalescense phenomenon.

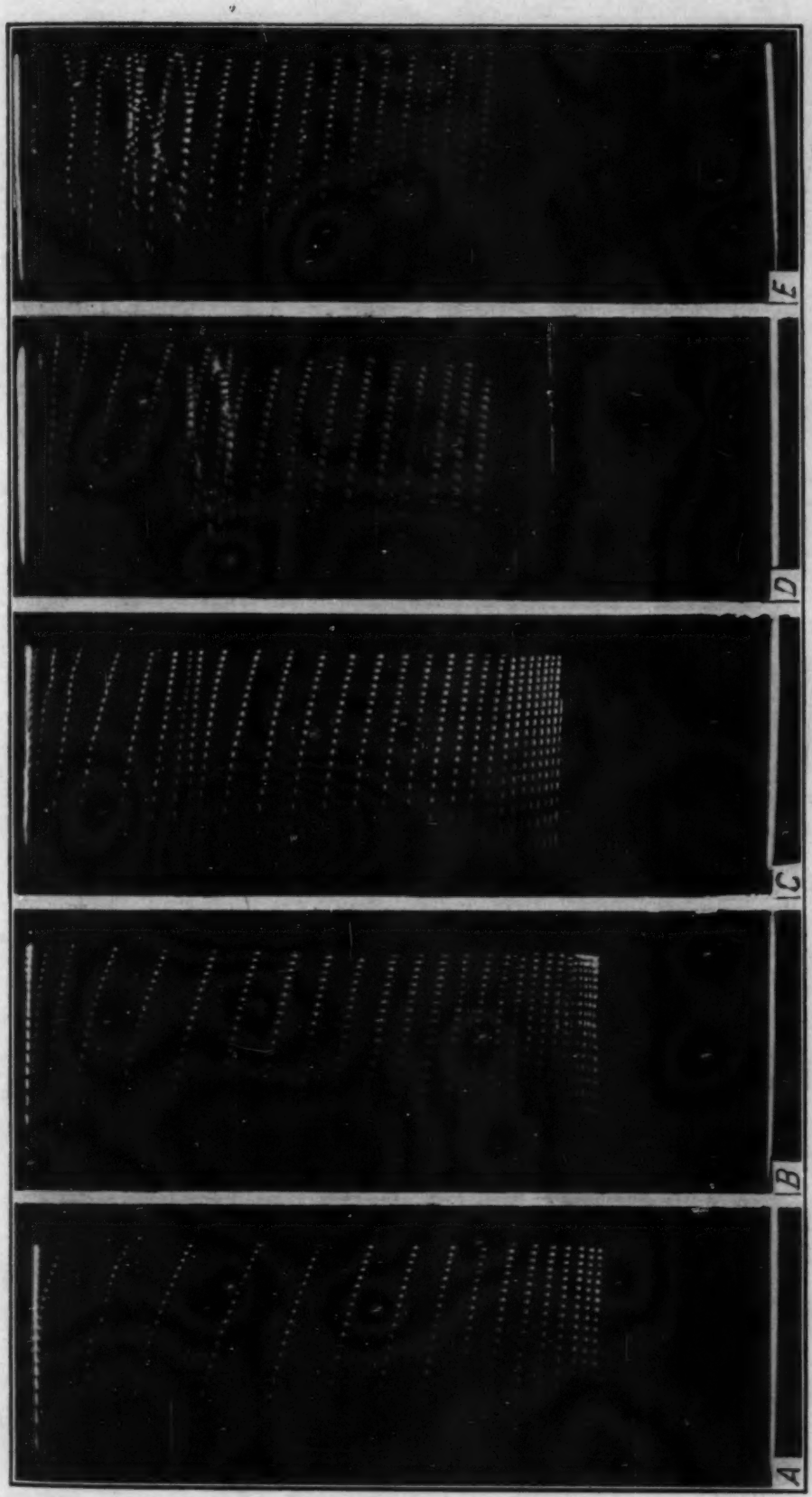

Fig. 8—Oscillograph Records Resulting From the Gas Quenching of Samples at Decreasing Rates of Cooling. Trace A Shows a Rate Sufficiently Rapid to Ensure a Completely Martensitic Structure. Trace E Shows a Rate Sufficiently Slow to Permit Complete Eutectoid Transformation.

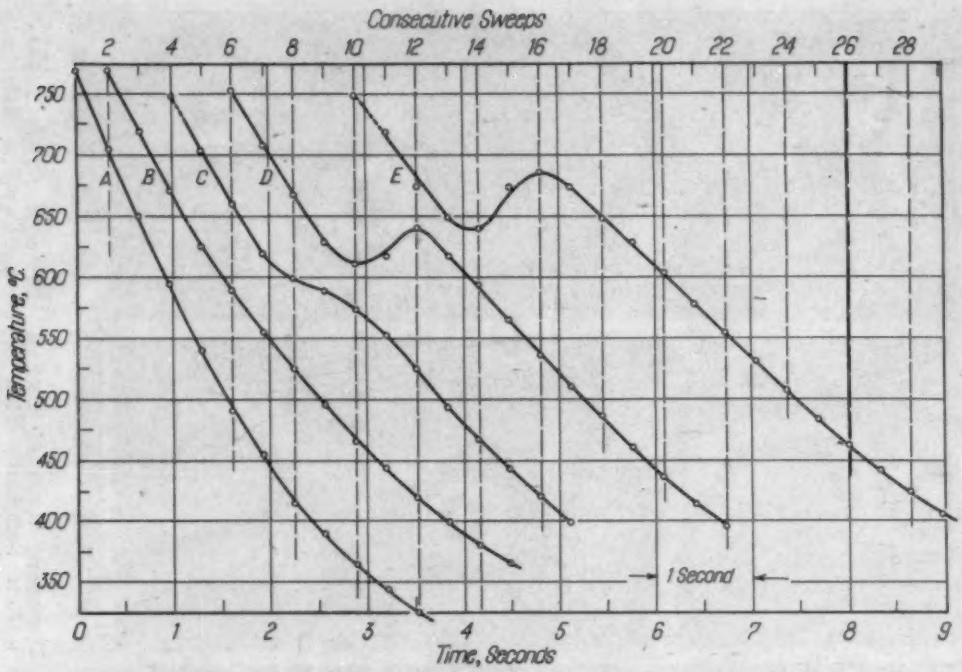

Fig. 9—Time-Temperature Cooling Curves Obtained From Analysis of the Oscillograph Traces Shown in Fig. 8.

Plots of these records obtained in the manner described in detail on page 760 result in the usual time-temperature cooling curves, reproduced in Fig. 9. The deduced curves were obtained by analysis of the negatives since the lines are more clearly defined than in the corresponding print. A comment should be added on the interpretation of Fig. 8-D and 8-E since some confusion might at first sight seem to exist. Because of the instantaneous return of the sweep after completion of its travel across the target in 0.3 second the origin of the next sweep necessarily lies in the same horizontal line with the final point of the previous sweep. Accordingly horizontal lines projected backward from the terminal of any trace identify immediately the origin of the next sweep. This simple principle permitted the identification of the sequence of sweeps recorded in Figs. 8-D and 8-E. It may be of interest to note that curve B (Fig. 9) shows a rate just sufficient to permit slight eutectoid transformation and exhibits a perceptible but minor retardation in its progress of cooling. From the curves shown in Fig. 9 cooling rates between 700 and 650 degrees Cent. were calculated with the following results:

Curve 9A	185 °C/sec	Curve 9D	120 °C/sec
Curve 9B	145	Curve 9E	100
Curve 9C	125		

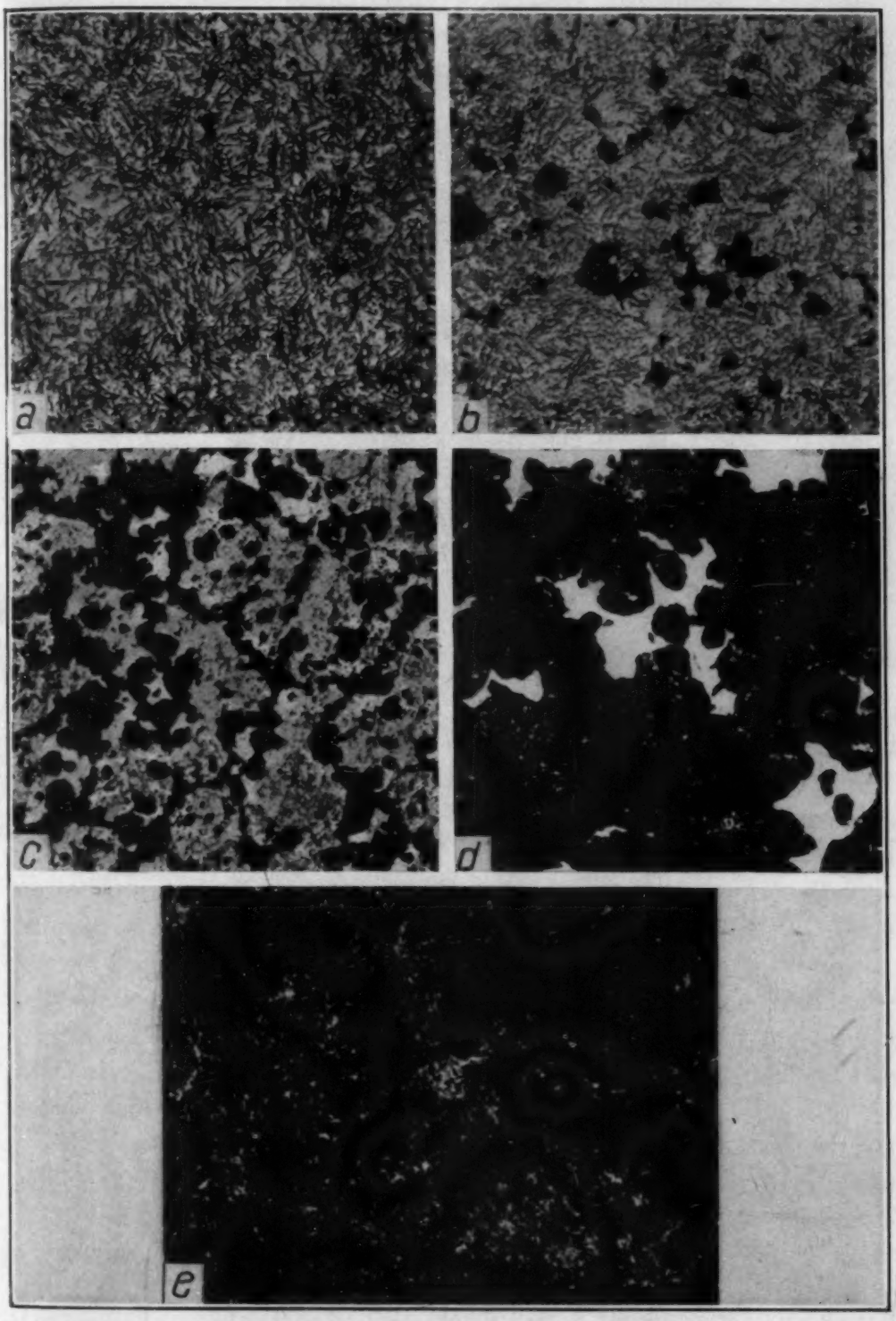

Fig. 10—Microstructures of Gas Quenched Samples. Figs. 10a to 10e Illustrate the Structures Observed From Treatments Typified in Fig. 9 A to E Respectively.

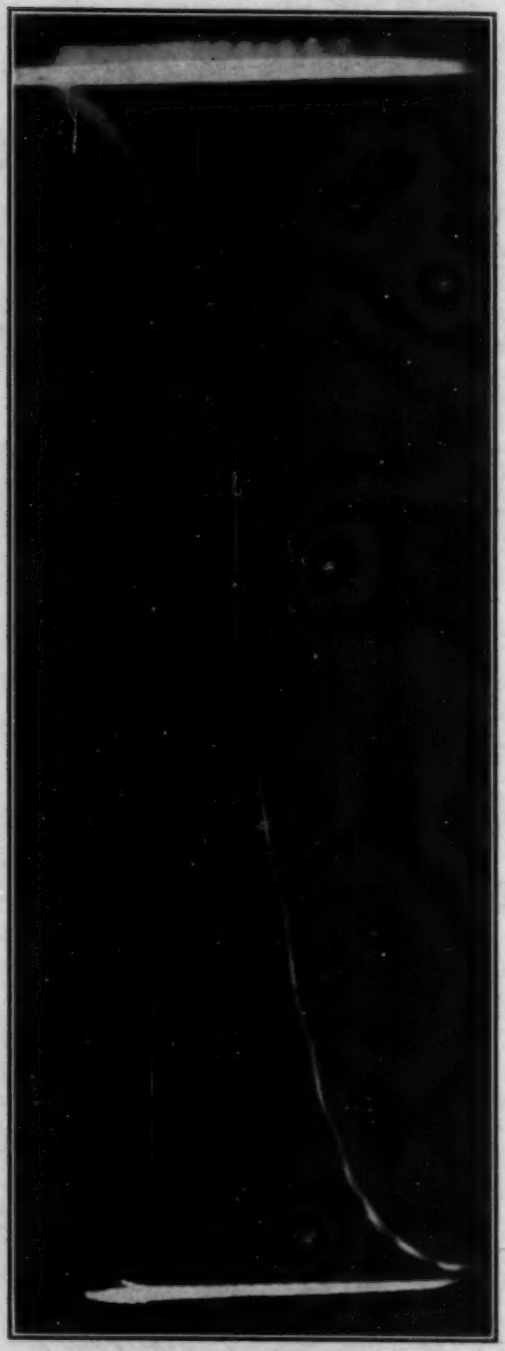

Fig. 11—Oscillograph Record Resulting From Quenching a Thermocouple Bead, Heated to 800 Degrees Cent., Into Cold Water.

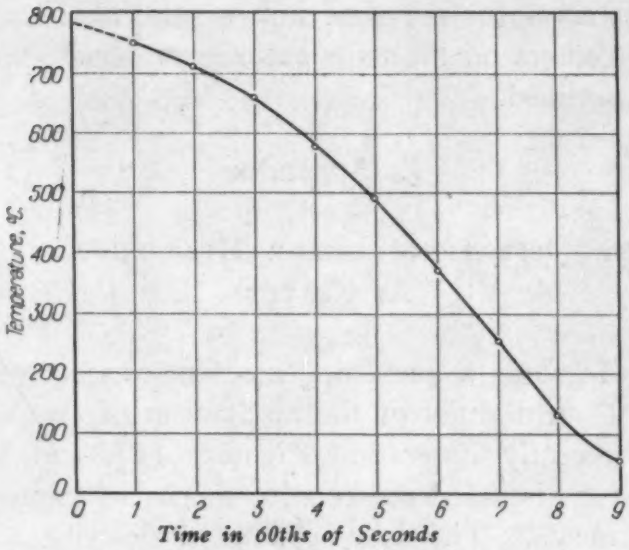

Fig. 12—Time-Temperature Cooling Curve Obtained From Analysis of the Oscillograph Trace Shown in Fig. 11.

The Rockwell C hardness values of the specimens from which these data were derived were 65, 63, 55, 49, and 50 respectively.

The microstructures of the samples have been reproduced in Figs. 10a to 10e, and need no comment. They merely serve to confirm that the metallography correlates with the other data. An added record is included to illustrate the response of the apparatus to the most severe quench which the authors have obtained with the equipment. Fig. 11 shows a print of the film resulting when a thermocouple bead, heated to approximately 800 degrees Cent. (1470 degrees Fahr.), was plunged into water and cooled to room temperature in less than 1/10 second. The corresponding cooling curve is given in Fig. 12 from which it may be calculated that the cooling rate between 600 and 300 degrees Cent. (1110 and 570 degrees Fahr.) is approximately 6500 degrees Cent. per second.

The method of derivation of the curve (Fig. 12) from the oscillograph record is slightly different from that used previously. In an earlier section the sensitivity of the amplification circuit to extraneous alternating currents was mentioned. In Fig. 8 it is noted that the traces are not continuous lines but rather are composed of small dashes of variable intensity. It appears that this phenomenon results from the slight pickup of the 60-cycle alternating current not excluded by shielding. Accordingly for very rapid cooling rates it is convenient to use successive centers of adjacent dashes as 1/60

second time interval for the time unit on the abscissa. The locations of these centers on the temperature co-ordinate were obtained as previously outlined.

I. Appendix

Assembly and Operation of the Heating and Quenching Apparatus

The use of gas as a quenching medium was early reported by Chevenard (10) in a study of the mechanism of tempering carbon steels. More recently Esser and Eilander (5), and Weaver and Engel (11) have discussed the relative merits of gases and liquids as quenching media. The former authors describe a method of heating in vacuum by high frequency induction, followed by rapid cooling, using a gas quench, and thereby attaining quenching rates as high as 3000 degrees Cent. (5430 degrees Fahr.) per second, with the small specimens used.

In both papers it was clearly indicated that the gas quenching technique provides more uniform and reproducible results than could be obtained with water.

The latest work of Digges (8) similarly provides data on gas quenching as applied to studies on the effect of austenitic grain size on critical cooling velocities of pure iron-carbon alloys. Reference to details of the new equipment was available some time after the apparatus described in the present paper had been designed and built by the authors. Details of the method employed by Digges, in rapidly heating the sample in vacuum or in nitrogen, are fully described in his work. A record of temperature change was obtained by use of the string galvanometer.

The assembly designed and used by the authors in the present investigation is described in detail in this appendix. Procedures differ appreciably from any of those employed in the references cited. Particularly on account of the special technique and problems involved in the application of a direct current amplifier-oscillograph unit it was considered desirable to provide precise information on the exact modus operandi of the complete procedure followed.

The assembled equipment may be considered to consist of three parts:

1. The furnace providing a means of heating the specimen in vacuum to the desired temperature.

2. A quenching chamber and mechanism for moving the speci-

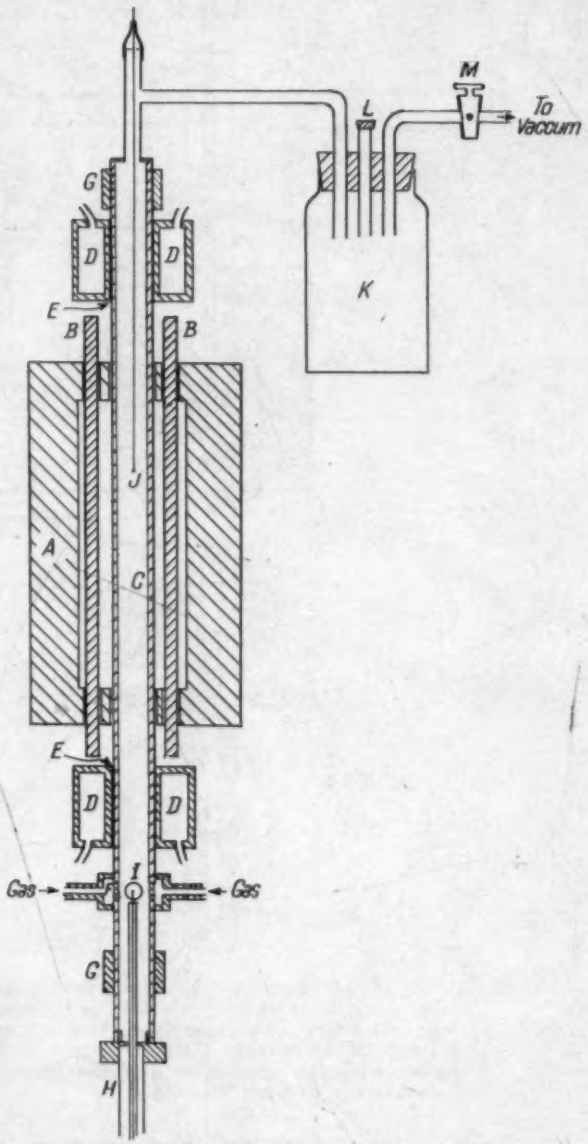

Fig. 13—Section Showing Details of Construction of Heating Furnace and Gas Quenching Chamber.

men rapidly from the furnace to this chamber while maintaining the vacuum and,

3. A system to introduce a desired gas velocity into this quenching chamber at the instant the steel sample reaches the quenching zone.

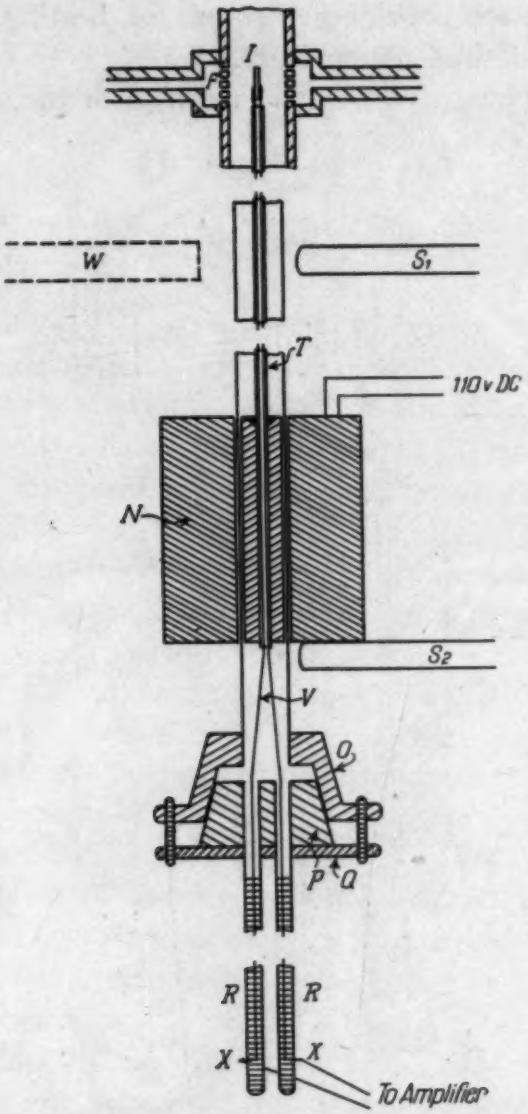

Fig. 14—Section Showing Solenoid and Iron Core in Lower Position For Quenching; Mercury Thermocouple Wells; and Method of Obtaining Vacuum Tight Union Between Couple Assembly and the Furnace Quenching Chamber Assembly.

The Evacuated Furnace

Details of the furnace are shown in section in Fig. 13. The furnace chamber, consisting of a ¾-inch bore nickel tube (C), is closed at the upper end by a tightly clamped piece of pressure tubing through which passes a thermocouple (J). The lower end, made vacuum tight by the method shown in Fig. 14, affords a means of introducing the 0.04-inch thick specimen disk for thermal treatment.

Evacuation is effected through the soldered metal tube which

passes into the pressure release chamber (K). Water cooling units (D) are clamped on the upper and lower end of the nickel tube to ensure a rapid temperature drop outside the furnace (A). This furnace consists of two refractory bricks suitably cut to accommo-

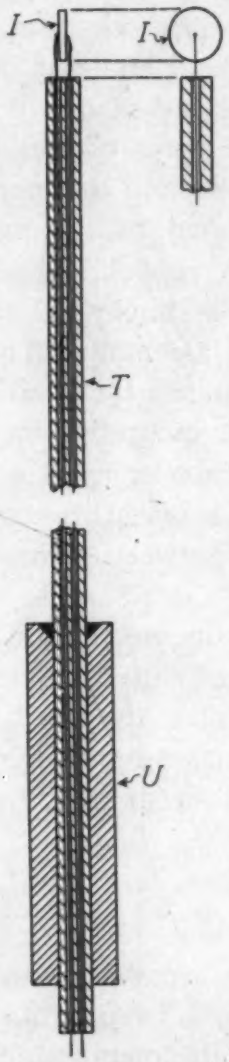

Fig. 15 — Section Showing Method of Assembly of Specimen, Thermocouple, Refractory Protection Tubing, and Iron Core.

date four globar units (B), and housed in a metal case so that the furnace can readily be opened to the position shown in the photograph (Fig. 3).

A brass block brazed on the lower end of the nickel tube serves

to afford a vacuum tight joint for the tube (H) which extends down to the mercury wells (R) shown in Fig. 14.

Gas Quenching Chamber

The gas quenching chamber (F) is connected to the pressure tank via the pressure release mechanism mounted on the board, in front of the tank (Fig. 3). Details of installation of the specimen, mounted by welding at the end of the thermocouple (I), are shown in Fig. 15. The separate wires of this couple are passed through the iron cylinder (U) down into the mercury wells (R) which are in turn electrically connected to the amplifier circuit by use of glass-metal seals (X). A rubber stopper (P) fitting the tapered brass union (O) provides a simple and rapid means of making and breaking the vacuum tight assembly. The location of the iron cylinder, which in turn determines the position of the specimen at the end of the thermocouple, is controlled by movement of the specially wound solenoid (N). This solenoid is so constructed as to provide a strong magnetic linkage between the coil and the iron core. Accordingly no lag obtains between movement of the solenoid and movement of the core.

The distance between the position of the specimen and the solenoid is controlled and fixed by use of a double holed refractory (T) held rigidly by picene cement in the small fillet shown.

On account of the marked sensitivity of the oscillograph to stray e.m.f.s, enamel-coated thermocouple wire has been used in these studies.

The Gas Quench

When the specimen is brought into the gas quenching zone by rapidly lowering the solenoid from S_1 to S_2 (Fig. 14) the tripper arm (W), clearly seen in the photograph, releases the catch which permits the weight to fall and thus causes rotation of the 3-way stopcock (not seen), fastened to the wooden disk. This permits the gas stream, previously adjusted by the reducing valve on the cylinder and discharging to atmosphere, to be introduced suddenly into the quenching chamber. The rate of quenching naturally is varied by the pressure of gas employed. Changes in orifice have also been used to extend the range of rates of gas flow which in turn increases the range of cooling velocity.

General Procedure

A brief description of the procedure should now clearly indicate the manner in which all tests have been conducted. The steel disk is welded to the thermocouple and assembled in the manner illustrated in Fig. 14. With the solenoid in the lower position on stop S_2 the assembly is then introduced into the brass tube (H) so that the position of the sample is automatically fixed in the quenching chamber (F, Fig. 13). The thermocouple wires (V) extending below the tapered brass union (O, Fig. 14) are then fed into the mercury columns (R) and the rubber stopper (P) pulled tightly into contact with the brass union holding the compression plate (Q).

The assembly is then evacuated and power of about 1.5 kilowatts sent through the four globar units. This brings the temperature of the furnace chamber as indicated by couple J, to about 900 degrees Cent. (1650 degrees Fahr.) in less than 10 minutes. When the desired temperature is attained the power is reduced to about ⅓ kilowatt. A direct current source of power is used to maintain temperature in order to eliminate evidence of A. C. pickup on the oscillograph trace.

The sample is then introduced into the heating chamber by raising the solenoid to the fixed position determined by the rest S_1. In this position the solenoid also rests on the tripper arm (W) (Fig. 14). The progress of heating of the sample is followed directly on the potentiometer (M V, Fig. 1) by merely pressing the contact button. As the sample approaches temperature, within a period of 2 to 3 minutes, accurate control of maximum temperature of the sample, as distinct from measured furnace temperature, is obtained by adjustment of a rheostat. While maintaining at temperature, for the desired time, the following details receive attention. The grid bias voltage is adjusted to give 0.5 milliamps output. This serves the same function as the adjustment of the reference line as described under Calibration of Oscillograph. The trace is then focused and adjusted for suitable intensity and for the minimum sweep frequency of three cycles per second. A light-tight shield is then placed between the oscillograph target and the camera lens, and the film holder placed in position for exposure.

As soon as the specimen has been held at temperature, the zero reference line is recorded upon the film. The desired gas velocity is then obtained by the valve adjustment, the stopcock M is closed to

protect the vacuum pump from the sudden pressure, the film sheath is withdrawn from film holder, the camera shutter is opened, the furnace current is stopped, and the solenoid is at once lowered so as to rest on stop S_2. This last operation automatically causes the quenching of the specimen to proceed as previously described.

The progress of the quench may be followed by observation of the milliammeter, and upon the specimen reaching a temperature of about 200 degrees Cent. (390 degrees Fahr.), the shutter is then closed. This prevents the registry of traces so slightly separated as to be indistinguishable. Switch S_3 is then closed in order to check that the initial zero reading of 0.5 milliampere has been maintained, and thus to check the record of its position on the film. An exposure for 1 or 2 seconds is then allowed, to record this reference line upon the film.

The gas flow is maintained after completion of the photographic record in order to prevent tempering of the test sample. The development of the film and the translation of the resulting record into a time-temperature curve are carried out as described.

Acknowledgment

The authors particularly desire to record their appreciation of the assistance given by Dr. Harold Saxton in the earlier phases of the development of the amplification circuit. Suggestions made by Dr. Francis Todd have also been appreciated.

Bibliography

1. M. A. Grossmann (a), "Hardenability as It Affects Heat Treated Parts", *Metal Progress*, April 1938, p. 373.
   (b), "Hardenability, Its Relation to Quenching, and Some Quantitative Data", Symposium of American Society for Metals, October 1938.
   W. E. Jominy, "Hardenability Tests", Symposium of American Society for Metals, October 1938, p. 66.
   Howard Scott, "Some Problems of Quenching Steel Cylinders", TRANSACTIONS. American Society for Metals, Vol. XXIII, 1934, p. 68.
   J. L. Burns, T. L. Moore and R. S. Archer, "Quantitative Hardenability", TRANSACTIONS, American Society for Metals, Vol. XXVI, 1938, p. 1.
   E. C. Bain, "Functions of the Alloying Elements in Steel", Metals Congress, American Society for Metals, October, 1939.
2. G. V. Luerssen, Discussion of Papers on Hardenability, Pennsylvania State Interchapter Meeting, May 3 and 4, 1940.
3. E. K. Spring and J. K. Desmond, "Hardenability Testing Tool Steels by Oil Quenching Small Cones", *Steel*, Vol. 107, October 1940, p. 60.
4. H. LeChatelier, "Etudes Sur la Tempre De L'Acier", *Revue de Metallurgie*, 1094, p. 473.
5. Carl Benedicks, "Experimental Researches on the Cooling Power of

Liquids on Quenching Velocities", *Journal,* Iron and Steel Institute, Vol. 27, 1908, p. 153.

A. M. Portevin and M. Garvin, "The Experimental Investigation of the Influence of the Rate of Cooling on the Hardening of Carbon Steels", *Journal,* Iron and Steel Institute, No. 1, Vol. 99, 1919, p. 469.

H. Esser and W. Eilander, Über die Stahlhärtung (Hardening of Steel), *Archiv für das Eisenhüttenwesen,* Vol. 4, 1930, p. 113.

T. G. Digges, "Effect of Carbon on the Critical Cooling Rates of High Purity Iron Carbon Alloys and Plain Carbon Steels", *Journal of Research,* National Bureau of Standards, XX RP1092, 1938, p. 571.

6. Ross Gunn, "Some Experiments on the Amplification of Thermocouple Electromotive Forces", *Review of Scientific Instruments,* Vol. 9, No. 9, Sept. 1938, p. 267.
7. M. A. Grossmann and R. L. Stevenson, "The Effect of Grain Size on Hardenability", TRANSACTIONS, American Society for Metals, Vol. XXIX, March 1941, p. 1.
8. T. G. Digges, "Influence of Austenitic Grain Size on the Critical Cooling Rate of High Purity Iron Carbon Alloys", American Society for Metals, Preprint No. 10, 1940.
9. C. R. Austin and M. C. Fetzer, "Cementite Stability and its Relation to Grain Size Abnormality and Hardenability", American Society for Metals, Preprint No. 29, 1940.
10. P. Chevenard, "Mechanism de la Tempe des Aciers au Carbone", *Revue de Metallurgie,* Vol. XVI, 1919, p. 17.
11. F. Weaver and N. Engel, "Über den Einfluss der Abkühlungsgeschwindigkeit auf die Temperatur der Umwandlungen, das Gefüge und der Feinbau der Eisen-Kohlenstoff Legierungen," *Mitteilungen,* Kaiser Wilhelm Institut für Eisenforschung, Vol. 12, 1930, p. 131.

DISCUSSION

Written Discussion: By Morse Hill, Jr., metallurgist, and R. E. Bowman, assistant electrical engineer, Materials Laboratory, Materiel Division, U. S. Army Air Corps, Wright Field, Dayton, Ohio.

The authors have accomplished something which must have seemed desirable in all recent cooling rate investigations. However, there are other types of oscillographs available which can be applied to cooling rate work with less difficulty. One such is the electromagnetic oscillograph with a sensitive galvanometer and a continuous drive film holder. The sensitive galvanometer is connected directly to the leads from the thermocouple. The temperature is recorded on a roll of Kodak film as it is wound from one spool to the other. The time can also be indicated on the film by an auxiliary galvanometer which can be connected to a 60-cycle Air Corps supply, or any suitable timing device. It is possible to obtain a deflection of 0.02 millimeter per degree Fahr., and to clearly read the trace to 0.1 millimeter. This is as good legibility as the usual recorder. However, since the total resistance of the galvanometer circuit may be as low as 15 ohms it is necessary to calibrate the galvanometer in such a way that the temperature distribution in the thermocouple is about the same as that which will prevail during measurement. This is readily accomplished by joining two thermocouples at the tip and making a record of one cooling curve with the oscillograph and the other with a high speed recorder or a portable potentiometer. In the calibration, the thermocouples are cooled

at a fairly slow rate so that the potentiometer will give an accurate indication. These oscillographs are commercially available from many of several sources.

Oral Discussion

MAXWELL GENSAMER:[1] Since we have a little bit of time left, I should like to take advantage of it by commenting about a similar setup that I have used recently. It is a lot simpler, but of course it will not work as quickly. By using a galvanometer of low sensitivity but with a period of one-half second, it is a jewel bearing type, not a suspension, with a distance from the mirror to the screen of two or three meters, thus avoiding a large angular deflection, I have been able to get cooling curves at pretty fast rates. It is a simple setup but one with which we have had a good deal of success. I do not mean to imply that it will handle cooling rates as fast as the authors' setup will handle, but it ought to determine the critical cooling rate for alloy steels and even the higher carbon plain carbon steels.

C. R. AUSTIN: Have you figures, Dr. Gensamer, on the maximum rate of cooling which you are able to get?

MAXWELL GENSAMER: No, I am afraid I have not, Dr. Austin. However, the light beam traverses the scale in a period of time which is certainly a very small fraction of a second, and presumably, then, it would be satisfactory for cooling rates in which you would get down to almost room temperature in a period of something like a second or two, at least that good, if not somewhat better.

B. A. ROGERS:[2] What was the relation between rate of cooling and transformation temperature?

R. M. ALLEN: The faster the cooling rate, the lower is the temperature at which the transformation begins, and as the cooling rate is decreased, the transformation begins at a correspondingly higher temperature. The lowest definite transformation temperature we reported is 625 degrees Cent. (1160 degrees Fahr.).

C. R. AUSTIN: The time-temperature cooling curves are shown in Fig. 9.

F. B. FOLEY:[3] There is some transformation in the Curve B.

C. R. AUSTIN: I think that is very interesting. In Curve B, to which reference has been made, there is some slight indication of a transformation at about 550 degrees Cent. (1020 degrees Fahr.).

I might mention that the primary reason for attempting to develop this particular instrument was to get some information on the effect of elements on the critical cooling rates of carbon steels, and on the effects of cooling rates on the degree of depression of the eutectoid transformation. For instance, we have in the laboratory a series of carbon steels, 0.5 per cent chromium, 0.5 per cent manganese, and so on, and we are using these pure iron-carbon third element alloys for this study.

The oscillograph records on thin steel disks are being correlated with the

[1]Associate professor of metallurgy, Metals Research Laboratory, Carnegie Institute of Technology, Pittsburgh.

[2]Supervising engineer, metallurgical division, Bureau of Mines, Pittsburgh.

[3]Superintendent of research, The Midvale Co., Nicetown, Philadelphia.

Jominy end quench treatments and it is hoped that we will be able to discuss this investigation at an early date.

Authors' Reply

We shall have to confess that we are not familiar with the use of the electromagnetic oscillograph as described by Messrs. Hill and Bowman. However, certain inherent difficulties must be expected with any method used to record rapid cooling rates, and it was our purpose in selecting the cathode ray oscillograph to reduce lag, such as obtained in galvanometers, to an absolute minimum. By so doing other difficulties were introduced, as evidenced by the pickup of alternating current through the amplifier, but by exercising certain precautions as given in the description in the text these may be overcome. In the light of the above a sensitive galvanometer may be used in many cases, but for very rapid cooling rates it would be necessary to resort to the cathode ray oscillograph.

We feel, therefore, that this valuable instrument should not be overlooked and that it may be made an extremely useful tool in the determination of critical cooling velocities and the hardenability characteristics of steels.

UREA PROCESS FOR NITRIDING STEELS

By Ray P. Dunn, W. B. F. Mackay and Ralph L. Dowdell

Abstract

A new nitriding process using synthetic urea is described in which Nitralloy G and S.A.E. X1314 and 1020 steels were nitrided in a closed container using various proportions of urea with different nitriding times, temperatures and pressures.

The results show the relation between the nitriding temperature and the hardness, type, and depth of case produced by this method. They indicate also that commercial hardness can be obtained and that with suitable revision of procedure and apparatus the process may have distinct commercial possibilities, especially considering the low cost of commercially pure urea.

THE use of urea as a source of ammonia for a nitriding process is new and is described here for the first time in view of its commercial possibilities.

The only reference found in the literature pertaining to such a use for urea was United States Patent Number 1,772,866, granted on August 12, 1930, to Marx Hirsch of New York and called "Use of Urea for Nitrogenizing Iron and Steel". This broad patent suggests the possible use of urea, cyanamide, sodium amide, hexamethylenetetramine, potassium amide, naphthylenediamine, dicyandiamide, phenylhydrazine, acetamide, or guanidine as a medium for setting up a nitrogen atmosphere in which a considerable amount of nascent nitrogen is available. In his claims, however, he limited his proposed process to the use of urea in a process for treating iron or molybdenum steel, which comprised introducing the same into a crucible or in an enclosed space in conjunction with urea and then heating to a temperature sufficient to release nitrogen from urea and cause nitrogenization.

Urea was selected for use in this research because it was known

---

A paper presented before the Twenty-third Annual Convention of the Society held in Philadelphia, October 20 to 24, 1941. Of the authors, Ray P. Dunn is research metallurgist, Electro Manganese Corporation, Minneapolis; W. B. F. Mackay is flying officer, Royal Canadian Air Force, and Ralph L. Dowdell is professor of metallography, University of Minnesota. Manuscript received April 19, 1941.

to evolve ammonia upon heating, was cheap, and was easy to handle and store. Its quoted price in large lots is about 4.25 cents per pound. Very little is presented in the literature on the pyrolysis of urea; a rather extensive discussion as to the decomposition process up to around 392 degrees Fahr. (200 degrees Cent.) is given by Emil A. Werner in his book of 1923 called "The Chemistry of Urea", but nothing over that temperature was found anywhere in the literature. The reaction products formed above the temperatures he worked at would be worth studying in order to better understand the results given in this paper.

In brief, the commercial nitriding process consists of holding steels, usually of the Nitralloy type, in an anhydrous atmosphere of ammonia with about 30 per cent dissociation at about 950 degrees Fahr. (510 degrees Cent.) under low pressure of a few inches of water for a specific period of time depending upon the type of case desired, anywhere from 24 to 100 hours.

Three steels were chosen for study as to their relative nitridability when using urea. Nitralloy 135 (type G) was selected as a representative commercial nitriding steel. Two other steels, S.A.E. 1020 and S.A.E. X1314, were selected for price and properties contrast. Their nominal compositions are shown in Table I.

Table I
Compositions of Steels Tested

Numbering Code	Nitralloy (G) 135 "Y"	S.A.E. 1020 "X"	S.A.E. X1314 "Z"
Carbon	0.30–0.40	0.15–0.25	0.10–0.20
Manganese	0.40–0.60	0.30–0.60	1.00–1.30
Phosphorus	.....	0.045 max.	0.045 max.
Sulphur	.....	0.045 max.	0.045 max.
Silicon	0.20–0.30	.....	.....
Aluminum	0.90–1.40	.....	.....
Chromium	0.90–1.40	.....	.....
Molybdenum	0.15–0.25	.....	.....

The Nitralloy steel was supplied in a sorbitic structure; it was used in the as-received form. The specimens were 1-inch cylinders cut from ¾-inch bar stock. The S.A.E. steels were 1-inch cylinders cut from 1-inch bar stock. The latter samples were quenched rapidly in cold water from 1735 degrees Fahr. (945 degrees Cent.) to obtain a good martensitic structure, then tempered for 1 hour at 1220 degrees Fahr. (660 degrees Cent.). The result was a sorbite or spheroidized structure. All of the S.A.E. specimens were centerless-ground to remove the decarburized zone.

Commercial nitriding furnaces use a continuous flow of anhydrous ammonia. In most of the present runs the urea was charged into the bottom of the nichrome retort of the pressure furnace with the specimens held directly above the urea; the furnace was sealed, and pressure and temperature controlled. Ammonia was evolved near 270 degrees Fahr. (130 degrees Cent.) at a rapid rate until high pres-

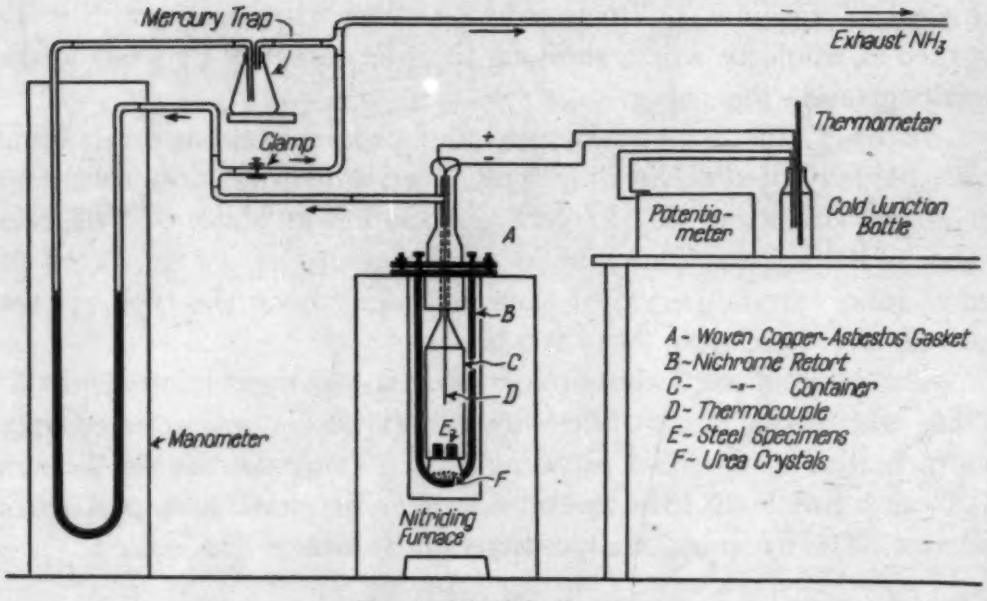

Fig. 1—Nitriding Apparatus.

sures were obtained. At this point it was necessary to bleed off excess ammonia in order to maintain the pressure at a maximum of about 42 inches of mercury in excess of atmospheric pressure. When the system reached a pressure equilibrium, it was sealed and the pressure held as long as it remained positive; but the pressure drop was fairly rapid even though no leaks were detected. The setup used is shown in Fig. 1.

After many revisions, the improved arrangement shown in Fig. 2 was developed. This setup differed from that in Fig. 1 in that the specimens were placed in a vitreous silica tube furnace and ammonia was supplied to them from an external generator; also, the revised plan operated at low pressure. The urea in the external generator was slowly heated to the temperature of ammonia evolution, but no higher; thus the rate of evolution was easily controlled by regulating the flame. While the generator was coming up to temperature with the valve closed, the tube furnace at temperature of 950 degrees

Table II

Run No.	Temperature Degrees Fahr.	Maximum Pressure Inches of Hg	Final Pressure Inches of Hg	Surface Vickers Hardness S.A.E. 1020	Surface Vickers Hardness Nitralloy G	Surface Vickers Hardness S.A.E. X1314	Case Depth in Inches S.A.E.1020	Case Depth in Inches Nitralloy G	Case Depth in Inches S.A.E. X1314
Pre-nitrided Condition		....	...	141	193	139	.....	.....	.....
6	936	15.5	0.4	174	694	254	0.005	0.006	0.055
8	1068	*42	0.7	197	651	298	0.0025	0.0055	0.0045
12	1173	*42	2.5	576	580	439	0.007	0.004	0.004
13	1116	*42	4.3	376	613	433	0.004	0.0065	0.005
14	1098	*42	2.5	289	588	337	0.004	0.007	0.006
15	817	38.3	4.3	199	492	236	0.002	0.006	0.006
18	1278	*42	5.8	400	426	400	0.005	0.004	?

*Excess gas bled off to keep maximum pressure of 42 inches of Hg, over atmospheric pressure.

Runs Nos. 6, 8, 12, 13, 14, 15 and 18 were held for 20-21 hours, using only 50 grams of urea in bottom of the furnace for the entire run.

Run No.	Temperature Degrees Fahr.	Maximum Pressure Inches of Water	Final Pressure Inches of Water	Surface Vickers Hardness Nitralloy G	Case Depth in Inches Nitralloy G	Time, Hours	Rate of Flow c.c./min.
Runs using Fig. 2 setup	950	¼	¼	902	0.028	26	25
	950	¼	¼	1124	0.028	70	10

Specimens from runs Nos. 6, 8, 12, 13, 14, 15 and 18 were all water-quenched following nitriding using Fig. 1 setup, while specimens from runs using Fig. 2 setup were buried in graphite to cool following nitriding.

Fahr. (510 degrees Cent.) was loaded with the clean specimens in a wire boat. The valve was then opened and the system purged for about 15 minutes with a high rate of ammonia flow into the ammonia absorbing bath where a ¼-inch back pressure was maintained. Then the system was regulated to optimum conditions of 270 de-

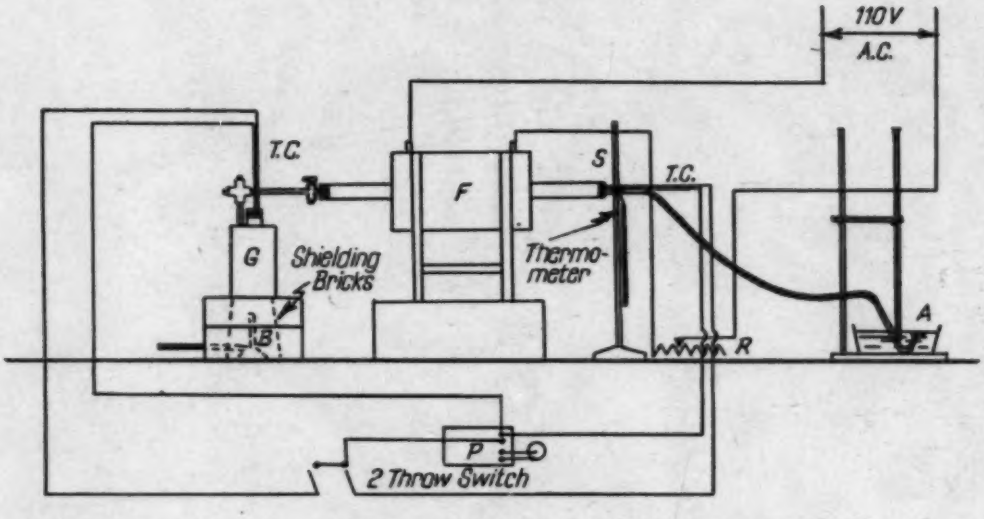

Fig. 2—Improved Nitriding Apparatus.

grees Fahr. (130 degrees Cent.) generator temperature with 10 cubic centimeters per minute flow. Every 12 hours the generator was recharged with 60 grams of urea. The specimens were cooled by removing them from the furnace upon completion of the run and burying them in graphite.

The operating data of all important runs are shown in Table II. The last runs shown were made using the Fig. 2 setup, but all of the others used the one in Fig. 1.

Difficulty was often encountered with clogging in the pipe leading from the pressure furnace (or leading from the ammonia generator in the improved setup) due to a white sublimate deposited in the cool tube. When the furnace was opened in several of the unsuccessful runs, not shown in Table II, at the stage where the ammonia evolution was decreasing, a white deposit was evident in the bottom of the nichrome retort. However, at the completion of the good runs, after the furnace had been at the high nitriding temperature of about 950 degrees Fahr. (510 degrees Cent.) for 20 to 21 hours, the furnace was found to be quite clean, with the exception of the appearance of a slight rust-like deposit on the bottom. Two

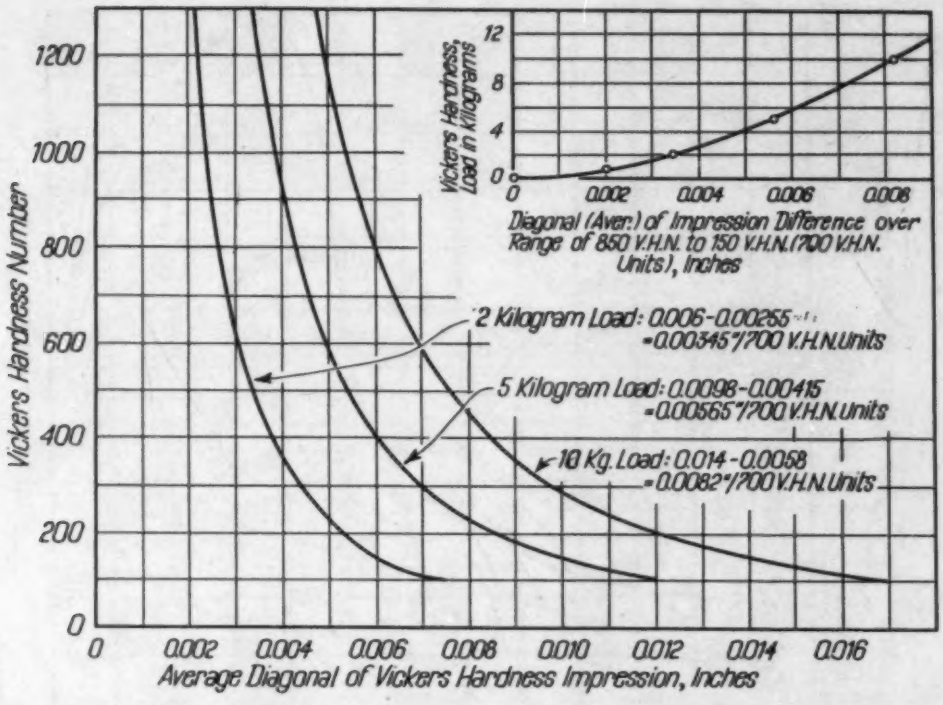

Fig. 3—Relationship Between Vickers Hardness Numbers and Average Vickers Hardness Impressions.

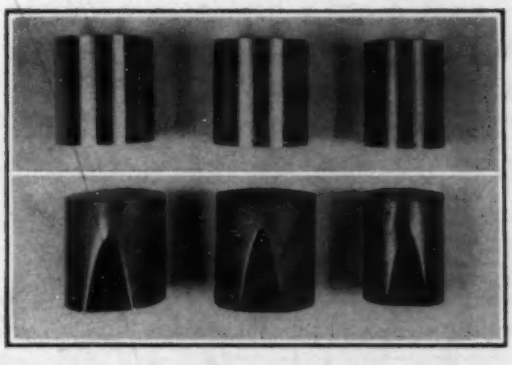

Fig. 4—Types of Specimens Used in this Investigation.

pressure maximums were noted for these high pressure runs; the first, at approximately 482 degrees Fahr. (250 degrees Cent.) was attributed solely to ammonia evolution, while the second at about 797 degrees Fahr. (425 degrees Cent.) was probably due to the decomposition of the white deposit, mentioned above, which was left in the bottom after the ammonia evolution had ceased. Also, upon opening the furnace at temperatures near the upper pressure maximum, a new odor was present with practically no ammonia detectable.

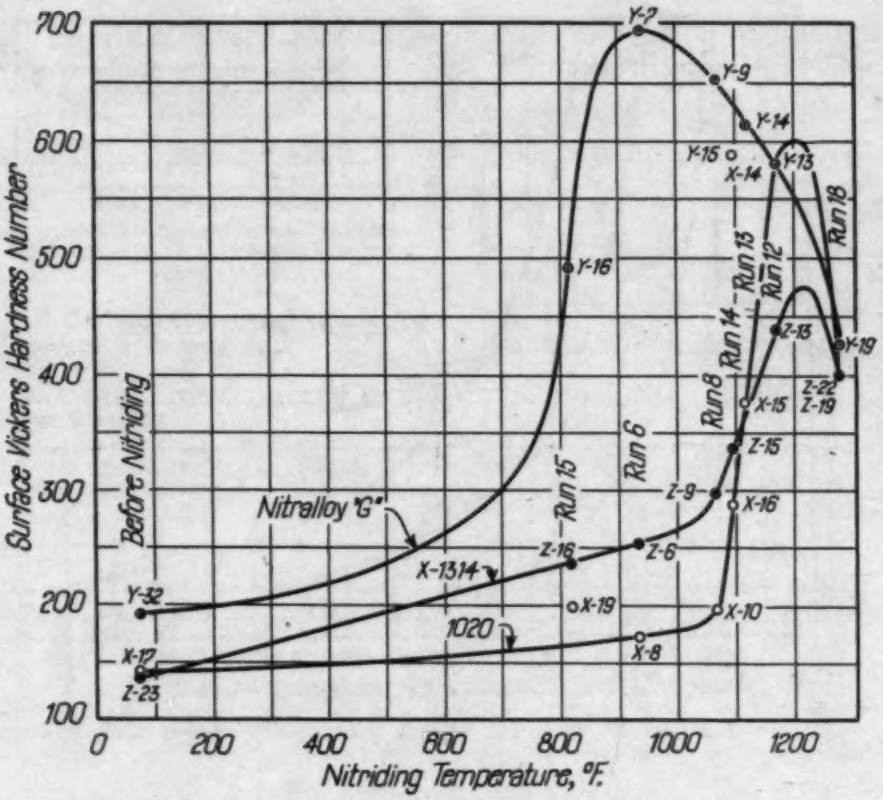

Fig. 5—Vickers Hardness Number Versus Nitriding Temperature for Three Steels Using 50 Grams of Urea for 20 to 21 Hours.

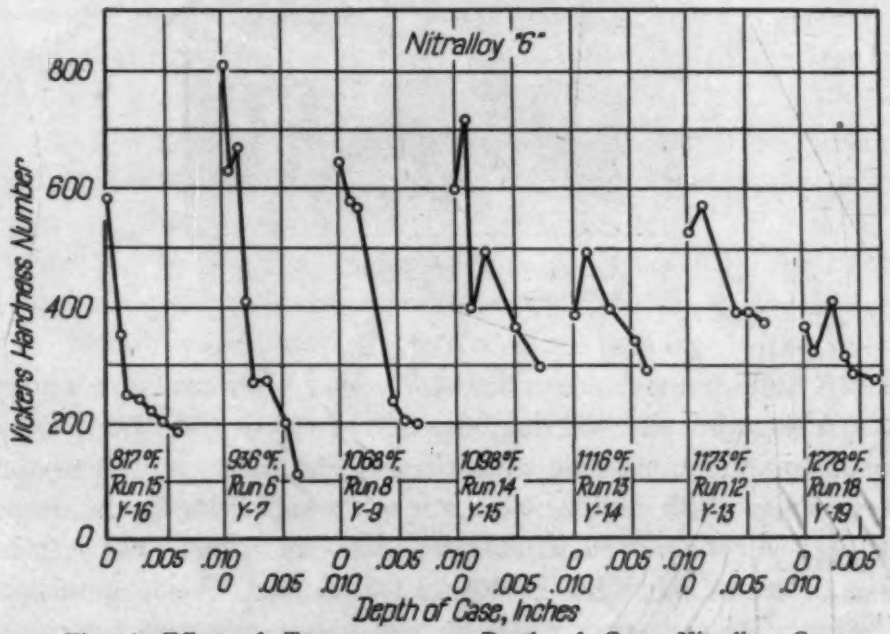

Fig. 6—Effect of Temperature on Depth of Case—Nitralloy G.

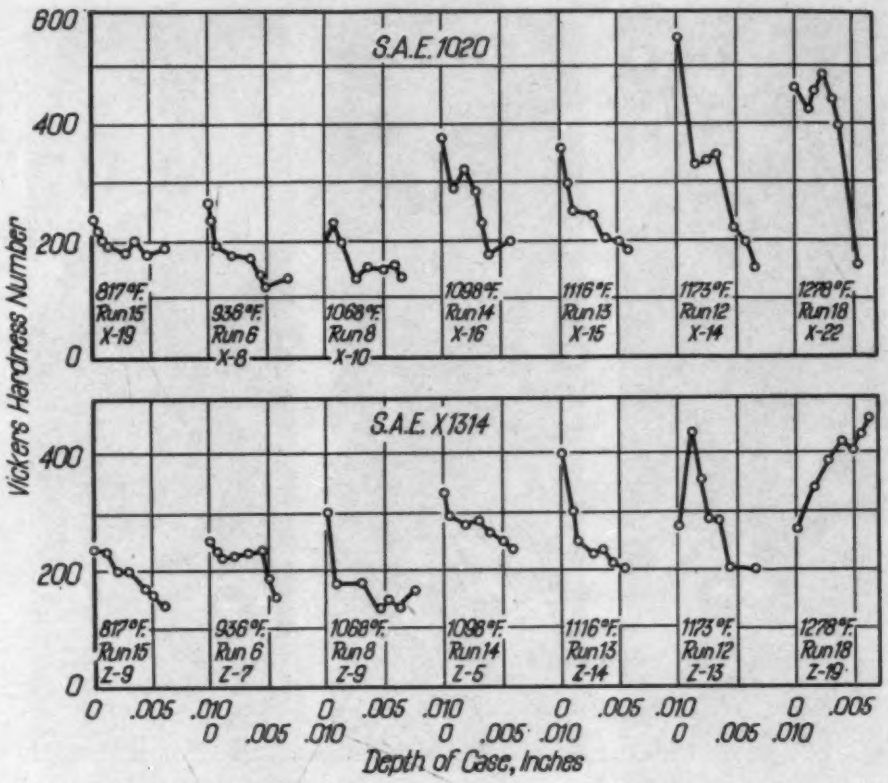

Fig. 7—Effect of Temperature on Depth of Case—S.A.E. 1020 and S.A.E. X1314.

The specimens of all steels from good runs were a bright finish upon entering the furnace and a smooth gray following nitriding. They were then ground while in a special vise in such a manner that a plane was cut through the cylindrical surface at 30 degrees 40 minutes to the axis, resulting in a shallow parabolic cross section through the case and core. Starting at the peak of this section (at the surface of the specimen) Vickers hardness impressions were made with a 5-kilogram (11 pounds) load at distances of 0.010 inch along the center-line. After experimental trials, a 5-kilogram load was found to give readable and reproducible hardness values, whereas a 2-kilogram load proved unsatisfactory. Fig. 3 shows that it is difficult to accurately differentiate between the high Vickers hardness impressions when using too low a load. Surface hardness was also determined on the cylindrical surface.

Before hardness impressions were made along the parabolic slope to measure the case depth, the specimens were polished on this slope, etched in 4 per cent nital, re-buffed, re-etched, and photographed at × 100 along the center line of the parabolic slope starting at the

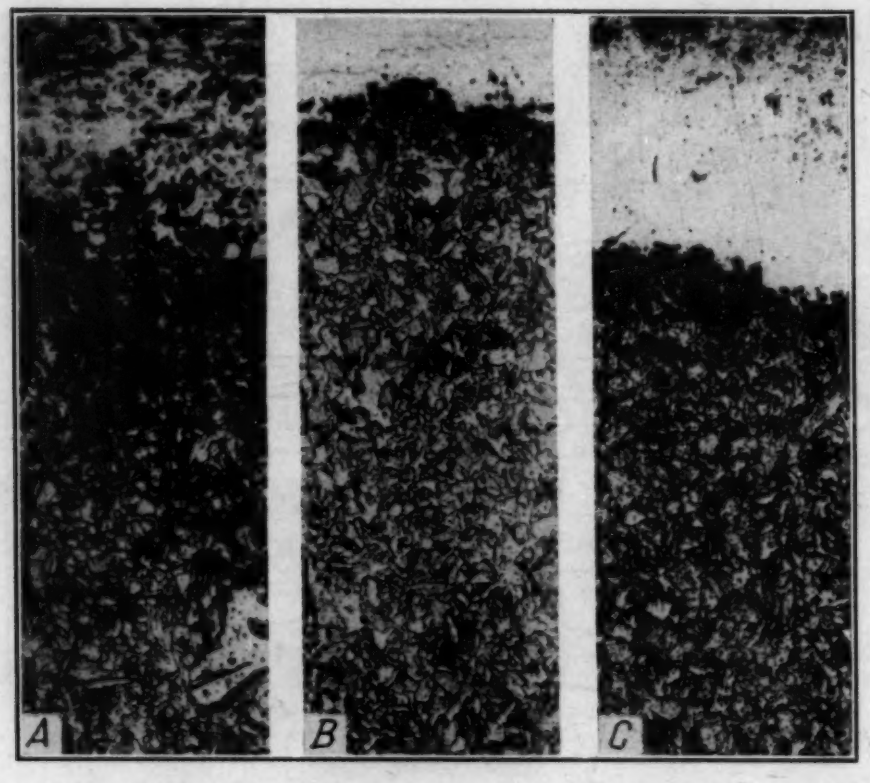

Fig. 8—Effect of Nitriding Temperature on the Type and Depth of Case Produced with S.A.E. 1020 Steel.

The following data cover the samples: All used 50 grams urea for 20 to 21 hours, were water-quenched and 4 per cent nital etched. × 100.

A. 817°F (436°C), X-19 of Run 15, 199 Vickers, 38.5″ Hg max. and 4.3″ Hg min. pressures.

B. 936°F (502°C), X-8 of Run 6, 174 Vickers, 15.5″ Hg max. and .3″ Hg min. pressures.

C. 1068°F (576°C), X-10 of Run 8, 197 Vickers, 42″ plus Hg max. and .75″ Hg min. pressures.

apex. Fig. 4 shows the appearance of the specimens of each steel, both before nitriding and after the parabolic slope on the nitrided samples had been polished.

In order to study the effect of nitriding temperature on surface hardness, type and depth of case, all of the runs in Table II except the last two were planned so that the temperature would be the variable, other factors being held constant. The results are shown as follows: Vickers hardness at the surface for various temperatures in Fig. 5; the case hardness gradient curves in Figs. 6 and 7; and the microstructures in Figs. 8, 9 and 10.

It is questionable as to whether hardness values on such thin cases of 0.005 to 0.006 inch can be relied upon for accuracy, due to the possibility of punctured cases caused by the Vickers diamond point. A hardness of 1000 Vickers gives an impression of 0.00053

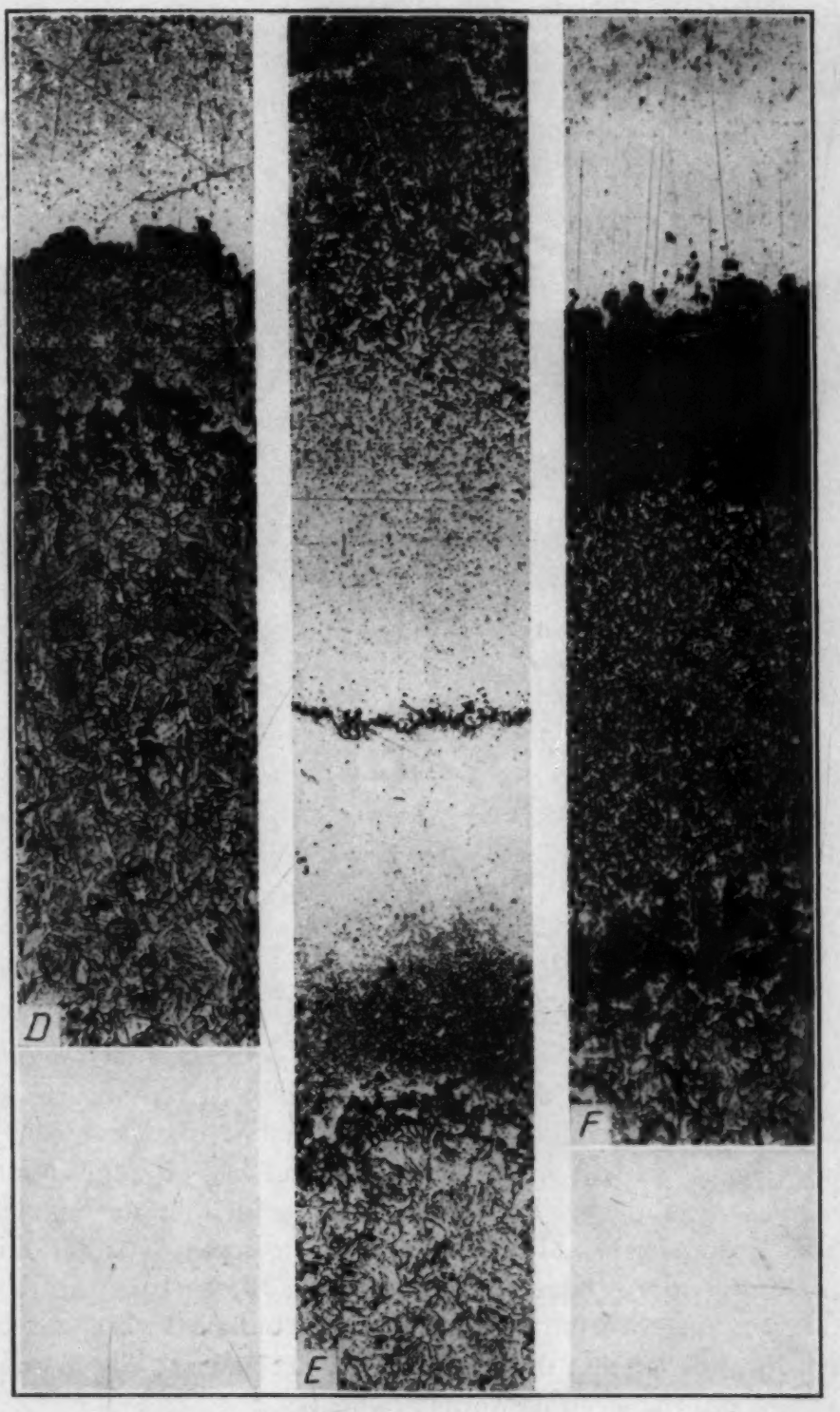

Fig. 8—Effect of Nitriding Temperature on the Type and Depth of Case Produced with S.A.E. 1020 Steel.

D. 1098°F (592°C), X-16 of Run 14, 289 Vickers, 42″ plus Hg max. and 2.5″ Hg min. pressures.

E. 1116°F (602°C), X-15 of Run 13, 376 Vickers. 42″ plus Hg max. and 4.3″ Hg min. pressures.

F. 1173°F (634°C), X-14 of Run 12, 576 Vickers, 42″ plus Hg max. and 2.5″ Hg min. pressures.

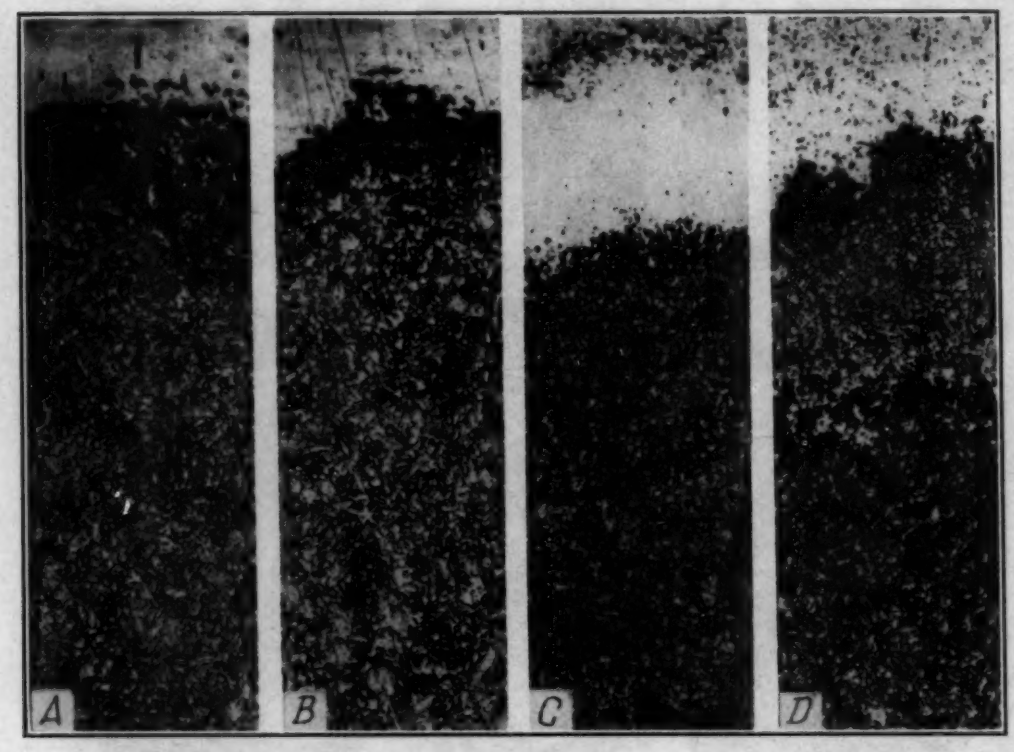

Fig. 9—Effect of Nitriding Temperature on the Type and Depth of Case Produced With S.A.E. X1314 Steel.

The following data cover the samples: All used 50 grams urea for 20 to 21 hours, were water-quenched and 4 per cent nital etched. × 100.

A. 817°F (436°C), Z-16 of Run 15, 236 Vickers. 38.5″ Hg max. and 4.3″ Hg min. pressures.
B. 936°F (502°C), Z-7 of Run 6, 254 Vickers, 15.5″ Hg max. and .3″ Hg min. pressures.
C. 1068°F (576°C), Z-9 of Run 8, 298 Vickers, 42″ plus Hg max. and .75″ Hg min. pressures.
D. 1098°F (592°C), Z-15 of Run 14, 337 Vickers, 42″ plus Hg max. and 2.5″ Hg min. pressures.

inch deep with a 5-kilogram load. It is often stated that the readings are affected by the metal beneath the impressions to a depth of 6 to 10 times the actual depth of the impression. By calculation of the depth of the impression, from the diagonal of the impression and the knowledge that the square-based pyramid has an angle between the angular faces of 136 degrees, it was found that the maximum hardness impression of 1124 penetrated to a depth of 0.00051 inch while the minimum hardness impression of 131 penetrated to 0.0015 inch. It would seem from this that the cases must have been punched through to some extent; this might partly account for the low hardness values and the steep hardness gradients.

The photomicrographs in Figs. 8 and 9 show that there is much similarity between the cases formed in the S.A.E 1020 and X1314 steels. Fig. 10 shows that the Nitralloy G steel gives practically no

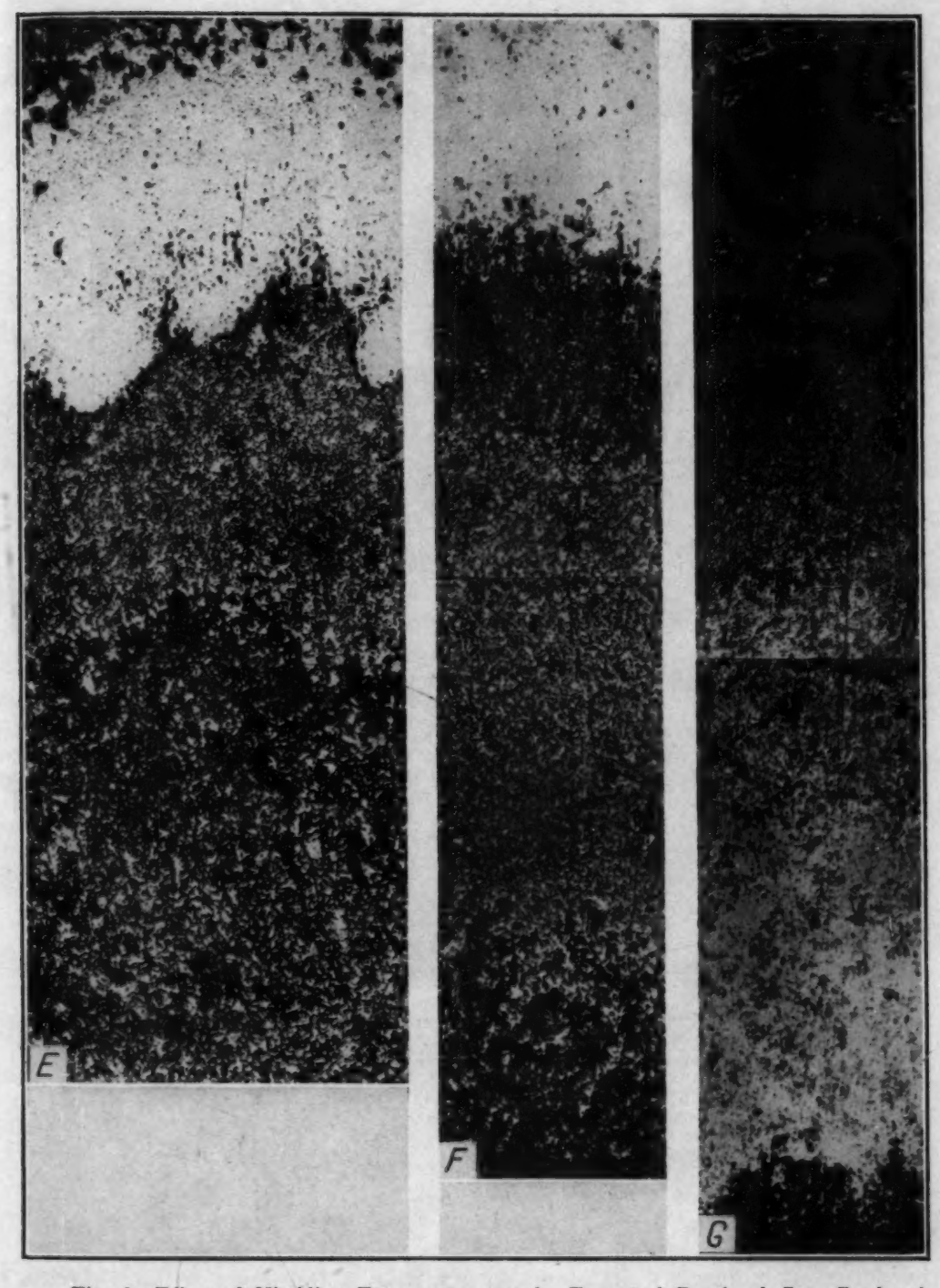

Fig. 9—Effect of Nitriding Temperature on the Type and Depth of Case Produced With S.A.E. X1314 Steel.

E. 1116°F (602°C), Z-14 of Run 13, 433 Vickers, 42″ plus Hg max. and 4.3″ Hg min. pressures.

F. 1173°F. (634°C), Z-13 of Run 12, 439 Vickers, 42″ plus Hg max. and 2.5″ Hg min. pressures.

G. 1278°F (692°C), Z-19 of Run 18, 400 Vickers, 42″ plus Hg max. and 5.75″ Hg min. pressures.

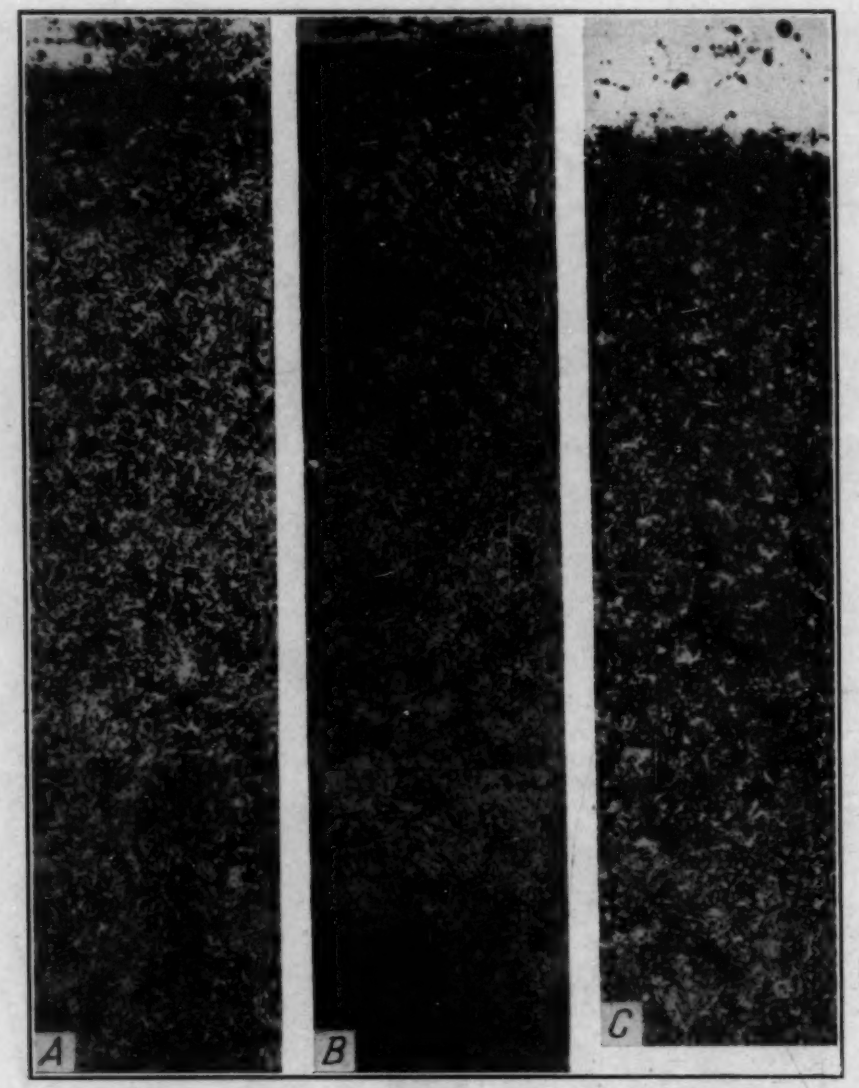

Fig. 10—Effect of Nitriding Temperature on the Type and Depth of Case Produced with Nitralloy G Steel.

The following data cover the samples: All used 50 grams urea for 20 to 21 hours, were water-quenched and 4 per cent nital etched. × 100.

A. 817°F (436°C), Y-16 of Run 15, 492 Vickers, 38.5″ Hg max. and 4.3″ Hg min. pressures.

B. 936°F (502°C), Y-7 of Run 6, 694 Vickers, 15.5″ Hg max. and .8″ Hg min. pressures.

C. 1068°F (576°C), Y-9 of Run 8, 651 Vickers, 42″ plus Hg max. and .75″ Hg min. pressures.

evidence of a case or of layers, other than a tendency to etch darker near the surface, until the maximum hardness range around 950 degrees Fahr. (510 degrees Cent.) had been passed.

The high Vickers hardness of the Nitralloy G specimen from the last run (using the Fig. 2 setup) in Table II illustrates that high commercial hardness can be obtained by the urea process.

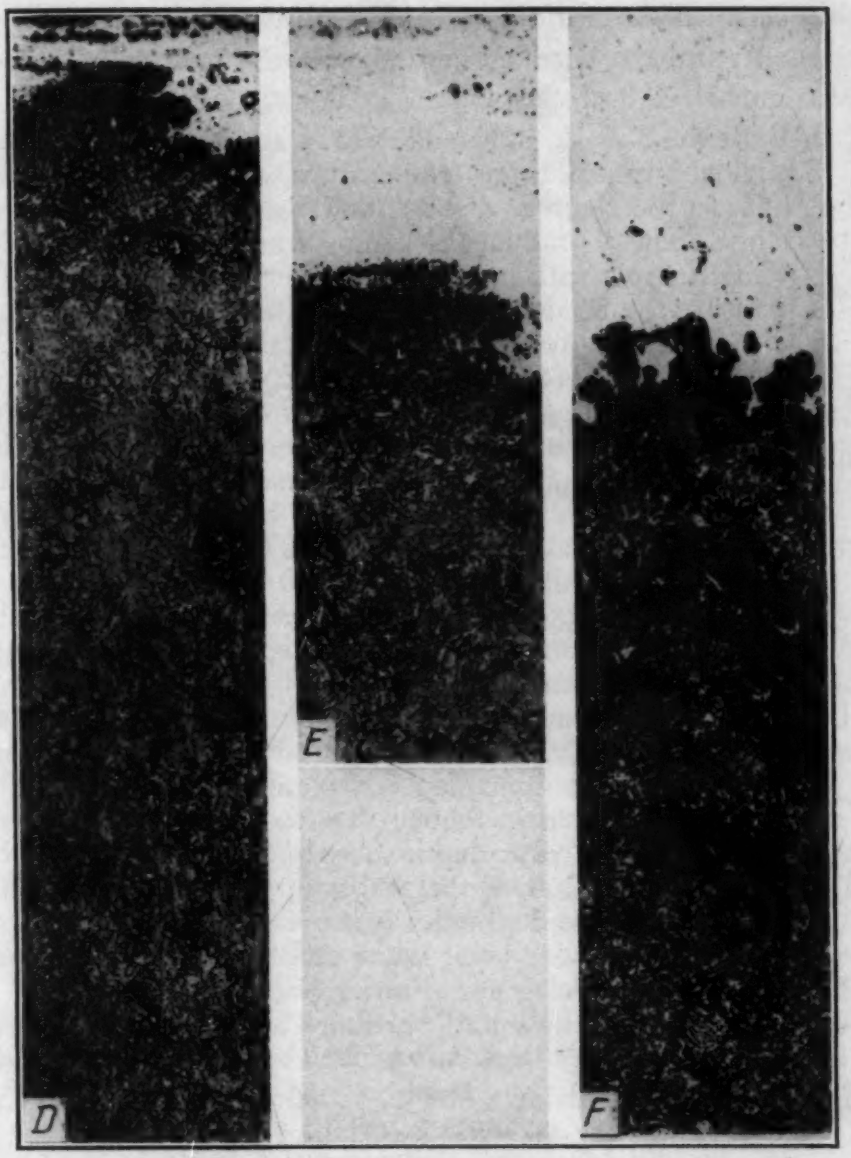

Fig. 10—Effect of Nitriding Temperature on the Type and Depth of Case Produced with Nitralloy G Steel.
D. 1098°F (592°C), Y-15 of Run 14, 588 Vickers, 42" plus Hg max. and 2.5" Hg min. pressures.
E. 1173°F (634°C), Y-13 of Run 12, 580 Vickers, 42" plus Hg max. and 2.5" Hg min. pressures.
F. 1278°F (692°C), Y-19 of Run 18, 426 Vickers, 42" plus Hg max. and 5.8" Hg min. pressures.

Conclusions

1. The steels tested, Nitralloy G and the S.A.E. steels 1020 and X1314, can be nitrided by this process using synthetic urea in a closed container.
2. The hardness data and microstructures both verify the relation-

ship between the nitriding temperature used, other factors being constant, and the hardness and structure of the case. This may be summarized as follows:

(a) Both the S.A.E. 1020 and X1314 steels showed only slight nitridability up to a temperature of about 1050 degrees Fahr. (566 degrees Cent.), and the micrographs over this range show a gradual thickening of the white outside layer of both steels with increasing temperature. Above that temperature the hardenability of the case increased very rapidly with increasing temperature up to a maximum of about 1200 degrees Fahr. (650 degrees Cent.) and the micrographs through this range showed the white outside layer with an additional second gray-colored layer below it. Both layers through this range gradually increased in thickness with increasing temperatures, as did the black interface between them, until the above maximum was reached; at this point, the Vickers hardnesses of the 1020 and X1314 steels were 600 and 475 (both surface hardnesses), respectively. Above this maximum hardness temperature, the hardness decreased but the case depth increased.

(b) The Nitralloy steel showed a maximum hardness at about 950 degrees Fahr. (510 degrees Cent.), which is the normal temperature recommended for obtaining the highest hardness with this steel. Above that temperature the hardness fell off and the case depth increased. The micrographs of samples nitrided at temperatures up to the maximum hardness point showed practically no evidence of a case other than a darker outer layer when etched with 4 per cent nital, until at 1278 degrees Fahr. (692 degrees Cent.) the Nitralloy G steel showed a definite tendency to stratify.

3. The case hardness gradient curves showed an average case depth after 20 hours of about 0.005 to 0.006 inch with 0.028 as the maximum depth for the Nitralloy G steel; the hardness gradient was quite steep for all of the samples. Although a small load of 5 kilograms was used for measuring the Vickers hardness, the cases were so thin that they probably punched through to some extent.
4. The effect of pressure upon the case of the samples was not determined. The decomposition of urea at high temperatures produced two pressure maximums, the first of which was due to the ammonia evolution, but the cause of the second was unknown.
5. A Vickers hardness of 1124 was obtained with a Nitralloy G sample after 70 hours, using the urea process; with suitable

revision of procedure and apparatus the process may have distinct commercial possibilities, especially considering the low cost of commercially pure urea.

Acknowledgment

The writers wish to thank Mr. Albert L. Stock for his valuable assistance in the experimental work.

DISCUSSION

Written Discussion: By V. O. Homerberg, technical director, Nitralloy Company, New York.

This interesting paper contains a number of statements which I should like to discuss.

Synthetic urea is made from carbon dioxide and ammonia. On heating, the products derived besides ammonia are biuret and cyanuric acid. It is quite likely that the white deposit which is formed and later decomposes is cyanuric acid.

Synthetic urea is made on such a large scale that the purchase of ammonia in tank cars is warranted with the result that the cost of production is much below that which would exist if the ammonia were purchased in 100-pound tanks. The users of the nitriding process on a large scale also purchase ammonia in tank cars. In such cases it is obvious that the cost involved in using the urea process cannot compete with the use of ammonia directly. I doubt that urea may have commercial possibilities even in competition with ammonia when purchased in 100-pound tanks. The use of ammonia directly also offers the advantages of greater convenience and control.

Table II shows that much higher hardness results were obtained with nitralloy when treated in the apparatus shown in Fig. 2 than in the equipment in Fig. 1. In Fig. 2 it is quite likely that only ammonia comes in contact with the steel specimens whereas in the apparatus of Fig. 1, the specimens may be affected by the decomposition products other than ammonia.

Table II also shows the same depth of case after 26 and 70 hours of exposure with a lower hardness for the shorter time. A greater rate of flow was used for the shorter run than for the longer one. The results would have been of even greater interest if the rate of flow had been the same in both cases. I should like to ask whether or not any dissociation determinations were made in this investigation.

A case depth of 0.028 inch after nitriding at 950 degrees Fahr. (510 degrees Cent.) for only 26 hours is most unusual and of great importance.

The differences in hardness shown by the three steels are in line with those observed when ammonia is used directly as in the usual nitriding process.

Oral Discussion

WILLIAM PENNINGTON:[1] I should like to ask Mr. Dunn just what effect the carbon content of the steel might have upon the rate of nitriding.

Authors' Reply

Urea nitriding was continued with successful results by R. L. Larson, a 1941 graduate of the University of Minnesota. The apparatus used was practically the same as Fig. 2. The furnace temperature was maintained at 950 degrees Fahr. (510 degrees Cent.) for all runs, the ammonia-from-urea generator was held at about 270 degrees Fahr. (130 degrees Cent.), nitriding periods were varied, and the urea recharging cycle was altered to 50 grams every 2 hours. Nitralloy G specimens were used throughout, and it was found suitable to water-quench the samples directly upon removal from the furnace. Case hardness values using a Vickers tester with a 10-kilogram load were all high—four of 1000, six of 1150, and one of 1250. Case depth measurements were visual and indicated case depths similar to those obtained in the previous work using the Fig. 2 setup.

The authors agree with Dr. Homerberg that tank car quantity users of ammonia would undoubtedly find the conventional ammonia nitriding process more economical than the urea process; however, the authors believe the latter has economic possibilities of development for those who are now using cylinder quantities of ammonia.

Regarding Dr. Homerberg's question, we did not carry on dissociation determinations, but feel that such information would have been very useful.

It is well to mention here, concerning the usual thickness of case obtained in the urea nitriding test period, that Dr. J. F. T. Berliner[2] has brought to our attention two additional patents pertaining to the use of urea in nitriding. One of these patents (U. S. 1,920,368 issued Aug. 1, 1933, to John J. Egan and assigned to the Electro Metallurgical Company) claims that conventional nitriding is accelerated in the presence of urea. The other patent (British 311,588 issued July 4, 1929, to J. L. F. Vogel of High Speed Steel Alloy Ltd.) pertains to hardening of molybdenum steel and iron by heating it in the presence of urea or similar compounds releasing nitrogen at or below temperatures necessary to release nascent nitrogen.

In response to Mr. Pennington's question, it has been found, not in our work, but in previous work, that the amount of carbon in the steel is very important. They have found that the steel with the higher carbon content tends to be the preferable composition, but if it becomes too high, then the toughness of the core of steel is reduced.

The authors wish to thank Dr. Homerberg, Mr. Pennington, and Dr. Berliner, for their contribution.

---

[1]Industrial Fellow, Mellon Institute, Pittsburgh.

[2]Ammonia Department of E. I. du Pont de Nemours & Company, Wilmington, Delaware.

A STUDY OF CUTTING OILS WITH AND WITHOUT ADDED SULPHUR

By O. W. Boston and J. C. Zimmer

Abstract

This paper presents the results of a study to determine the effects on performance of cutting oils with and without added sulphur. The machinability data show a relationship between the cutting speed and tool life when turning an S. A. E. 3140 steel, and the torque and thrust when drilling several steels such as the S.A.E. 3140, 1035, 1020 and 1112 steels.

THE five oils used were designated as A, B, A_s, B_s and A + s, respectively, as indicated with their various properties in Table I. The oils A and B were the two base oils differing mainly in sulphur content. Oil A contained 0.10 per cent sulphur in its natural state while oil B contained 2.03 per cent naturally occurring sulphur. Oil B had a slightly lower gravity and flash point. The two oils had a viscosity of 105/110 Saybolt Universal at 100 degrees Fahr. They were pale oils obtained from lubricating oil distillates of domestic, naphthenic or "low cold test" crudes. They were conventionally refined by acid treatment and distillation over caustic soda.

Oils A_s and B_s were sulphurized products using the base oils A and B, respectively. They were prepared by heating 15 gallons of each oil from 285 to 290 degrees Fahr. using mechanical agitation to facilitate heat transfer from the direct fired bottom surface of the kettle. When this temperature was reached, 0.8 per cent of elementary sulphur was added to the oil after which the temperature was raised to 325 degrees Fahr. during the course of 50 minutes. Heating was discontinued at this time and the oil was allowed to cool to 225 degrees Fahr. by air radiation during a 2-hour period. These oils represent commercially available products which have been used for metal fabrication purposes.

The fifth oil, sample A + s, was prepared by simply adding

A paper presented before the Twenty-third Annual Convention of the Society held in Philadelphia, October 20 to 24, 1941. Of the authors, O. W. Boston is professor, College of Engineering, University of Michigan, Ann Arbor, and J. C. Zimmer is associated with the Esso Laboratories, Standard Oil Development Co. Manuscript received June 23, 1941.

1.6 per cent of an oil soluble, synthetic, sulphur compound to the 0.1 per cent natural sulphur content oil at 100 degrees Fahr. and mixing thoroughly.

Since oils A_s and B_s show wide variations in their total sulphur content, it was believed desirable to ascertain if it were possible to differentiate between the natural sulphur and the added sulphur content of these sulphurized oils. It was believed that only the added (or "active") sulphur was effective in cutting operations. A method which appears suitable for determining the amount of active added sulphur in this type of cutting oil containing no fatty oil is to contact the oil with metallic copper powder as described below:

Active Added Sulphur Content

One hundred grams of the cutting oil and 20 grams of copper powder were weighed into a 250-cubic centimeter lipless beaker. The oil and copper powder were agitated vigorously by a mechanically driven glass stirrer, and heated to 280 to 300 degrees Fahr. in 5 minutes. The temperature was held for 1 hour, while continuing the agitation. The copper was removed from a portion of the oil by filtration and a sulphur determination was made by the A.S.T.M. procedure D-129-39. A sulphur determination was also made on a sample of the oil which had not been treated with copper. The per cent sulphur of the copper powder treated sample was subtracted from the per cent sulphur in the untreated sample. This difference is called the "active added sulphur."

The results obtained with the copper powder method on the five oils studied are shown in Table I, along with other inspection characteristics of the oils. As expected, the copper powder has little or no effect on the natural sulphur content of mineral oil, but does remove "active" or free sulphur.

The load carrying capacity or extreme pressure properties of the several cutting oils also were determined on the Almen extreme pressure lubricant test machine. The usual test procedure, as outlined in Appendix, was employed (i.e. adding the weights at 10-second intervals) and by a shock loading procedure (all the weights being added at one time). These data, given in Table I, indicate that all three oils with added sulphur have a much greater load carrying capacity than the untreated base oils, A and B, as discussed later.

Table I
The Cutting Oils and Their Properties

Sample	A	A_s	A+s	B	B_s
Designation	A	A sulphurized	A plus additive	B	B sulphurized
Gravity, °API	25.8	25.2	25.1	23.0	22.8
Flash, deg. F.	325	315	315	355	345
Vis/100 deg. F.	107.2	108.9	106.8	107.3	107.6
Vis/210 deg. F.	38.5	38.3	38.4	38.4	38.5
Pour	–40	–45	–45	–40	–40
Color (Robinson)	18½*	5¾†	17½*	10¼†	4¼‡
Total sulphur, %	0.10	0.85	1.02	2.03	2.69
Active added sulphur, % (Copper Powder method)	0.00	0.75	0.90	0.08	0.70
Inactive sulphur	0.10	0.10	0.12	1.95	1.99
Almen machine					
Gradual loading	5	15	15	5	15
Shock loading	§	5	5	§	7
Tool-life minutes at 120 f.p.m. (T_{120})	124	162	182	115	204
Net kw. in turning	1.43	1.41	1.48	1.47	1.39

*Light golden.
†Light tan—darker than light golden.
‡Light blue-green.
§Tests were not run since seizure usually occurs with one weight.

The Tool-Life Cutting-Speed Tests

The test log used in the cutting-speed tool-life tests, as originally purchased, was a forging 12 inches in diameter and 4 feet long, weighing 1680 pounds. The analysis conformed to an S.A.E. 3140 steel and showed elements in percentages of 0.38 carbon, 0.17 phosphorus, 0.62 manganese, 0.19 silicon, 0.75 chromium and 1.25 nickel. The log was normalized and annealed giving a resulting tensile strength of 96,000 pounds per square inch, a yield point of 57,500 pounds per square inch, an elongation in 2 inches of 22 per cent, and a reduction in area of 38.8 per cent. The Brinell hardness was 207.

The log was marked A at one end and D at the other end and was divided into four zones—A, B, C and D. All of these tests were run on sections C and D, the diameter of which was 9.15 inches at the beginning of the tests but gradually reduced to 7.87 inches at the conclusion. One cutting tool was repeatedly ground and tested at frequent intervals under dry conditions. This tool gave data on which to base corrections in the variation in machinability of the test log so that all data of the tests were corrected to correspond to that of the original diameter. This variation amounted to less than 1 per cent on the cutting speed.

The tools used were of the 18-4-1 type of Red Cut Superior high speed steel in the form of ⅜-inch square bits each 3 inches long. They were held in a special solid steel holder having a holder angle of 10½ degrees. The tool point in this position was ground to have an 8-degree back rake, 14-degree side rake, 6-degree side and end relief, 6-degree end cutting edge angle, 15-degree side cutting edge angle, and $\frac{3}{64}$-inch nose radius. The grinding was accomplished with a 3846 J5BE cup wheel manufactured by the Norton Company. The setting angle of the tool was 90 degrees, a depth of cut in all cases of 0.100 inch, and the feed was 0.0125 inch per revolution. Tool life was indicated by the complete breakdown of the tool.

These tool-life tests were run on a 30-inch by 14-foot geared head engine lathe provided with a variable speed drive of the Reeves type. A special cutting fluid tank was provided. Five gallons of the oil to be tested were placed in the tank and its temperature maintained at 105 degrees Fahr. by means of electric coils. The oil was discharged vertically downward on the tool face and chip at

a rate of 4.5 gallons per minute through a ¾-inch diameter pipe having a bore of $\frac{25}{32}$ inch at the nozzle. This gave a velocity of 180 feet per minute.

The experimental data resulting from the tests are shown as a straight line for each oil on a modified log-log chart, Fig. 1. This chart is modified so that the ordinate is exactly six times the value of abscissa.

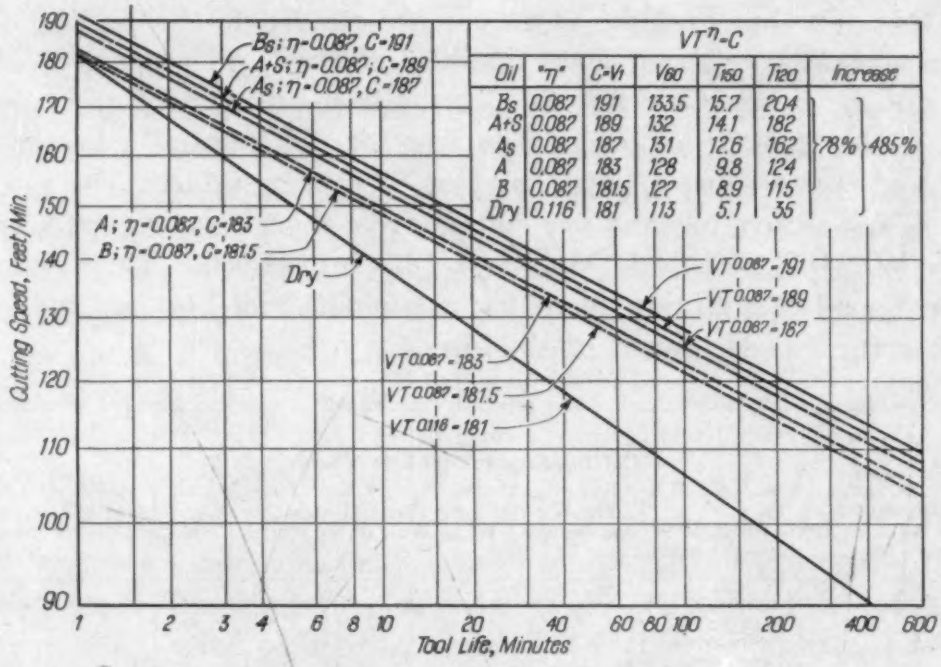

Fig. 1—Cutting-Speed Tool-Life Tests for Five Oils with and without Added Sulphur When Turning Annealed and Normalized S.A.E. 3140 Steel with Tools ¾-Inch Square of High Speed Steel Ground to a Shape of 8, 14, 6, 6, 6, 15, $\frac{3}{64}$. The Depth of Cut Was 0.100 Inch and the Feed 0.0125 Inch. The Curves Are Plotted on Modified Log-Log Co-ordinate, the Vertical Being Six Times the Horizontal.

Each straight line is determined by a number of experimental points. Each point was obtained by operating the specific tool under the standardized cutting conditions outlined above at one cutting speed, and observing the resulting tool life at the time of complete tool breakdown. The speeds were kept high enough so that the maximum tool life observed was not in excess of 20 minutes. The various lines indicated in Fig. 1 are the experimentally determined lines extended further to the right.

Each line on log-log paper may be represented by the equation $VT^n = C$ in which V is the cutting speed in feet per minute, T is the time for total tool failure in minutes, n, the exponent of T, represents

the slope of the line from the horizontal, and C represents the height or vertical displacement of the line for a tool life of 1 minute. Each line is indicated by the symbol of the oil. At the right of each symbol is given the value of n and C. The highest line is for oil B_s which was the basic oil B containing 2.03 per cent natural sulphur which, by being sulphurized, contains a total of 2.69 per cent sulphur, 0.70 per cent of which is found to be active by the copper powder test. The slope of the line, as represented by the value of n, is 0.087. The lines for the other oils are parallel to the B_s line, but are vertically displaced lower in the following order: A + s, A_s, A and B, B being the lowest. As the lines are parallel, the values of n are equal in all cases. The line for dry cutting is lowest of all and is at a greater slope, its value of n being 0.116. The values of C for all five oils and dry cutting from the highest to the lowest are 191, 189, 187, 183, 181.5 and 181, respectively. These values correspond to a cutting speed for a 1-minute tool life, and indicate the vertical displacement of the lines.

Table II

Cutting-Speed Tool-Life Tests

An annealed S.A.E. 3140 steel was cut with Red Cut Superior high speed steel tool bits ground to 8, 14, 6, 6, 6, 15, $\frac{3}{64}$. A depth of cut of 0.100 inch and a feed of 0.0125 inch per revolution was used. The cutting oil was applied at the rate of 4.5 gallons per minute from a $\frac{3}{32}$-inch diameter nozzle.

Oil	Equation	V_{10}	V_{60}	T_{150}	T_{120}
B_s	$VT^{0.087} = 191$	163.5	133.5	15.7	204
A + s	$VT^{0.087} = 189$	161.5	132	14.1	182
A_s	$VT^{0.087} = 187$	160	131	12.6	162
A	$VT^{0.087} = 183$	156.5	128	9.8	124
B	$VT^{0.087} = 181.5$	155	127	8.9	115
Dry	$VT^{0.116} = 181$	147	113	5.1	35

The complete equations showing the values of n and C for the five oils and dry cutting are summarized in the upper right corner of Fig. 1 and in Table II. Values of V_{10} and V_{60} are also given which represent, respectively, the cutting speed for a 10-minute tool life and a 60-minute tool life. For example, oil B_s has a value of C (equal to V_1) equal to 191 feet per minute, V_{10} equals 163.5 feet per minute (from Table II), and V_{60} equals 133.5 feet per minute. Values of T_{150} and T_{120}, which represent, respectively, the tool life for a cutting speed of 150 and 120 feet per minute, are also given for each oil and dry cutting.

From the values summarized in the upper right-hand corner of Fig. 1, oil A, having the lower inactive sulphur content, has a tool

life for a cutting speed of 120 feet per minute (T_{120}) of 124, which compares with 115 for B, the high natural sulphur content oil. Upon sulphurization, the relative positions of the two types of oil are reversed, B_s having a tool life at 120 feet per minute of 204 minutes in comparison with 162 for oil A_s. In other words, the sulphurization of the high natural sulphur content oil B results in a 78 per cent increase in tool life at 120 feet per minute (T_{120}), in comparison with a 47 per cent increase upon sulphurization of the low natural sulphur content oil A. These data indicate that a high natural sulphur content in a mineral oil is of no value in metal-cutting operations with untreated mineral oils. However, upon sulphurization of the mineral oils, a high natural sulphur content evidently plays some role in combining the added sulphur into the mineral oil, which results in a more active form of sulphur or a more effective sulphurized cutting oil. The overall increase in tool life (T_{120}) noted when using a sulphurized, high natural sulphur content mineral oil is 485 per cent over the tool life (T_{120}) when dry cutting.

Comparing oils A, A_s and A + s indicates that cutting oils of slightly greater tool life under the conditions of these tests can be prepared by adding the sulphur to the mineral oil in the form of an organic sulphur compound instead of thermally sulphurizing the mineral oil with elementary sulphur. The tool life at 120 feet per minute (T_{120}) for oil A, the base stock, is 124. This is increased to 162 by thermal sulphurization, and to 182 by adding the synthetic sulphur compound. Reference to Table I indicates that the active added sulphur content values do not correlate with the relative cutting performance of the sulphurized oils, as oil B_s with 0.70 per cent active sulphur has a T_{120} of 204 minutes, while oil A_s with 0.75 per cent active sulphur has a T_{120} of only 162 minutes. The unsulphurized oil B, with 0.08 per cent active sulphur, is inferior to A with no active sulphur. The Almen shock loading test, however, did pick out the most effective oil B_s as described under Lubrication Tests.

To visualize better the relative values of V_1, V_{60} and T_{120}, these values are plotted over the cutting oil symbols in order of increasing value in Fig. 2. It is seen that T_{120} (the tool life for a cutting speed of 120 feet per minute) is increased from 35 minutes for dry cutting to 204 for oil B_s, giving an overall increase of 485

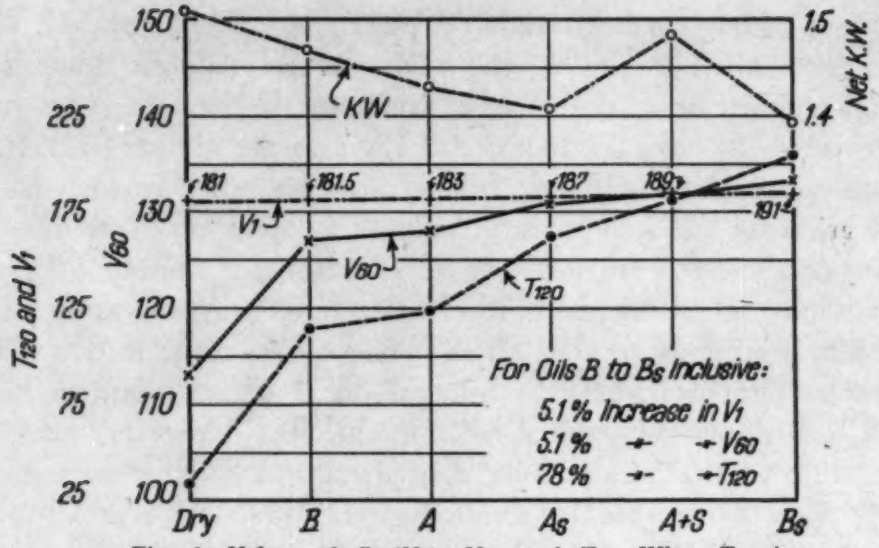

Fig. 2—Values of C (V_1), V_{60}, and T_{120} When Turning S.A.E. 3140 Steel with Five Oils with and without Added Sulphur under Conditions Outlined in Fig. 1.

per cent (also see Fig. 1). T_{120} for B_s is 78 per cent higher than that for oil B. V_{60} is increased from 113 for dry cutting to 133.5 for the best oil B_s, or an 18 per cent increase, whereas the increase of V_{60} for the best oil B_s over the poorest oil B is 5.1 per cent. Inasmuch as the cutting-speed tool-life lines for the five oils are parallel, the percentage of increase for V_1 is the same as it is for V_{60}.

Power in Turning

A recording wattmeter was attached to the motor operating the lathe during all of the cutting-speed tool-life tests. The gross and tare values of power were determined from a number of these charts produced at speeds of approximately 153 feet per minute for each of the cutting fluids. The tare has been subtracted from the gross to give the net power. Averages of from five to eight such tests for each cutting fluid were determined. They are shown plotted over the cutting fluid as net kilowatts in Fig. 2 when turning the S.A.E. 3140 steel. The highest value of 1.52 kilowatts was obtained when cutting dry. Oil A + s gave the next highest power consumption of 1.48 kilowatts, followed in order by oil B with 1.47, oil A with 1.43, A_s with 1.41, and B_s, the lowest, with 1.39.

The power required to cut with the different cutting fluids is seen to fall off from left to right and become the reverse of the cutting speed for a given tool life as V_{60}. This is as normally would

be expected inasmuch as the less the power consumption, the less the heat developed at the tool point, and the longer would be the tool life. The power for oil A + s, however, is out of step, and, for some reason, is extremely high—almost as high as dry cutting and higher than corresponding values for any of the other cutting oils.

Chip Formation

Most of the oils broke the chips up fairly well. For the first one-tenth of the life of the cut, the chips were continuous and straight. After that they became broken into small "C" shaped chips approximately 1 inch in diameter at first, but were reduced to ¼ inch in diameter as the tool face became cupped. The chips remained stringy and continuous for the longest period of time for oil B_s, although, when cutting dry, the chips remained continuous for a much longer period of time. Some chips from oil B were slightly colored, while all of those from oils A_s and B_s were slightly discolored, probably due to the action of the sulphur. This chip discoloration might also be due to higher temperatures caused by insufficient cooling of the chip at the time of its formation.

Drilling Tests

In order to determine additional factors to compare with those of tool life, drilling tests were conducted. Equipment was available consisting of a modern Barnes Drill Company No. 201¼ drill press provided with a small recording-type dynamometer designed to record the drill torque and thrust as a function of the depth of hole.[1] A single ⅜-inch diameter drill used in the previous tests was used here. This drill had a helix angle of 30 degrees, and a web thickness of 0.068 inch. The flutes were sandblasted rather than polished. The drill was operated at 573 revolutions per minute, equivalent to a peripheral speed of 56.4 feet per minute, and a feed per revolution of 0.006 inch. The drill was ground at the beginning of the tests on each metal.

The values of torque and thrust when drilling the S.A.E. 3140 steel used in the turning tests previously discussed are plotted

[1] O. W. Boston and W. W. Gilbert, "The Torque and Thrust of Small Drills Operating in Various Metals," *Transactions*, American Society of Mechanical Engineers, February, 1936.

over the oils in Fig. 3. The oils are arranged as abscissas from left to right in order of increasing cutting speed such as V_{60} in Fig. 2. The torque, which is the principal factor of power consumption in drilling, is decreased from left to right, except the value for oil

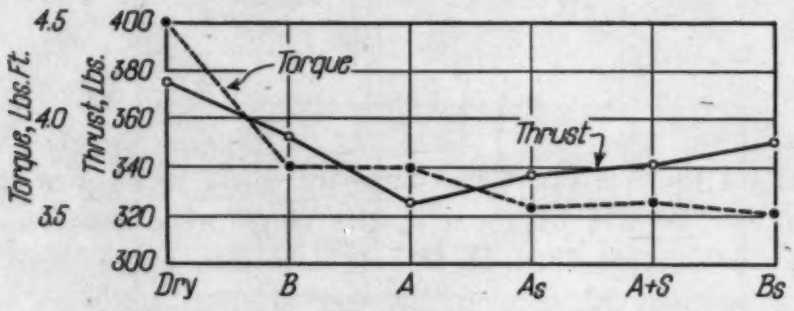

Fig. 3—Torque and Thrust When Drilling Normalized and Annealed S.A.E. 3140 Steel with Cutting Oils with and without Added Sulphur. A ⅜-Inch Diameter Drill Having a Helix Angle of 30 Degrees with Sand-Blasted Flutes and Web Thickness of 0.0685 Inch Operated at 573 R.P.M. (56.4 F.P.M.) and 0.006-Inch Feed.

A + s which is slightly higher than that for oil A_s. There is a much greater difference between the value of torque for dry cutting, and any of the oils, than between values for different oils. This same general relationship holds for the V_{60} line in Fig. 2. The thrust is highest for dry cutting, and next highest for oils B and B_s which are approximately equal, the thrust for oils A + s and A_s are slightly lower and about equal, while that for oil A is lowest. This thrust curve confirms what has previously been observed—that is, the values of thrust for different cutting fluids do not vary in the same proportion as the corresponding values of torque. The thrust is lowest for oil A, but the turning power and the cutting speed V_{60} for oil A are intermediate when compared with corresponding values for the other oils.

Drilling Other Steels

It has been observed previously that the performance of several cutting fluids on one metal does not necessarily predict their performance on another metal. For this reason, the drilling tests were conducted on three additional steels, as an annealed S.A.E. 1020 steel, 1¾-inch by 4-inch section; annealed S.A.E. 1035 steel, 1¾-inch by 4-inch section; and a cold drawn S.A.E. 1112 steel, 1½-inch by 1½-inch section. These steels were used in the paper of footnote, page 801.

The values of torque resulting from these three added metals, as well as the S.A.E. 3140 steel, are shown plotted over the cutting oils in Fig. 4. The oils are arranged from left to right in order of increasing value of V_{60}, as in Fig. 2. It is observed in Fig. 4 that the highest torque for each metal is obtained when drilling dry. The lowest torque is obtained in S.A.E. 1020 and 1112 with oil

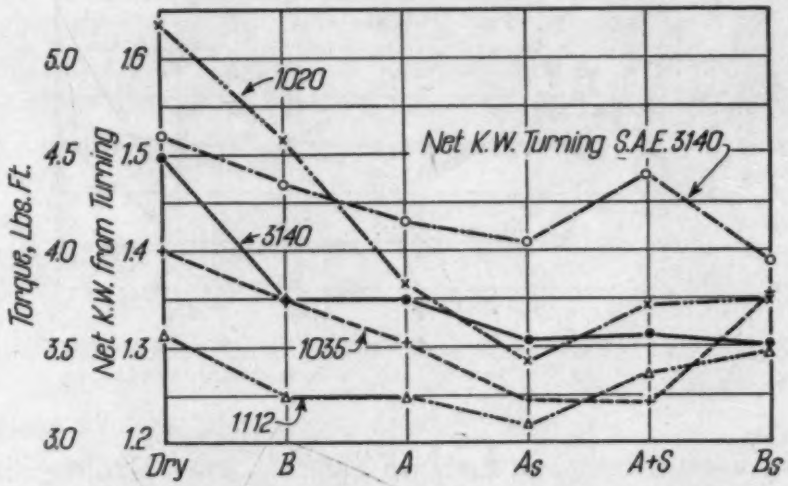

Fig. 4—Torque When Drilling Several Steels with Each of Several Cutting Fluids with and without Added Sulphur. Drilling Conditions Are Outlined in Fig. 3. The Net Kw. in Turning the S.A.E. 3140 Steel Was Calculated for a Speed of 153 F.P.M.

A_s, although in the S.A.E. 1035 and 3140 steels, the value of torque is also very low for oil A + s. Oil B_s gives the lowest value of torque for S.A.E. 3140 steel, but the highest of all oils for the S.A.E. 1035 steel. It is also interesting to observe the appreciable increase in torque produced by oil B_s over oil A_s in the steels S.A.E. 1035, 1112 and 1020. It is also observed that when drilling the S.A.E. 1112 steel, the torque obtained with the oils is only slightly lower than that obtained when drilling dry. For this steel, the lowest torque is obtained with oil A_s, while the next lowest torque is obtained with oils B and A.

The net kilowatt required in turning the S.A.E. 3140 steel has been added to Fig. 4 so that the power in turning for the different oils might be compared with the torque (99 per cent of the power) in drilling the four metals with the various oils. In a general way, these curves are similar, all having a tendency to become less from the left (dry cutting) to the right as far as oil A_s. Oil A + s produces a high turning power value in the S.A.E. 3140

steel, and also a high torque for the S.A.E. 1020 steel. The net power in turning the S.A.E. 3140 steel is lowest for oil B_s, and next lowest for oil A_s. The torque also is lowest for steel 3140 for oil B_s. For the other metals, the value of torque with oil B_s is higher than that of oil A + s.

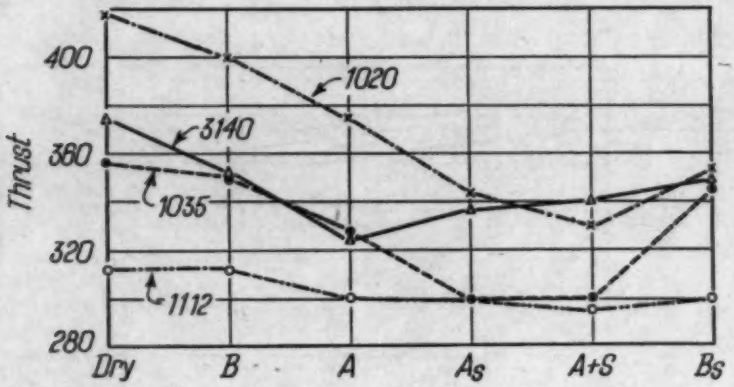

Fig. 5—The Thrust When Drilling S.A.E. Steels with Several Cutting Fluids with and without Added Sulphur as Outlined in Fig. 3.

Values of thrust for each of the oils when drilling the four steels are given in Fig. 5. In general, the values are reduced from left to right. Minimum values are reached for all metals for oil A + s, except for the S.A.E. 3140 steel which has a minimum value for oil A. The thrust for all steels is increased for oil B_s over other minimum values. The thrust is lowest for the S.A.E. 1112 steel when oil A + s is used. It is lowest for the S.A.E. 1035 steel when oils A + s, A_s and A are used. It is lowest for the S.A.E. 3140 steel when oil A is used, and for the S.A.E. 1020 steel when A + s is used.

Lubrication Tests

To obtain other performance data from these five oils, a set of lubrication tests was run on the Almen extreme-pressure lubricant testing machine, as described in more detail in the Appendix. Tests were run first with a gradual loading, and secondly with shock loading. The results are listed for each oil under the Almen Machine heading in Table I. Oils A and B, having practically no added or active sulphur, carried only five weights, or the equivalent of 5000 pounds up to the time of seizure. All of the oils containing active sulphur, that is, oils A_s, A + s, and B_s, carried the full load of

fifteen weights on the beam, equivalent to 15,000 pounds per square inch on the ¼-inch diameter journal, without seizure. It may be assumed that resistance to seizure is a function of active sulphur whether it is added in the form of an organic sulphur compound or by thermosulphurization.

The shock loading tests show that when the whole load is applied instantly to the journal, the oils A_s and A + s gave a reading of 5, whereas the sulphurized oil B_s gave a reading of 7. Oil B_s also had the highest value of T_{120}. It therefore appears that the shock loading tests on the Almen Machine indicate, with some degree of certainty, the cutting performance of the oils.

Conclusions

General conclusions may be drawn from this investigation involving two base oils with little or no active sulphur, one having very little combined or natural sulphur, and the other having considerable combined sulphur. Each of these oils was then treated so as to retain a quantity of added active sulphur.

1. In determining the tool-life cutting-speed relationship when turning an annealed S.A.E. 3140 steel forging with high speed steel tools operating under constant conditions, a straight line on log-log paper is obtained for each of the five oils and cutting dry, which have equations of the type $VT^n = C$ (see Fig. 1).

(a) The line for cutting dry is lowest and steepest, $VT^{0.116} = 181$.

(b) The lines for the oils are higher and parallel, $VT^{0.087} = C$ in which C represents the vertical displacement of the line and corresponds to the cutting speed in feet per minute for a 1-minute tool life. The plain oil B, having high natural sulphur, is lowest. The plain oil A, with low natural sulphur, is slightly higher. The addition of active sulphur to both oils gives values of C higher than for the oils without the added active sulphur.

(c) By thermally sulphurizing the oil B with high inactive sulphur to give oil B_s, the performance factor C is increased from the poorest to the best, that is, 181.5 to 191, or a 5.1 per cent increase. The tool life is increased 78 per cent (Fig. 2).

(d) By thermally sulphurizing the oil A with low inactive sulphur to give oil A_s, the performance C is increased appreciably, that is, 183 to 187, or 2.2 per cent. The corresponding increase in tool life is 31 per cent.

(e) By adding an oil soluble, synthetic, sulphur compound to oil A with low inactive sulphur to give oil A + s, the speed is increased from 183 to 189, or 3.3 per cent. The corresponding increase in tool life is 47 per cent.

(f) The increase in speed of the best oil B_s over that of cutting dry is from 181 to 191, or 5.5 per cent, while T_{120} is increased 485 per cent.

2. The added active sulphur content values do not correlate with the relative cutting performance of the sulphurized oils (Table I).

3. High natural sulphur does not give high cutting performance, but seems to aid sulphurization to give a superior product.

4. The net power in turning seems to be inversely proportional to the cutting speed for a given tool life (C, V_1, or V_{60}), and the tool life for a given cutting speed (T_{120}), Fig. 2. The power for oil A + s is high and out of order.

5. All tools failed in turning by the usual cupping process.

6. All oils caused the chips to be formed in a normal way, and the chips broke up into small pieces in a shorter time with the oils than when turning dry. With the oils, the chips were continuous and straight for about one-tenth of the tool life, then they became broken into small "C" shaped chips about 1 inch diameter at first, and then as small as ¼ inch diameter as the tool face became deeply cupped. The chips remained stringy and continuous for the longest period of time for oil B_s.

7. The drilling torque in the S.A.E. 3140 steel, which is the principal factor of power, follows the turning power line as a function of the oils. It is highest for cutting dry, reduced for the plain oils A and B, and reduces still further for the sulphurized oils. The torque for oil A + s is slightly higher than that for A_s and B_s, as was the case in turning (see Figs. 2 and 3).

8. The drilling thrust is highest for cutting dry and lowest for the plain oil A. That for all sulphurized oils is lower than that for the plain oil B. The thrust for the oil B_s giving the highest cutting speed is higher than that for all other oils except the plain oil A (Fig. 3).

9. Torque values indicate fairly well the cutting performance for these oils, but thrust values do not (Fig. 3).

10. Torque and thrust values obtained for various oils in one steel do not necessarily have the same relation in another steel.

11. The Almen lubricant testing machine shows a high load carrying capacity for those oils containing high active sulphur and low capacity for those oils with low active sulphur. The shock loading test seems to give the best correlation with cutting speed performance of the oils.

Acknowledgments

The oil samples were prepared by the Esso Laboratories, and the experiments were performed in the Metal Processing Laboratories at the University of Michigan. Assistant Professor W. W. Gilbert and L. P. Hartung, a research assistant in the department, helped in carrying out the tests.

Appendix

The Almen Lubricant Testing Machine.[2] Many types of laboratory testing machines have been proposed for evaluating or classifying extreme pressure lubricants. All of these test machines will show differences in load-carrying ability of the different lubricants, since they use dissimilar test pieces and operate under different pressures, rubbing velocities, temperatures, etc. Consequently, for each laboratory testing machine a set of operating conditions must be drawn up, which will rate the lubricants in the same order of merit, as indicated by actual service. A testing machine which has been standardized in the terms of preliminary service data becomes a secondary standard for determining uniformity in production and for evaluating new lubricants with respect to extreme pressure characteristics.

The Almen extreme-pressure lubricant testing machine was designed to simulate the conditions of extreme pressures which are encountered with hypoid gears. It employs a ¼-inch diameter drill rod journal and ½-inch split bushing made from S.A.E. 2315 cold drawn steel. Both the journal and bushing are used in the heat treated "as-received" condition. The journal is polished and the bushing after splitting is ground on the bearing surface with a fine grinding wheel. A 0.007-inch clearance is provided between the journal and the normal diameter of the bushing. Pressure is applied to the split bushing through a mechanical and hydraulic system.

[2] "Proceedings of the Petroleum Institute," Section III, 13th Annual Meeting, Nov. 14, 1931, p. 13, and U. S. Patent 2,001,861.

The journal and bushing are held in a cup fixture which also serves as a container for the lubricant being tested. The entire assembly including the oil sample cup and the loading cylinder is cradled around the center of rotation of the journal. The torque developed is indicated through a second hydraulic system by a test gage shown. The machine is belt-driven and is operated at a journal speed of 600 revolutions per minute. Two-pound weights are applied on the loading beam at 10-second intervals. The test is continued until seizure occurs, or until a total of 30 pounds is applied (fifteen 2-pound weights). Each 2-pound weight is equivalent to 1000 pounds per square inch projecting bearing area. Thus, the full load of 15 weights on the beam is equivalent to 15,000 pounds per square inch on the bearing surface on the ¼-inch journal.

The Almen shock loading test is run by starting up the journal rotation and placing all weights on the beam, while the beam is supported so as not to apply any pressure to the bushing and journal. The beam with the added weights is then released so that all of the load is applied instantaneously to the journal.

DISCUSSION

Written Discussion: By Joseph Geschelin, Detroit editor, Automotive Industries, and chairman, Independent Research Committee on Cutting Fluids.

The authors of the paper are to be congratulated upon the completion of an important investigation in the field of metal cutting. In particular, as chairman of the Independent Research Committee on Cutting Fluids, I wish to express the gratitude of our membership for the excellent and continuing program of research in metal cutting carried on by Professor Boston and his associates.

It is discouraging to find that few people concerned with machine shop practice realize the basic role of cutting fluids. Anything that can be done to encourage a better knowledge of the utilization of cutting fluids will go far to promote more economical metal cutting. And that is something of vital significance in the present national emergency.

The paper demonstrates quite unmistakably the importance of "free" sulphur additions in certain types of cutting fluids, brings to the fore the fact that sulphurized cutting fluids have a definite place in the picture of machine shop practice. It might be noted that many varieties of extreme pressure fluids, including sulphurized and chlorinated materials, are being used successfully in regular production. It is certainly important to confirm the current practice by scientific studies such as the one under discussion.

Undoubtedly there is some question as to the maximum percentage of free sulphur required to give optimum results. The authors have presented the results of test work with free sulphur additions not exceeding 1 per cent,

which is consistent with good field practice. Have they any comments as to the effectiveness or limitations of additions exceeding 1 per cent?

One of the moot questions that has troubled chemists and others concerned with cutting fluids has been the difficulty of accurately identifying the sulphur content of sulphurized cutting fluids. While I am not qualified to discuss this phase of the matter, I have been told on many occasions that it has been quite difficult, if not impossible, to isolate the sulphur content and to indicate how much is "native" sulphur and how much is "free" sulphur. On page 794 the authors give a simple method for making this determination.

It would be most constructive if the authors and others qualified to discuss this would indicate whether the method they have employed can be generally recognized as making a good yardstick or whether it is a new method which should be given due consideration by experts in the field of cutting fluids. If this method is indeed foolproof, it should be given wide publicity and may be accepted as a standard procedure by the producers and users of cutting fluids.

Written Discussion: By W. H. Oldacre, president, D. A. Stuart Oil Co., Chicago.

It is always a pleasure to comment on the work of Dr. Boston and his associates. By persistent pioneering they have added much to our knowledge of the art of cutting metals.

This paper deals with a very practical and timely subject. The use of cutting oils containing sulphur, while approaching the universal, suffers from a lack of accurate scientific analysis and clear understanding. In this time of tool steel scarcity and urgent production needs, this addition to our knowledge of metal cutting processes must be profitable.

It is perhaps unavoidable that a paper of this nature (preliminary, we hope) suffers from over-simplification. Certainly Dr. Boston will be the first to confirm the assertion that this investigation of three very simple sulphur bearing oils should in no wise be taken as an inclusive study of "sulphurized oils."

Sulphur is a very "versatile" element. It forms a large number of oil soluble compounds that vary widely in activity. In this paper the copper powder method of determining activity is used. It is interesting to note that the use of iron powder, which theoretically should correlate more closely with service, will give results much different from those secured by using copper.

As indicated in recent studies of sulphurized gear lubricants, sulphur functions as an anti-weld agent and also under some conditions as a wear accelerator. Apparently these two characteristics are also effective in metal cutting. Thus, in machining a free cutting steel the use of a highly active sulphurized oil will definitely shorten tool life due to front clearance (end relief) wear, while the use of the same oil in machining a soft, tough steel will increase tool life by preventing scuffing at points of contact between chip and tool. With steels between these two extremes it is profitable to study and adjust the sulphur activity to the requirement.

Obviously then we should not draw too definite conclusions regarding the intrinsic merit of sulphurized oils from simple tool-life tests. The relationship between metal, oil and sulphur can be of considerable complexity and

the effect of this relationship on the complex mechanism of chip formation merits our most respectful approach.

Written Discussion: By H. L. Moir, The Pure Oil Co., Chicago, Ill.

We wish to congratulate the authors upon their timely presentation of this excellent paper on a subject about which, in our opinion, too little information has been made available. There is very little to add to the data except that it would appear a more complete picture could have been presented had oil B plus the synthetic sulphur additive been included in the data. We are in agreement with the findings of the authors as tool life is now measured, and only wish that some other test machine data, such as Timken or S.A.E., could have been given as added information. We note the Almen machine data run at one temperature shows oils A and B to be considered equal, yet the actual cutting data show oil A superior to oil B. Perhaps other test machine data on these oils might have explained this.

It would be well, along these lines, to see some data upon this series of oils with reference to surface finish. There seems to be some doubt that tool life alone, as measured to tool failure, is a complete criterion of a good cutting oil. It may be that tool life is the time during which the tool cuts without a change of surface finish.

We have done a considerable amount of work along these lines, and have prepared a slide of a thermally sulphurized cutting oil, which was tested under the following conditions:

Material Cut—S.A.E. 1045
Cutting Speed—187 Feet per minute
Feed—0.0094 Inch/Revolution
Depth—0.050 Inch
Tool Material—Rex AA H.S.S.
Tool Shape—6-8-8-8-8-5-1/32 R
Oil Used—Thermally Sulphurized Oil
Oil Rate of flow—2 gal/minute @ 7.9 feet/second
Tool Life—11.03 minutes
Approx. time for finish change—7 minutes

It will be seen that there is an abrupt change in surface finish at a tool-life time, as measured by finish, slightly more than half of the total tool-life time, as measured by Boston and Zimmer. Where similar cases have been noted, cutting oils have been given two ratings, derived from a lathe test similar to the set-up used by the authors, based upon a finish failure and a tool failure. It is our feeling that an analysis of the test results, based upon such a principle, might reverse the findings of oils A and B.

The drilling tests are quite interesting, inasmuch as oil B$_s$, which showed up quite well in the tool-life tests, did not show as well as oil A$_s$ when drilling 1020, 1112 and 1035, and is not much better than oil A$_s$ on the other steels. It is doubtful whether the difference of 0.05 per cent active sulphur between oils A$_s$ and B$_s$ would entirely account for the differences obtained between these oils, but would like to have the authors' verification regarding this. Again, in this series of curves, particularly Fig. 4, it appears that the assumption is made that the finish produced by all of the oils on one or more steels is either proportional to the forces measured, or is disregarded as an unimportant fac-

tor. Perhaps here, again, some criterion of finish might be introduced in the interpretation of these tests results.

It may be that some of the discrepancies which have occurred between laboratory tests and actual field tests on both experimental and commercial cutting oils do occur because of the misinterpretation of laboratory data. In practice, tests for the determination of tool life are generally based upon finish failure of the tool rather than complete failure of the cutting edge. It is our opinion, therefore, that laboratory data should be interpreted in the same manner as is practice, so that some of the vagaries which occur between laboratory and field tests may be avoided.

Written Discussion: By M. E. Merchant, physicist, Research Department, The Cincinnati Milling Machine Co., Cincinnati, Ohio.

This paper is a valuable contribution to the literature on the practical aspects of metal cutting. It at last provides a quite definite answer to the much discussed question as to the relative values of added and natural sulphur in cutting oils. The view has often been expressed that added sulphur, only, is effective in the cutting of steel, but it is most gratifying to find that a careful investigation of the relative merits of the two, under practical yet scientifically controlled test conditions, has been made. The tool-life cutting-speed tests on S.A.E. 3140 steel are particularly conclusive, and the correlation between these results and the results obtained from the shock loading tests on the Almen machine is most interesting.

The results obtained in the measurements of net power required in turning with the different oils are also noteworthy. It is surprising to find that the addition of the oil soluble sulphur compound to oil "A" actually caused an increase in power consumption, yet gave increased tool life. The writer cannot help but feel that measurements of other fundamental physical quantities, namely, cutting ratio, tool temperature, and coefficient of friction between chip and tool, made simultaneously with the present measurements, would have thrown considerable light on this seemingly anomalous result, as well as on the nature of the changes produced in the cutting action by all of the various oils. It is the changes in such fundamental variables as these which produce the over-all changes in the observed practical quantities.

The results obtained in the drilling tests on the various materials under controlled practical conditions provide an excellent demonstration of the fact that a given cutting fluid varies in its effectiveness as the chemical composition of the work material is changed. The result is not surprising when one considers the fact that the action of a cutting fluid, apart from cooling, depends mainly on its ability to enter into chemical combination with the chip material, under the conditions of pressure and temperature existing at the chip-tool interface. This same result has been observed in the course of an investigation of the fundamentals of cutting fluid action made in the Research Laboratory of the Cincinnati Milling Machine Company, and reported in a paper[3] given at the 1940 Metal Congress. The accompanying Table A is from that publication and provides another illustration of the fact that a cutting fluid may give good results on one material, poor results on another.

[3]Hans Ernst and M. E. Merchant, SURFACE TREATMENT OF METALS, published by American Society for Metals, 1941, p. 299.

Table A

Case	Cutting Fluid	Work Material	Condition of Surface	Cutting Ratio = (Length of Chip) ÷ (Length of Cut)		Cutting Force (F_c) (Lbs.)	
					S.A.E.		S.A.E.
				Alum.	1020	Alum.	1020
I	Acetic anhydride	Aluminum	Bad	0.18	....	154	...
	Acetic anhydride	S.A.E. 1020 Steel	Good	....	0.41	...	363
II	Turpentine	Aluminum	Good	0.35	....	78	...
	Turpentine	S.A.E. 1020 Steel	Bad	....	0.25	...	493
III	Carbon Tetrachloride	Aluminum	Excellent	0.39	....	65	...
	Carbon Tetrachloride	S.A.E. 1020 Steel	Excellent	....	0.48	...	212
IV	Benzene	Aluminum	Very bad	0.13	....	182	...
	Benzene	S.A.E. 1020 Steel	Very bad	....	0.22	...	535

The measurement of torque in drilling is not quite as straightforward a test as the measurement of tool life in turning, for demonstrating the differences between various cutting fluids, because of the increased number of variables that are present in the drilling process. It is unfortunate that turning tests, with measurements of tool life, could not have been made for all the materials investigated in the drilling tests. The writer realizes, however, that such tests would have required a large additional amount of time and material, and were perhaps not feasible for this reason.

In almost all of the cutting tests described in this paper, the oils containing added sulphur were found to be superior to the natural sulphur-bearing base oils. However, it should be noted that the authors have not generalized to the extent of saying that the former oils are universally superior, as they have evidently recognized that this is not likely to be universally true. On the other hand they have succeeded in showing conclusively that cutting oils containing "active" sulphur ordinarily behave quite differently from those containing only natural sulphur, and also that the latter may be expected to be superior to the former in a large percentage of cutting applications, on ferrous metals. Thus their paper should serve to remove much of the confusion now existing in regard to the usefulness of sulphur in cutting oils, and should help to clarify and simplify the problems in this field.

Oral Discussion

SAM TOUR:[4] Might I add to Dr. Oldacre's comments? We must consider not only what the oil is supposed to lubricate, and so forth, but we must also consider the basic oil to which the sulphur is added. The addition of a certain amount of sulphur to one oil is not necessarily comparable to the addition of that same amount of sulphur to some other base oil. In this case the effect of sulphur addition to a specific oil has been studied. Also a specific high sulphur oil has been studied. It has not been shown that similar results are obtained or obtainable with any other oils.

[4]Vice President, Lucius Pitkin, Inc., New York.

Authors' Reply

We sincerely appreciate the interest shown in this paper as has been made evident by the many comments. We wish to reiterate that the purpose of the paper was to deal with a simple case of cutting oils. Two were straight mineral oils, one with little and the other with considerable natural sulphur. Two additional oils were made using these same oils to which active sulphur had been added by cooking. The fifth oil was prepared by adding an organic sulphur compound to the low natural sulphur oil. These oils were not selected to cover the range of cutting fluids generally available for metal cutting operations. In this paper, no attempt is made to anticipate results which might be obtained with other oils such as those containing fat, fat plus sulphur, chlorine, or combinations of sulphur and chlorine. It is recognized, however, that there is a definite lack of information dealing with this complete picture.

It probably is true that the difference in cutting performance and the power required for turning in the various steels is due to some extent to the difference in activity of the added sulphur. This activity is believed to be a function of the amount of active sulphur present in the oil. The inactive sulphur presumably aids the active sulphur to some extent.

Mr. Oldacre brought up the question of active sulphur determinations with iron powder instead of copper powder. We have determined the active sulphur content of the test oils using both copper and iron powder in accordance with the procedure written up in the paper, and find that the iron powder shows somewhat lower active sulphur content than does the copper. The results of our tests are shown in Table B.

Table B

Designation Sample No.	Active Added Sulphur, Per Cent	
	Copper Powder	Iron Powder
Oil A	0.00	0.02
Oil A_s	0.75	0.72
Oil A + s	0.91	0.41
Oil B	0.02	0.01
Oil B_s	0.76	0.61

The results obtained with the copper powder are in closer agreement with a known amount of added sulphur in each of these cutting oils, whereas the iron powder shows somewhat lower values with two of the oils containing active sulphur, and checks the copper in one case. Both methods show the unsulphurized oil to contain substantially no added sulphur. Comparing the active sulphur values from the copper and iron powder with the results of the machining tests, it would appear that the copper powder method is the more reliable.

The iron powder method we think certainly should be compared with copper because, naturally, it is the more satisfactory type of material to use, since the cutting oil operation involves the reaction of the sulphur with the iron, rather than with copper. The copper has one particular disadvantage and that is the reason we have not offered it or publicized it widely for general use.

It is not particularly applicable in the presence of appreciable quantities of fatty oils because of the complicating effect of copper soap formation.

The Almen Lubricant Testing Machine has been used in the Esso Laboratories with considerable satisfaction. It is recognized, however, that lubrication data obtained on other machines of this general nature are not always in close agreement. For this reason, samples of the oils have been tested in the S.A.E. extreme-pressure lubricant testing machine and the following results were obtained:

Table C
Results of Lubrication Tests for Each of the Oils

Oil Sample	S.A.E. Extreme Pressure Lubricant Testing Machine Scale Load in Lbs. (1000 RPM; 14.6:1 Rubbing Ratio; 80 Lbs./Sec. Loading Rate)	Almen Lubricant Testing Machine* Scale Load in 1000 Lbs. Gradual Loading	Almen Lubricant Testing Machine* Scale Load in 1000 Lbs. Shock Loading
A	Less than 20	5	8
A_s	150	15	5
A + s	165	15	5
B	Less than 20	5	8
B_s	190	15	7

*Values taken from Table I.

The oils containing active sulphur have the highest load-carrying capacity. The oils A and B with no active sulphur have very low load-carrying capacity. Referring to Fig. 2 of the paper, the cutting values of T_{120}, V_{∞}, and V are low and about equal for oils B and A as are the results of all three lubrication test results given in Table C. The power for these oils is relatively high. The cutting values of oils A_s, A+s, and B_s are relatively high, improving from A_s to B_s. These high values are accompanied by high but equal values of the gradual loading on the Almen machine. The shock loading on the Almen machine does give equal values for oils A_s and A+s, but the highest value for B_s, which correlates well with the cutting values. The S.A.E. values as given seem to correlate best with the cutting values as the load is very low for oils A and B, but greatly improved for oils A_s, A+s, and B_s, in the order named. There is an increase of 7.1 per cent in T_{120} for oil B_s over A_s in Fig. 2, and an increase in S.A.E. scale load of 26.8 per cent in S.A.E. machine load for oil B_s over A_s. There is a directly indicating tendency, but on a different ratio basis, between the cutting values of Fig. 2 and the S.A.E. machine load. It is seen in Fig. 2, however, that the net K.W. curve does not follow the tendency of the cutting curves in that the K.W. value for oil A+s is unusually high and apparently out of order.

If the values of these lubrication tests were plotted over the oils in Fig. 4 of the paper, it would be seen that the high lubricating values for the three sulphurized oils do not seem to correlate satisfactorily with the normal values of torque for the several steels drilled. The value of torque for all steels for these three oils containing active sulphur is low, but the torque for oil B_s on three of the steels is considerably higher than that for oil A_s. This is indicated by the S.A.E. loading, but not by the Almen tests. The torque for the oils

A and B containing no active sulphur appear to be about the same as that for oils A+s and B_s for most of the steels, whereas the lubrication test data show considerably lower values. This would indicate that the lubrication test is of little value in throwing true light upon the torque required to drill various steels with various types of oils.

There is also little of definite value in determining the thrust values when drilling with various steels by using the lubrication tests as the lubrication tests for oils B and A in Fig. 5 are definitely of a lower order than the corresponding values for the sulphurized oils.

Mr. Harry L. Moir, of the Pure Oil Company, also ran lubrication tests on the S.A.E. machine as well as on the Falex. He has correlated these data in Table D which summarizes data of tool life, power in turning, etc., to show the relative merits of the various oils.

Table D
A Summary of Data to Show Relative Merits of Each Oil

Oil	A	B	A_s	A+s	B_s
Tool life at 120 fpm, T_{120}	4	5	3	2	1
Net K.W. in turning	3	4	2	5	1
S.A.E. rating (750 rpm)	3	5	2	4	1
Falex test—maximum load	4	3	2	5	1
Almen machine, Gradual loading	3	3	1	1	1
Shock loading	5	5	2	2	1
Inactive sulphur	4	2	4	3	1
Active sulphur, Cu powder	5	4	3	1	2
Fe powder	4	5	1	3	2
Total sulphur	5	2	4	3	1

Note: Low numbers depict best results, i.e., 1 means highest tool life, lowest turning power, highest load on S.A.E. machine, highest sulphur, etc.

Mr. Merchant's analysis of these data, in view of his own experimental data on lubrication, is of very great interest and value. His discussion indicates the complexity of the subject and the need for further work. Mr. Moir raises some very interesting questions as to a preliminary tool failure in which the surface quality is changed before the total tool-life time. Such observations have been made many times, although by changing the tool shape, such as the side cutting-edge angle or the nose radius, or even the ratio of depth to feed, this preliminary tool failure may occur without affecting the finish on the work or the work size. Many tests have been run to determine the relation between the time of preliminary tool failure or the local breaking down of the cutting edge of the tool and the time of total tool failure. In many instances, this preliminary tool failure occurs after 90 per cent of the effective tool life, or it may occur after one-third to one-half of the total tool life. Further, the cutting-speed tool-life line on log-log paper for the preliminary tool failure may be parallel to the line for total failure, or it has been found to have a steeper slope. This relationship is believed to be variable, and to date no answer to the general relationship can be given. It is entirely possible that the cutting oil plays an influential part in this relationship, although no information as to this point is available at this time.

Mr. Geschelin has raised one question as to the effectiveness of active

sulphur in excess of 1 per cent. Many tests have been run in which the apparent active sulphur content is considerably in excess of 1 per cent, even up to 3 or 4 per cent. It is believed that active sulphur up to 1 per cent is very beneficial, but that in excess of this amount it becomes less and less effective, so that the actual sulphur in excess of some arbitrary value such as 2 per cent or possibly 3 per cent would be of no immediate value.